This electronic thesis or dissertation has been downloaded from the King's Research Portal at https://kclpure.kcl.ac.uk/portal/

Temporal and spatial controls of cell fate specification in the cerebellum

Green, Mary

Awarding institution:
King's College London

The copyright of this thesis rests with the author and no quotation from it or information derived from it may be published without proper acknowledgement.

END USER LICENCE AGREEMENT

Unless another licence is stated on the immediately following page this work is licensed

under a Creative Commons Attribution-NonCommercial-NoDerivatives 4.0 International

licence. https://creativecommons.org/licenses/by-nc-nd/4.0/

You are free to copy, distribute and transmit the work

Under the following conditions:

- Attribution: You must attribute the work in the manner specified by the author (but not in any way that suggests that they endorse you or your use of the work).
- Non Commercial: You may not use this work for commercial purposes.
- No Derivative Works - You may not alter, transform, or build upon this work.

Any of these conditions can be waived if you receive permission from the author. Your fair dealings and other rights are in no way affected by the above.

Take down policy

If you believe that this document breaches copyright please contact librarypure@kcl.ac.uk providing details, and we will remove access to the work immediately and investigate your claim.

Download date: 06. Jan. 2025

This electronic theses or dissertation has been downloaded from the King's Research Portal at https://kclpure.kcl.ac.uk/portal/

KING'S College LONDON

Title: Temporal and spatial controls of cell fate specification in the cerebellum

Author: Mary Green

The copyright of this thesis rests with the author and no quotation from it or information derived from it may be published without proper acknowledgement.

END USER LICENSE AGREEMENT

This work is licensed under a Creative Commons Attribution-NonCommercial-NoDerivs 3.0 Unported License. http://creativecommons.org/licenses/by-nc-nd/3.0/

You are free to:

- Share: to copy, distribute and transmit the work

Under the following conditions:

- Attribution: You must attribute the work in the manner specified by the author (but not in any way that suggests that they endorse you or your use of the work).
- Non Commercial: You may not use this work for commercial purposes.
- No Derivative Works - You may not alter, transform, or build upon this work.

Any of these conditions can be waived if you receive permission from the author. Your fair dealings and other rights are in no way affected by the above.

Take down policy

If you believe that this document breaches copyright please contact librarypure@kcl.ac.uk providing details, and we will remove access to the work immediately and investigate your claim.

Temporal and spatial controls of cell fate specification in the cerebellum

Mary Jane Green

MRC Centre for Developmental Neurobiology

King's College London

Thesis submitted for the degree of Doctor of Philosophy (PhD)

September 2012

Abstract

The domain of the developing cerebellum in dorsal rhombomere 1 is specified by signals from two adjacent organising centres, the midbrain-hindbrain boundary (isthmus) and the roof plate of the fourth ventricle. Two major precursor pools give rise to all the cells of the cerebellum: the ventricular zone and the cerebellar rhombic lip. The rhombic lip comprises a dorsal progenitor population, defined by the expression of the transcription factor Atoh1, which gives rise to different cell types contributing to both extra-cerebellar and cerebellar populations. In chick embryos, I have investigated the timing, morphology and gene expression of successive cohorts of rhombic lip derivatives using a combination of *in ovo* electroporation and *in situ* hybridisation. Using this approach, I first derived an accurate spatiotemporal map of cell production within rhombomere 1, which helps illuminate the evolutionary mechanisms generating diversity in the structure and function of the cerebellum. I then explored how signals from the roof plate and isthmus specify distinct neuronal derivatives of the cerebellar rhombic lip at different time points. In these experiments, I show that the isthmus abuts an expanded region of *Atoh1* expression from which early, extra-cerebellar, *Lhx9*-expressing rhombic lip derivatives are born. Through surgical manipulation of the isthmus in cultured explants and through induction of an ectopic isthmic organiser through *in ovo* electroporation of early genetic regional determinants (*Otx2*), I demonstrate that this expanded region of *Atoh1* is dependent upon the isthmus for its induction and maintenance. I also demonstrate the role of the isthmic gene, *Fgf8*, in the maintenance of the expanded domain through *in ovo* electroporation of plasmids encoding *Fgf8* and a dominant-negative FGF receptor. This FGF-dependent domain of *Atoh1* is regulated independently from the specification of rhombic lip derivatives, suggesting a novel role for both *Atoh1* and FGF signalling in rhombomere1. Analysis of triple knockout FGF receptor mutants and FGF hypomorph mice confirmed the results of dominant negative overexpression in chick. To investigate temporal factors influencing the specification of temporal cell fate, I examined the role of thyroid hormone, which is synthesised in the fourth ventricle choroid plexus adjacent to the rhombic lip. I show that pharmacological manipulations of thyroid signalling can specifically disrupt the expression of markers of late-born rhombic lip derivatives, pointing to an important role for steroid hormone receptor signalling in specifying the fate of specific temporal cohorts in the rhombic lip lineage.

Acknowledgements

Thanks must go first and foremost to my supervisor, Richard, for always sparking my interest, for all the (endless hours of) discussions and ideas and for encouraging me throughout my PhD. Thank you to all the members of the Wingate lab, past and present: Emma, for teaching me my way around a lab and setting a fantastic example to follow; Tom, who answered every stupid question I ever had, provided excellent Friday afternoon discussion and taught me about the animals “not in the zoo”; Leigh for all the help, encouragement and snacks; and Flo for egging me on to the finishing line. Thank you to Tom and Kate, who went through it all from start to finish with me and to all the other people in my office who made it such as fun place to work: Liam (my photoshop/illustrator guru), Oniz (my early morning buddy), Ellen and Peter. Thanks also to the members of the Lumsden group meetings who gave me so much helpful feedback and advice. The MRC centre has been a brilliant place to work, so thank you to all the people who I have met and worked with here. Finally, thank you to all my family and friends who have supported me and kept me sane.

Table of Contents

Table of Figures

Table of Tables

Chapter 1 Introduction

1.1 The cerebellum: anatomy and function.

1.1.1 Functions of the cerebellum.

In any controlled system, be it biological or mechanical, there is a requirement for both instruction and feedback which can modulate output. This feedback process requires a calculation of error. For example, a simple thermostat system must calculate the error between the temperature of the surrounding environment and the temperature set on the thermostat. The thermostat must then be able to signal to an effector (eg. a heater) to enact the appropriate response. This same principal is applicable in the nervous system where sensory feedback must be interpreted, error calculated, and response modulated accordingly. Furthermore, the nervous system can combine sensory inputs and previous experiences to predict appropriate output before errors are made. This "feed-forward" control allows for more accurate, and faster, responses because errors are anticipated rather than detected. These feed-back and feed-forward systems are contained within the circuitry of the cerebellum.

This model of cerebellar function has evolved over several decades by the interpretation of anatomical and physiological observations in the light of clinical descriptions of cerebellar dysfunction. Historically, the majority of clinical observations regarding cerebellar damage or congenital malformation pertain to the loss of motor coordination (Holmes, 1917, 1922b, a). Cerebellar injuries do not cause paralysis but instead result in ataxia (uncontrolled movements) and problems with posture and balance and the ability to learn simple motor tasks, all of which require feed-back and feed-forward information processing. These clinical traits are mirrored by the majority of cerebellar circuits feeding into sensorimotor pathways in the central nervous system. Therefore the majority of studies of cerebellar function have focussed on its role in motor systems to calculate error and as a mechanism for motor-learning.

The cerebellum has also been implicated in non-motor tasks relating to error-predication, attention, language, mental calculations and working memory through connections with non-motor regions of the cerebral cortex (reviewed by Ito (2008)). Clinically, damage to specific regions of the cerebellum are associated with these cognitive defects as are several syndromes characterised by, or associated with cerebellar malformations: Dandy-Walker syndrome, Jouberts syndrome, Fragile-X syndrome, Down's syndrome, William's syndrome

and autism (reviewed by Steinlin (2008) and Millen and Gleeson (2008)). Cerebellar mutism, autism, dyslexia and schizophrenia have also been associated with cerebellar function and/or pathology (reviewed by Ito (2008)). Furthermore, neuroimaging studies have provided evidence for pronounced activity in these cerebellar regions during various mental tasks (Reviewed by Ito (2008)). These cognitive functions can be related to processes requiring error calculations and learning (ie. planning and adapting). Therefore it is currently believed that similar processes are used for calculations in both cognitive and motor pathways and learning.

1.1.2 Cerebellar circuitry.

The cerebellum consists of a foliated cortex of three layers (molecular layer, Purkinje cell layer, and granule cell layer) surrounding a central white matter containing discrete cerebellar nuclei. The cerebellar cortex is entirely uniform in its intrinsic circuitry with two types of input from mossy fibres of precerebellar nuclei in the hindbrain and climbing fibres of the inferior olivary complex. Efferently, the cerebellar cortex connects to the cerebellar and vestibular nuclei. This circuitry is outlined in **Figure 1-1** and is reviewed by Voogd and Glickstein (1998).

Glutamatergic granule neurons in the granule cell layer have axons which project up to the molecular layer and bifurcate into parallel fibres. Parallel fibres form excitatory synapses with the broad dendritic arbours of underlying Purkinje cells which are arranged at right angles to parallel fibre axons. Purkinje cells constitute all of the output of the cerebellar cortex to cerebellar or vestibular nuclei via GABAergic, inhibitory signals. Multiple classes of inhibitory interneurons, chiefly stellate and basket cells of the molecular layer and Golgi cells of the granule layer, act to modulate connections within the cerebellar cortex. Additional cells types within the mammalian cerebellar cortex include inhibitory Lugaro cells and candelabrum cells and excitatory unipolar-brush cells (Lainé and Axelrad, 1994; Flace et al., 2004; Kalinichenko and Okhotin, 2005).

Input to the cerebellum is in two forms: mossy fibres and climbing fibres. Mossy fibres originate from five distinct nuclei in the hindbrain: pontine grey, reticulotegmental, vestibular, lateral reticular and external cuneate. Mossy fibres project to the cerebellum forming synapses with granule neurons. Climbing fibres originate from cells of the inferior olivary nuclei and project directly to Purkinje cells. Every Purkinje cell has input from a single climbing fibre which progressively encompasses its entire dendritic tree. Both climbing fibres and mossy fibres have collateral connections to cerebellar nuclei.

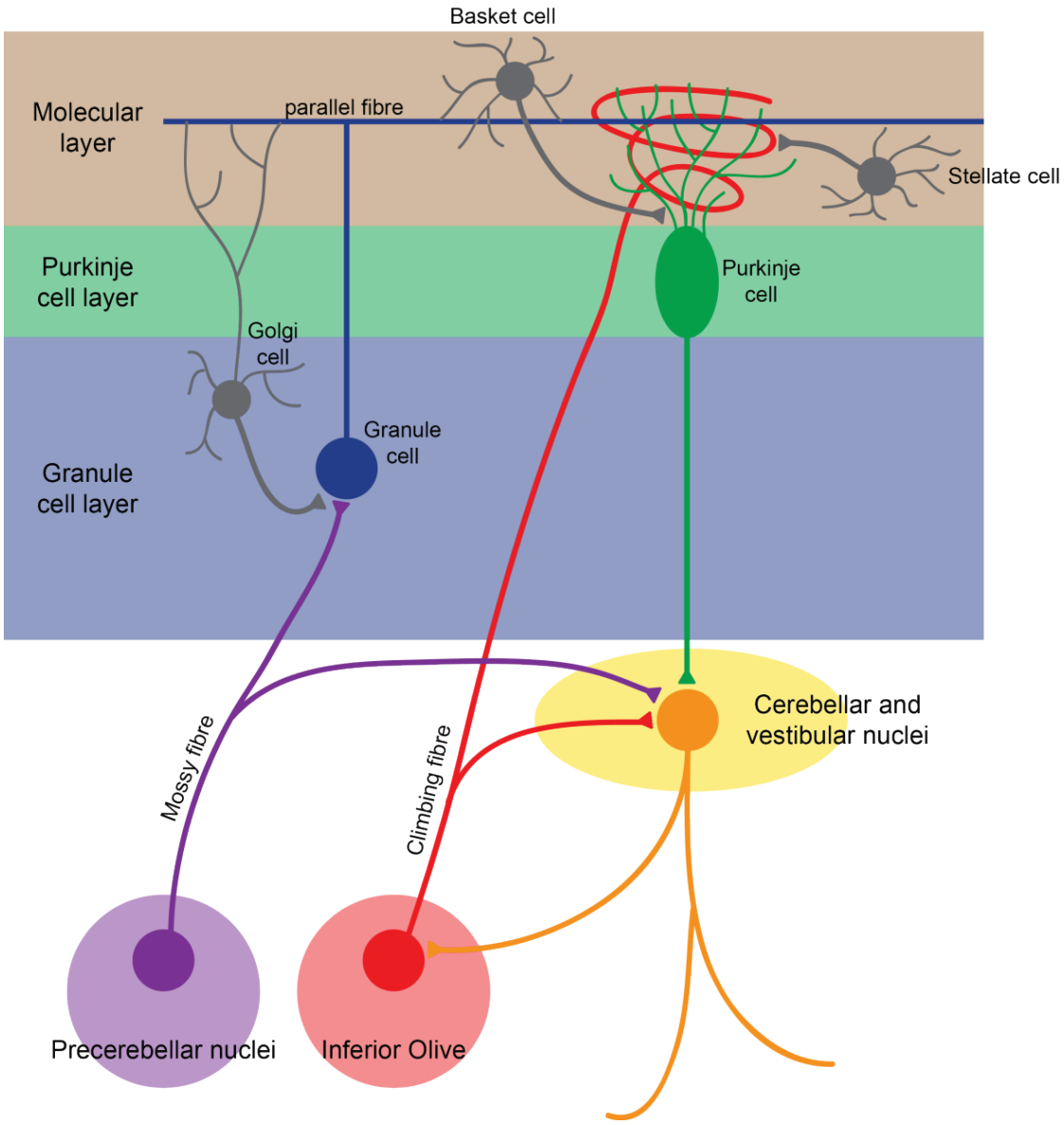

Figure 1-1 Cerebellar circuitry.

Schematic representing all of the cell types of the avian cerebellum. The cerebellar cortex is divided into 3 layers: the granule layer contain granule cells (blue), the Purkinje cell layer containing Purkinje cells (green) and the molecular layer (brown) containing the parallel fibres of granule cell axons and Purkinje cell dendrites. Golgi cells of the granule layer and basket/stellate cells of the molecular layer are interneuron populations (grey). Input to the cerebellum is via mossy fibres (purple) from the precerebellar nuclei in the hindbrain and climbing fibres (red) of the inferior olive to granule cells and Purkinje cells respectively. All of the output of the cerebellum is via Purkinje cells to cerebellar and vestibular nuclei (orange).

The first model of cerebellar function as a computational processing system was proposed by Eccles, Ito and Szentagothai (Eccles, 1967) suggesting that microzones, constituting the minimal functional unit within the cerebellar cortex, were established by the connection of single climbing fibres to single Purkinje cells. Dual input of single climbing fibres and thousands of mossy fibre connections, via granule cell parallel fibres, caused Purkinje cells to elicit two distinct types of action potential, simple spikes (normal action potentials) and complex spikes. Complex spikes are unique to Purkinje cells and are only observed following firing of climbing fibres. These anatomical and physiological descriptions lead to the proposal of models explaining how cerebellar microcircuits could confer motor learning (Marr, 1969; Albus, 1971). The "Marr-Albus" model of motor learning proposes that the low frequency firing rate of complex spikes implies these signals do not directly confer motor commands and instead, constitute an error or teaching signal and thus could modulate the circuits, resulting in motor learning.

The first direct evidence supporting this theory was obtained in 1982 when Ito and colleagues observed that combined input of parallel fibres and climbing fibres resulted in depression of Purkinje cell outputs (Ito et al., 1982). Further work has confirmed that long-term depression (LTD) in Purkinje cells and synaptic silencing mediates learning within the cerebellum (reviewed by Daniel et al. (1998)). It has also been identified that parallel fibre firing when not accompanied by climbing fibre firing leads to positive reinforcement of synapses by long-term potentiation, and that GABAergic interneurons can modulate and support the potentiation of circuits (reviewed by Dean et al. (2010)) . This work and the establishment of these models in several behavioural systems has led to the general acceptance that the cerebellum functions as an "adaptive filter" which leads to motor learning and coordination (reviewed by Dean et al. (2010)).

1.1.3 Connections within the central nervous system.

Further to the specific connections and circuits within the cerebellum, the efferent and afferent connections made with the rest of the central nervous system define the information which is process by the cerebellar cortical circuits. The cerebellar cortex is subdivided into several parasagittal domains which confer specific functional connections. The first evidence of this patterning within the cerebellar cortex was demonstrated by the late embryonic expression of a gene called Zebrin which was found to be expressed in Purkinje cells in a parasagittal banding pattern (Hawkes et al., 1985). Subsequent work demonstrated that several genes were expressed in similar patterns in the cerebellar cortex and mapping the input and output of specific longitudinal regions reveals topographic connections between

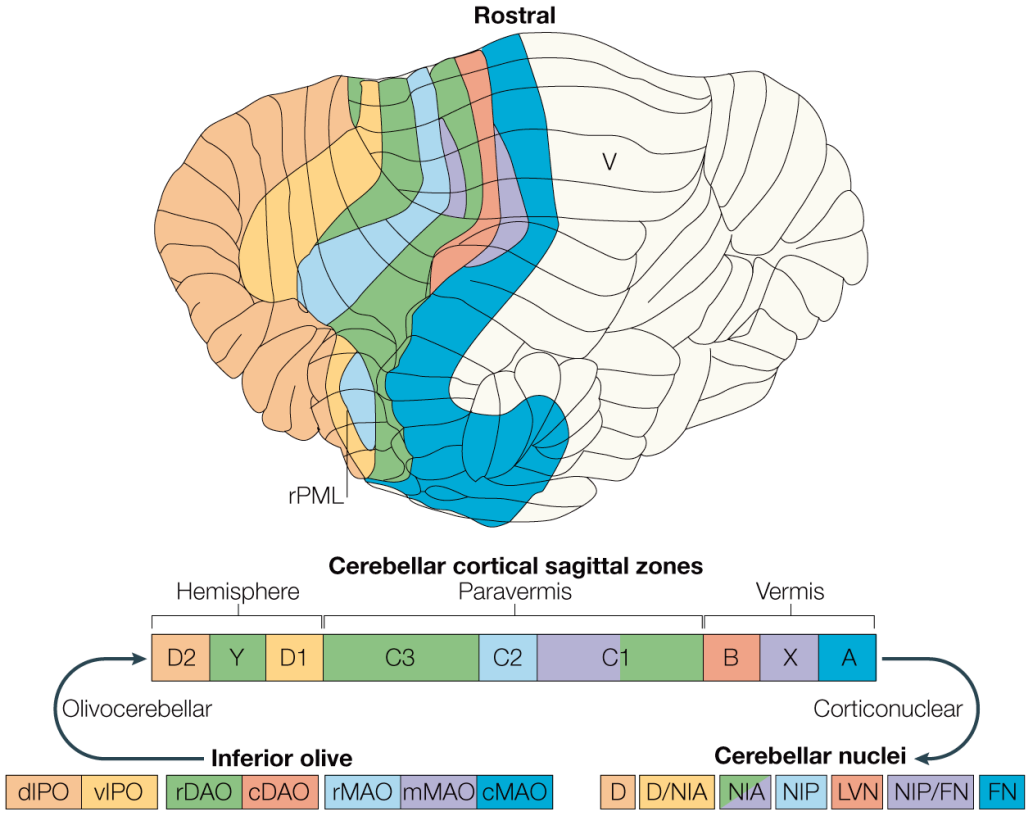

Figure 1-2 Topographical organisation of parasagittal domains of the cat cerebellum

Adapted from review by Apps and Garwicz (2005). Diagram indicating the spatial organisation of projections from the inferior olive to Purkinje cells in specific regions of the cerebellar cortex and the respective organisation of Purkinje cell outputs to the cerebellar nuclei.

the inferior olive, mediolateral domain of the cerebellar cortex and output to cerebellar nuclei (reviewed by Hawkes (1992) and Voogd and Glickstein (1998)). This topgraphic organisation is summarised in **Figure 1-2**. Furthermore, distinct peripheral sensory domains also showed regionally specific representation in the cerebellar cortex (reviewed by Apps and Garwicz (2005)).

Through the different mediolateral regional connections to the different cerebellar nuclei, different regions of the cerebellar cortex are broadly categorised into three zones based on their subsequent efferent connections within the brain: the corticocerebellum, spinocerebellum and vestibulocerebellum. The corticocerebellum defines lateral regions of the cerebellum which connect to the cerebral cortex, via the dentate nucleus and thalamus (**Figure 1-3** red pathway) (Nieuwenhuys, 1998). Both motor cortex and non-motor cortex (frontal, parietal and occipital cortex) are linked to the cerebellum through this pathway, broadly defining the region of the cerebellum involved in cognitive, non-motor function (reviewed by Strick et al. (2009)). Cerebellar-cortical connections form closed loops back to the cerebellar cortex via the pons (Kelly and Strick, 2003). The spinocerebellum encompasses the cerebellar vermis (medial region of the cerebellum) and intermediate parasagittal zone and forms descending tracts through the spinal cord via the interposed and fastigial cerebellar nuclei and subsequently the red nucleus, reticular nuclei and vestibular nuclei (**Figure 1-3** blue and green pathways) (Nieuwenhuys, 1998). Finally, the vestibulocerebellum, which, in mammals is defined by connections from a small posterior region of the cerebellum, the foccular lobe, projects directly to the vestibular nuclei and subsequently to descending tracts (F**igure 1-3** orange pathway) (Nieuwenhuys, 1998). Afferent connections of these pathways are also specifically from vestibular nuclei.

1.1.4 Evolutionary variation in structure and function of the cerebellum.

When considering the structure, function and development of the cerebellum, it is also helpful to consider the evolutionary variation in morphology, cell type and circuitry across species. The cerebellum is present as a distinct brain structure in all gnathostomes (jawed vertebrates), and for the most part displays remarkable conservation in the basic circuits within the cerebellar cortex (granule cells and Purkinje cells)(Nieuwenhuys, 1998). However, across species the gross morphology of the cerebellum is vastly variable, most distinctly through variation in the degree of foliation of the cerebellar cortex (reviewed by Butts et al. (2011)).

Foliation of the cerebellum varies within tetrapods from the flat amphibian cerebellum to the highly foliated cerebellum of mammals. The degree of foliation in the cerebellum relates to

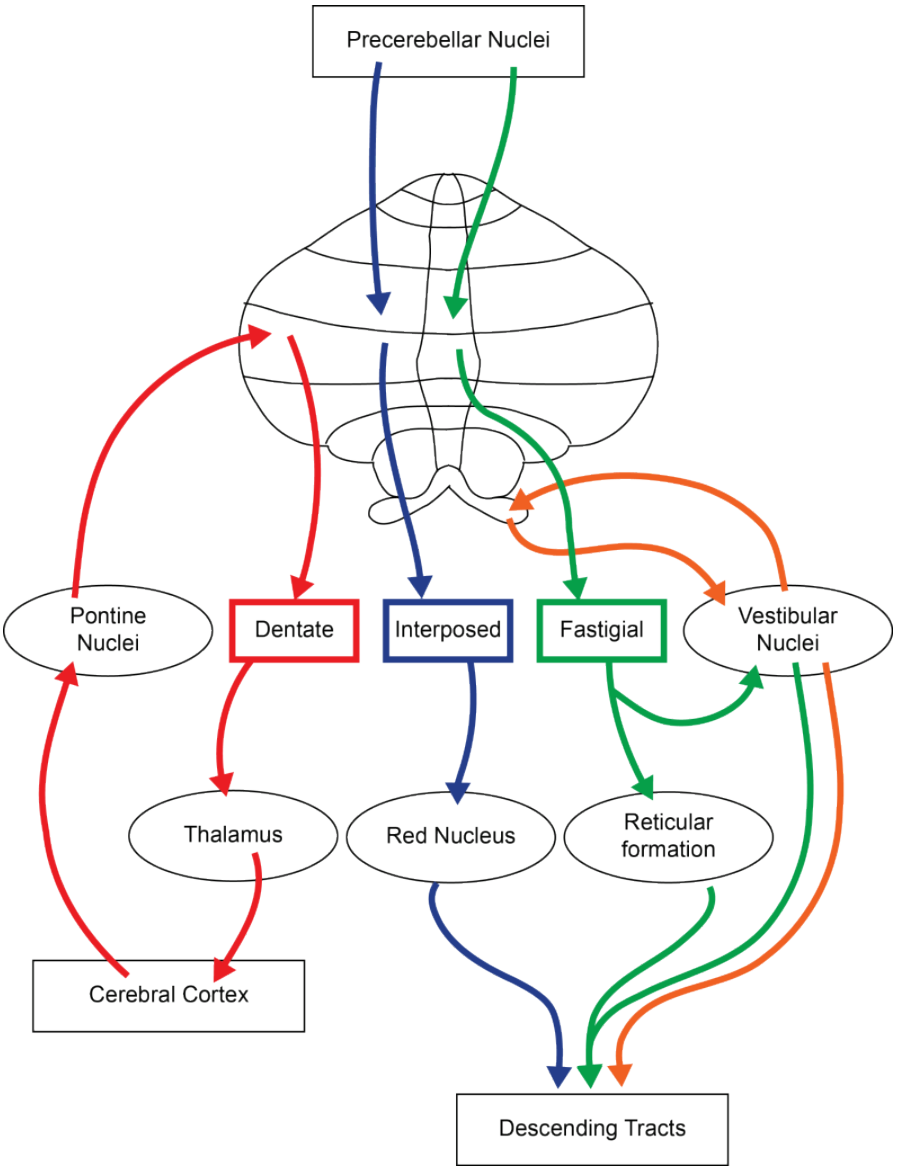

Figure 1-3 Cerebellar Pathways

Schematic representing the pathways throughout the central nervous system involving the cerebellum. Four distinct pathways are present: 1) the cerebellar-cortical pathway (red): projections from the lateral cerebellar cortex, through the dentate nucleus to the thalamus and on to the cerebral cortex. Projections then pass back to the cerebellar cortex via the pons. 2&3) cerebellar-spinal pathways (blue and green): spinal input, via the precerebellar nuclei to the medial regions of the cerebellar cortex and efferent pathways occur via the interposed and fastigial cerebellar nuclei and through the red nucleus, reticular formation or vestibular nuclei, to form descending tracts to the spinal cord. 4) vestibulo-cerebellar pathways (orange); projections from and to the vestibular nuclei to the posterior cerebellum which also form descending tracts through the spinal cord.

the absolute size of the cerebellum and is determined by the degree of transit amplification of granule cells during development. This transit amplification of the granule cell population is dependent on the amplitude of Sonic hedgehog signalling from Purkinje cells (Corrales et al., 2004; Corrales et al., 2006) and the expression of the transcription factor Atonal in the proliferating granule cells (Zhao et al., 2008; Flora et al., 2009). Molecular changes in the regulation of transit amplification and migration of granule cells through evolution account for the variations in cerebellar morphology (Butts et al., 2011).

As well as differences in the foliation of the cerebellum, some variation is also seen in the gross structures within the cerebellum associated with specific functional output. The cerebellar vermis (medial region of the cerebellar cortex) and floccular lobe are present only in mammalian lineages and teleost fish possessing a unique structure called the valvulus at the anterior end of the cerebellum which has been shown to produce cerebellar cells throughout adult life in these fish (Nieuwenhuys, 1998; Grandel et al., 2006; Kaslin et al., 2009).

Regardless of the numbers of cells, there is a remarkably conserved circuitry within the cerebellum comprising granule cell axons that are orthogonally aligned to Purkinje cell dendrites. By contrast, there is significant evolutionary variation in other cerebellar cell types, namely GABAergic interneurons and cerebellar nuclei.

The frog cerebellum only contains stellate interneurons in the molecular layer. Reptiles additionally have Golgi interneurons in the granule cell layer. Birds have stellate, Golgi and basket interneurons and mammals have stellate, basket, Golgi, Lugaro and candelabrum cells (Llinás, 1969).

The number of cerebellar nuclei and the connections which they make within the brain are variable across vertebrates. Teleost fish alone possess no cerebellar nuclei, whilst other ray-finned fish, chondrichthyans and amphibians possess a single cerebellar nucleus, reptiles and birds possess two, and mammals have up to five cerebellar nuclei (Nieuwenhuys, 1998). This diversification of cerebellar nuclei number is matched by distinct efferent connections within the brain. The addition of extra cerebellar nuclei in mammals coincides with the evolution of cerebellar-cortical connections in the brain, via the thalamus, which are not present, or substantially reduced, in other vertebrates. The function of these circuits in relation to cognitive functions of the cerebellum suggests profound consequences in the evolution of cerebellar function with regard to evolution of the cerebellar nuclei.

The various cerebellar interneurons and cerebellar nuclei develop from cell lineages common with Purkinje cells and granule cells respectively, and their production is controlled by a temporal sequence of cell specification (Hoshino et al., 2005; Machold and Fishell, 2005; Wang et al., 2005; Leto et al., 2006). Therefore the evolutionary changes in diversity within these cell types are likely controlled by evolutionary changes in temporal controls of cell fate specification.

1.2 Spatial patterning of the developing cerebellum.

The entire complement of cells of the cerebellum is derived from two distinct progenitor domains in the dorsal aspect of the anterior hindbrain. These two progenitor domains, the cerebellar rhombic lip and cerebellar ventricular zone, segregate the generation of glutamatergic and GABAergic cells of the cerebellum respectively and are established by their spatial coordinates within the embryonic brain. The territory within which the cerebellum forms is first established by patterning the anterior-posterior axis of the brain followed by dorsoventral patterning to specify the distinct progenitor domains. Superimposed onto this developmental regime is a temporal sequence of production of different cells types which migrate and undergo morphological rearrangements to integrate the glutamatergic and GABAergic cell types to create the functional circuits of the adult cerebellar cortex and cerebellar nuclei. **Figure 1-4** depicts an overview of the developmental processes which are described hereafter.

1.2.1 Allocation of cerebellar precursor territory.

In embryonic development, the neural tube is patterned into distinct regions along the anterior-posterior axis to generate the forebrain, diencephalon, midbrain/mesencephalon, hindbrain and spinal cord. The hindbrain region is further subdivided into a series of metameres known as rhombomeres (Lumsden and Keynes, 1989). Rhombomere 1 is the most anterior rhombomere abuting the midbrain. Various studies suggest dorsal rhombomere 1 is the origin of the cerebellum (Hallonet and Le Douarin, 1993; Millet et al., 1996; Wingate and Hatten, 1999).

Initial studies mapping the territorial boundaries of the cerebellum by chimeric quail-chick grafting used the physical constriction between the mesencephalon and anterior region of the hindbrain (the metencephalon) to map the origin of cerebellar cells. Using this technique, studies found that, excluding the granule cells which are entirely derived from the metencephalon, the anterior one third of the cerebellum was derived from tissue of the mesencephalon (Hallonet et al., 1990; Hallonet and Le Douarin, 1993; Le Douarin, 1993).

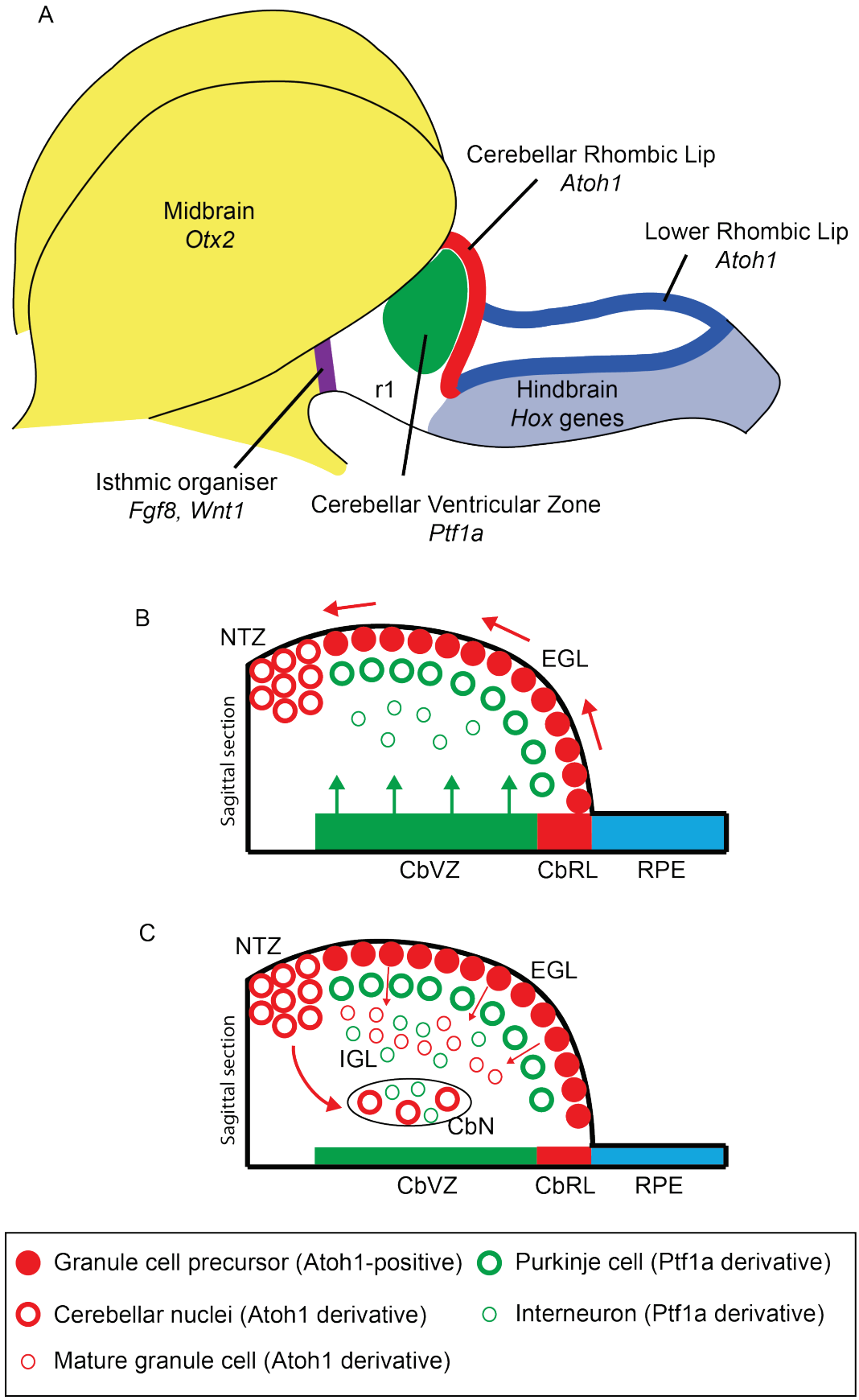

Figure 1-4 Cerebellar development.

Previous page:

Figure 1-4 Cerebellar development

A) shows diagram of midbrain and hindbrain indicating the distinct spatial regions of the *Otx2*$^{+ve}$ midbrain (yellow) and *Hox*-expressing lower hindbrain (rhombomeres 2-8; light blue) abutting rhombomere 1 (r1). The isthmic organiser (purple) is located between the midbrain and rhombomere1.The dorsal population of the cerebellar and lower rhombic lip which express *Atoh1* are shown in red and blue respectively and the position of the cerebellar ventricular zone, which expresses *Ptf1a,* is indicated in green. B&C) diagrams of section through the cerebellum in early (B) and late (C) cerebellar development. Progenitor domains of *Ptf1a*$^{+ve}$ cerebellar ventricular zone (CbVZ; green) and *Atoh1*$^{+ve}$ cerebellar rhombic lip (CbRL; red) abutting the roof plate epithelium (RPE; blue). In B post-mitotic GABAergic Purkinje cells (large green circles) and interneurons (small green circles) migrate radially from the CbVZ (green arrows). Cells from the CbRL migrate over the surface of the brain (red arrows) making post-mitotic cells in the nuclear transitory zone (NTZ; red circles) and proliferative cells in the external granule layer which maintain *Atoh1* expression (solid red circles). In C cells in the NTZ move internally to make the cerebellar nuclei (CbN) and cells in the EGL become post-mitotic, lose *Atoh1* expression and migrate radially to populate the internal granule layer (IGL).

However, later studies assessing the molecular boundary between the midbrain and the hindbrain showed that the posterior limit of *Otx2* expression, which defines the region of forebrain and midbrain (Acampora et al., 1995), lies rostral to the physical constriction between the mesencephalon and metencephalon (Millet et al., 1996). Throughchick-quail fate mapping of the molecular boundary between *Otx2*-positive midbrain tissue and *Otx2*-negative hindbrain tissue Millet and colleuges showed the cerebellum to be entirely derived from *Otx2*-negative tissue (Millet et al., 1996). Mice with reduced *Otx* gene dosage show an expansion of cerebellar territory at the expense of mesencephalic and diencephalic tissues (Acampora et al., 1997) and conversely, overexpression of *Otx2* in rhombomere 1 (both by electroporation in chick and in mice expressing *Otx2* in the Engrailed1 locus) causes a loss of cerebellar tissue and an expansion of midbrain tissue (Broccoli et al., 1999; Katahira et al., 2000), thus demonstrating the requirement for an *Otx2*-negative region to specify cerebellar fate. The expression of *Otx2* in the midbrain abuts the expression of *Gbx2* in the hindbrain. As with *Otx2* for the midbrain, *Gbx2* is necessary and sufficient for the hindbrain territory with a knockout of *Gbx2* resulting in deletion of the metencephalon (and a caudal expansion of *Otx2*) and ectopic expression of *Gbx2* in the midbrain causing a rostral expansion of the cerebellar territory at the expense $Otx2^{+ve}$ territory (Wassarman et al., 1997; Millet et al., 1999; Katahira et al., 2000).

Posteriorly, the boundary of the territory which gives rise to the cerebellum coincides with the anterior boundary of Hox gene expression. Hox genes are expressed throughout the hindbrain and spinal cord in a combinatorial code defining specific regions and, ultimately, the length of the axis (reviewed by Keynes and Krumlauf (1994)). The most anteriorly expressed Hox gene in the neural tube is *Hoxa2*, the anterior limit of which coincides with the rhombomere 1-2 boundary (Prince and Lumsden, 1994). *Hoxa2*-null mice show a caudal expansion of the lateral regions of the cerebellum and a loss of rhombomere 2 identity (Gavalas et al., 1997), whereas overexpression of *Hoxa2* in rhombomere 1 in chick results in a loss of cerebellar granule neurons (Eddison et al., 2004). Finally, fate mapping of granule cells with respect to the boundary of *Hoxa2* expression showed the precursors to be entirely derived from *Hoxa2*-negative region of rhombomere 1(Wingate and Hatten, 1999).

Together these studies demonstrate the identity of rhombomere 1 as *Hox*- and *Otx*-negative regions is vital for the formation of the cerebellum (**Figure 1-4A**).

Whilst the expression of *Otx2* in the midbrain and *Gbx2* in the hindbrain determines the identity of their respective compartments and are required to position the boundary (see above), these properties are also dependent on the function of the isthmic organiser which is

induced by interaction between midbrain and rhombomere 1 tissue (Irving and Mason, 1999). Key signalling molecules, WNT1(McMahon and Bradley, 1990), FGF8 (Crossley and Martin, 1995) and Engrailed 1 and 2 (EN1/2) (Gardner et al., 1988) are expressed at the isthmic boundary and collectively regulate growth (McMahon et al., 1992; Lee et al., 1997; Xu et al., 2000), patterning (Martinez and Alvarado-Mallart, 1990; Marin and Puelles, 1994; Crossley et al., 1996; Lee et al., 1997; Martinez et al., 1999; Sgaier et al., 2007) and positioning (Sato et al., 2001; Jaszai et al., 2003; Sato and Nakamura, 2004) of the adjacent territories. Isthmic induction/function is also mediated by the regional expression of *IRX* genes (Matsumoto et al., 2004), *Lmx1b* (Matsunaga et al., 2002; Guo et al., 2007) and *Pax2* (Ye et al., 2001; Hidalgo-Sanchez et al., 2005) and through delta-notch interactions (Tossell et al., 2011).

Within the midbrain, loss of isthmic signalling can lead to the loss or repatterning of the territory (McMahon and Bradley, 1990; Wurst et al., 1994; Meyers et al., 1998; Chi et al., 2003; Basson et al., 2008). For example, the caudal midbrain is particularly affected in Fgf8 mutants (Chi et al., 2003) and retinotectal map formation is globally altered in *Engrailed* overexpression studies (Itasaki and Nakamura, 1996; Logan et al., 1996). In contrast the midline cerebellum is particularly sensitive to the loss of isthmic gene expression (Chi et al., 2003; Basson et al., 2008), possibly due to the morphogenic rotation of cerebellar hemispheres during midline fusion whereby the initially anterior tissue forms medial cerebellar structures and more posterior tissue forms lateral cerebellar structures (Sgaier et al., 2005). Alternatively midline sensitivity to isthmic signalling could be due to interactions with roof plate signalling prior to midline fusion (Alexandre and Wassef, 2003; Louvi et al., 2003; Basson et al., 2008). Isthmic influences on anterior-posterior patterning of the cerebellum are harder to interpret than regional patterning in the midbrain due to the morphological changes in the tissue. For example mutations in *Engrailed* genes can lead to deficits of specific folia of the cerebellum (Millen et al., 1994; Cheng et al., 2010), but it is unclear how this relates to the initial patterning of the region through the influences of the isthmic organiser compared to later functional requirements for Engrailed gene expression.

Some studies have suggested that isthmic FGF8 is required as an instructive signal for the specification of the cerebellum due to its ability to induce cerebellar tissue ectopically in the midbrain (Irving and Mason, 1999; Liu et al., 1999; Martinez et al., 1999; Sato et al., 2001; Sato and Nakamura, 2004) and because of its absolute requirement for the development of the cerebellum in rhombomere 1 (Meyers et al., 1998; Reifers et al., 1998; Chi et al., 2003) and for the regeneration of ablated cerebellar tissue in zebrafish (Koster and Fraser, 2006). However, more recent studies suggest that FGF8 is required indirectly for the cerebellum

through its action to restrict or inhibit *Otx2* expression (Foucher et al., 2006; Sato and Joyner, 2009).

A single study in chick by Irving and Mason (2000), has also suggested that the isthmic organiser may also be involved in regulating the position of the rhombomere 1-2 boundary of *Hoxa2* expression. However these results could also be interpreted as changes in growth and overall size of rhombomere 1 following excessive or reduced FGF signalling, rather than a specific interaction with Hoxa2. Furthermore, *Fgf8* is not initiated until after a *Hoxa2*-free rhombomere 1 territory is established (Eddison et al., 2004).

1.2.2 Glutamatergic and GABAergic lineages are allocated along the dorsoventral axis.

Across the entire hindbrain the dorsal-most population of cells, abutting the expanded roofplate of the fourth ventricle, is the rhombic lip (reviewed by Wingate (2001)). The rhombic lip is characterised by the expression of the basic helix-loop-helix transcription factor *Atonal1* (*Atoh1*; called *Cath1* in chick and *Math1* in mouse) and throughout development produces cells which migrate tangentially over the pial surface of the hindbrain to populate distinct nuclei. The rhombic lip and all of the cells derived from it are critically dependent on the expression of *Atoh1* at the rhombic lip (Ben-Arie et al., 1997; Machold and Fishell, 2005; Wang et al., 2005; Rose et al., 2009a). The rhombic lip is subdivided into two regions, the cerebellar (upper) rhombic lip of rhombomere 1 and the lower rhombic lip of rhombomeres 2-8 (**Figure 1-4A**).

The cerebellar rhombic lip produces all of the glutamatergic cells of the cerebellum comprising cerebellar granule cells and projection neurons of the cerebellar nuclei. Glutamatergic unipolar brush cells have also been shown to originate from the rhombic lip, but follow a unique migratory path through the white matter of the cerebellum (Englund et al., 2006). Cerebellar nuclei projection neurons migrate from the rhombic lip over the pial surface of the cerebellum to form a transient pool of cells at the lateral edge of the cerebellar primordium, the nuclear transitory zone. Later in development, these neurons form distinct nuclei within the white matter of the cerebellum (**Figure 1-4 B,C**) (Altman and Bayer, 1985a, b; Machold and Fishell, 2005; Wang et al., 2005; Fink et al., 2006).

Cerebellar granule cell precursors migrate tangentially from the cerebellar rhombic lip and form a transient, proliferative layer covering the pial surface of the cerebellar primordium, the external granule layer (**Figure 1-4B**) (Alder et al., 1996; Wingate and Hatten, 1999). Unlike other rhombic lip derivatives, granule cell precursors in the external granule layer retain their expression of *Atoh1* which is critical for their transit amplification (Zhao et al.,

2008; Flora et al., 2009) in response to Sonic hedgehog signalling from underlying Purkinje cells (Dahmane and Ruiz i Altaba, 1999; Wallace, 1999; Wechsler-Reya and Scott, 1999; Lewis et al., 2004). This phase of secondary, transit amplification results in the production of a vast number of granule neurons that appears to be the principal driver of foliation of the cerebellar cortex (Corrales et al., 2006). The external granule layer has been shown to uniquely produce granule neurons (Alder et al., 1996; Klein et al., 2005; Espinosa and Luo, 2008) despite earlier reports of contributions to other lineages in the hindbrain (Lin et al., 2001). Cells in the external granule layer continue to proliferate into postnatal development and, upon exiting the cell cycle, cells differentiate and migrate radially through the underlying Purkinje cell layer to populate the internal granule layer of the adult cerebellum (**Figure 1-4C**) (Miale and Sidman, 1961; Cajal, 1990 (1894))

In contrast to the glutamatergic cells born from the cerebellar rhombic lip, all of the GABAergic cells types of the cerebellum (Purkinje cells, small neurons of the cerebellar nuclei and basket, stellate and Golgi interneurons) are born from the cerebellar ventricular zone, just ventral to the rhombic lip and migrate radially to populate the cerebellum (**Figure 1-4 A,B**). The cerebellar ventricular zone is characterised by and dependent on the expression of the basic helix-loop-helix, transcription factor *Ptf1a*. The *Ptf1a* mutant, *cerebellarless*, lacks the entire the entire cerebellum through failure to specify GABAergic neurons and the subsequent gradual loss of granule cells and cells of pontine and olivary precerebellar nuclei (Hoshino et al., 2005). *Ascl1 (*Achaete-Scute homolog 1 also called *Cash1/Mash1* in chick/mouse) also defines the *Ptf1a* population of the cerebellar ventricular zone, distinctly from the *Atoh1*$^{+ve}$ rhombic lip (Kim et al., 2008).

The function of *Atoh1* and *Ptf1a* to specify glutamateric and GABAergic cells types respectively is conserved in various populations in the brain including the dorsal spinal cord and cochlea nucleus (Helms and Johnson, 1998; Bermingham et al., 2001; Glasgow et al., 2005; Miesegaes et al., 2009). However these transcription factors are not always expressed in precursors of glutamatergic/GABAergic neurons elsewhere in the brain. In the cerebellum, loss of *Ptf1a* allows cells of the cerebellar ventricular zone to enter the external granule layer and express *Atoh1* (Pascual et al., 2007). However, following the loss of *Atoh1*, rhombic lip cells enter the roof plate of the fourth ventricle (*Gdf7*-expressing) lineage (Rose et al., 2009a).

Dorsalising signals are critically important for the precursor populations which produce the cerebellum. Roof plate TGFβ signals are required for the specification of dorsal interneurons from an *Atoh1*$^{+ve}$ progenitor domain in the spinal cord (Lee et al., 1998; Lee et al., 2000b;

Millonig et al., 2000; Helms and Johnson, 2003). Genetic ablation of the roof plate of the fourth ventricle results in a complete failure to specify the *Atoh1*$^{+ve}$ domain of the rhombic lip and all of its subsequently derivatives (Chizhikov et al., 2006). TGFβ signalling has also been shown to be sufficient to induce *Atoh1* expression in vitro culture systems and TGFβ-treated progenitor cells were capable of producing cerebellar granule neurons when transplanted into the external granule layer (Alder et al., 1999). More recent studies have demonstrated that TGFβ-dependent rhombic lip expression of *Atoh1* and neurogenesis at the rhombic lip is mediated through direct contact with the roofplate epithelium via Notch signalling (Machold et al., 2007; Broom, 2011). As well as its requirement in roofplate formation (Millonig et al., 2000; Chizhikov et al., 2006), *Lmx1a* has been shown to be expressed in granule cells of posterior lobes and is required for the correct specification and migration of these cells and in maintaining the rhombic lip progenitor pool (Chizhikov et al., 2010).

Despite the requirement of roofplate signalling for the rhombic lip precursor pool, expression of *Ptf1a* in the cerebellar ventricular zone is not lost following ablation of the roofplate (Chizhikov et al., 2006). It is not known how the spatial domain of *Ptf1a*-expression is determined.

Other dorsal patterns in the hindbrain include the dorsal expression of *Wnt1* and *Pax6*. *Wnt1* is expressed in a domain overlapping the *Atoh1*$^{+ve}$ rhombic lip extending into the *Lmx1a*$^{+ve}$ domain of the roofplate epithelium and marks all of the same cells as the *Atoh1* lineage of the rhombic lip (Volkmann et al., 2010; Hagan and Zervas, 2012). It is not clear, however, how *Wnt1* functionally regulates cerebellar development as *Wnt1*-null mice show a severe loss of cerebellar territory, due to a requirement for early, broad regional expression of *Wnt1* in the maintenance of the isthmus (McMahon and Bradley, 1990; McMahon et al., 1992). In the rest of the hindbrain, *Wnt1* is expressed in the rhombic lip but expression is seen in a broader dorsoventral domain than *Atoh1* expression and encompasses a precursor domain expressing *Neurogenin1* (*Ngn1*). The *Wnt1*$^{+ve}$ region of lower hindbrain is responsible for the production all of the precerebellar nuclei but the inferior olive is specified from the *Wnt1*$^{+ve}$ domain which is *Math1*-negative and expresses *Ngn1* (Rodriguez and Dymecki, 2000; Landsberg et al., 2005). In the hindbrain, *Pax6* has been demonstrated to determine the balance of the *Atoh1*/*Ngn1* precursors pools, possibly though disruption of roof plate signalling (Landsberg et al., 2005). However, in the cerebellum loss of *Pax6* affects rhombic lip derivatives (not the rhombic lip itself). In the *Pax6*-small eye mutant, development of granule cells is disturbed affecting the migration, proliferation and axon organisation and

having secondary effects on the development of Purkinje cells (Engelkamp et al., 1999; Yamasaki et al., 2001; Swanson et al., 2005; Swanson and Goldowitz, 2011).

1.3 Temporal patterning and cell fate diversity at the rhombic lip.

The specific progenitor domains which broadly determine the glutamatergic or GABAergic cells of the cerebellum are specified through a series of spatial patterning events in both the anterior-posterior and dorsoventral axes. However the specification of individual cell types derived from both the cerebellar ventricular zone and the cerebellar rhombic lip are determined by a temporal sequence of cell production.

1.3.1 Temporal fate-maps of the cerebellar rhombic lip.

Although associations between the external granule layer and the rhombic lip had been made previously through molecular analyses (Akazawa et al., 1995; Ben-Arie et al., 1997) and histological observations (Miale and Sidman, 1961; Altman and Bayer, 1978; Ryder and Cepko, 1994), the first fate map of cerebellar rhombic lip derivatives was performed using microsurgical quail to chick chimeric grafting by Wingate and Hatten (1999). Chimeric grafting performed at E2 and analysed at E6 showed specific transplantation of the cerebellar rhombic lip tissue and cells which were derived from the rhombic lip were found in the external granule layer, but also unexpectedly in a population of cells in ventral/rostral regions of rhombomere 1. This was the first time that non-granule cell populations were identified as originating from the rhombic lip. Wingate and Hatten also used DiI labelling and time-lapse microscopy to observe the tangential migration of cells from the rhombic lip, but not from more ventral progenitor regions.

Following this, another study by Gilthorpe et al. (2002) identified that the two populations of cells derived from the cerebellar rhombic lip had different temporal origins. DiI labelling of the rhombic lip at E4 and E6 identified the early migration of cerebellar rhombic lip derivatives into ventral rhombomere 1 and late migration of cells to populate the external granule layer.

In 2005, two independent studies used genetically inducible fate maps of the *Atoh1* lineage to define the temporal populations of cells born from the rhombic lip (Machold and Fishell, 2005; Wang et al., 2005). Wang and colleagues analysed the production and migration of cells from the rhombic lip in a series embryonic stages in mice with a *LacZ* gene knocked into the *Math1* locus ($Math1^{LacZ/+}$) and compared these with a Math1- null ($Math1^{LacZ/null}$). They identified cells throughout the entire hindbrain originating from the rhombic lip and found that the cerebellar rhombic lip produced not only the population of cells in ventral

rhombomere 1 (previously identified in chick) and granule cells, but also an intermediate population which migrated to the nuclear transitory zone and subsequently formed the cells of the cerebellar nuclei. All of the populations identified were absent in *Math1*$^{LacZ/null}$ mice showing an absolute requirement for *Math1* in specifying these cells. This study was, however, limited in it accuracy of identifying the temporal origin of cell types as conclusions were made by studying a series of different stages of the entire rhombic lip lineage and individual temporal cohorts were not labelled. Furthermore, the origin of cells from the cerebellar or hindbrain rhombic lip was not confirmed, and again was inferred from static images of a dynamic migratory system.

At the same time Machold and colleagues, used transgenic mice carrying a Tamoxifen-inducible Cre-recombinase under the control of the *Math1* enhancer (previously characterised by Helms et al. (2000)) crossed to the R26R-stop-lacZ reporter line such that after transient activation of the CreER^{T2} recombinase activity by Tamoxifen administration, the R26R stop cassette, flanked by loxP sites was excised resulting in permanent β-galactosidase expression, allowing for analysis at embryonic stages or at P21 to assess initial and final identity of specific temporal populations. Tamoxifen-induced labelling on different days between E10.5 and E16.5 compared to *Math1*^{LacZ} knock-in mice allowed for identification of the temporal window in which each population of cells was born from the rhombic lip. Here they identified nuclei in ventral/rostral rhombomere 1 as the first populations born from the rhombic lip between E10.5-12.5. Also labelled in this temporal window, though more heavily in later E11.5-12.5 window, were cells of the cerebellar nuclei. Finally, in tamoxifen injections between E12.5 and E16.5 granule cells were exclusively labelled, with earlier and later temporal cohorts only contributing to anterior and posterior lobes of the cerebellum respectively. Once the specific populations has been identified, they were compared to an En1-Cre::R26R-stop-LacZ transgenic mouse to verify the origin of cells as exclusively from rhombomere 1 *Math1* populations and not from the lower rhombic lip. Again, this study showed the absence of all rhombic-lip derived populations in *Math1*$^{LacZ/null}$ mice. Whilst this study complemented the study by Wang et al., providing evidence of temporal birth-dating and rhombomere 1 origin of cells, the accuracy of timing was limited to broad temporal windows of unspecified length based on previous studies reporting translocation of the CreER fusion protein to cell nuclei within 6 hours of tamoxifen administration and labelling over a subsequent 24 hour period (Danielian et al., 1998; Zervas et al., 2004). This meant that a temporal distinction between different ventral nuclei and cerebellar nuclei could not be distinguished. Furthermore, the efficiency of cell labelling by this method appeared markedly reduced compared to the *Math1-LacZ* knock-in.

This issue was later circumvented using the more sensitive Cre-PR fusion protein (Wunderlich et al., 2001) in the *Math1* locus leading to similar conclusions but labelling previously unidentified nuclei within ventral rhombomere 1 (Rose et al., 2009a).

These three studies (Machold and Fishell, 2005; Wang et al., 2005; Rose et al., 2009a) identify the first-born ventral/rostral population of cells in rhombomere 1 derived from the cerebellar rhombic lip as contributing to the following nuclei: Parabigeminal nucleus, pedunculopontine tegmental nucleus, pontomesencephalic tegmental nucleus (Wang et al. only), microcellular tegmental nucleus, laterodorsal tegmental nucleus, dorsal nucleus of the lateral lemniscus, medial paralemniscal nucleus*, lateral parabrachial nucleus, medial parabrachial nucleus*, pontine reticular-oral nucleus* and Kölliker-Fuse nucleus* (* only identified by Rose et al.). All of these nuclei have functions associated with arousal (parabigeminal, pontine, tegmental and medial parabrachial), hearing (lemniscal) and interoception/breathing (lateral parabrachial and Kölliker-Fuse). Although these populations derived from the cerebellar rhombic lip do not form cerebellar circuits they do contribute to a large network of neurons throughout the hindbrain and spinal cord derived from *Math1*$^{+ve}$ progenitor populations involved in unconscious behaviours relating to proprioception, interoception and arousal (Rose et al., 2009a).

A recent study (Hagan and Zervas, 2012) has also temporally mapped the derivatives of the *Wnt1*$^{+ve}$ population in dorsal rhombomere 1. *Wnt1* is expressed in a broader domain than *Math1*, but lead to similar conclusions regarding cell production at the rhombic lip. This study demonstrated a temporal sequence of cell production within the cerebellar nuclei with the most lateral, dentate nucleus being labelled earlier than the more medial fastigial nucleus. In addition, this study highlighted a discrepancy in timing between labelling from *Math1* and *Wnt1* progenitor pools suggesting that progenitor cells express *Wnt1* earlier than they express *Math1*. Mapping of the *Wnt1*$^{+ve}$ progenitor population has also been performed in zebrafish embryos showing the presence of early-born cerebellar rhombic lip cells in ventral rhombomere 1, similarly to mice and chick (Volkmann et al., 2010).

The cerebellar ventricular zone also shows temporal progression of cell specification (Leto et al., 2006; Kim et al., 2008; Leto et al., 2011), but there is also evidence for molecular heterogeneity within the *Ptf1a*-progenitor pool which can at least partially account for the production of different cell types from the cerebellar ventricular zone (Chizhikov et al., 2006; Morales and Hatten, 2006; Zordan et al., 2008; Mizuhara et al., 2010).

These detailed studies have delineated the temporal component of cell specification in the cerebellum but, thus far, it is unknown how this temporal progression occurs. Studies in

other regions of the central nervous system have establish several models of temporal cell fate specification which may help provide a framework for understanding temporal fate in the cerebellum

1.3.2 Temporal fate allocation models in other developmental systems.

As a general principal, the allocation of temporal identity can occur by the integration of spatial identity with intrinsic or extrinsic factors which change over time (**Figure 1-5**; reviewed by Pearson and Doe (2004)). This model can be used to explain the acquisition of temporal identity in several developmental systems including fate allocation in Drosophila neuroblasts, retina and cerebral cortex. In these models is it important to distinguish between factors that are required for the differentiation of specific cell types in a lineage and the factors which control a temporal transition between cell types.

In the ventral nerve cord of the Drosophila embryo, 30 neuroblasts (for each side of the embryo) are spatially divided into rows and columns. Each neuroblast produces a distinct lineage of a specific number of cells in an invariant temporal sequence which is repeated in serial segments throughout the embryo (Higashijima et al., 1996; Novotny et al., 2002; Pearson and Doe, 2003; Pearson and Doe, 2004). Interactions with genes determining regional identity along the axis such as *Hox* genes and *Pbx/Meis* can result in region specific variation in the neuroblast lineages of different segments (Karlsson et al., 2010). The asynchronous production of cells within each lineage and the apparently normal sequence of cell production in an isolated culture system (Broadus and Doe, 1997) lead to the assumption that intrinsic, rather than extrinsic factors must control the sequence of cell types produced.

In 2001, Isshiki and colleagues identified a specific temporal sequence of transcription factors (*Hunchback* → *Krüppel* → *Pdm* → *Castor*) that are expressed in each neuroblast lineage in the same order (Isshiki et al., 2001). These transcription factors confer broad temporal identity and not specific fate identities as subsequent cell division can produce different cell types from a single progenitor expressing one of these genes. Furthermore this study (Isshiki et al., 2001) showed that overexpression or knockdown of these genes could alter the temporal identity of cells produced, for example, overexpression of Hunchback, the gene expressed earliest, converted all of the subsequent lineage into early-born cell types. Cells also demonstrate a gradual restriction in competence to respond to early temporal identity genes (Pearson and Doe, 2003) and the transition between different temporal genes is mediated by cell division (Isshiki et al., 2001; Grosskortenhaus et al., 2005) suggesting a possible model in which asymmetric divisions can partition factors into specific daughter cells. Within broad temporal windows of one of these five transcription factors, further

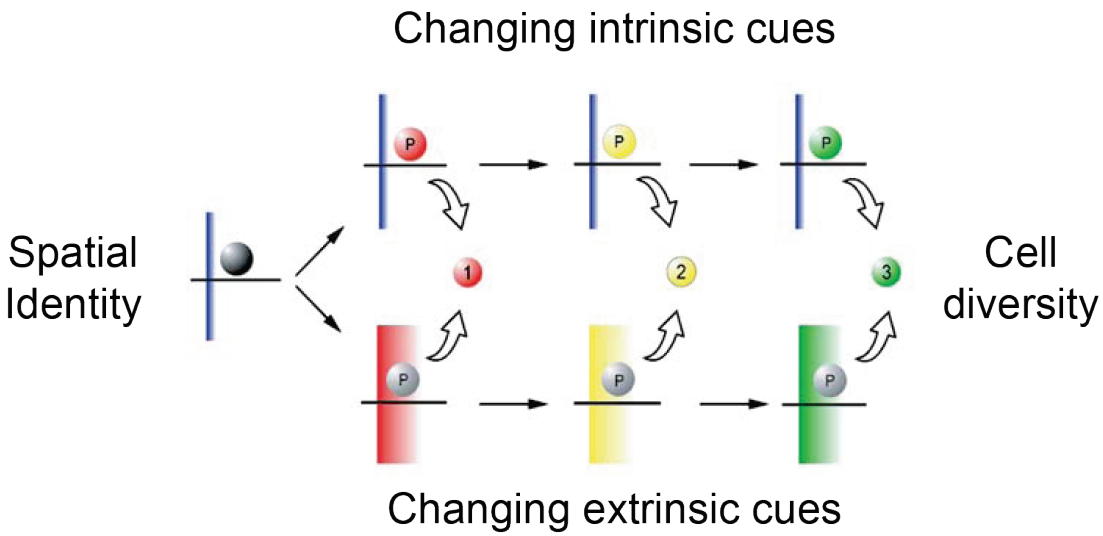

Figure 1-5 Models of temporal fate specification by intrinsic and extrinsic factors

Schematic depicting models of temporal cell fate specification. Following allocation of a spatial identity, progenitor cells can be subject to temporally changing intrinsic or extrinsic cues to generate distinct cell fates in a temporal sequence.

subdivision of lineages can occur by opposing feed-forward signalling systems downstream of that transcription factor (Baumgardt et al., 2009) elegantly demonstrating a molecular mechanism for different temporal programs of development being controlled by a single transcription factor.

Whilst this model provides insight into intrinsic molecular mechanisms in temporal fate specification, the ways in which it relates directly to rhombic lip lineage specification is limited. It is not clear whether the rhombic lip comprises multipotent progenitors or whether different progenitors contribute to different populations of rhombic lip derivatives. Temporal labelling of the *Math1*$^{+ve}$ progenitor pool has suggested that single progenitors do not remain at the rhombic lip (Machold and Fishell, 2005) but there could be a population of *Math1*-negative progenitors which transiently activate *Math1* expression before exiting the rhombic lip. Furthermore the rhombic lip represents a whole population of progenitor cells which must operate in a coordinated manner whereas Drosophila neuroblasts lineages progress in a more isolated fashion.

Another developmental system which shows temporal changes in cell specification is the vertebrate retina. The retina consists of 7 distinct cell types which are generated in a stereotyped but broadly overlapping sequence which can be subdivided into two major, overlapping stages of early ganglion, horizontal, cone and amacrine cell production and late biopolar, rod and Müller glial cell production (Cepko et al., 1996; Chang and Harris, 1998). All of these cells are derived from a single pool of multipotent progenitors which are vastly heterogeneous in the cells which they produce (Turner and Cepko, 1987; Holt et al., 1988; Wetts and Fraser, 1988). The general model of how this is achieved relies on changing intrinsic factors regulating competence of progenitors to produce specific cell types under the influence of extrinsic signals (reviewed by Livesey and Cepko (2001)). An intrinsic early or late identity is demonstrated in heterochonic transplantation and co-culture studies (Belliveau and Cepko, 1999; Belliveau et al., 2000; Rapaport et al., 2001) but these studies demonstrate that the normal cohort of cells cannot be generated in an ectopic temporal environment suggesting an additional requirement for extrinsic signals. Specific extrinsic signalling mechanisms have also been described, such as feedback mechanisms which supresses the production of specific early born cells by the presence of those cell types in the older retina (Waid and McLoon, 1995; Waid and McLoon, 1998; Belliveau and Cepko, 1999; Zhang and Yang, 2001). Retinal progenitors display a requirement for factors which maintain their multipotency, for example *Pax6* is expressed in all early, but not late, progenitors and when lost, only one specific cell type can be made (Marquardt et al., 2001). More recent work has identified a role for the gene *Ikaros*, a mammalian orthologue of the

Drosphila gene, *Hunchback*, which is involved in specifying early lineages in Drosphila neuroblasts. *Ikaros* is expressed exclusively in early retinal progenitors and misexpression in late progenitors can drive the production of early born cell types (Elliott et al., 2008). This suggests a general function of Hunchback/Ikaros in generating early fate identity in two distinct systems.

Compared to retinal development the cerebellar rhombic lip temporal lineage appears to be organised into more discrete temporal windows, though current studies cannot distinguish the degree of overlap between different derivatives. Another stark difference is that rhombic lip cells undergo long distances of migration and therefore local feedback mechanisms are unlikely to control the subsequent cell types produced. Furthermore, compared to the broad field across which retinal cell specification occurs, the rhombic lip is a relatively discrete progenitor population that could be more amenable to global signalling cues. However, the retinal model highlights the potential integration mechanisms of both intrinsic and extrinsic cues in the formation of a temporal lineage.

The developing cerebral cortex also demonstrates a temporal dimension in cell specification. Glutamatergic cells of the cortex are derived from multipotent progenitors in the ventricular zone (Reid et al., 1997) which sequentially produce cells of different cortical layers, populating first the most superficial layer 1 and then subsequent layers 2-6 are born in an "inside-out" fashion with deep layers 5 and 6 being populated first and more superficial layers 2/3 being populated last (Berry et al., 1964; Berry and Rogers, 1965; Luskin and Shatz, 1985; McConnell, 1988). Cells in different layers of the cortex form different projections. Heterochronic transplants of early progenitors into late cortex causes progenitors which are still mitotic to switch their temporal identity to making late cells (McConnell, 1988; McConnell and Kaznowski, 1991) demonstrating that temporal identity is not instrinsically committed prior to the final cell division. However older progenitors lose their ability to produce early layer neurons demonstrating progenitors become intrinsically limited in the cells which they can make (Frantz and McConnell, 1996). Isolated progenitors in culture can produce early, followed by late cells types (Qian et al., 2000) and the transcription factor Foxg1 is required to supress the production of early-born layer 1 neurons for subsequent layers to form (Hanashima et al., 2004). Several genes have been shown to be expressed in specific layers for the cortex to regulate cell fate and targeting of specific projections but these genes are not sufficient to explain temporal transitions between the formation of different cortical layers.

This model of cell specification provides a much closer approximation of cerebellar rhombic lip temporal transitions than either of the previous two models. Cells of the cortex migrate away from their progenitor domain as they are specified and migration is systematically varied between different temporal populations, much like the rhombic lip (Gilthorpe et al., 2002). A further comparison between cortical and cerebellar rhombic lip lineages is that both, within their late born cohorts, develop cells which undergo transit amplification before terminal differentiation (Noctor et al., 2004). Given the similar cohorts of genes expressed within these two glutamatergic populations (reviewed by (Hevner et al., 2006)) it is possible that common mechanisms unite these processes. However, the molecular mechanisms which regulate fate transitions in cortical progenitors are largely unknown.

Very few studies have focussed on temporal controls of cell fate allocation in rhombic lip populations. It has been observed that throughout the whole hindbrain rhombic lip population there is a general switch from the early production of cells expressing *Lhx2*/9 to the production of cells expression *Barhl1* (Rose et al., 2009a). However this does not account for all of the cells of the rhombic lineage and it is not known how this switch occurs, though both *Lhx9* and *Barhl1* expression are downstream of *Atoh1* (Rose et al., 2009a). This suggests a possible role for intrinsically controlled fate specification downstream of *Atoh1*, but does not account for all of the diversity seen within these two broad temporal populations.

A single study in chick embryos using a heterochronic grafting strategy has suggested that cerebellar rhombic lip cells are intrinsically committed to a specific temporal identity but an extrinsic signal is required to mediate the transition between different cell fates (Wilson and Wingate, 2006). However, these experiments also used a heterotopic transplantation and therefore it is not known how different spatial cues may alter the properties of these populations. A subsequent gene-expression study highlighted the specific expression of genes regulating retinoic acid signalling in and around the rhombic lip which could possibly implicate retinoic acid in regulating development of the rhombic lip (Wilson et al., 2007).

Within the various models of temporal fate specification outlined above little attention has been paid to the possible roles that ageing organisers with changing temporal signals may act to control temporal as well as spatial aspects of cell fate specification. Whereas these other systems may not be directly under the influence of local organisers, the rhombic lip/cerebellum is directly adjacent to (and dependent upon) two well characterised organisers, the roof plate of the fourth ventricle and the isthmic organiser.

1.4 Re-examining cell specification at the rhombic lip.

In this thesis I examine the temporal and spatial roles of cell fate specification in the rhombic lip of chicken embryos. The chicken provides an excellent model for studying temporal mechanism during development due to the ease with which focal manipulations can be made at any time point during early development. Since fate mapping of the cerebellar rhombic lip derivatives in chick (Wingate and Hatten, 1999), it has been demonstrated that cells of cerebellar nuclei also originate from this same progenitors pool (Machold and Fishell, 2005; Wang et al., 2005). I therefore begin my work by fully characterising the temporal origin of the cerebellar nuclei in chick using focal cell labelling and generate a detailed framework of temporal and spatial cell specification from the cerebellar rhombic lip. Following a detailed characterisation of the temporal progression of molecular markers of individual temporal cohorts, I use this framework as a basis to examine the molecular mechanisms which regulate cell diversity in cerebellar rhombic lip derivatives, focussing particularly on the potential changing signalling sources of the isthmus and roofplate of the fourth ventricle. I also use this detailed map of cerebellar fate determination for comparative analysis of the evolution of cerebellar anatomy and function.

Chapter 2 The temporal origin of cerebellar rhombic lip derivatives in chick

2.1 Background

This chapter aims to establish a detailed temporal characterisation of the different cell types born from the cerebellar rhombic lip in chick and to compare and contrast this to the mammalian model system. This will provide a detailed framework for subsequent chapters in which I will investigate the mechanism by which such diversity is generated.

Advances in the understanding of the cerebellar rhombic lip and its contribution towards the cells of the hindbrain have largely come from three sources: Firstly, chimeric, quail to chick grafting experiments, which showed the external granule layer and a ventral population of cells to be derived from the rhombic lip of rhombomere1 (Wingate and Hatten, 1999); secondly, DiI labelling of the chick cerebellar rhombic lip at different time points demonstrated temporal segregation of the different rhombic lip populations (Gilthorpe et al., 2002) and finally genetic fate mapping in mouse mapped all of the cells derived from the *Atoh1*$^{+ve}$ rhombic lip (Machold and Fishell, 2005; Wang et al., 2005).

Genetic mapping of the *Atoh1*$^{+ve}$ cerebellar rhombic lip lineage characterised the identity of the first born populations of cells which migrate into ventral rhombomere 1 as contributing to various nuclei including: parabigeminal, pontine, tegmental, parabrachial and lemniscal nuclei (Machold and Fishell, 2005; Wang et al., 2005). These nuclei do not form part of the cerebellum and are instead part of a wider network of nuclei derived from *Atoh1*$^{+ve}$ populations throughout the hindbrain and spinal cord which are involved in unconscious behaviours (Rose et al., 2009a). Hereafter, I shall refer to these nuclei as ventral or extra-cerebellar cells/nuclei.

Of the techniques used to map the rhombic lip lineage, only *Atoh1*$^{+ve}$ genetic studies in mouse identified that cells of the cerebellar nuclei are born from the cerebellar rhombic lip (Machold and Fishell, 2005; Wang et al., 2005). Cerebellar nuclei cells initially migrate tangentially and populate the nuclear transitory zone, a domain at the lateral edge of the cerebellar primordium, dorsal to the extra-cerebellar populations in ventral rhombomere 1, and subsequently move internally to populate the distinct cerebellar nuclei (Altman and Bayer, 1985b, a; Fink et al., 2006). Subsequent genetic mapping of the *Atoh1*$^{+ve}$ and *Wnt1*$^{+ve}$ rhombic lip lineage demonstrated that all three of the mouse cerebellar nuclei are born in a temporal sequence with the most lateral, dentate nucleus born first followed by the more medial interposed and fastigial nuclei (Rose et al., 2009a; Hagan and Zervas, 2012).

The discovery that cells of the cerebellar nuclei are derived from the rhombic lip marked a distinct change from the previous model in which all of the cells of the cerebellar nuclei were thought to be derived exclusively from the cerebellar ventricular zone populating the nuclear transitory zone by radial migration (Altman and Bayer, 1985b, a). The cerebellar nuclei comprise a mixed population of both glutamergic projection neurons from the cerebellar rhombic lip (Fink et al., 2006) and GABAergic interneurons. Radially migrating, GABAergic neurons of the cerebellum are derived from the *Ptf1a*$^{+ve}$ cerebellar ventricular zone (Hoshino et al., 2005) and thus the cerebellar nuclei are formed by the integration of cells via two distinct migratory pathways (See introduction **Figure 1-4**). There is also evidence for a third source of cerebellar nuclei cells from a progenitor population found ventral to the *Ptf1a*$^{+ve}$ cerebellar ventricular zone. This domain expresses *Lmx1a* and, by gene expression, appears to contribute cells to the region adjacent to the nuclear transitory zone and subsequently a region at the base of the cerebellum (Chizhikov et al., 2006). However, a later study mapping derivatives of *Lmx1a*$^{+ve}$ progenitor populations did not identify any *Lmx1a*-derived cells in the cerebellar nuclei, though these populations were not the direct focus of this study (Chizhikov et al., 2010). Therefore it is currently unclear if an *Lmx1a*$^{+ve}$ progenitor domain also contributes cells to the cerebellar nuclei along with cells from the cerebellar rhombic lip and cerebellar ventricular zone.

In chick, the origin of the cerebellar nuclei has not previously been established. Surgical fate mapping experiments did not include detailed analysis of axon projections. An observation (Gilthorpe et al., 2002) that "granule cell precursors" appear to accumulate at the lateral edge of the external granule layer could point to a previously uncharacterised population of cells which make the nuclear transitory zone in chick.

Previous temporal analysis of cerebellar rhombic lip derivatives in chick (Gilthorpe et al., 2002; Wilson and Wingate, 2006) focus on the time points of a transition between production of ventral cells at embryonic day (E) 4 and granule cell precursors at E6. If chick and mouse rhombic lip produce equivalent populations then the cerebellar nuclei would be expected to be produced between these two time points.

In this chapter I therefore outline a detailed temporal fate map of the cerebellar rhombic lip using acute cell labelling. I focus on all the stages between E3/Hamburger and Hamilton stage (St)16, when *Atoh1* expression is first observed at the rhombic lip (Broom, 2011) and E6/St29 when granule cell precursors are born from the rhombic lip (Gilthorpe et al., 2002). The identity of the cerebellar nuclei is assessed by axonal projections on criteria derived from anatomy of the adult pigeon (Arends and Zeigler, 1991a). Summarised in **Figure 2-1,**

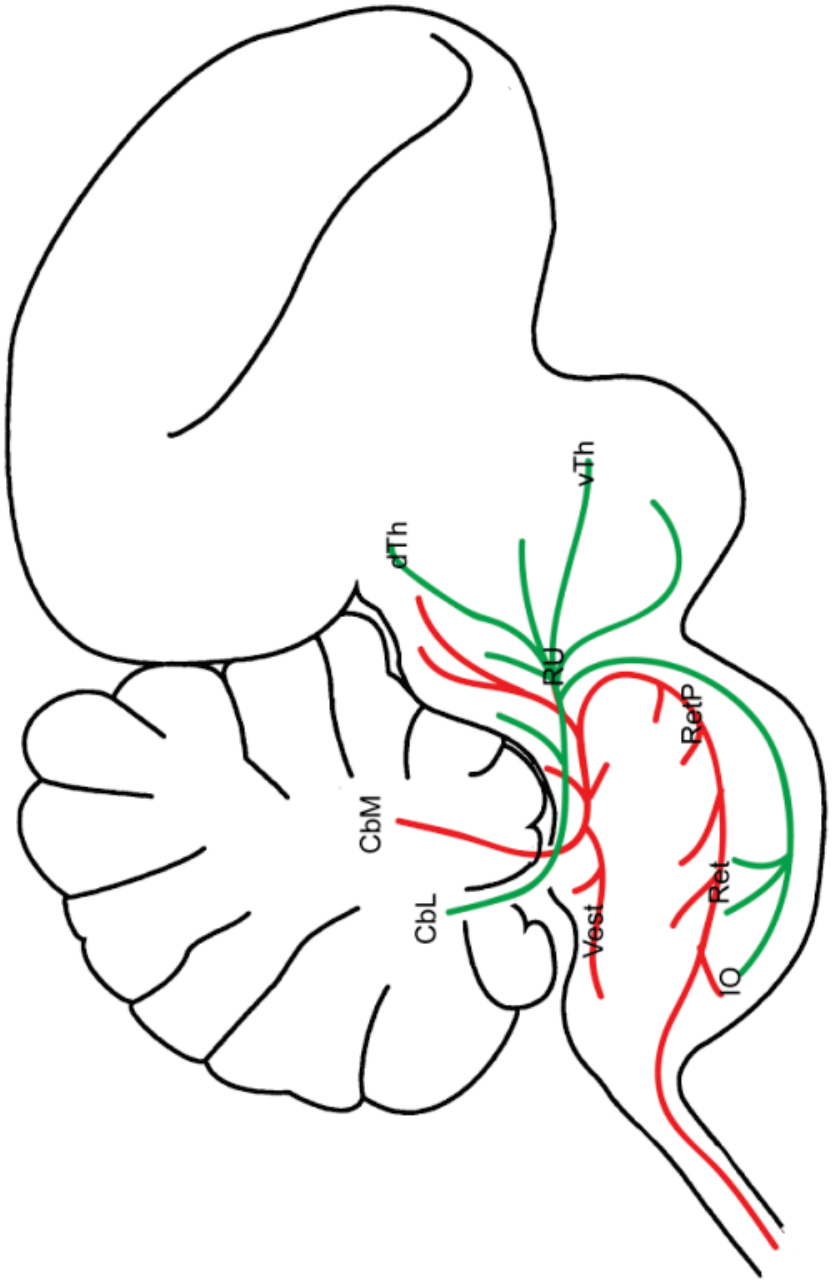

Figure 2-1 Summary of projections of the cerebellar nuclei of chick.

Adapted from Arends and Zeigler, 1991. Diagram indicating the efferent connections of the medial (red) and lateral (green) cerebellar nuclei in chick. Abbreviations: CbM: medial cerebellar nucleus, CbL: lateral cerebellar nucleus, RU: red nucleus, dTh: dosal thalamus, vTh: ventral thalamus, Vest: vestibular nuclei, RetP: reticular pontine nuclei, Ret: reticular nuclei, IO: inferior olive.

Arends and Zeigler (1991a) described the presence of two (medial and lateral) cerebellar nuclei in birds which carry most of their efferents within two main branches: the fasciculus uncinatus, an axon tract across the dorsal midline (medial nucleus) and the brachium conjunctivum/superior cerebellar peduncle (lateral nucleus). The major output of the medial cerebellar nucleus was reported to be to the vestibular and reticular nuclei in the dorsal/ventral hindbrain respectively, whilst the lateral cerebellar nucleus forms the majority of projections to the red nucleus of the ventral tegmentum, with minor branches to the thalamus and ventral hindbrain. The majority of projections described are contralateral, but ipsilateral connections from the medial cerebellar nucleus to vestibular nuclei are also present. Based on these projections, the medial cerebellar nucleus is considered homologous to the mammalian fastigial nucleus, whilst the lateral cerebellar nucleus is considered homologous to the mammalian interposed nucleus. None of the populations in the pigeon cerebellum resemble the mammalian dentate nucleus which forms major projections to the cerebral cortex, via the thalamus.

The presumptive identity of cerebellar nuclei and other cerebellar rhombic lip derivatives is then contrasted with molecular markers of mouse cerebellar rhombic lip derivatives. During mouse development, two transcription factors, *Lhx9* and *Barhl1*, are both activated down-stream of *Atoh1* in different temporal subsets of cells and mark all of the derivatives of the cerebellar rhombic lip (Rose et al., 2009a).

Lhx9 is a LIM-homeobox (LHX) transcription factor, which in combination with various other LHX genes play a significant role in the specification of different classes of neurons with specific axon projections throughout the nervous system (Hobert and Westphal, 2000). LHX genes are known to be of particular importance in the specification of specific classes of motor neurons and interneurons of the spinal cord (Thor et al., 1999; Wilson et al., 2008; Avraham et al., 2009). In rhombomere 1, the role of *Lhx9* has not been established but it is specifically expressed in early born, extra-cerebellar rhombic lip derivatives in ventral rhombomere 1 and in the interposed and dentate cerebellar nuclei (Morales and Hatten, 2006; Rose et al., 2009a).

In mouse, *Barhl1* specifically labels the fastigial cerebellar nucleus and cerebellar granule cells precursors, both of which are born after *Lhx9*$^{+ve}$ rhombic lip derivatives (Rose et al., 2009a). In the absence of a probe for *Barhl1* in chick, I used an alternative marker, *Tbr1*, which in mouse labels the fastigial cerebellar nucleus (Fink et al., 2006). *Tbr1* (T-Box-brain1), a member of the T-box family of transcription factors, is required for the development and specification of certain classes of neurons, particularly neurons of the

cerebral cortex (Bulfone et al., 1995; Hevner et al., 2001). In the cerebellum, *Tbr1* expression is specific to the cells of the fastigial nucleus, but no obvious defects in the development or projection of these cells was observed in *Tbr1*-null mice (Fink et al., 2006).

2.2 Results

2.2.1 Cell production from the cerebellar rhombic lip occurs in a strict temporal sequence in chick.

To precisely map the derivatives of the cerebellar rhombic lip, a CAβ-*gfp* overexpression construct (hereafter just called *gfp*) was electroporated focally into dorsal rhombomere 1 (**Figure 2-2 A**) at every Hamburger and Hamilton stage (St) between St16 and St29 (E3-6; for a full list of staging compared to day of embryonic development see **Appendix A**). All embryos were harvested at St31/E7 to create a cumulative fate map of cerebellar rhombic lip derivatives. Comparing populations that were excluded from progressively later electroporations then allowed the precise birthdate of populations of cells to be inferred.

Using this technique the region of the rhombic lip can be targeted by the positioning of the positive and negative electrodes. However, especially in younger embryos where a broader region is electroporated, rhombic lip cells are not likely to be the only cells labelled. Rhombic lip-derived cells can be differentiated from other cells by three unique morphological characteristics compared to cells in the surrounding regions: 1) the rhombic lip migratory stream is only found on the pial surface of the hindbrain, 2) rhombic lip derivatives are excitatory neurons with large cell bodies and leading processes or projecting axons which are clearly distinct from the small cell bodies and local connections of interneurons derived from the adjacent ventricular zone, 3) rhombic lip cells are the only tangentially migrating population from the most dorsal part of rhombomere 1, therefore any cells which are seen at a distance from the electroporated region can be presumed to have originated in the rhombic lip.

Figure 2-2 shows a representative example of E4, E5 and E6 *gfp* electroporations all fixed at E7. Variation in the projections labelled was seen between electroporations at the same stages. This may be due to the position or the size of each individual electroporation and suggests that heterogeneity may exist within the cerebellar rhombic lip within specific temporal cohorts. This variability will be discussed in more detail in chapter 5 but for the purposes of temporal fate mapping I have described the results of electroporations which mark all of the cell types seen at a particular time. The full collection of images of electroporations at individual stages can be found in **Appendix B**.

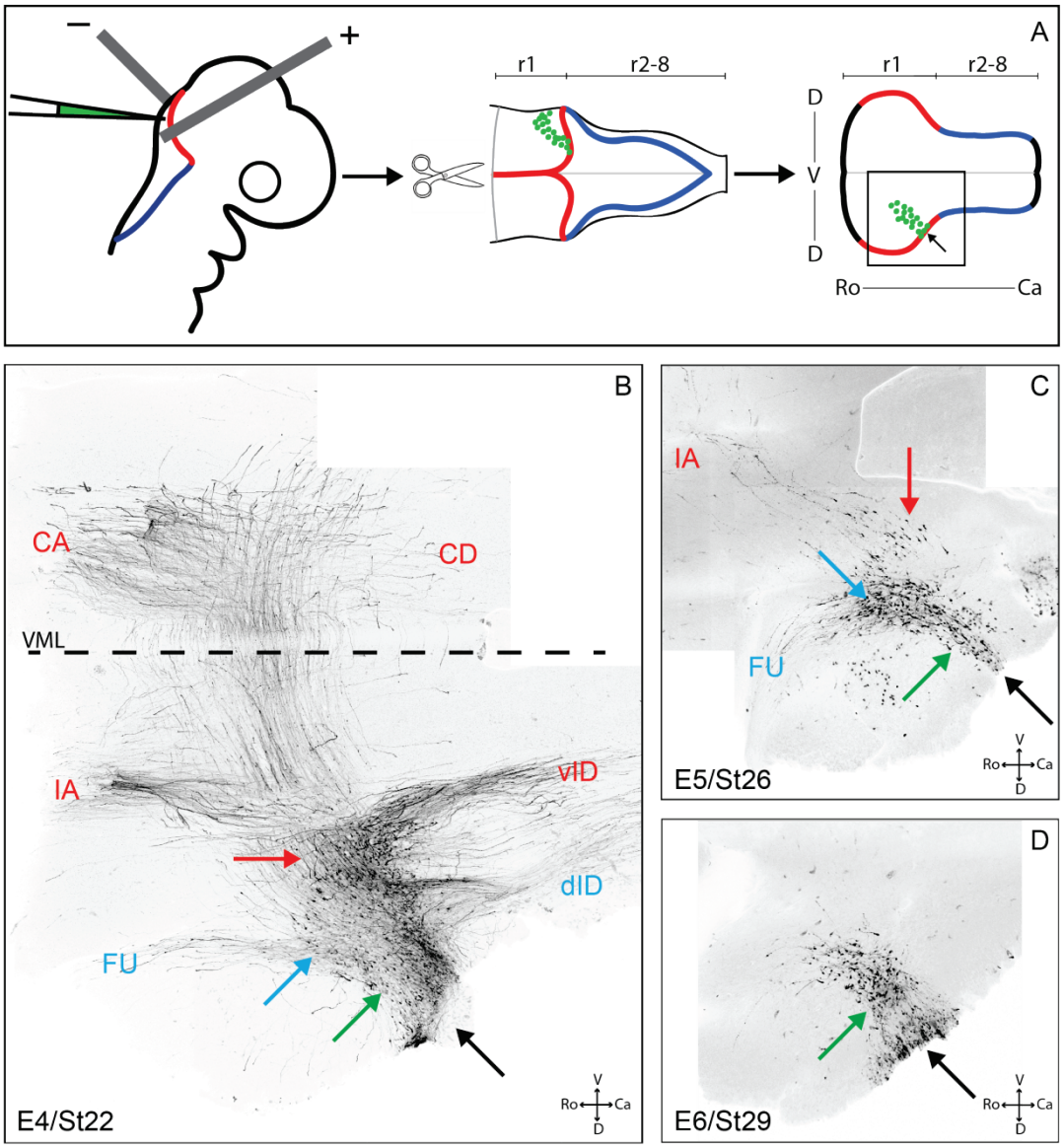

Figure 2-2 Temporal fate mapping of cerebellar rhombic lip derivatives.

Previous page:

Figure 2-2 Temporal fate mapping of cerebellar rhombic lip derivatives.

A) schematic diagram of how embryos were electroporated positioning the positive and negative electrodes to target the cerebellar rhombic lip (red) and prepared in flat-mount for confocal imaging by cutting the dorsal midline and mounting on a slide, pial surface uppermost. B-D) show composite projections of confocal Z-stacks taken of flat-mounted E7 hindbrains, orientated rostral to the left, with stage and position (black arrow) of electroporation indicated. B) E4 electroporation labels cells in ventral rhombomere 1 (red arrow and projection labels), the nuclear transitory zone (blue arrow and projection labels) and on the pial surface of the cerebellum, the external granule layer (green arrow). Ventral midline is marked by dashed line. C) E5 electroporation labels a few cells in ventral rhombomere 1 (red), the nuclear transitory zone (blue) and cells in the external granule layer (green). D) E6 electroporation only labels cells in the external granule layer (green). Abbreviations: D: dorsal, V: ventral, Ro: rostral, Ca: caudal, VML: ventral midline, CA: contralateral ascending, CD: contralateral descending, IA: ipsilateral ascending, vID, ventral ipsilateral descending, dID: dorsal ipsilateral descending, FU: fasciculus uncinatus.

At all stages, rhombic lip electroporations of *gfp* label a continuous stream of cells extending from the electroporated region. Electroporated cells all migrate ventrally and slightly rostrally irrespective of the position and timing of electroporation. As previously reported (Gilthorpe et al., 2002) rhombic lip derivatives show a gradual dorsal restriction in their migration paths with later electroporations labelling only more dorsal cells but early electroporation labelling ventral and dorsal cells. Occasionally, E3/4 electroporations only labelled ventral cells and the subsequent dorsal cells were not seen. This was presumed to be a result of dilution of *gfp* through cell divisions.

Electroporations at E3/E4 labelled similar cohorts of cells which contained all of the cell types produced between E3/4 and E7 (**Figure 2-2B**, E3 not shown, see **Appendix B**). Three major populations of cells were observed: 1) cells in ventral rhombomere 1 outside of the cerebellar primordium, 2) cells accumulated at the lateral edge of the cerebellum, 3) cells on the pial surface of the cerebellum.

The most ventral population (1) shows four major axon projections: contralateral ascending (CA), contralateral descending (CD), ipsilateral ascending (IA) and ventral ipsilateral descending (vID). A small, dorsal subset of these extra-cerebellar cells were labelled in later electroporations at E5 (**Figure 2-2C** red arrow), but not at E6 (**Figure 2-2D**). Intermediate time points showed the dorsal restriction of cell migration within this population was gradual (between St16 and St27) and thus, ventral cells of this population are born first.

Cells clustering at the lateral edge of the cerebellar primordium (population 2) were labelled in all electroporations between St 16 and St27 (**Figure 2-2B,C**), with a small contribution to this population in St28 electroporations. The most prominent labelling of this population was seen in electroporations at St26 and S27, suggesting this to be the peak time of labelling these cells. This population also demonstrates a slight rostral shift compared to the rest of the cells in the lineage which formed a uniform column of labelled cells from the rhombic lip. This shift is most clearly seen in **Figure 2-2C**, where cells appear to turn rostrally and are distinctly orientated. This apparent migratory turn has been reported previously by Gilthorpe et al. (2002) as granule cell precursors turning at the edge of the cerebellum. However, in these electroporations an axon tract can be seen from this population projecting dorsally, over the dorsal midline, to the contralateral cerebellum. This is the characteristic axon path of the fasciculus uncinatus (hook bundle of Russell), from the medial cerebellar nucleus (Arends and Zeigler, 1991a; Fink et al., 2006) and therefore this region at the lateral edge of the cerebellum is the nuclear transitory zone, containing immature neurons of cerebellar nuclei. This nuclear transitory zone population of cells also forms an ipsilateral descending

axon tract to the dorsal hindbrain (dID),labelled clearly in E4 electroporations (**Figure 2-2B**) and variably labelled in electroporations at E5 (up to St26). This temporal discrepancy between labelling ascending and descending axons from the nuclear transitory zone suggests a slightly earlier termination of production of cells with descending axons.

The population of cells on the pial surface of the cerebellum (population 3), was labelled in all electroporations from E3-E6 but is the only population of cells labelled in electroporations after St28 (**Figure 2-2B-D**) demonstrating this to be the last population of cells born from the cerebellar rhombic lip within the stages analysed. These cells do not have identifiable axons at E7 and their position in the pial surface of the cerebellum (the presumptive external granule layer) and the timing of their production at E6 lead to the conclusion that these cells are cerebellar granule cell precursors.

2.2.2 Scattered labelling of cells reveals heterogeneous populations of cells within nuclei.

Each temporal cohort of cells from the cerebellar rhombic lip shows several distinct axon projection tracts. This could represent a homogenous population of cells with branching axons or a heterogenous population of mixed cell types which project to different targets. To distinguish between these two possibilities I examined individual cell morphology in sparsely labelled cells from the cerebellar rhombic lip by electroporating a conditional GFP reporter (pFlox-pA-EGFP; hereafter called Stop-*gfp*) with a diluted cre-recombinase (pCx-*Cre*) (Morin et al., 2007). The Stop-*gfp* construct contains a β-actin promoter linked to *gfp* preceded by a floxed stop cassette. When Cre-recombinase is expressed in the same cell, the stop cassette is removed and GFP is expressed. By using a diluted concentration of cre-recombinase, recombination becomes an infrequent event and results in sparse cell labelling.

To test these constructs, I co-electroporated the cerebellar rhombic lip at E4 with equal concentrations of CAβ-*rfp* and Stop-*gfp* and 1:100, 1:1000 or 1:10,000 dilutions of Cre-recombinase. Comparing the GFP and RFP labelling in these embryos showed that 1:1000 and 1:10,000 dilutions of Cre-recombinase allowed for single cell resolution to be seen (**Figure 2-3A-C**).

Using this technique I observed that all cerebellar rhombic lip derivatives have single axons that do not branch (at least proximally) (**Figure 2-3D-F**) and thus all the nuclei comprise heterogeneous populations of cells with differently projecting axons. Within an individual temporal cohort different projections appear to be dependent on the position of the cell body within the nucleus (**Figure 1-3D**) with descending projection neurons mostly found in the

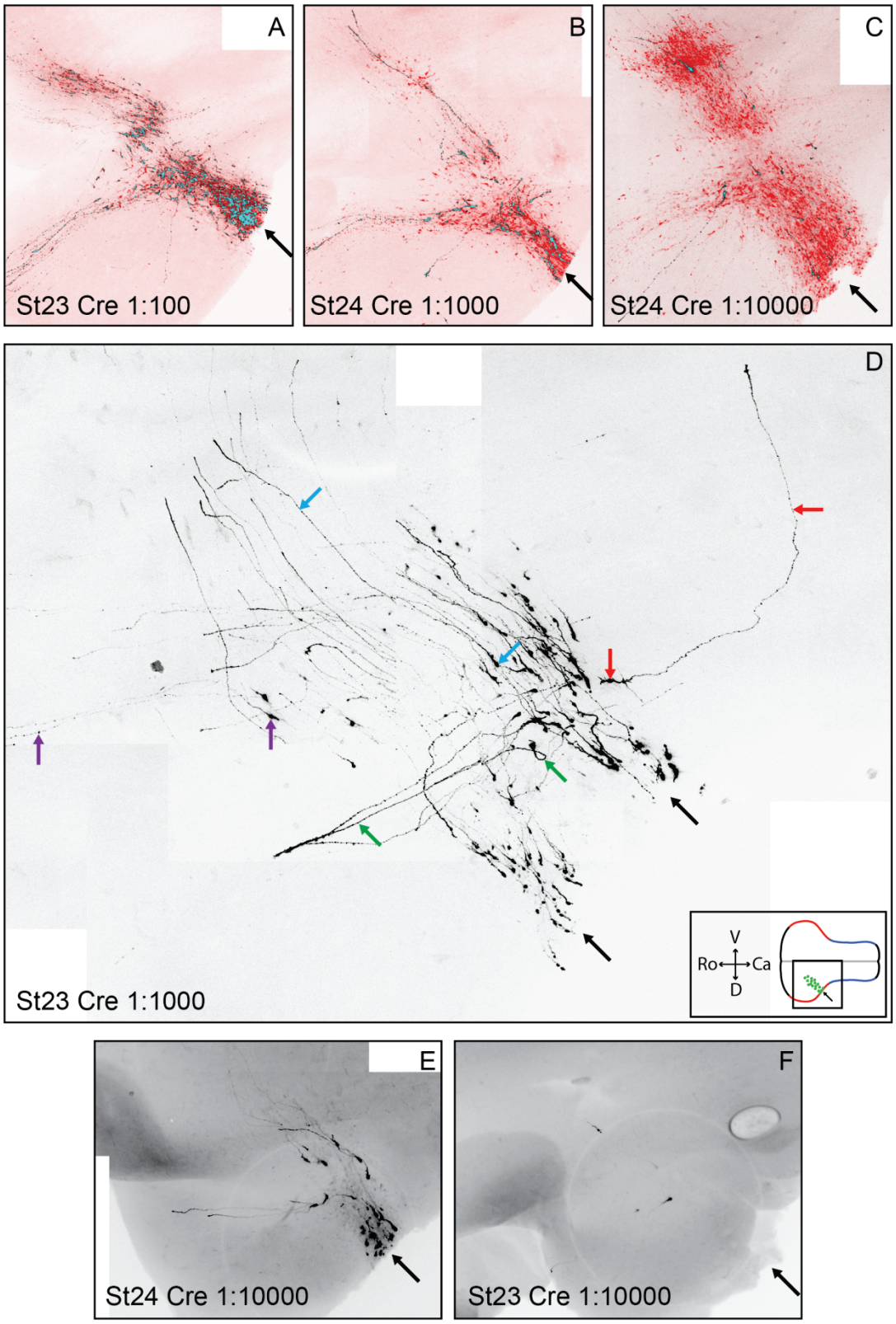

Figure 2-3 Scattered labelling of individual cells from the cerebellar rhombic lip.

Previous page:

Figure 2-3 Scattered labelling of individual cells from the cerebellar rhombic lip.

Composite projections of confocal Z-stacks taken of flat-mounted E7 hindbrains (orientation inset (D)) electroporated in the cerebellar rhombic lip at E4. Individual stage and position (black arrow) of electroporation are indicated on each picture. A-C) show coelectroporations of *rfp*, *cre* and Stop-*gfp* constructs with *cre* diluted 1:100 (A), 1:1000 (B) and 1:10000(C). RFP^{+ve} cells shown in red, GFP^{+ve} cells shown in black, RFP^{+ve}/GFP^{+ve} are shown in blue (colours manipulated in photoshop). D-F) show coelectroporations of *cre* and Stop-*gfp* with *cre* diluted 1:1000 (D) or 1:10000 (E,F). Individual cells are marked with coloured arrows marking both the cell body and axon. Heterogeneous populations of cells with single axons are seen within early (purple and blue) and later-born (red and green) populations of cerebellar rhombic lip derivatives. D shows two sites of electroporation arising from movement of electrodes during the same single electroporation.

caudal part of each population. Such topography appears to be conserved to the adult nuclei (Arends and Zeigler, 1991a). Using this technique it was not possible to determine the clonal origin of cells from the rhombic lip, even when as few as 2 cells were labelled (**Figure 1-3F**) because cells are born over several days and the progenitor cells were not always visible at the time of dissection.

2.2.3 Axonal projections of cerebellar rhombic derivatives.

To identify the cerebellar rhombic lip derivatives labelled in electroporations I traced the axon projections through the brain. Embryos electroporated with *gfp* at E3-4 (St16-24) were analysed at E7 and brains were hemisected or flat-mounted. No projections were seen to enter the dorsal midbrain, so this region was removed to make mounting the embryos easier. Due to variability between electroporations, and the different dissection required for optimal visualisation of each axon tract, **Figure 2-4** represents a collection of E3/4 electroporations which collectively label all of the observed axon tracts.

Rhombic lip derivatives in ventral rhombomere 1, only labelled in E3 and E4 (St16-24) electroporations, showed four distinct projections, two ascending and two descending. These pairs of axon tracts appeared to mirror each other on the ipsilateral and contralateral side of the embryo (**Figure 2-4A**). Embryos fixed at E7 showed ipsilateral ascending projections terminating in the hypothalamus and thalamus (**Figure 2-4 B,C,E,F** black and red arrows) and possibly occasionally into the ventral telencephalon (not shown). Contralateral ascending axons were mostly seen to project to the ventral mesencephalon (**Figure 2-4 A-C** green arrows) but were occasionally seen projecting to the contralateral thalamus/hypothalamus (**Figure 2-4 F'** green arrows). Therefore it is not clear whether axons terminate in the ventral mesencephalon or whether these axons are still growing towards their thalamic targets.

Descending projections were seen to project ipsilaterally towards the spinal cord through the ventral hindbrain (**Figure 2-4 A,D,E** purple arrows). Whilst contralateral descending projections appeared to mirror the ipsilateral projections, these axons did not project as far caudally (**Figure 2-4 A** orange arrow). Again this may be a consequence of axons being examined whilst still growing towards their targets, rather than an accurate reflection of the final termination.

The nuclear transitory zone population of cells at the lateral edge of the cerebellum labelled in E3/4/5 electroporations has two distinct axon bundles: one ipsilateral projection into the dorsal hindbrain (**Figure 2-4 A,B,E,F** dark blue arrow) and the fasiculus uncinatus

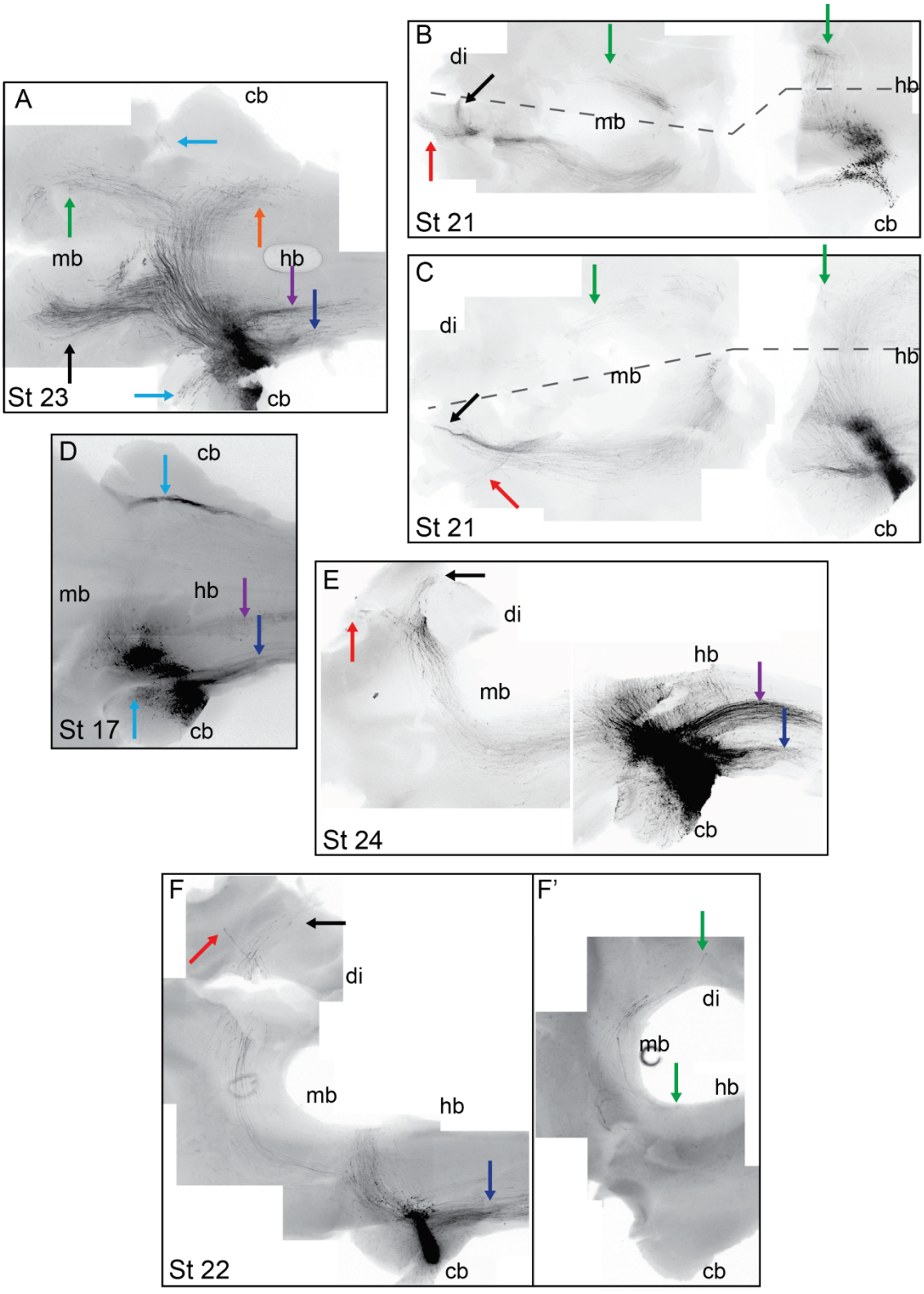

Figure 2-4 Axon tracing of cerebellar rhombic lip derivatives.

Previous page:

Figure 2-4 Axon tracing of cerebellar rhombic lip derivatives.

Composite projections of confocal Z-stacks taken of E7 brains electroporated in the cerebellar rhombic lip at E3/4 (individual stages of electroporation indicated on each picture). A-D) show flat-mount preparations of hindbrain and ventral midbrain (A,D) or hindbrain with ventral midbrain and diencephalalon mounted separately (B,C) where continuation of ventral midline is indicated by grey dashed line. Rostral orientated to left. E-F) show hemisected tissue of hindbrain, ventral midbrain and diencephalon orientated dorsal to the bottom. F' shows the contralateral side of brain to F in the same orientation. In A-F different axon projections are labelled with different colour arrows: black: ipsilateral projection to ventral thalamus/hypothalamus, red: ipsilateral projection to dorsal thalamus, green: contralateral projection to ventral midbrain, orange: contralateral projection to ventral hindbrain, purple: ipsilateral projection to ventral hindbrain, dark blue: ipsilateral projection to dorsal hindbrain, light blue: fasciculus uncinatus projection to contralateral dorsal hindbrain. Abbreviations: cb: cerebellum, hb: hindbrain, mb: midbrain, di: diencephalon.

(**Figure 2-4 A,D** light blue arrows). The fasiculus uncinatus projects in a rostro-dorsal direction but once it crosses the dorsal midline (which is cut in mounted hindbrains) these axons turn caudally and project into the dorsal hindbrain on the contralateral side of the embryo, mirroring the ipsilateral projection from the same populations of cells. These two axon tracts match the reported projections of the medial cerebellar nucleus to the vestibular nuclei in ipsilateral and contralateral dorsal hindbrain (Arends and Zeigler, 1991a) but, projections to the contralateral ventral hindbrain nuclei (via the fasciculus uncinatus) are not apparent from this nuclear transitory zone population (see F**igure 2-1**).

In mouse development, cells of both the medial and lateral cerebellar nuclei initially migrate to the nuclear transitory zone (Machold and Fishell, 2005; Wang et al., 2005; Fink et al., 2006). By contrast, in chick, axons that project contralaterally to cerebellar nuclei targets of the ventral midbrain (red nucleus), thalamus and ventral hindbrain (pontine and reticular nuclei) (see **Figure 2-1**) are only labelled from more ventrally located cells. This implies that in chicken, cells which contribute to the cerebellar nuclei are initially located ventrally to the nuclear transitory zone, though molecular markers will be needed to confirm this. The early born population of cells in ventral rhombomere 1 also has several axon tracts which are not reported targets of the cerebellar nuclei, including ipsilateral connections to the thalamus and ventral hindbrain and axons projecting to the (ipsilateral and contralateral) hypothalamus and possibly to the ventral telencephalon. Therefore the early-born population of cerebellar rhombic lip derivatives in ventral rhombomere contains non-cerebellar nuclei, likely similar to the mouse *Atoh1*-derived parabigeminal, pontine, tegmental, parabrachial and lemniscal nuclei.

2.2.4 Verification of cerebellar rhombic lip fate mapping.

Although, as previously stated, cerebellar rhombic lip derivatives are easily identifiable based on their cell morphology, migratory capacity and position over the pial surface of the brain, it is important to verify that no other populations of cells were included in my fate map analysis. Populations that could contribute to confusing or erroneous identification of rhombic lip derivatives could include cells of the locus coeruleus or Lmx1a^{+ve} neurons, both derived from progenitors just ventral to the *Ptf1a*$^{+ve}$ cerebellar ventricular zone (Aroca et al., 2006; Chizhikov et al., 2006). Furthermore, a subset of Purkinje cells, derived from *Ptf1a*$^{+ve}$ cerebellar ventricular zone have direct projections to vestibular nuclei (Arends and Zeigler, 1991b). Dorsal targeting of electroporations should exclude these cells from analysis but to verify that the *gfp*-electroporated populations identified thus far are solely derivatives of the

cerebellar rhombic lip, I compared my results with two alternative methods of labelling cerebellar rhombic lip derivatives: chimeric grafting and an *Atoh1*-reporter.

In previous work (Wingate and Hatten, 1999), orthotopic grafting of quail rhombic lip into dorsal rhombomere 1 of St10 chick was used to create a cumulative fate map of all the derivatives of the cerebellar rhombic lip. I analysed chimeric embryos (kindly generated by Amata Hornbruch) in which dorsal rhombomere 1 of a St10/E2 *gfp*-transgenic chicken embryo was grafted into dorsal rhombomere 1 of a wild-type St10 chicken embryo. The chimeric embryos were then harvested and fixed at St29 (E6) or St34 (E8) and the brains were flat-mounted or hemisected for analysis (**Figure 2-5**). Using this method only cells derived from the most dorsal neural tube are GFP-positive. Furthermore, grafts were performed at St10/E2 at a stage much earlier than specific labelling by electroporation can be achieved. This method of cell labelling should therefore highlight whether any rhombic lip derived populations are born between St10 and St16, when the earliest electroporations were performed.

Chimeric embryos showed all of the same cells that were seen in the earliest electroporated embryos and all of the same axon tracts (**Figure 2-5**). Two additional populations were found in chimeric embryos that were not seen in electroporated embryos: A small population of ventral cells, just caudal to the rhombic lip stream and neural crest cells (**Figure 2-5**A,B). Most of the neural crest cells were dissected away before analysis but in some embryos neural crest cells were seen in the trigeminal ganglion (**Figure 2-5B**). Separate axons were not clearly visible from the additional ventral population so it was not possible to identify these cells. Given the ventral position of this extra population and the previously observed dorsal restriction of cell position with time it is possible that this extra population represents cells which are born prior to the earliest electroporations performed.

To further verify the origin of cells in *gfp* electroporations as rhombic lip specific, I used a *Math1* specific reporter (Math1-*LacZ*). This reporter consists of two conserved elements of the *Math1* enhancer region fused to a βGlobin/*LacZ* and has been shown to be sufficient to drive β-Gal expression in all *Math1* expressing cells in transgenic mice (Helms et al., 2000). Conservation between the mouse and chick *Atoh1* enhancer regions suggest this construct should also be sufficient to drive expression in *Cath1* expressing cells in chick. I therefore electroporated this construct into chick rhombic lip at St22/23, fixed the embryos are St31 (E7) and stained for β-galactosidase.

Cells stained positive for β-gal were found in ventral positions distal to the rhombic lip. The position of these cells in ventral rhombomere 1 was equivalent to the populations of cells

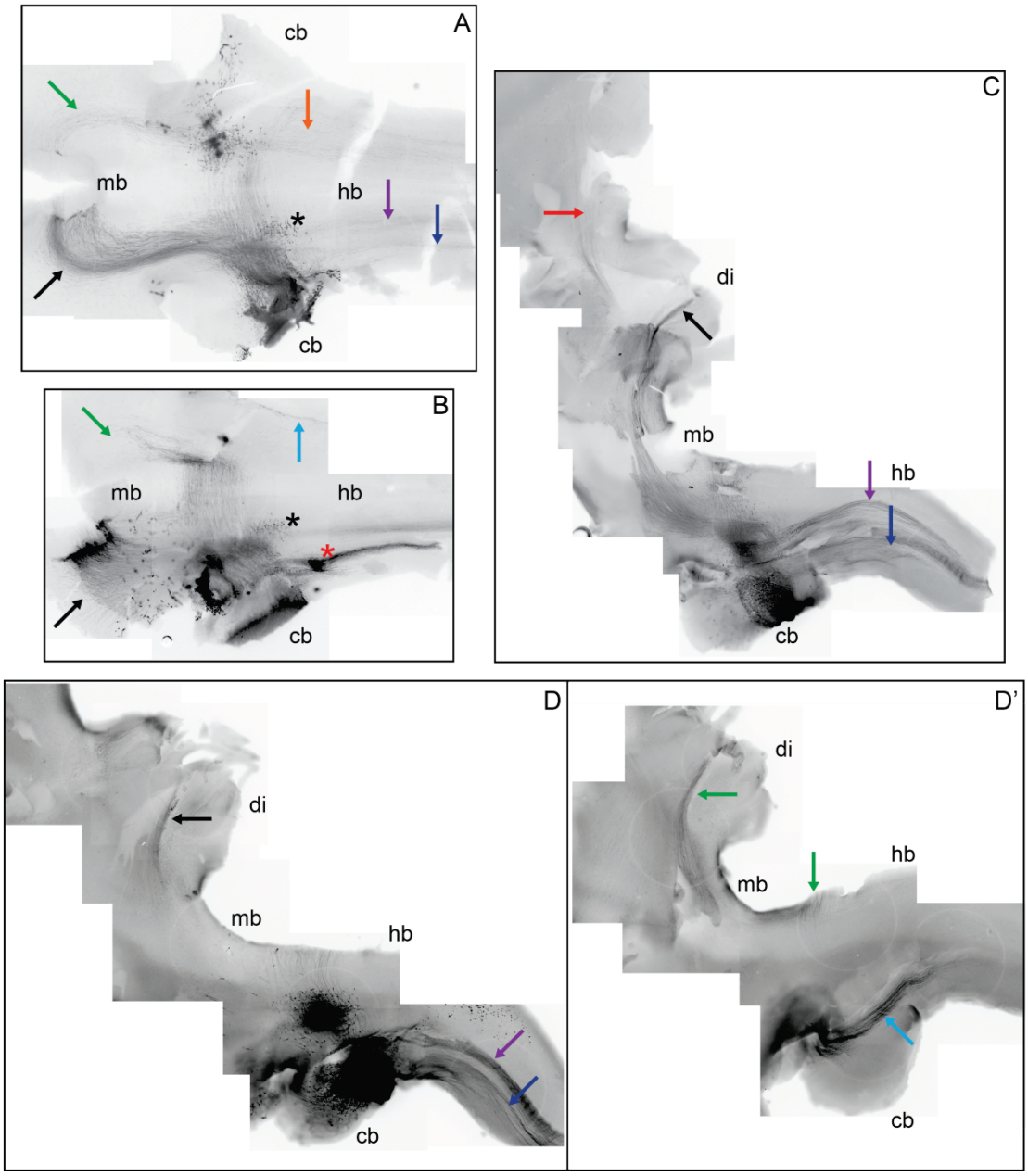

Figure 2-5 Orthotopic chimeric grafts of the cerebellar rhombic lip.

Previous page:

Figure 2-5 Orthotopic chimeric grafts of the cerebellar rhombic lip.

Composite projections of confocal Z-stacks taken of brains following orthotopic grafting of cerebellar rhombic lip tissue of *gfp*-transgeneic chicken embryos into wildtype hosts at E2. A-B) show E6 flat-mounted hindbrain and midbrain tissue orientated rostral to the left. Black asterisk marks additional (not labelled by electroporation) ventral population of labelled cells and red asterisk marks additional labelling in the trigeminal ganglion. C-D) show E8 hemisected hindbrain, midbrain and diencephalon orientated dorsal to the bottom. D' shows the contralateral side of brain to D in the same orientation. In A-D different axon projections are labelled with different colour arrows: black: ipsilateral projection to ventral thalamus/hypothalamus, red: ipsilateral projection to dorsal thalamus, green: contralateral projection to ventral midbrain, orange: contralateral projection to ventral hindbrain, purple: ipsilateral projection to ventral hindbrain, dark blue: ipsilateral projection to dorsal hindbrain, light blue: fasciculus uncinatus projection to contralateral dorsal hindbrain. Abbreviations: cb: cerebellum, hb: hindbrain, mb: midbrain, di: diencephalon.

labelled in *gfp* electroporations at E3/E4 (**Figure 2-6**). This is further confirmation that the cells marked in other electroporations were indeed derived from the *Atoh1*-positive rhombic lip. However, little or no β-gal^{+ve} cells were seen more dorsally in the rhombic lip, nuclear transitory zone or external granule layer (**Figure 2-6**). The Math1-*LacZ* reporter therefore did not fully recapitulate the results seen in GFP electroporations. This is likely due to weak expression of the reporter and a dilution of the construct through rounds of cell division at the rhombic lip such that only the first born cells after electroporation had sufficient concentration of the construct to allow the cells to be seen. This dilution effect was also occasionally seen in *gfp* electroporations. Attempts to re-engineer the Math1-*LacZ* construct to make a fluorescent reporter (see materials and methods) were unsuccessful and therefore axon labelling from this *Atoh1*-derived population was not possible.

From chimeric embryos and Math1-LacZ electroporations it can be concluded that my technique for temporally mapping cerebellar rhombic lip derivatives was effective and my analysis has not included any cell populations outside of the rhombic lip.

2.2.5 *Lhx9* marks only a subset of the early-born cerebellar rhombic lip derivatives in ventral rhombomere 1.

To help differentiate the terminal identity of rhombic lip derivatives which migrate into ventral rhombomere1 and to the nuclear transitory zone in chick, I combined GFP electroporations into the cerebellar rhombic lip at St16-29 with *in situ* hybridisation at St31 (E7). I first looked at the expression of *Lhx9*, a marker of mouse, early-born rhombic lip derivatives, in cells from the rhombic lip in chick.

At St31 *Lhx9* is expressed in a broad domain throughout rhombomere 1 from dorsal at the rostral end of rhombomere1 to more ventral in caudal rhombomere 1 (**Figure 2-7 A,C,E**). Of the early-born (E3/4) population, ventral to the nuclear transitory zone, *Lhx9* marks only a ventral subset (**Figure 2-7 A,B** red arrow, green arrow: *Lhx9*$^{-ve}$). E3 (St16/17) *gfp* electroporations label cells within the *Lhx9*$^{+ve}$ territory (**Figure 2-7 A,B** red arrows) whereas the majority of cell bodies in E4 electroporations (St20-24) are positioned dorsal to *Lhx9*$^{+ve}$ expression, but have GFP^{+ve} axons which overlap with the *Lhx9*$^{+ve}$ domain (**Figure 2-7 C,D** green arrows: cell bodies, blue arrows axons). All of the four major axon tracts attributed to early-born cells in ventral rhombomere 1 are seen in the *Lhx9*-negative cells labelled at E4 (**Figure 2-7 C'**). *Lhx9*$^{+ve}$ cells which are exclusively labelled by E3 electroporations, do not contribute to the ipsilateral descending tract but with this cumulative labelling analysis it is not possible to determine which particular subsets of the other 3 axon tracts are from *Lhx9*$^{+ve}$

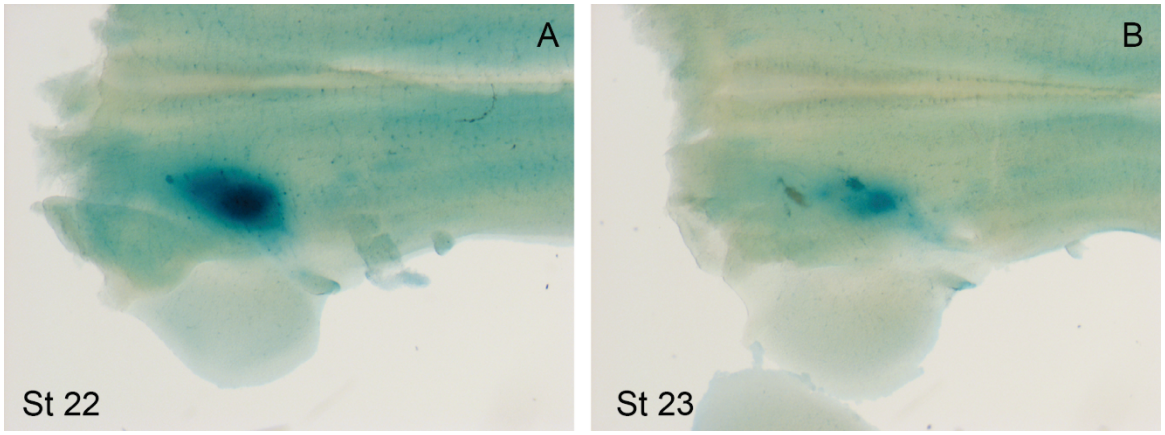

Figure 2-6 Math1-*LacZ* reporter electroporations.

E7 flat-mount hindbrains (rostral to left) stained with X-gal following electroporation of Math1-*LacZ* reporter construct at E4 (A: St22, B: St23 electroporation). LacZ^{+ve} cells from the cerebellar rhombic lip can be seen in the ventral hindbrain.

Next Page:

Figure 2-7 *Lhx9* is expressed in the most ventral rhombic lip derivatives.

E7 flat-mount hindbrains (rostral to left) following electroporation with *gfp* into the cerebellar rhombic lip (black arrows) at St17/E3 (A/B), St20/E4 (C,D) or St26/E5 (E,F) and *in situ* hybridisation for *Lhx9*. Column 1 shows bright field pictures of *Lhx9* expression. Column 2 (A',B' etc.) shows inverted colour pictures of GFP. Column 3 (A",B" etc.) shows GFP overlaid on *Lhx9* expression. B,D and F show magnified region of A,C and E marked by black box. Red and green arrows indicate Lhx9^{+ve} and Lhx9^{-ve-} populations of early born cells in ventral rhombomere 1. E3 electroporations (A,B) label cells within the *Lhx9*$^{+ve}$ domain (red arrows) but later electroporations (E4 and E5 (C-F)) only label cells outside of the *Lhx9*$^{+ve}$ domain (green arrows) though axons are often labelled which pass through the Lhx9^{+ve} domain (blue arrow).

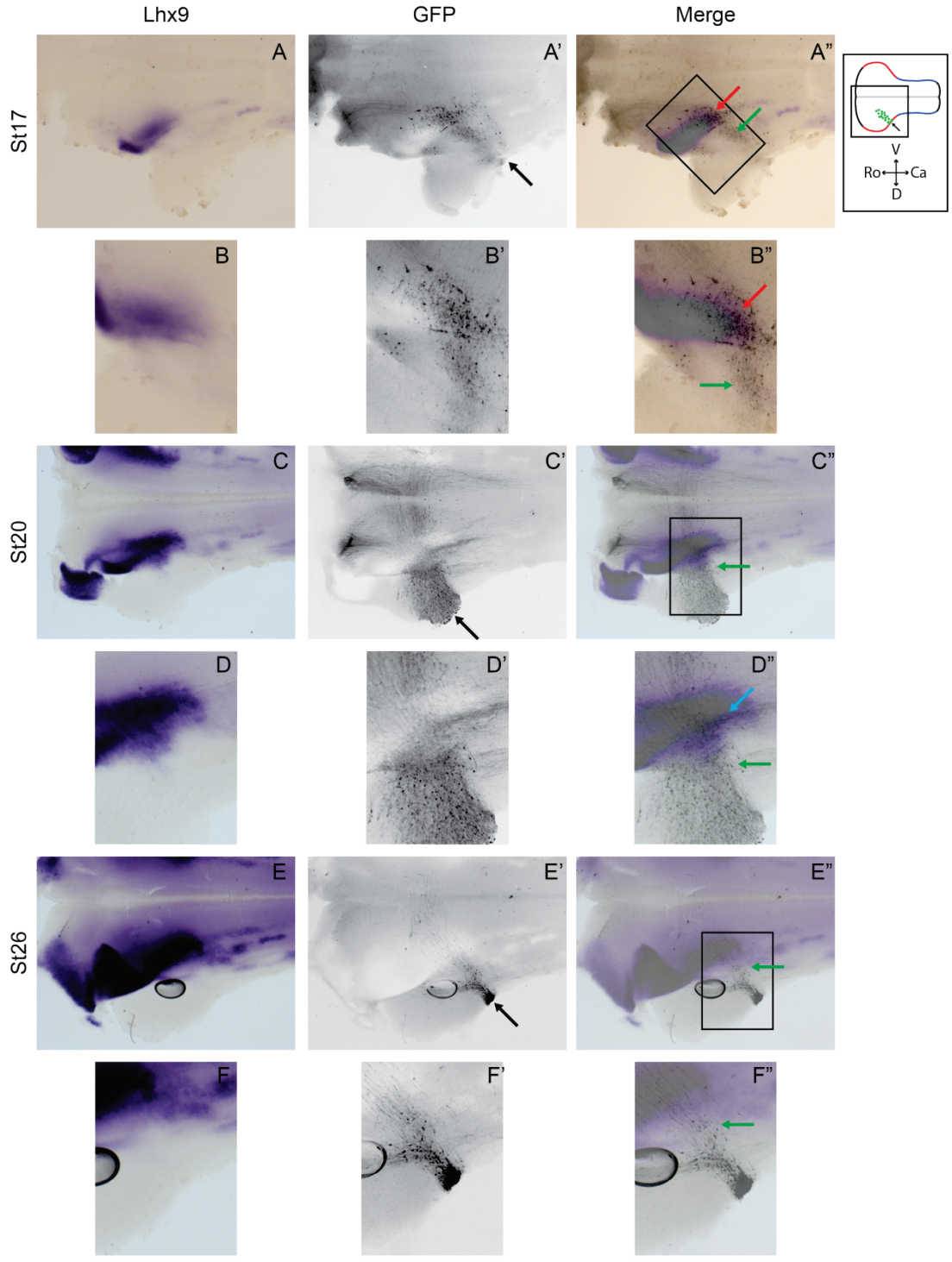

Figure 2-7 *Lhx9* is expressed in the most ventral rhombic lip derivatives.

cells. E5 (St26/27) *gfp* electroporations do not label any cells within the *Lhx9*$^{+ve}$ domain but contribute

a small number of cells (with axons projecting rostrally or contralaterally) to the *Lhx9*-negative population ventral to the nuclear transitory zone (**Figure 2-7 E,F** green arrows).

Therefore the early-born population of rhombic lip derivatives in ventral rhombomere 1 can be subdivided into an *Lhx9*$^{+ve}$ population born at E3 and an *Lhx9*-negative population born at E4. The presence of a mixed population of cells in ventral rhombomere 1 is consistent with the hypothesis that some cells of the cerebellar nuclei may initially be found in this population, ventral to the nuclear transitory zone. This also shows that, unlike in mouse, cells in the nuclear transitory zone do not express *Lhx9*.

The domain of *Lhx9* expression extends from ventral rhombomere 1, where rhombic lip cells born at E3 were labelled, to dorsal rhombomere 1 rostrally, abutting the isthmus. If, as previously reported in mouse (Rose et al., 2009a) all *Lhx9*$^{+ve}$ cells in rhombomere 1 originate from the rhombic lip, this would imply that cells born from the rhombic lip in the most rostral part of rhombomere 1, do not migrate as far ventrally. To label these cells, I performed *gfp* electroporations at E3 and E4 into the most rostral part of the cerebellar rhombic lip. When electroporations were analysed at E7, electroporated cells were found in a more caudal region of rhombomere 1, in a stream extending from the cerebellar rhombic lip and the rostral/dorsal *Lhx9*$^{+ve}$ population could not be labelled (data not shown). The consistent caudal shift observed in electroporated cells in rostral rhombomere 1 from the time of electroporation to the time of analysis may be indicative that these cells are pushed caudally by growth from isthmic region of rhombomere 1.

2.2.6 *Tbr1* is expressed in the nuclear transitory zone marking cells of the medial cerebellar nucleus.

To confirm the conclusions of *gfp* electroporation axon mapping, that cells accumulated at the lateral edge of the cerebellum, the nuclear transitory zone, form the medial cerebellar nucleus which primarily projects through the fasciculus uncinatus, I combined E4/5/6 (St20-29) electroporations with *in situ* hybridisation for *Tbr1*, a gene which specifically marks the medial/fastigial nucleus in mouse (Fink et al., 2006).

At E7, *Tbr1* is expressed in a stripe at the lateral edge of the cerebellum, (**Figure 2-8 A,C,E**). Electroporations at E4 and E5 showed that GFP-labelled cells in the nuclear transitory zone, all reside within the *Tbr1*$^{+ve}$ domain. These cells mostly project through the fasciculus uncinatus and make a small contribution to the ipsilateral descending projection

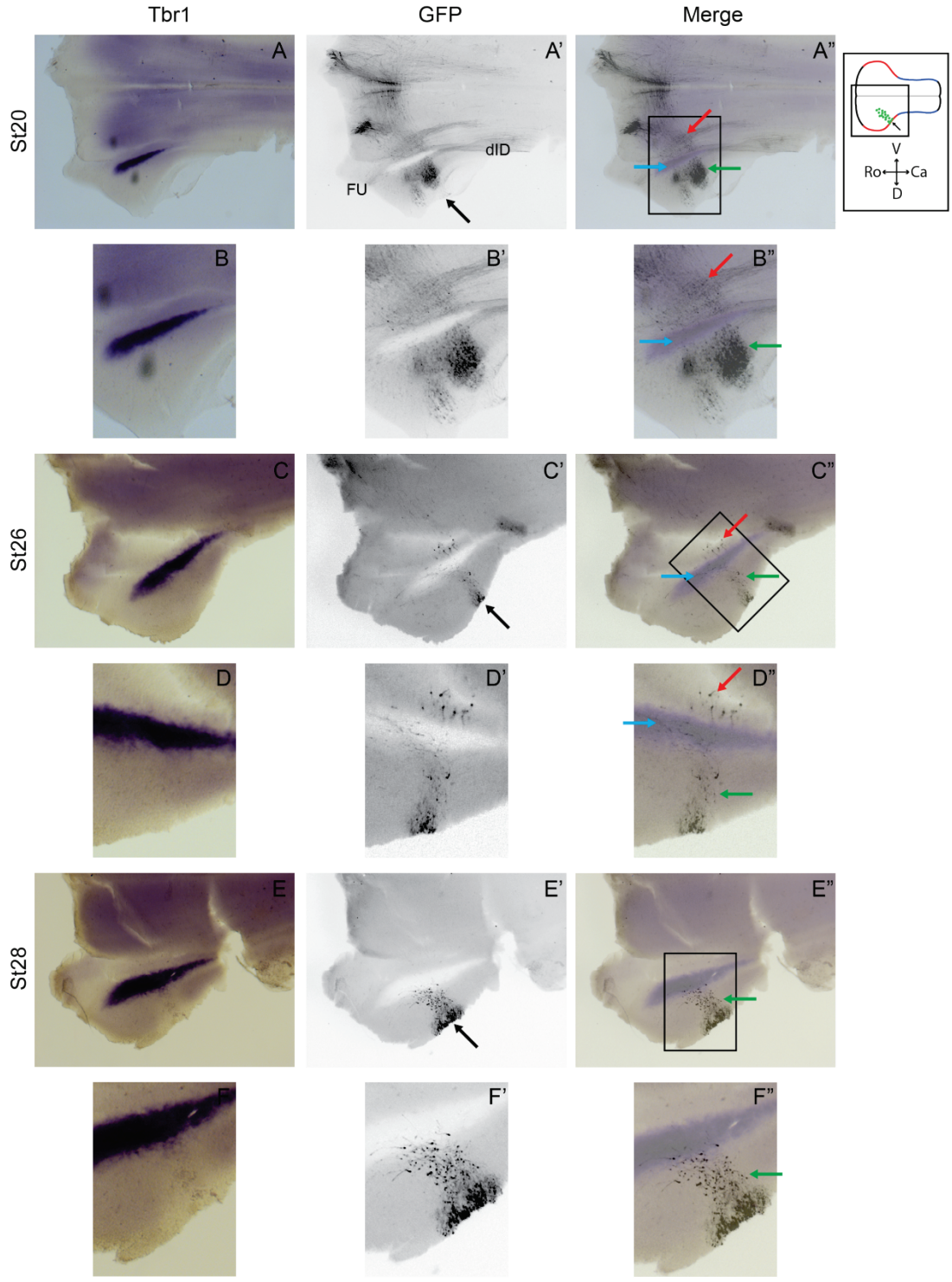

Figure 2-8 *Tbr1* expression in the nuclear transitory zone marks rhombic lip derivatives born at E5.

Previous page:

Figure 2-8 *Tbr1* expression in the nuclear transitory zone marks rhombic lip derivatives born at E5.

E7 flat-mount hindbrains (rostral to left) following electroporation with GFP into the cerebellar rhombic lip (black arrows) at St20/E4 (A/B), St26/E5 (C,D) or St28/E6 (E,F) and *in situ* hybridisation for *Tbr1*. Column 1 shows bright field pictures of *Tbr1* expression which is present in the nuclear transitory zone at the edge of the cerebellum. Column 2 (A',B' etc.) shows inverted colour pictures of GFP. Column 3 (A",B" etc.) shows GFP overlaid on *Tbr1* expression. B,D and F show magnified region of A,C and E marked by black box. Red arrows: early-born ventral populations, blue arrows $Tbr1^{+}$ nuclear transitory zone cells, green arrows: late-born dorsal population. E4 and E5 electroporation (A-D) show a subset of cells labelled fall within the $Tbr1^{+ve}$ domain which form projections of the fasciculus uncinatus (FU) and ipsilateral projections into the dorsal hindbrain (dID). E6 electroporations (E,F) label very few cells in the $Tbr1^{+ve}$ domains and most cells are found dorsal to *Tbr1* expression (green arrows).

into the dorsal hindbrain (**Figure 2-8 A-D** blue arrows). No cells labelled ventral to the nuclear transitory zone expressed *Tbr1* (**Figure 2-8** red arrows**)**. Electroporations at E6 (St28/29) only labelled cells dorsal to the domain of *Tbr1* expression, consistent with their identity as cerebellar granule cell precursors (**Figure 2-8 E,F** green arrows).

These observations confirm the identity of the medial cerebellar nucleus, which form the only population of cells in the nuclear transitory zone. As previously reported (Arends and Zeigler, 1991a), these cells are orthologous to the fastigial nucleus of mouse which also expresses *Tbr1* and forms projections through the fasciculus uncinatus (Fink et al., 2006). However, contrary to previous reports this population does not contribute axons which project to the contralateral ventral hindbrain, to reticular nuclei and the inferior olive (**See figure 2-1**).

2.2.7 How do *Lhx9*$^{+ve}$ and *Tbr1*$^{+ve}$ temporal cohorts compare with developing mouse?

In situ hybridisation for *Lhx9* and *Tbr1* using digoxigenein- and fluorescein-labelled riboprobes to allow for staining in two colours, was performed on E7 hindbrain tissue. This reveals a distinct gap between the expression domains of these two genes in rhombomere 1 (**Figure 2-9 A**). This intermediate *Tbr1*$^{-ve}$*/Lhx9*$^{-ve}$ population of rhombic lip derivatives forms the whole of the ipsilateral descending projection to the ventral hindbrain and contributes projections to the contralateral midbrain and ventral hindbrain and the ipsilateral thalamus (see above). At E10, *Tbr1* expression can be seen within the cerebellum marking the medial cerebellar nucleus (**Figure 2-9 B**), however *Lhx9* expression is limited to extra-cerebellar regions (**Figure 2-9 C**).

To compare chick expression of *Tbr1* and *Lhx9* to mouse, I performed *in situ* hybridisation on cryostat sections of hindbrain tissue from E16.5 mouse embryos. In serial sections, the expression of *Tbr1* could be seen in the nuclear transitory zone (**Figure 2-9 D**) immediately abutting the expression of *Lhx9* (**Figure 2-9 E**). In more lateral sections, *Lhx9* expression could be seen in two distinct domains in rhombomere 1: a broad population in ventral rhombomere 1, and in the nuclear transitory zone (**Figure 2-9 F**).

Comparing the expression of *Lhx9* in mouse and chick, it is evident that the *Lhx9*$^{+ve}$ nuclear transitory zone domain in mouse, is absent in chick but the more ventral domain of *Lhx9* expression is conserved between species. This distinction between species, combined with the E10 expression of *Lhx9* in chick show that chick do not have a *Lhx9*$^{+ve}$ cerebellar nucleus.

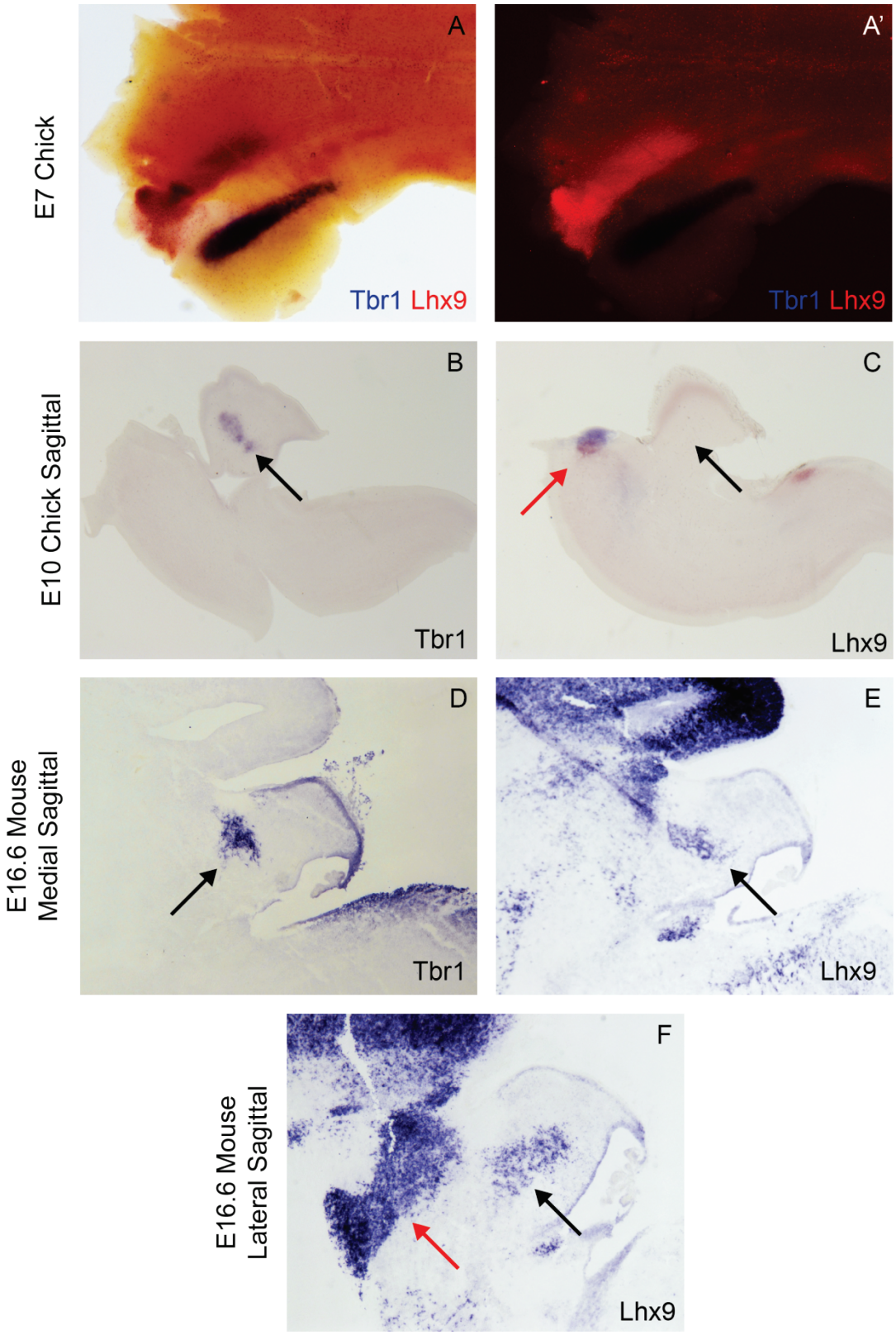

Figure 2-9 Comparative expression of *Tbr1* and *Lhx9* in chick and mouse.

Previous Page:

Figure 2-9 Comparative expression of *Tbr1* and *Lhx9* in chick and mouse.

A) E7 hindbrain of a chick embryo flat-mounted following double *in situ* hybridisation for *Tbr1* (blue) and *Lhx9* (red). A') red fluorescence of fast-red stained *Lhx9* expression. A clear gap is seen between the expression of *Lhx9* in ventral rhombomere 1 and *Tbr1* in the nuclear transitory zone. B-C) Sagittal sections through E10 chick hindbrains showing clear expression of *Tbr1* (B), but no expression of *Lhx9* (C) in the cerebellar nuclei (black arrows). Instead *Lhx9* is confined to a rostral region outside of the cerebellum (red arrow). D-F) sagittal sections of the brain of an E16.5 mouse embryo. D and E are serial sections in a mid-parasagittal region stained by *in situ* hybridisation for *Tbr1* (B) and *Lhx9* (C) showing expression of both genes in the nuclear transitory zone in a complementary manner with *Tbr1* caudal to *Lhx9* (black arrows). F shows a *Lhx9* expression in a lateral region showing two distinct domains of expression in rhombomere 1, one in a ventral/rostral region (red arrow) and the other in the nuclear transitory zone (black arrow). All tissue and sections orientated rostral to the left.

2.3 Discussion

In this chapter I have shown a specific temporal sequence of cell production from the cerebellar rhombic lip between St16 and St29 (E3-E6) in chick. Cells were characterised by axon mapping and analysis of molecular markers to reveal four distinct temporal populations: 1) *Lhx9*$^{+ve}$ population of extra-cerebellar nuclei (labelled at E3), 2) *Lhx9*$^{-ve}$*/Tbr1*$^{-ve}$ population (labelled at E4), 3) *Tbr1*$^{+ve}$ cells in the nuclear transitory zone which form the medial cerebellar nucleus (labelled at E5), and 4) cerebellar granule cell precursors in the external granule layer (labelled at E6). These data are summarised in **Figure 2-10**.

I have also shown that each of the temporal cohorts formed by the cerebellar rhombic lip comprise a mixed populations of cell types which contribute to the different axon tracts. Variation in the cohorts of cells labelled within each temporal stage and the observation that topography exists within each nucleus suggest that, within each temporal window of cell production, different regions of the cerebellar rhombic lip may contribute different cell types. I will look at this observation in more detail in chapter 5.

Finally I have identified a difference in the expression of *Lhx9* in temporal cohorts of the cerebellar rhombic lip between mouse and chick, highlighting key differences in cell specification in these two species.

2.3.1 Limitations of the experimental approach

In mapping the derivatives of the cerebellar rhombic lip I have used cumulative data to identify populations which are successively eliminated from labelling at later time points. Using these data I can infer the time point at which production of an individual population stops. However, I cannot establish the time of onset of production and therefore the degree of overlap between different populations. My conclusions are therefore based on the assumption that cell production is sequential without overlap, which has not been definitively proved in this or previous studies (Machold and Fishell, 2005; Wang et al., 2005). Analysis of the temporal onset of molecular markers of each individual population will help to clarify this (see chapter 3).

A further limitation of using a cumulative fate map is that overlapping axon tracts can mask the identity of axons from the earliest-born cohorts of cells. The axons of later-born populations can be assessed in later electroporations. Particularly for *Lhx9*$^{+ve}$ population of extra-cerebellar nuclei it is difficult to assess exactly which axons are labelled from this population. Furthermore, it has not been possible to determine the identity of these *Lhx9*$^{+ve}$ neurons. In mice, the first-born, *Lhx9*$^{+ve}$ cells of the cerebellar rhombic lip contribute to

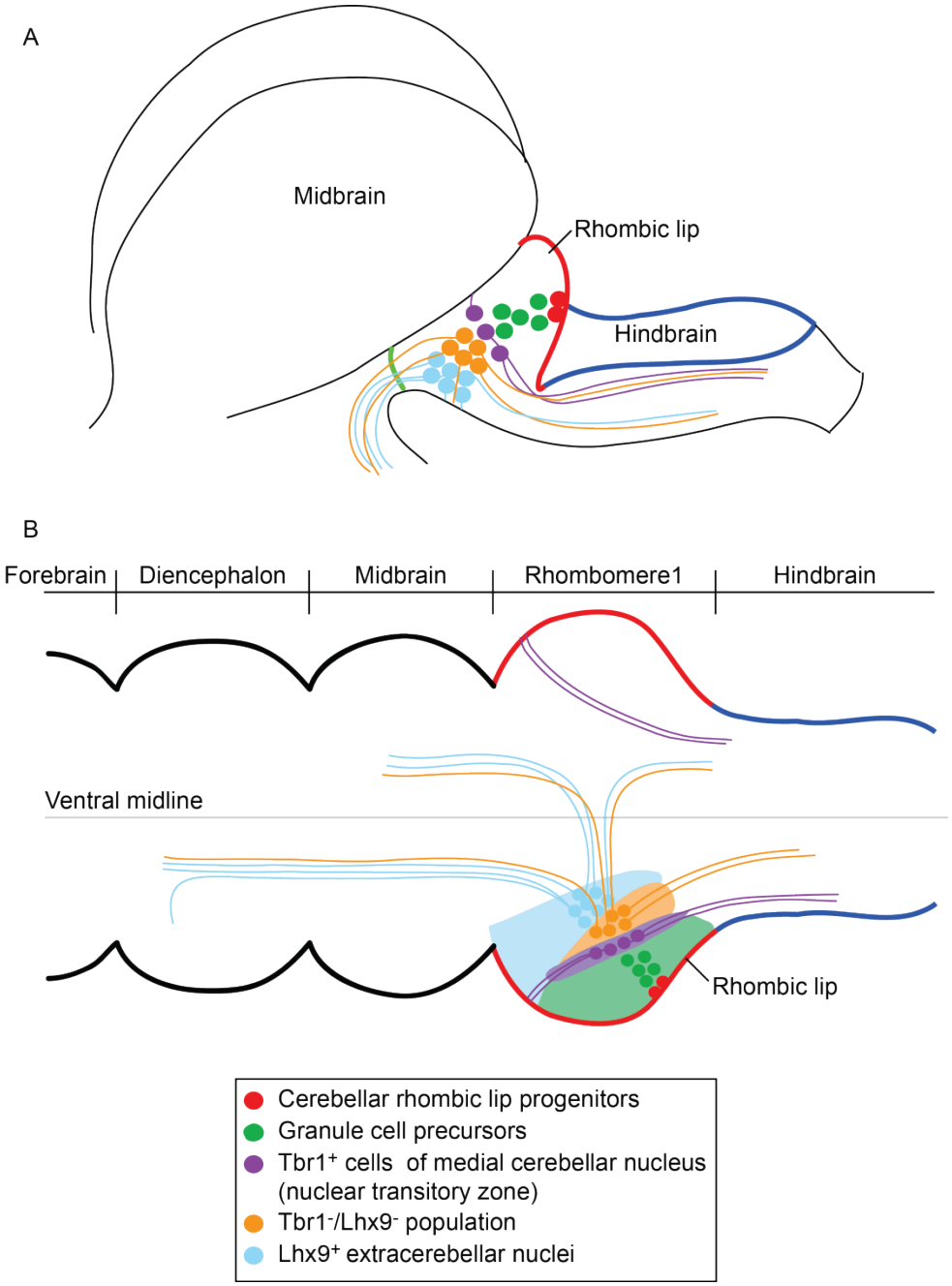

Figure 2-10 Summary of derivatives of the chick cerebellar rhombic lip from E3-E7.

Schematic of cells born from the cerebellar rhombic lip (red) between E3 and E7 and their respective axon projections shown on wholemount (A) and flatmount (B) preparations. Lhx9^{+ve} cells in ventral rhombomere 1 (blue) are born first and then subsequently more dorsal populations forming: intermediate population of Lhx9^{-}/*Tbr1*$^{-}$ cells (orange), cells of *Tbr1*$^{+ve}$ medial cerebellar nucleus which populate the nuclear transitory zone (purple) and finally granule cell precursors in the external granule layer (green).

multiple nuclei in ventral rhombomere 1 (Rose et al., 2009a) but at the embryonic stages studied, chick cerebellar rhombic lip cells are orientated into a continuous column of cells which are not segregated into individual nuclei. However, I have identified that different cell types contribute to different axon tracts from this population. It is possible that the subsequent organisation of these distinct cells may contribute to distinct nuclei within ventral rhombomere 1.

It was not possible to map the origin of entire population of *Lhx9*$^{+ve}$ cells in rhombomere 1. Attempts to electroporate the most rostral region of rhombomere 1, containing cells expressing *Lhx9* dorsally, consistently labelled more anterior populations. It is not clear whether this is representative of a caudal shift in cells within rhombomere 1 between labelling and analysis or whether this region, by its position at a deep cleft in the neural tube can simply not be labelled by electroporation.

Focal electroporations of the cerebellar rhombic lip gives a spatial resolution of label that cannot be achieved by genetic fate mapping of chimeric grafting. Furthermore, this technique allows for precise temporal characterisation and manipulations can be performed, *in vivo* at any time point. However, the technique used was not specifically selective for rhombic lip cells and required deductive elimination of other cell types based on cell morphology and prior knowledge of the origins of different populations within rhombomere 1: For example that GABAergic populations from the adjacent cerebellar ventricular zone only migrate radially (Hoshino et al., 2005). Comparisons with chimeric orthotopic grafts of the cerebellar rhombic lip provide convincing evidence that the criteria for identifying cells from the cerebellar rhombic lip were sufficient but results of electroporations with a conditional *Atoh1* reporter were not very informative.

The final limitation of the results in this chapter is that analysis was only performed at embryonic time points. Therefore the final identity of populations of cells is made by inferences based on adult avian anatomy reported in pigeons and comparison with other model organisms, namely the mouse, which in this chapter I have demonstrated has distinct differences in temporal progression of cerebellar rhombic lip derivatives both molecularly (differences in *Lhx9* expression) and morphologically (only cells of the medial cerebellar nucleus populate the nuclear transitory zone). Analysis of axons during development shows their initial trajectory and in several cases did not appear to mark the final termination point of axons, especially in the contralateral part of the brain, presumably due to the longer distances of axon growth required. Furthermore, in several different systems throughout the vertebrate central nervous system considerable remodelling of axons and selective cell death

are common mechanisms for generating mature connections within the brain (examples include: Ramoa et al. (1989), Heffner et al. (1990), O'Leary et al. (1986), reviewed by O'Leary (1987)). Therefore it cannot be assumed that early embryonic patterns of axon projections reflect connections within the adult brain.

2.3.2 What is the origin of the cerebellar nuclei in chick?

Despite these variation limitations, mapping of cerebellar rhombic lip derivatives has clearly revealed the temporal origin and position of the medial cerebellar nucleus during these developmental stages. Clearly labelled in E5, but not E6 electroporations are *Tbr1*$^{+ve}$ cells which form a morphologically distinct population of cells (due to their slight rostral migration and cell orientation) at the lateral edge of the cerebellum, the nuclear transitory zone. Axons of these cells project through the fasciculus uncinatus, a very unique axon tract across the dorsal midline, to the contralateral cerebellum and into the dorsal contralateral hindbrain. Other cells in this nucleus form ipsilateral descending tracts into the dorsal midbrain. All of these characteristics match previous reports of medial cerebellar nuclei in birds (which project to the contralateral and ipsilateral vestibular nuclei located in dorsal hindbrain) and their orthologous population in mice, the fastigial nucleus (Arends and Zeigler, 1991a; Fink et al., 2006). The only discrepancy between this population and the medial cerebellar nucleus of pigeon, described by Arends and Zeigler, is that there is no projection to the contralateral ventral hindbrain; however, such projections are observed originating from more ventral populations of rhombic lip derivatives. The method used to trace the efferents of the pigeon cerebellum used broad injections of anterograde axon tracers into the pigeon cerebellum, and thus cross over between the two cerebellar nuclei could have resulted in erroneous allocation of axon tracts to the medial or lateral nucleus (Arends and Zeigler, 1991a). Alternatively this discrepancy may point to differences in the origin in these tracts between different bird species.

The identity of rhombic lip derivatives found ventrally to the nuclear transitory zone show four distinct axon tracts and can be distinguished into two temporally distinct populations which are *Lhx9*$^{+ve}$ or *Lhx9*$^{-ve}$. Only one axon tract (ventral ipsilateral descending) was definitely confined to one of these two populations (*Lhx9*$^{-ve}$). The observation that *Lhx9* is not expressed in the E10 chicken cerebellum and is confined to extra-cerebellar cells shows that, unlike mouse, chick does not have an *Lhx9*$^{+ve}$ cerebellar nucleus. So can any of the other rhombic lip derived cells account for the cells of the lateral cerebellar nucleus?

According to Arends and Zeigler (1991a), the cerebellar efferents which are not accounted for by the *Tbr1*$^{+ve}$ medial cerebellar nucleus are projections to the red nucleus, ventral

hindbrain nuclei of the reticular formation and the spinal cord, all of which should be contralateral projections. All of these projections are potentially accounted for by the *Lhx9*$^{-ve}$/*Tbr1*$^{-ve}$ population of rhombic lip derivatives, just ventral to the nuclear transitory zone, assuming projections to the spinal cord have not yet grown this far. I therefore propose that this population is the origin of the lateral cerebellar nucleus. Additional axon tracts to ipsilateral brain targets, including the hypothalamus and possibly ventral telencephalon, which is not a target of any cerebellar circuits, can be explained by the presence of other nuclei derived from the cerebellar rhombic lip, which are not part of the cerebellar system. Alternatively, significant remodelling may occur by selective cell death of ipsilaterally projecting neurons. This interpretation of the data remains consistent with the model in mouse that cerebellar nuclei are born in temporal sequence, with the more lateral being born first (Rose et al., 2009a; Hagan and Zervas, 2012).

To confirm this hypothesis, the cells proposed to form the lateral cerebellar nucleus must be analysed into later development, when the cerebellar nuclei are internalised into the white matter of the cerebellum. Sparse cell labelling, using the Cre;Stop-*gfp* system, could also help identify the axon projections of specific populations within the cerebellar rhombic lip derivatives born between E3 and E5 to help determine their terminal identity. Molecular characterisation of these cells would also aid their identification and differentiation from other populations in the cerebellar rhombic lip lineage.

2.3.3 What is the significance of evolutionary changes in temporal patterning?

The results of this chapter highlight key differences in the development of cerebellar nuclei of chickens and mice, which may point to major differences in cerebellar function between these two species. Mammals possess a dentate nucleus which forms connections to the thalamus, but birds do not. Given the well characterised role of LHX genes in establishing cell identity and connections within the brain (see background), this difference in specification of the cerebellar nuclei in the two species may be explained by the presence of *Lhx9* expression in the dentate/interposed nuclei of mouse, but not in the lateral cerebellar nuclei of chick. Through evolution, a heterochronic shift in the window of *Lhx9* expression may have resulted in the addition of cerebellar nuclei which connect to the thalamus. This could be tested experimentally by driving the expression of *Lhx9* in chick cerebellar rhombic lip derivatives, after its normal temporal window of expression to see if the output of the cerebellum could be modulated. Alternatively, can loss of *Lhx9* expression in mouse alter the connections of the dentate/interposed nuclei?

A further difference between the mouse and chick models, is the definition of the nuclear transitory zone. In mouse, this region appears to contain cells that contribute to all of the cerebellar nuclei, expressing both *Lhx9* and *Tbr1* (Fink et al., 2006; Morales and Hatten, 2006). However, in chick, only cells of the medial cerebellar nucleus appear to accumulate in this specific region. This suggests differences in the migratory mechanisms which govern these cells during development. In the cerebellar rhombic lip lineage, migratory distances are closely associated with temporal origin (Gilthorpe et al., 2002; Wilson and Wingate, 2006) and therefore changes in the temporal identity and migration of cells of the cerebellar nuclei in chick and mouse may also point to heterochronic changes in the allocation of cells to a cerebellar fate.

Chapter 3 Molecular characterisation of the cerebellar rhombic lip and its derivatives.

3.1 Background

In this chapter I characterise the temporal progression of gene expression of cerebellar progenitor domains (cerebellar rhombic lip and cerebellar ventricular zone), cerebellar rhombic lip derivatives and the isthmic organiser, located at the rostral boundary of rhombomere 1. Genes were selected for analysis based on their previously reported expression or functions in cerebellar development. By analysing the temporal onset and dynamics of specifically expressed genes, I provide a detailed framework and hypothesis for subsequent experiments investigating the temporal specification of cell types in the cerebellum. Furthermore, I aim to confirm conclusions from chapter 2 regarding the timing of specific temporal cohorts of cells derived from the rhombic lip.

The following genes were selected for analysis in chick: *Cath1* and *Wnt1* (rhombic lip); *Ptf1a* (cerebellar ventricular zone); *Lhx9*, *Tbr1*, *Pax6* and *NeuroD1* (subsets of rhombic lip derivatives); *Otx2*, *Gbx2* and *Fgf8* (isthmus).

Atonal (Atoh1), also called *Cath1* in chick and *Math1* in mouse, is a basic helix-loop-helix transcription factor and a member of a group of genes which have been defined as having "proneural" function. Proneural genes, are necessary and sufficient to initiate a pan-neuronal identity and are expressed in specific regions in the developing nervous system to promote the generation of progenitors that are committed to differentiate into specific types of neurons and glia (reviewed by Bertrand et al. (2002)). *Atoh1* is expressed in the rhombic lip of the hindbrain and in cerebellar granule cell precursors in the external granule layer (Akazawa et al., 1995; Ben-Arie et al., 1997; Helms and Johnson, 1998) and its expression is dependent on roof plate signalling (Chizhikov et al., 2006). *Atoh1* is required for all rhombic lip derivatives, including all of the glutamatergic cells of the cerebellum, and defines the progenitor domain of the rhombic lip (Ben-Arie et al., 1997; Bermingham et al., 2001; Machold and Fishell, 2005; Wang et al., 2005; Rose et al., 2009a). *Atoh1* expression is downregulated in all rhombic lip derivatives as they leave the rhombic lip except cerebellar granule cell precursors which continue to express *Atoh1* in the external granule layer and downregulate *Atoh1* as they differentiate (Ben-Arie et al., 1997).

Ptf1a is a basic helix-loop-helix, proneural transcription factor, which is expressed in the progenitor domain of the cerebellar ventricular zone in a manner that is complementary to the expression of *Atoh1*. *Ptf1a* is required to specify all of the GABAergic neurons of the

cerebellum (Hoshino et al., 2005). *Ptf1a* has been shown to be required for GABAergic cell fate in many different populations of neurons whilst *Atoh1* generally specifies glutamatergic fate. The spatial separation of *Ptf1a* and *Atoh1* expressing progenitor domains is a well-established convention which is used to create cell neuronal diversity in multiple different systems as well as in the cerebellum (Glasgow et al., 2005; Hoshino et al., 2005; Machold and Fishell, 2005; Wang et al., 2005; Fujiyama et al., 2009).

Wnt1, a secreted signalling molecule, is expressed in the cerebellar rhombic lip precursor pool and at the isthmus (Wilkinson et al., 1987; Hollyday et al., 1995; Rodriguez and Dymecki, 2000) . *Wnt1* mutant mice show a complete deletion of the cerebellum and caudal midbrain due to its requirement to maintain the isthmic organiser (McMahon and Bradley, 1990; McMahon et al., 1992). Because of this major deletion in *Wnt1*-null mice, the function of *Wnt1* within the rhombic lip is not known. Mapping of of the *Wnt1* lineage within the hindbrain reveals that all of the precerebellar nuclei of the hindbrain and all cerebellar rhombic lip derivatives are derived from *Wnt1*$^{+ve}$ precursors (Rodriguez and Dymecki, 2000; Landsberg et al., 2005; Hagan and Zervas, 2012). The caudal midbrain is also derived from a small domain of *Wnt1*$^{+ve}$ cells at the isthmus (Zervas et al., 2004).

Lhx9, a LIM-homeodomain transcription factor is expressed in a subset *Math1*$^{+ve}$ cells throughout the hindbrain and spinal cord (Bermingham et al., 2001; Rose et al., 2009a). Within the hindbrain in mouse, *Lhx9* is expressed in the first-born cohorts of cells from the rhombic lip, which in rhombomere 1 constitutes extra-cerebellar cells in ventral rhombomere 1 and the dentate and interposed cerebellar nuclei (Rose et al., 2009a). The expression of *Lhx9* is dependent on the expression of *Atoh1* (Bermingham et al., 2001; Wang et al., 2005; Rose et al., 2009a), but in the cerebellar rhombic lip derived populations the specific function of *Lhx9* is not known. In spinal cord populations, loss of *Lhx9* or other LIM-homeodomain genes results in major alterations in the axon projections and cell specification of several classes of interneurons and motor neurons (Thor et al., 1999; Wilson et al., 2008; Avraham et al., 2009). Rose et al. (2009a) have identified that across the entire hindbrain, rhombic lip derivatives can be broadly categorised into early-born *Lhx9*-expressing and late-born *Barhl1*-expression neurons. This observation suggests that there may be a global temporal transition across the hindbrain in neuronal specification. I therefore include analysis of lower-hindbrain expression in my temporal characterisation of different genes.

Tbr1 is a T-box transcription factor which is expressed in cells of the medial/fastigial cerebellar nucleus (Fink et al., 2006). *Tbr1*-null mice show only a mild disruption of the morphology of the medial/fastigial nucleus but no change in cell number or axon projections

(Fink et al., 2006). *Tbr1* is also expressed in postmitotic neurons of the cerebral cortex (Bulfone et al., 1995) and is required for the correct specification and axon projection of specific subsets of cortical neurons (Hevner et al., 2001; Hevner et al., 2002). *Tbr2*, a close relative of *Tbr1* is also expressed in the developing cerebellum, transiently labelling cerebellar granule neurons and unipolar brush cells (Bulfone et al., 1999; Englund et al., 2006).

Pax6, a paired-homeodomain transcription factor, which is expressed in a large number of populations in the developing central nervous system (Walther and Gruss, 1991) and has a wide variety of functions in neural and non-neural tissues, including regulating proliferation, specification, differentiation, cell death, migration and cell adhesion (for review see Simpson and Price (2002)). In the developing cerebellum , *Pax6* is expressed in granule neurons (Engelkamp et al., 1999). Analysis of the "smalleye" *Pax6* mutant mouse (*Pax6*$^{sey/sey}$) shows that although granule cells are still produced from the rhombic lip in the absence of *Pax6*, their migration and terminal differentiation is disrupted (Engelkamp et al., 1999; Swanson et al., 2005). *Pax6* has also been shown to be expressed transiently in other cerebellar rhombic lip populations in the nuclear transitory zone and in unipolar brush cells (Englund et al., 2006; Fink et al., 2006). In the lower hindbrain, *Pax6* has been shown to regulate the dorsal progenitor domains which contribute to different populations of hindbrain nuclei, including the precerebellar nuclei (Engelkamp et al., 1999; Landsberg et al., 2005).

NeuroD1, a basic helix-loop-helix transcription factor, is expressed in post mitotic granule cells but has not been identified in any other cells of the cerebellar rhombic lip lineage (Miyata et al., 1999; Lee et al., 2000a). When *NeuroD1* expression is lost, cerebellar granule cell precursors in the external granule layer are unable to differentiate into mature granule cells (Miyata et al., 1999). Overexpression of *NeuroD1* prevents tangential migration of granule cell precursors and drives immediate differentiation (Thomas Butts, unpublished data).

Pax6, *Tbr2*, *NeuroD1* and *Tbr1* are all transcription factors which mark populations of cerebellar rhombic lip derivatives (see above). These transcription factors are also expressed in sequential order during the specification of glutamatergic cortical neurons and granule cells of the hippocampus. It has been suggested that this network of transcription factors could create a general program for the specification of glutamateric cells (Hevner et al., 2006) but the individual genes are expressed in many different populations of neurons (not only glutamatergic) and have been shown to have many different functions in controlling proliferation, migration and specification.

The isthmus is the boundary between *Otx2*$^{+ve}$ midbrain tissue and *Gbx2*$^{+ve}$ hindbrain tissue. *Otx2* and *Gbx2,* both homeobox transcription factors, are required for and are sufficient to induce and position the respective compartments of the midbrain and hindbrain (Acampora et al., 1995; Acampora et al., 1997; Broccoli et al., 1999; Millet et al., 1999; Katahira et al., 2000). The secreted signalling molecule, FGF8 is induced at the boundary between these two tissue (Crossley and Martin, 1995; Irving and Mason, 1999) and is required for the development of the caudal midbrain and anterior hindbrain (Meyers et al., 1998; Reifers et al., 1998; Chi et al., 2003)

FGFs are secreted ligands which bind to receptor tyrosine kinases (FGFRs) to activate intracellular signalling cascades which can alter transcription of specific genes in a context-dependent manner to control a variety of developmental processes including regulating proliferation, growth, differentiation and cell death (for review see Dailey et al. (2005)). Although there are several intracellular signalling pathways downstream of FGF signalling, the Ras-ERK pathway has been shown to mediate the known effects of FGF8 signalling at the isthmus (Sato and Nakamura, 2004). *Sprouty* genes are activated in response to FGF signalling through the Ras-ERK signalling pathway (Ozaki et al., 2001) and act to negatively regulate FGF signalling (Kramer et al., 1999). *Sprouty2* is expressed at the isthmus in response to FGF8 signalling (Chambers and Mason, 2000; Chambers et al., 2000).

3.2 Results

3.2.1 Rhombic lip markers *Wnt1* and *Cath1* show rostrocaudal polarity within rhombomere1

To examine how the rhombic lip changes over time as different temporal cohorts are produced I looked the expression of two rhombic lip markers, *Wnt1* and *Cath1,* by *in* situ hybridisation at different time points.

At E3 (St16), the earliest time point analysed, *Wnt1* is expressed in the rhombic lip throughout the hindbrain, at the isthmus and in the dorsal midline of the midbrain (**Figure 3-1 A**). *Wnt1* expression in the midbrain, isthmus and hindbrain rhombic lip remain unchanged until E6 (St29), the latest stage analysed (**Figure 3-1 B-D**). Within rhombomere 1, *Wnt1* is initially expressed in the E3 cerebellar rhombic lip in a gradient with expression lowest near the isthmus and highest at the boundary with rhombomere 2. This gradient is also seen at E4 and E5 (**Figure 3-1 A-C**) but, by E6, *Wnt1* is expressed uniformly throughout the cerebellar rhombic lip except for a region in the most rostral part of rhombomere 1, abutting the isthmus, from which *Wnt1* expression is excluded (**Figure 3-1 D**). The most rostral

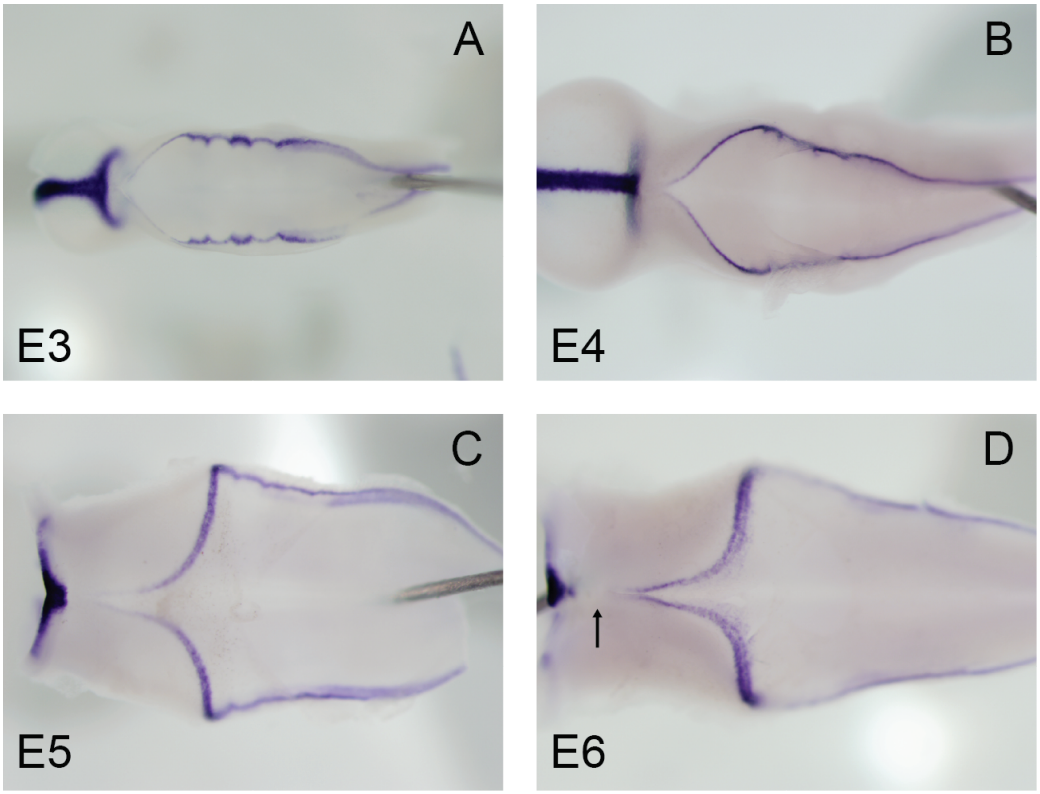

Figure 3-1 *Wnt1* expression from E3 to E6

Dorsal view of hindbrain stained by i*n situ* hybridisation for *Wnt1* at E3 (A), E4 (B), E5 (C) and E6 (D). Orientated rostral to left. At all stages *Wnt1* is expressed in the rhombic lip, isthmus and dorsal midline of the midbrain. In rhombomere 1 *Wnt1* is expressed in a gradient (A-C) or is exluded from rostral rhombomere 1 (D, arrow).

expression of rhombic lip *Wnt1* lies at the point where the roofplate expands at the fourth ventricle. Therefore the most rostral region of dorsal rhombomere 1 is molecularly distinct from the rest of the rhombomere.

At all stages analysed between E3 (St16) and E6 (St29) *Cath1* is expressed in the cerebellar rhombic lip of the entire hindbrain (**Figure 3-2**). At E3 and E4 expression in the cerebellar rhombic lip of rhombomere 1 is seen in a broader domain than in the rest of the hindbrain (**Figure 3-2 A-C**). At E5 (St27) *Cath1* expression is expressed in two distinct, but continuous domains in rhombomere 1: a broad domain in the rostral third of dorsal rhombomere 1, abutting the isthmus, and rhombic lip expression in the caudal two thirds of the rhombomere. In contrast to E3/4, at E5 rhombic lip expression is of uniform width between rhombomere 1 and the rest of the hindbrain (**Figure 3-2 D-E**). At a slightly earlier E5 stage, St26, a faint, or graded expression of *Cath1* can be seen broadly in the cerebellum which is no longer present by St27 (**Figure 3-2 E,F**). Vibratome sections of St27 hindbrain reveal that that the broad rostral domain of *Cath1* expression extends throughout the depth of the tissue from the ventricular to the pial surface (**Figure 3-2 G-I**). Ventricular expression of *Cath1* suggests this may be a progenitor domain rather than an accumulation of rhombic lip derivatives which migrate across the pial surface of the hindbrain.

At E6, the first *Cath1*$^{+ve}$ cerebellar granule cell precursors can be seen on the pial surface of the cerebellum forming the external granule layer. At this stage the rhombic lip and broad rostral domain (which abuts the external granule layer) still express *Cath1* (**Figure 3-2 J,K**). By E7, the broad rostral domain of *Cath1* expression become confined to a region outside of the cerebellum which is no longer continuous with the rhombic lip or external granule layer expression of *Cath1* (**Figure 3-2 L,M**). At E7, *Cath1* is also no longer expressed in the hindbrain rhombic lip caudal to rhombomere 1. From E8 to E10 (the latest stage analysed), as the cerebellum expands and begins to foliate, *Cath1* expression is only found in the cerebellar rhombic lip and the external granule layer (**Figure 3-2 N,O**).

Additional sites of *Cath1* expression are seen ventrally in the lower hindbrain (rhombomeres 2-8) in postmitotic neurons of the paratrigiminal nucleus of rhombomere 2 and the parafacial nucleus of rhombomere 5 (Rose et al., 2009b). *Cath1* expression can be seen in the paratrigeminal nucleus from St25 (E4.5) and parafacial nuleus from St28 (E6). *Cath1* expression in both of these nuclei is no longer seen at E7. These sites of expression can clearly be seen in **Figure 3-2 E,F,H,K (*)** but not as easily visible in whole-mount pictures.

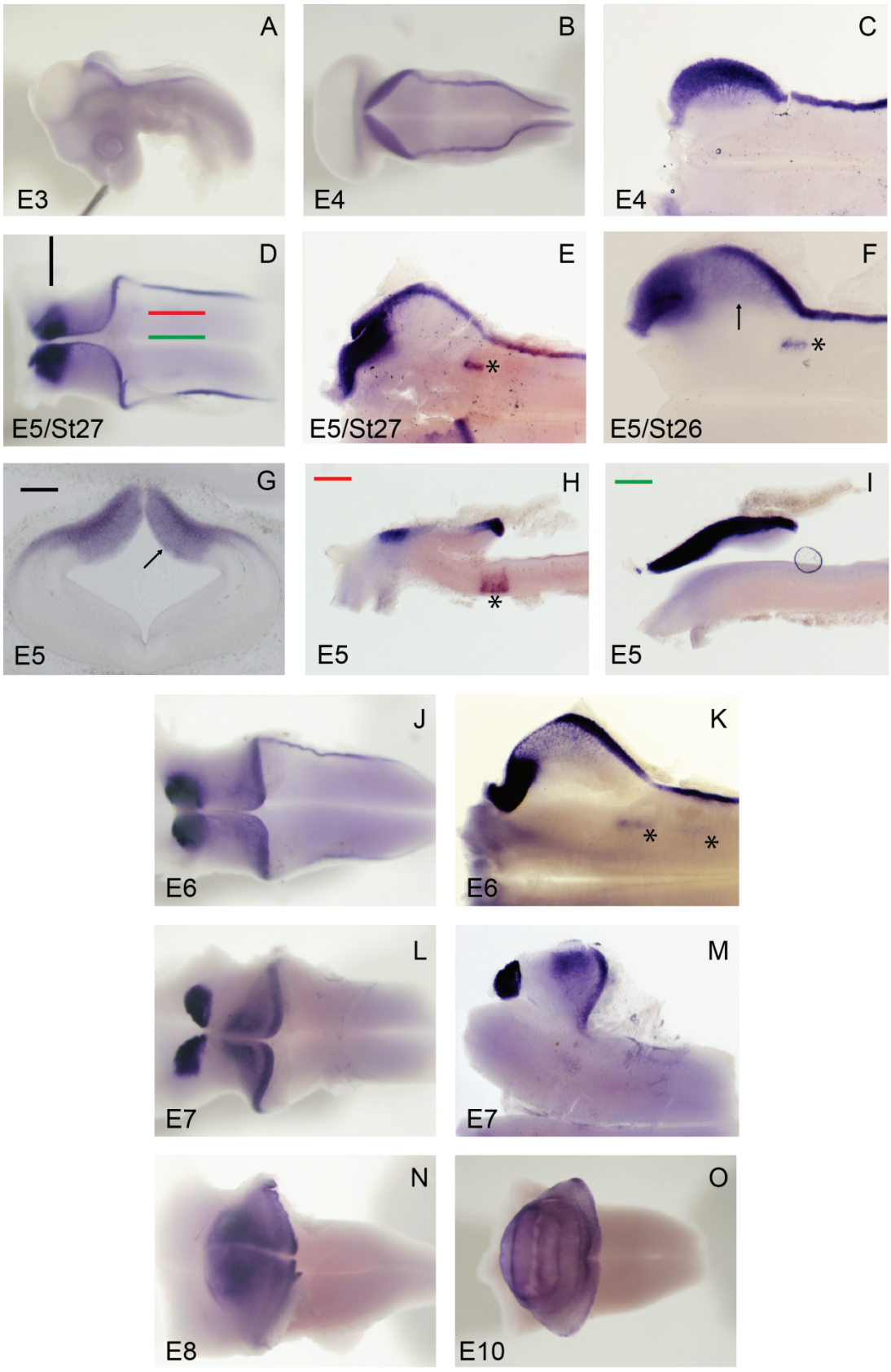

Figure 3-2 *Cath1* expression from E3 to E10

Previous page:

Figure 3-2 *Cath1* expression from E3 to E10

In situ hybridisation of *Cath1* between E3 and E10 (age indicated on picture) in lateral (A), dorsal (B,D,J,L,N,O) or flat-mount (C,E,F,K,M) view on in coronal (G) or sagittal section (H,I) at the level indicated in D. Orientated rostral to left. Expression is seen: in the rhombic lip (A-O), but is broader in rhombomere 1 at E3/4 (A-C); in broad rostral domain (D-M) extending to the ventricular zone (G, arrow); in faint broad domain across cerebellum (F, arrow); in external granule layer (J-O); and in hindbrain nuclei (E,F,H,K *).

Together the expression patterns of *Wnt1* and *Cath1* demonstrate that from St26/E5 the rostral domain of dorsal rhombomere 1 is molecularly distinct from the rest of dorsal rhombomere 1. This domain subsequently forms extra-cerebellar tissue between the rostral extent of the external granule later and the isthmus.

3.2.2 *Tbr1* marks the nuclear transitory zone and medial cerebellar nucleus

Electroporation mapping experiments show that *Tbr1*-positive cells in the nuclear transitory zone give rise to the medial cerebellar nucleus and are born between St26 and St28 (E5-6), just before the onset of granule cell production. To follow the movement of these cells and assess their final position in the cerebellum I examined *Tbr1* expression from St27/E5 onwards. At St27/E5, no expression of *Tbr1* is detected anywhere in the hindbrain (**Figure 3-3 A**). At St28/E6, *Tbr1* expression can be seen in the in the nuclear transitory zone but not in any cells in the pial migratory stream from the rhombic lip (**Figure 3-3 B-D**). Thus *Tbr1* is not expressed in rhombic lip derivatives until cells reach the nuclear transitory zone at the end of their tangential migration. At E7, *Tbr1* is still expressed in the nuclear transitory zone (**Figure 3-3 E**) but from E8-10 the *Tbr1*$^{+ve}$ domain moves internally into the centre of the cerebellum to form the medial cerebellar nucleus (**Figure 3-3 F-I**).

Double in situ hybridisation for *Tbr1* and *Cath1* at E6 (completed by Anna Myat) demonstrates that in the most rostral region of rhombomere 1, *Tbr1* expression in the nuclear transitory zone partially overlaps the broad rostral domain of *Cath1* expression at the pial surface (**Figure 3-3 J**). In contrast, in more caudal rhombomere 1, *Tbr1* expression abuts the lateral edge of the *Cath1*$^{+ve}$ external granule layer (**Figure 3-3 K**).

3.2.3 *Pax6* and *NeuroD1* have multiple sites of expression in rhombomere 1

In chick, *Pax6* is not expressed anywhere within dorsal rhombomere1 until St28/E6 where expression can be seen in the cerebellar rhombic lip, nuclear transitory zone and external granule layer (**Figure 3-4 A-G**). Since cells of medial cerebellar nucleus are born prior to E6, *Pax6* therefore does not mark these cells as they migrate towards the nuclear transitory zone and, much like *Tbr1*, is expressed in cells once they reach the nuclear transitory zone. Between E6 and E8 *Pax6* expression in the external granule layer becomes stronger and is downregulated in cells of the nuclear transitory zone as they migrate internally into the cerebellum (**Figure 3-4 H-L**). At E10, *Pax6* is only expressed in the external granule layer (**Figure 3-4 M**).

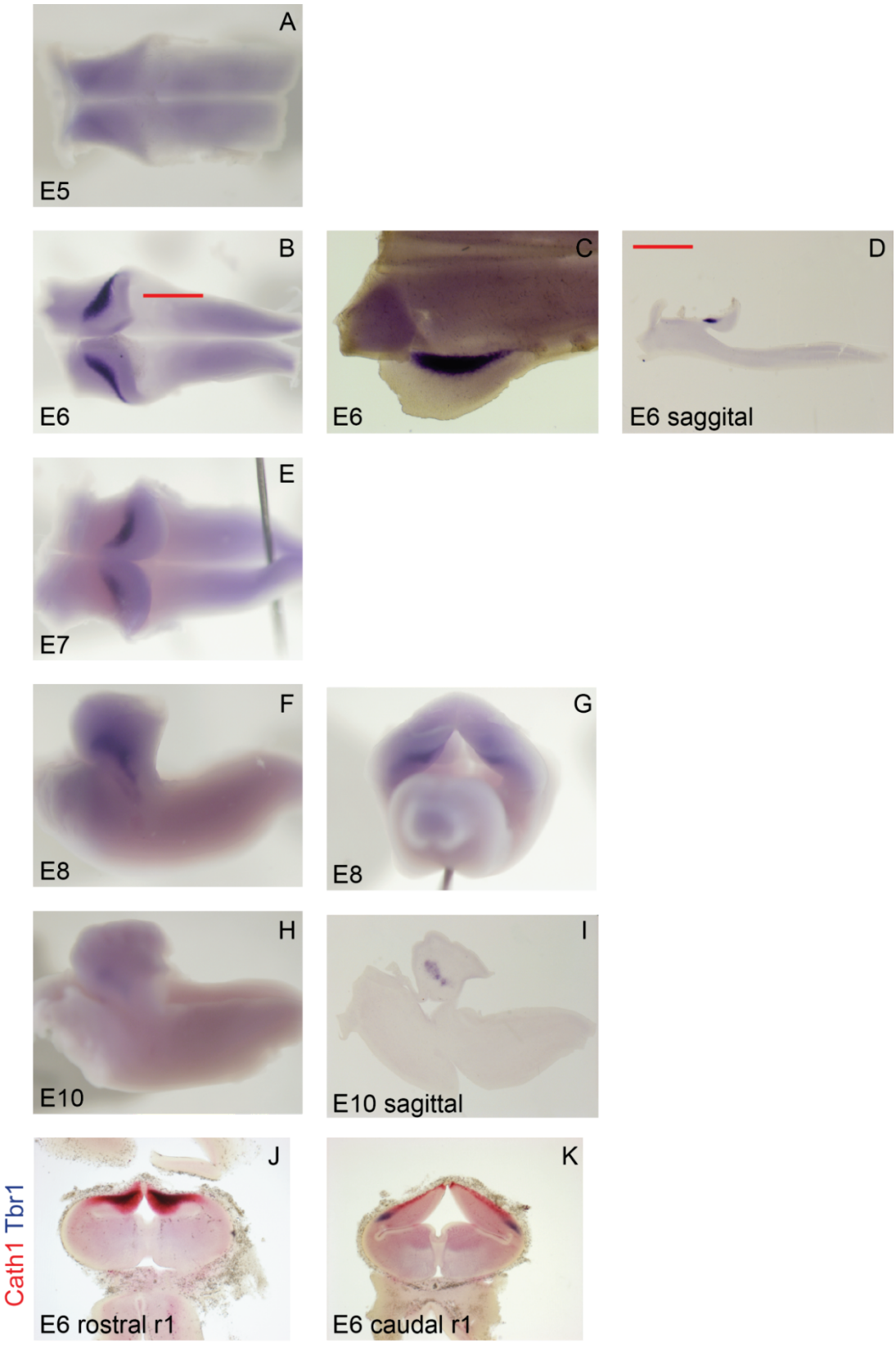

Figure 3-3 *Tbr1* expression from E5 to E10

Previous page:

Figure 3-3 *Tbr1* expression from E5 to E10

In situ hybridisation for *Tbr1* (A-I) or *Tbr1* and *Cath1* (J,K) between E3 and E10 (age indication on picture). Hindbrain shown in dorsal (A,B,E), flat-mount (C), lateral (F,H) or posterior (G) view or in sagittal (I and D at level indicated in B) or coronal section (J,K). Orientated rostral to left or dorsal top. Expression is seen in the nuclear transitory zone/medial cerebellar nucleus and shows partial overlap with broad domain of *Cath1* (J) but complementary expression with *Cath1* in external granule layer (K). Double *in situ* hybridisation sections (J,K) by Anna Myat.

Next page:

Figure 3-4 *Pax6* expression from E3 to E10

In situ hybridisation of *Pax6* between E5 and E10 (age indicated on picture). Hindbrain shown in dorsal (A,B,C,E,H,J,M) or flat-mount (D,F,I,K) view or sagittal section (G,L). Orientated rostral to left (or rostral top:K). Expression is seen in: ventral hindbrain stripes (A-I), rhombic lip (E-M), nuclear transitory zone (E-I), external granule layer (E-M), cerebellar ventricular zone (G), lower hindbrain populations (F,I,K). Abbreviations: NTZ: nuclear transitory zone, EGL: external granule layer, VZ: cerebellar ventricular zone.

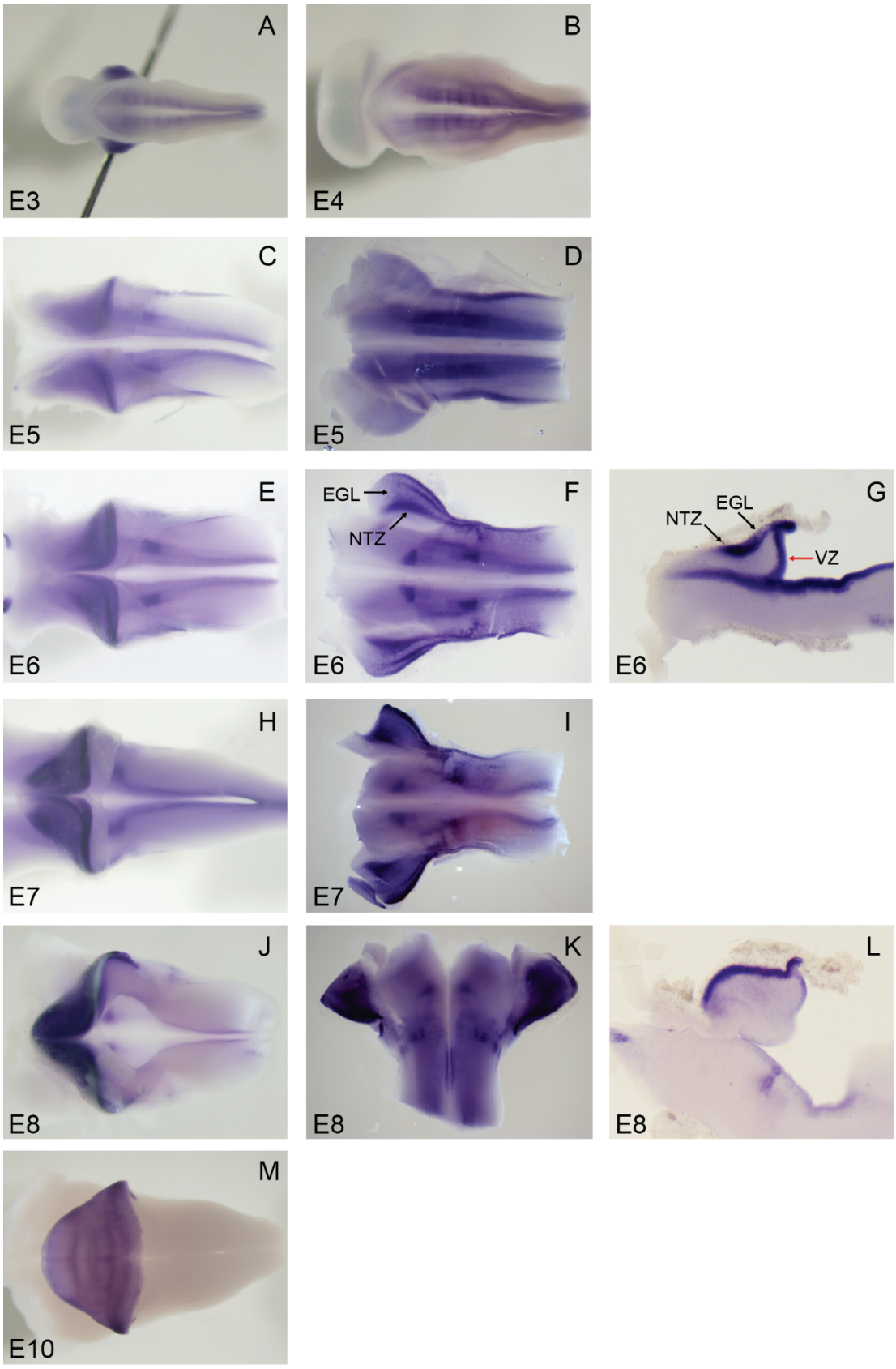

Figure 3-4 *Pax6* expression from E3 to E10

Sagittal sections through the cerebellum at E6 surprisingly reveal that *Pax6* is also expressed in cerebellar ventricular zone (**Figure 3-4 G**). This site of expression has not previously been reported and demonstrates that *Pax6* expression is not specific to the rhombic lip and rhombic lip derivatives. By E8, cerebellar ventricular zone expression of *Pax6* is absent or very faint (**Figure 3-4 L**)

In the lower hindbrain (rhombomere 2-8) *Pax6* is expressed in the rhombic lip from E5 to E7 and *Pax6*$^{+ve}$ rhombic lip derivatives can be seen on the pial surface of the hindbrain from E6-E8 (**Figure 3-4 D-K**). Caudal to rhombomere 1, *Pax6* expression is also seen from E3 to E7 in two distinct stripes in the ventral ventricular zone along the anterior-posterior length of the hindbrain. Within these stripes, particularly strong expression is seen from E6 in rhombomeres 2 and 5, which remains through to E8.

NeuroD1 is not expressed in dorsal rhombomere 1 until St28/E6 when expression can be seen in the nuclear transitory zone and faintly within the external granule layer and ventricular zone of the cerebellum (**Figure 3-5 A-E**). *NeuroD1* expression in the external granule layer gradually increases until E8 when expression covers the entire surface of the cerebellum (**Figure 3-5 C-H**). *NeuroD1* is downregulated in cells of the nuclear transitory zone by E8, when cells of the cerebellar nuclei begin to move internally into the cerebellum. Throughout the ventral hindbrain *NeuroD1* is expressed in the ventricular zone in two stripes from E5 to E6 (**Figure 3-5 A-D**). Therefore, *NeuroD1* is expressed in the same regions in rhombomere 1 as *Pax6*.

Throughout the entire hindbrain *NeuroD1* is expressed in two ventral stripes between E5 (the earliest stage analysed) and E6. In rhombomeres 2-8, *NeuroD1* is expressed in pial populations throughout the dorsal hindbrain from E6, including a population which is continuous with the rhombomere 1 nuclear transitory zone. These cells are may also be rhombic lip derivatives but do not mark the same populations as *Pax6* (compare **Figure 1-5 D,G** with **Figure 1-4 F,I,K**). *NeuroD1* expression is retained in these hindbrain populations until E8, the latest stage analysed (**Figure 3-5 C-H**).

3.2.4 *Ptf1a* is transiently expressed within the rhombic lip

I next examined the expression of *Ptf1a*, a marker of the cerebellar ventricular zone progenitor domain which contributes GABAergic cells to the cerebellum, to compare temporal changes with rhombic lip populations. *Ptf1a* is expressed caudally to rhombomere 1 in distinct progenitor domains which form longitudinal stripes in the hindbrain from St21, the earliest stage analysed. This hindbrain expression then extends into rhombomere 1 at

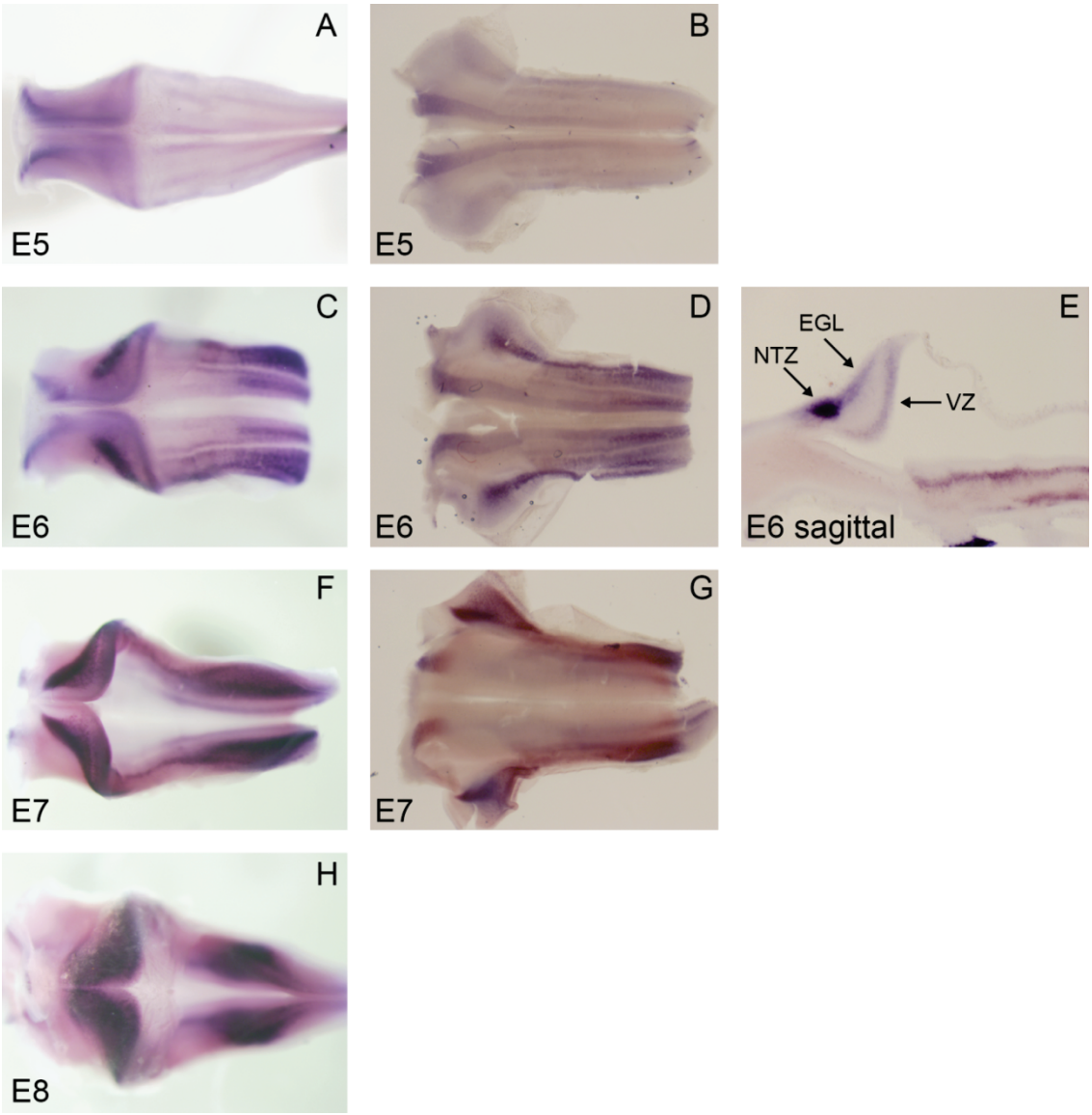

Figure 3-5 *NeuroD1* expression from E5 to E8

In situ hybridisation of *NeuroD1* between E5 and E8 (age indicated on picture). Hindbrain shown in dorsal (A,C,F,H) or flat-mount (BDG) view or sagittal section (E). Orientated rostral to left. Expression is seen in: ventral hindbrain stripes (A-E), nuclear transitory zone (C-G), external granule layer (C-H), cerebellar ventricular zone (E), lower hindbrain populations (C-H). Abbreviations: NTZ: nuclear transitory zone, EGL: external granule layer, VZ: cerebellar ventricular zone.

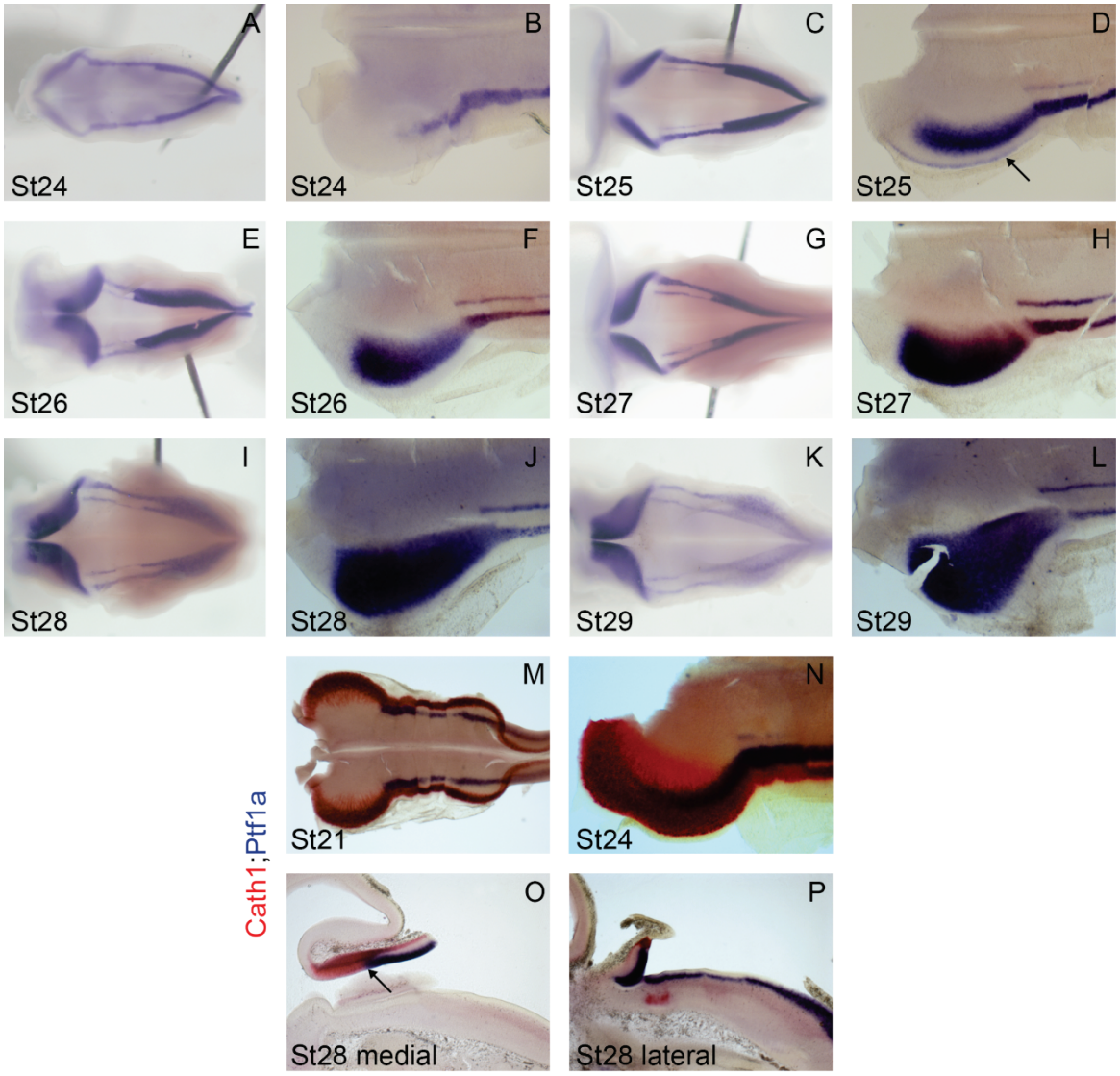

Figure 3-6 *Ptf1a* expression from St24/E4 to St29/E6

In situ hybridisation of *Ptf1a* (A-L) or *Ptf1a* and *Cath1* (M-P) between St24/E4 and Sr29/E6 (age indicated on picture). Hindbrain shown in dorsal (A,C,E,G,I,K) or flat-mount (B,D,F,H,J,L,M,N) view or sagittal section (O,P). Orientated rostral to left. *Ptf1a* expression seen in ventricular zone (A-P) complmentary to *Cath1* expression (M-P) and *Ptf1a* is expressed in rhombic lip (D only). *Cath1;Ptf1a* double *in situ* hybridisation (M-P) by Anna Myat.

St23/24 to be expressed in the cerebellar ventricular zone, where it is expressed up to E6, the latest stage analysed (**Figure 3-6 A-L**).

Double in situ hybridisation for *Ptf1a* and *Cath1* (performed by Anna Myat), demonstrates complementary expression of these two genes at E4 and E6 in dorsal rhombomere 1, including the broad rostral domain of *Cath1* expression abutting the isthmus (**Figure 3-6 M-P**). In E4 flat-mounted hindbrains *Cath1* expression, appears to overlap *Ptf1a*, however *Cath1* expression is confined to the pial surface and *Ptf1a* to the ventricular surface (not shown). Despite this complementary expression, *Ptf1a* expression was also transiently seen in the rhombic lip at St25 (E4.5) (**Figure 3-6D**). This rhombic lip expression of *Ptf1a* has never previously been reported and brings into questions the model of allocation of different cerebellar cells from spatially distinct progenitor domains.

3.2.5 *Lhx9* expression marks early rhombic lip derivatives and highlights an extra-cerebellar, rostral domain in dorsal rhombomere 1.

In rhombomere 1, *Lhx9* is expressed in the cerebellar rhombic lip from E3-E5 and can be seen in cells in a pial migratory stream from the rhombic lip at E3 and E4 (**Figure 3-7 A-H**). *Lhx9*$^{+ve}$ cells which migrate ventrally from the rhombic lip form a a population of extra-cerebellar cells extending from ventral rhombomere 1 caudally, to dorsal rhombomere 2 rostrally. *Lhx9* is expressed in this population of cells up to E10, the latest stage analysed.

Lhx9 expression in the lower hindbrain mirrors the temporal changes in rhombomere 1 with rhombic lip expression seen from E3 to E5 and *Lhx9* expression retained in more ventrally located rhombic derivatives at all stages analysed up to E10, though expression is much weaker than in rhombomere 1 from E7 to E10 (**Figure 3-7**).

In dorsal rhombomere 1, *Lhx9* expression is restricted a rostral domain, outside of the cerebellum, abutting the isthmus. From E5-E7 this region of rhombomere 1 is marked by the broad domain of *Cath1* expression. To examine the relationship between *Cath1* and *Lhx9* expression I performed double *in situ* hybridisation of these two genes between E4 and E6.

At E3/E4, when the expression of *Cath1* is broader in the cerebellar rhombic lip than the lower hindbrain (rhombomere 2-8), *Lhx9*$^{+ve}$ cells migrate from the broad cerebellar rhombic lip (**Figure 3-8 A**). At E5, the broad domain of *Cath1* expression is only seen in rostral rhombomere 1 whilst caudal rhombomere 1 shows narrow rhombic lip expression. At this time point *Lhx9*$^{+ve}$ cells are seen in a domain that overlaps with, and extends from, the broad rostral domain of Cath1 (**Figure 3-8 B**). This pattern is maintained at E6 when the caudal cerebellar rhombic lip, marked by a narrow domain of *Cath1*, begins to produce *Cath1*$^{+ve}$

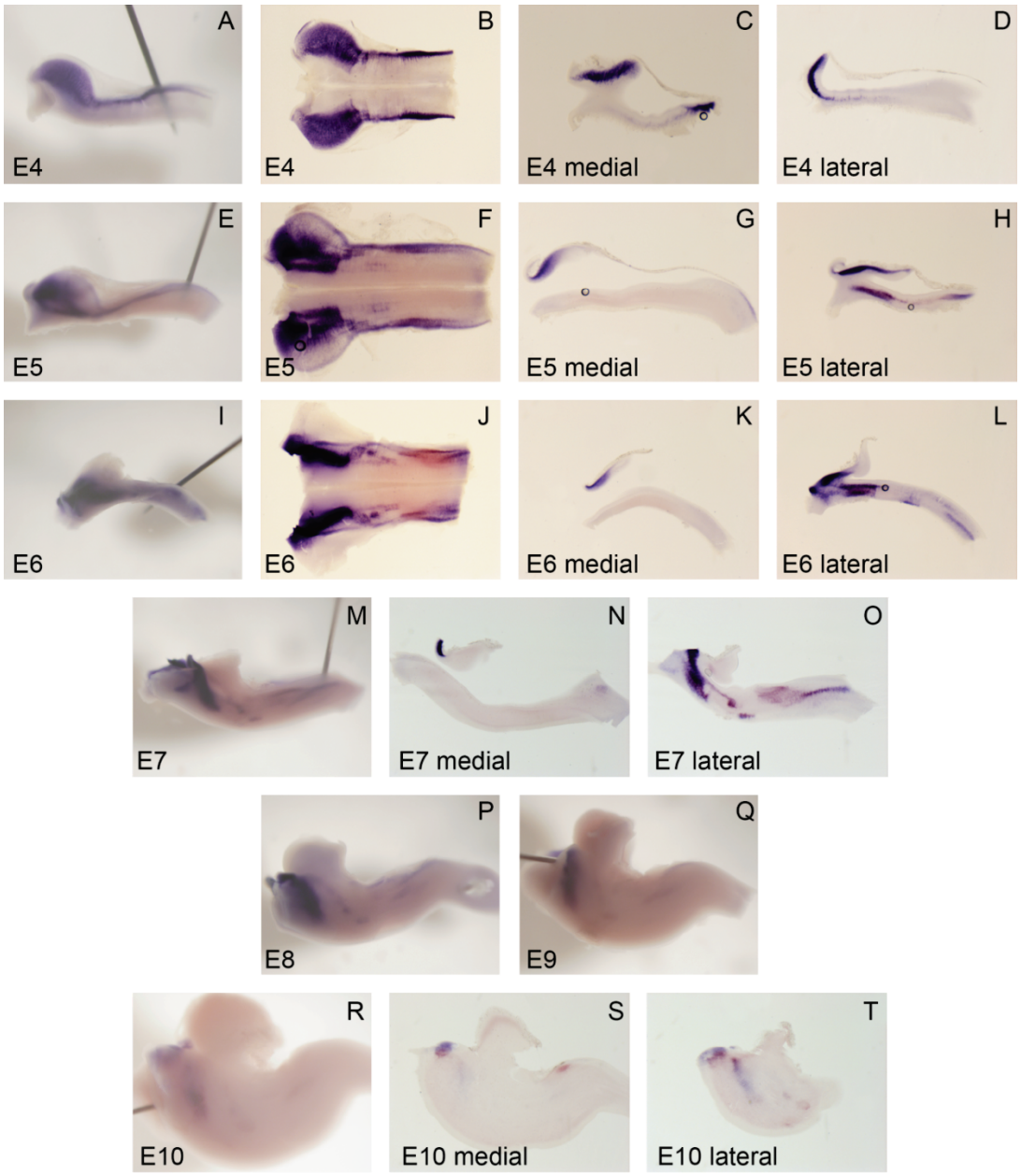

Figure 3-7 *Lhx9* expression from E4 to E10

In situ hybridisation of *Lhx9* between E4 and E10 (age indicated on picture). Hindbrain shown in lateral (A,E,I,M,P,Q,R) or flat-mount (B,F,K) view or sagittal section (C,D,G,H,K,L,N,O,S,T). Orientated rostral to left. *Lhx9* expression is seen in rhombic lip (A-H) and rhombic lip derivatives (A-T). In rhombomere 1 *Lhx9* is expressed in extra-cerebellar populations extending from dorsal (rostral rhombomere 1) to ventral (caudal rhombomere 1).

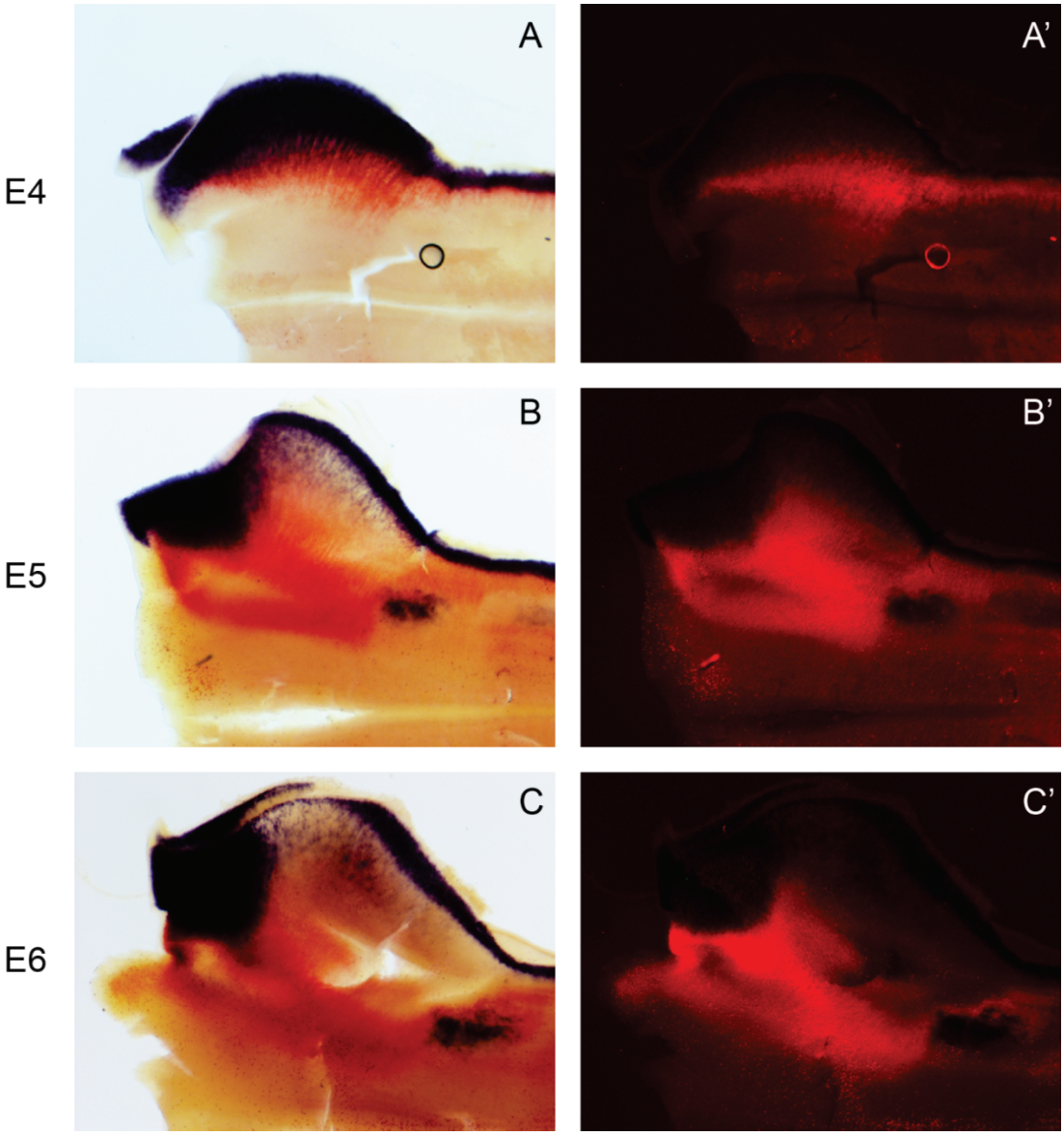

Figure 3-8 *Cath1* and *Lhx9* expression from E4 to E6

Double *in situ* hybridisation of *Cath1* and *Lhx9* between at E4 (A), E5 (B) and E6 (C). Half of rostral hindbrain shown in flatmount (rostral to left). A',B'C' show red fluorescence. *Cath1* and *Lhx9* expression overlap at E4 at the broad rhombic lip and in dorsal rostral domain at E5/6.

cerebellar granule cell precursors (**Figure 3-8 C**). This demonstrates a close association between dorsal *Lhx9* expression and broad expression of *Cath1*, both throughout the whole cerebellar rhombic lip at E4 and in the broad rostral domain from E5. Therefore, between E4 and E5, both of these genes show a rostral restriction towards the midbrain-hindbrain boundary (isthmus). Does signalling from the isthmus orchestrate this graded pattern of gene expression?

3.2.6 Changes in isthmic gene expression are associated with polarisation of rhombomere 1.

In order to study the function of the isthmus I first analysed the temporal progression of the isthmic gene *Fgf8* and regional determination genes *Otx2* and *Gbx2*.

Double *in situ* hybridisation for *Otx2* and *Gbx2* show that at E3 (St18), the earliest stage analysed, *Otx2* is expressed throughout the midbrain and *Gbx2* is expressed throughout whole of the hindbrain (**Figure 3-9 A**). At this time point *Fgf8* is expressed uniformly throughout the dorsoventral axis within the *Gbx2*-positive domain at the boundary of these two compartments (**Figure 3-9 B,C**).

At all subsequent stages analysed, up to E6, *Otx2* expression remains constantly expressed in midbrain tissue. However, from E4 to E5 *Gbx2* expression is down regulated in ventral rhombomere 1 except in a small domain abutting the expression of *Otx2* (**Figure 3-9 D,G**). This change in *Gbx2* expression coincides with a dorsal expansion and ventral reduction of *Fgf8* expression at the isthmus (**Figure 3-9 E,F,H**).

At E6 *Gbx2* expression is only present in dorsal rhombomere 1 (**Figure 3-9 I**). Between E6 and E7 *Fgf8* expression is gradually lost ventrally to leave only a small dorsal domain (Figure 3-9 J). *Fgf8* is no longer seen at the isthmus from E8 (not shown).

The time point (E5) at which *Fgf8* expression first becomes expanded dorsally and reduced ventrally coincides with restriction of the broad *Cath1*$^{+ve}$ domain to rostral rhombomere 1. Double *in situ* hybridisation for *Fgf8* and *Cath1* (by Anna Myat) shows an overlap in the expression of these two genes in dorsal, rostral rhombomere 1 (**Figure 3-10 A,B**). *Cath1* expression does not extend into *Otx2*$^{+ve}$ midbrain tissue at the isthmus (**Figure 3-10 C**).

I next analysed the expression of *Sprouty2*, a direct downstream target (and negative regulator) of FGF signalling (Suzuki-Hirano et al., 2005), compared to *Cath1*. At St18 (E3) and St22 (early E4) when the broad domain of *Cath1* is seen throughout rhombomere 1, *Sprouty2* expression extends from the isthmus throughout the whole of rhombomere 1.

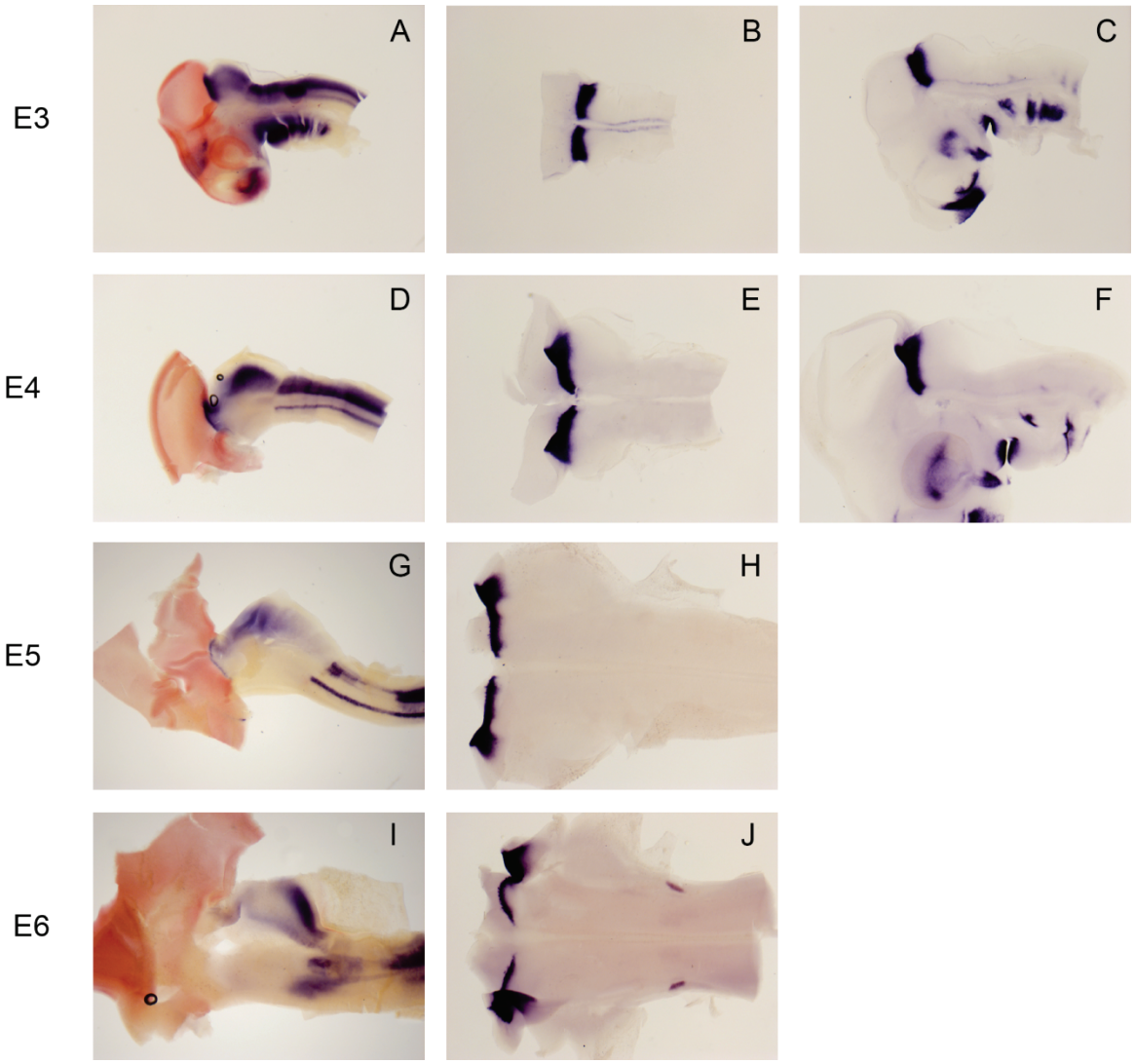

Figure 3-9 *Otx2, Gbx2* and *Fgf8* from E3 to E6

In situ hybridisation for *Otx2* and *Gbx2* in hemisected heads/brains (A,D,G,I) or *Fgf8* in flat-mount (B,E,H,J) or hemisected head (C,F). Stage indicated to left, orientated rostral to left. *Otx2* expressed in midbrain, *Gbx2* in hindbrain showing gradual dorsal restriction in rhombomere 1, *Fgf8* in isthmus showing dorsal expansion at E5/6.

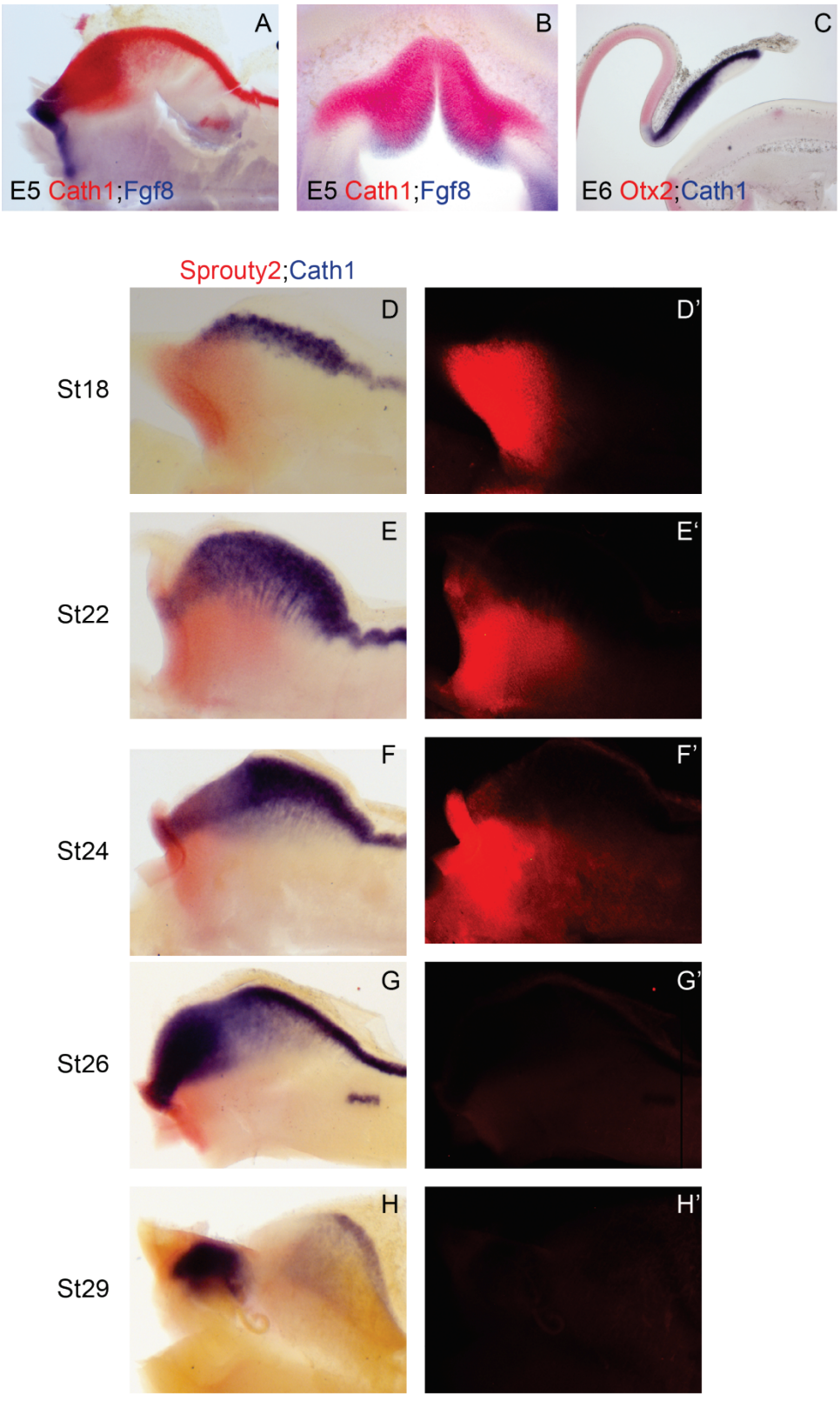

Figure 3-10 FGF signalling and *Cath1* expression from St18/E3 to St29/E6

Previous page:

Figure 3-10 FGF signalling and *Cath1* expression from St18/E3 to St29/E6

Double *in situ* hybridisation for A,B) *Fgf8* (blue) and *Cath1* (red), C) *Cath1* (blue) and *Otx2* (red) or D-H) *Cath1* (blue) and *Sprouty2* (red). Shown in flatmount (A, D-H), coronal section (B) or sagittal section (C). Orientated rostral to left, stage indicated on picture, D' to H' show red fluorescence. *Fgf8* is coexprssed with broad rostral domain of *Cath1* (A,B), which abuts $Otx2^{+ve}$ midbrain (C). Broad expression of *Cath1* is associated with the caudal extent of *Sprouty* 2 expression (D-H). Double *in siu* hybridisation A-C by Anna Myat.

(**Figure 3-10 D,E**). Between St24 (late E4) and St26 (E5), *Sprouty2* expression becomes limited to the rostral part of rhombomere 1. This coincides with the restriction of broad *Cath1* expression to rostral rhombomere 1 (**Figure 3-10 F,G**). At St29 (E6) *Sprouty2* expression is only detected in dorsal, rostral rhombomere 1 overlapping with the broad *Cath1*$^{+ve}$ domain (**Figure 3-10 H**). The expression of *Fgf8*, *Cath1* and *Sprouty* 2 are no longer detected in tissue between the midbrain and cerebellum by E8 (not shown).

3.3 Discussion

In this chapter I have examined temporal changes in the expression of genes marking the cerebellar progenitor domains, rhombic lip derivatives and isthmus in chick. A summary of these data can be found in **Table 3-1**.

This data has revealed the presence of a previously undescribed domain in dorsal, rostral rhombomere 1 from E5. This domain is molecularly and morphologically distinct from other populations in dorsal rhombomere 1 which all contribute to the cerebellum.

Furthermore, I have highlighted novel, transient sites of expression for several genes including: expression of *Ptf1a* at the cerebellar rhombic lip, expression of *NeuroD1* in the nuclear transitory zone and expression of *Pax6* and *NeuroD1* in the cerebellar ventricular zone. These observations have important consequences for the putative function of these genes in cerebellar development.

3.3.1 The temporal origin of cerebellar rhombic lip derivatives.

One of the aims in characterising the temporal expression of markers of rhombic lip derivatives was to complement data (from chapter 2) characterising the temporal cohorts born from the cerebellar rhombic lip. The expression of *Lhx9* in early rhombic lip derivatives, born between E3 and E4, and *Cath1*, in cerebellar granule neurons from E6, provides confirmation for the temporal allocation of these two populations.

An ambiguity remains regarding the expression of *Cath1* and the temporal onset of granule cell production. At St26 (early E5), diffuse expression of *Cath1* is seen across the cerebellum in cells which are not part of the rhombic lip or broad rostral domain of *Cath1* (**Figure 3-2 F**), possibly suggesting granule cells may be born at E5. However, this conclusion is not consistent with the lack of *Pax6* (another granule cell marker) at this time point and the observation that later, at St27, *Cath1*$^{+ve}$ cells are not observed over the surface of the cerebellum. Therefore, this transient expression is likely to be part of the broad domain of *Cath1* expression which is refined to rostral rhombomere 1 by St27. Alternatively, this

Table 3-1 Summary of temporal gene expression in rhombomere 1 from E3 to E10.

Gene	CbRL	RLS	V r1	NTZ	CbN	EGL	CbVZ	DR r1
Wnt1	E3-6[a]	-	-	-	-	-	-	-
Cath1	E3-10	-	-	-	-	E6-10	-	E5-8
Tbr1	-	-	-	E6-7	E8-10	-	-	E6-7[d]
Pax6	E6-10	-	-	E6-7	-	E6-10	E6-7	-
NeuroD1	-	-	E3-6[b]	E6-7	-	E6-10	E6[a]	-
Ptf1a	E4.5	-	-	-	-	-	E4-6[a]	-
Lhx9	E3-5	E3-4	E4-10	-	-	-	-	E5-10
Fgf8	-	-	E3-6[bc]	-	-	-	-	E5-8

a: later time points not analysed, b: not rhombic lip derivatives c: expression only at the isthmus, d: partial overlap

Abbreviations: CbRL: Cerebellar rhombic lip, RLS: rhombic lip stream (pre EGL), Vr1: ventral rhombomere 1, NTZ: nuclear transitory zone, CbN: cerebellar nuclei, EGL: external granule layer, CbVZ: cerebellar ventricular zone, DRr1: dorsal rostral rhombomere 1 (from E5)

expression may suggest that a specific cohort of rhombic lip derivatives retains *Cath1* expression for a short time after exiting the cerebellar rhombic lip.

This molecular characterisation has not provided any further clarity on the origin or identity of the lateral cerebellar nucleus. None of the genes analysed were expressed in rhombic lip derivatives which fall in the domain between *Lhx9* and *Tbr1* expression, where I have proposed lateral cerebellar nucleus cells to be positioned based on axon projections (see chapter 2). *Tbr1, Pax6* and *NeuroD1* expression mark cells of the medial cerebellar nucleus in the nuclear transitory zone, but not whilst the cells migrate from the rhombic lip. When these cells are first produced and whether there is any overlap in the production of different temporal cohorts from the cerebellar rhombic lip remains unclear.

3.3.2 Molecular clues to temporal changes in the hindbrain

The temporal windows of *Lhx9* and *Pax6* expression in all rhombic lip derivatives of rhombomere 1 and 2-8 point towards a single temporal transition that occurs across the whole hindbrain. *Lhx9* is expressed in all cells born from the rhombic lip from E3-E4/5, and *Pax6* is expressed in all rhombic lip derivatives born from E5/6-7. Rose et al. (2009a) have previously identified this unified transition between *Lhx9* and *Barhl1* expression in rhombic lip derivatives (Rose et al., 2009b). In mouse *Barhl1* is expressed in the same cell types that I have identified express *Pax6* in chick (the medial cerebellar nucleus and granule cell precursors).

Despite this global temporal transition in rhombic lip cell production rhombomere 1 there are still clear differences between the cerebellar and hindbrain rhombic lip. In rhombomere 1, rhombic lip derivatives display a gradual dorsal restriction in migration over time, whereas cells of the hindbrain rhombic lip show *Lhx9*$^{+ve}$ cells accumulate in dorsal positions but *Pax6*$^{+ve}$ cells generally migrate more ventrally. The cerebellar rhombic lip produces cells for longer than the hindbrain rhombic lip, which loses *Cath1* expression at E7. And finally, the cerebellar rhombic lip produces a population of cells which retain *Cath1* expression and is still proliferative, which is not a characteristic of any hindbrain rhombic lip derivatives. These differences lead to the idea that the cerebellar rhombic lip is clearly distinct from the rest of the hindbrain but may be following a similar temporal program to produce *Lhx9*$^{+ve}$ and *Pax6*/*Barhl1*$^{+ve}$ cells.

In the cerebellum, *Pax6* and *NeuroD1* both label cells in the nuclear transitory zone, cerebellar ventricular zone and external granule layer, although *NeuroD1* is only expressed in post-mitotic cells (Miyata et al., 1999). Mice with mutations in these genes show that both

affect granule cells development (see background) (Engelkamp et al., 1999; Miyata et al., 1999; Swanson et al., 2005). However, the expression of *Pax6* and *NeuroD1* in both the nuclear transitory zone and cerebellar ventricular zone suggest their functions are probably not limitedc to granule cell development.

In the lower hindbrain *Pax6* and *NeuroD1* are expressed in distinct subsets of cells. It has not previously been shown which populations of cells are *NeuroD1*$^{+ve}$ in the hindbrain and therefore these cells may not be rhombic lip derivatives. Furthermore *Pax6* is expressed in both cells from *Atoh1*$^{+ve}$ and *Neurogenin1*$^{+ve}$ progenitors of the hindbrain which form precerebellar nuclei contributing mossy fibres and climbing fibres respectively (Landsberg et al., 2005). Therefore in the hindbrain, *Pax6* and *NeuroD1* are not specific to *Atoh1*-derivatives. The fact that these populations show a similar temporal onset to the cerebellum suggests than non-rhombic lip populations may also exhibit temporal transitions by similar mechanisms.

3.3.3 Progenitor domains in the cerebellum

It has previously been shown that the *Atoh1*$^{+ve}$ rhombic lip and *Ptf1a*$^{+ve}$ cerebellar ventricular zone exclusively give rise to glutamatergic and GABAergic cells of the cerebellum respectively (Hoshino et al., 2005; Machold and Fishell, 2005; Wang et al., 2005). The observation that *Ptf1a* is transiently expressed within the rhombic lip provides evidence of a more complicated regulation of cell specification within the cerebellum. It is not possible to determine if *Pft1a* and *Cath1* are co-expressed in cells at the cerebellar rhombic of whether *Ptf1a* is expressed in a subset of *Cath1*-negative cells. The timing of this transient expression is between the production of *Lhx9*$^{+ve}$ and *Pax6*$^{+ve}$ rhombic lip derivatives at St25/E4.5. If this transient expression of *Ptf1a* expression resulted in the production of cells in the rhombic lip pial migratory stream, in a manner similar to Cath1^{+ve} rhombic lip derivatives, cells may contribute to a population of cells just ventral to the nuclear transitory zone, proposed to form the lateral cerebellar nucleus. Furthermore, if the *Ptf1a*$^{+ve}$ domain in the rhombic lip produced GABAergic cells, this could demonstrate a novel mechanism for generating mixed cell types within a single nucleus which is in contrast to the established model that glutamatergic and GABAergic cell types are born from spatially distinct progenitor domains in the cerebellum. Electroporation of conditional *Ptf1a* and *Atoh1* reporters into the cerebellar rhombic lip could be used to further investigate this transient population.

Results in this chapter have also led to the characterisation of three distinct *Cath1*$^{+ve}$ populations within rhombomere 1: 1) a broad rhombic lip domain which is later confined to rostral rhombomere 1, 2) a narrow rhombic lip domain, present from E5, throughout the

caudal two thirds of rhombomere 1, and 3) granule cell precursors in the external granule layer (see schematic in **Figure 3-11**). The temporal and spatial change in the two progenitor domains coincides with the switch from the production of *Lhx9*$^{+ve}$ extra-cerebellar cells and cells which contribute to the cerebellum (cerebellar nuclei and granule cells). The overlap between the broad rostral domain of *Cath1* and *Tbr1* expression in the nuclear transitory zone can be explained by the rostral migration of these cells after their tangential migration to the nuclear transitory zone. These observations lead to a hypothesis that two distinct progenitor domains, which are regulated temporally and spatially, produce extra-cerebellar and cerebellar cells respectively.

It is important to highlight that spatial changes in the *Cath1* progenitor domains are not due to cells regressing into rostral rhombomere 1. Instead only the expression of *Cath1* is altered within a field of cells. This can be delineated from data in chapter 2 in which specific regions of the rhombic lip were labelled by *gfp* electroporation at E4 but did not move into rostral rhombomere 1. In fact, to the contrary, a caudal shift in cells was observed between labelling at E4 and analysis at E7.

A further important question regarding the broad *Cath1*$^{+ve}$ domain, is whether it continues to produce *Lhx9*$^{+ve}$ cells after it is confined to the most rostral region of rhombomere 1. This rostral region is *Wnt1*-negative. Cells derived from *Wnt1* lineage in mouse have previously been described to form all the same populations and the *Math1*$^{+ve}$ lineage (Hagan and Zervas, 2012) suggesting an *Atoh1*$^{+ve}$*/Wnt1*$^{-}$ domain does not produce any cells in mouse. However, it is not known what differences there are in *Atoh1* expression between mice and chick and the specific function of *Wnt1* within the cerebellar rhombic lip is not known. Attempts to label this rostral domain by electroporation in chapter 2 were unsuccessful.

3.3.4 The influence of an aging organiser.

In this chapter I have characterised the progressive changes and ultimate loss of isthmic signalling between E3 and E8. The loss of *Gbx2* from ventral rhombomere 1 precedes the loss of ventral *Fgf8* expression. This implies that a continual interaction between *Gbx2* and *Otx2*, which initially establishes the isthmic boundary, may also be important to maintain isthmic expression of *Fgf8* until it is eventually lost at E8.

FGF8 is a secreted protein, so in the absence of an anti-body for FGF8, I used the expression of a direct downstream target of FGF signalling, *Sprouty2*, to assess the functional activity of the isthmus at different time points. *Sprouty2* has been demonstrated to be downstream of

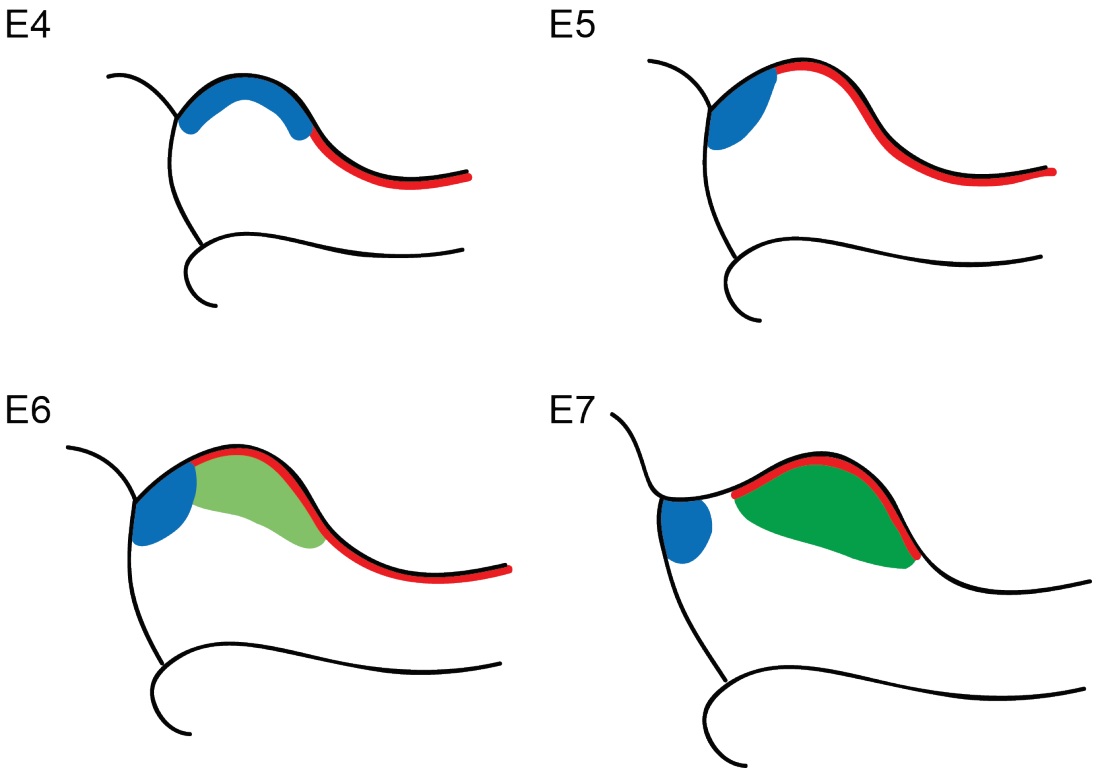

Figure 3-11 Temporal changes in 3 distinct domains of *Cath1* expression

Schematic indicating 3 modes of *Cath1* expression in rhombomere 1 between E4 and E7: blue) E4 broad rhombic lip resolves to domain in dorsal, rostral rhombomere 1, abutting the isthmus; red) narrow rhombic lip expression in lower hindbrain at E4 then cerebellar rhombic lip from E5; green) granule cell precursos from E6.

FGF8 signalling at the isthmus both via the Ras-ERK signalling cascade and by ERK-independent nuclear translocation of FGF8 (Chambers et al., 2000; Suzuki-Hirano et al., 2005; Suzuki et al., 2012) and is therefore likely to be a good functional read out of isthmic FGF signalling. The progressive rostral restriction of *Sprouty2* therefore suggests that FGF signalling in rhombomere 1 reduces over time. However, after the initial induction of *Sprouty2* it is not known how its expression is regulated compared to FGF signalling.

The caudal extent of FGF signalling, as shown by *Sprouty2* expression is correlated with the caudal extent of broad *Cath1* expression in rhombomere 1. Furthermore, *Fgf8* expression overlaps with the broad rostral domain of *Cath1* at E5 and *Fgf8* and the rostral domain of *Cath1* expression are both finally lost at the same time, E8. Together these observations lead to the hypothesis that isthmic signalling, namely *Fgf8*, may act to induce a broad domain of *Cath1* in rhombomere 1 and that reduced signalling from the isthmus over time causes a rostral restriction in the extent of this domain. The broad domain of *Atoh1* is correlated with *Lhx9* expression, suggesting that temporally changing signals at the isthmus may coordinate the temporal transition in cell production from the cerebellar rhombic lip. This hypothesis will be the focus of my next chapter.

Chapter 4 The role of the isthmus in patterning rhombomere 1.

4.1 Background

In the preceding chapter I have identified three distinct modes of *Cath1* expression in dorsal rhombomere 1: 1) a broad expression domain which is first evident throughout the whole of the cerebellar rhombic lip and is then refined to the most rostral region of rhombomere 1 at E5, 2) rhombic lip specific expression evident from E5 when broad expression regresses to rostral rhombomere 1, and 3) expression in granule cell precursors in the external granule layer of the cerebellum from E6. The broad domain of *Cath1* expression is correlated with the expression of *Lhx9*, a marker of early born post-mitotic rhombic lip derivatives, and an expanded $Fgf8^{+ve}$domain at the isthmus. In this chapter, I explore whether there is a functional relationship between these genes, hypothesising that isthmic FGF signalling may induce a broad expression domain of *Cath1*, to specify $Lhx9^{+ve}$ cerebellar rhombic lip derivatives and that the temporal reduction of isthmic signalling may then limit the broad domain of *Cath1* and *Lhx9* to rostral rhombomere 1, allowing for the specification of later-born populations from the more caudally located cerebellar rhombic lip.

Studies of cerebellar development have clearly established that spatially segregated progenitor domains, expressing *Atoh1* and *Ptf1a*, contribute different cell types to the cerebellum and that both of these populations contribute multiple cell types to the cerebellum by temporal modification (Hoshino et al., 2005; Machold and Fishell, 2005; Wang et al., 2005). The induction of the $Atoh1^{+ve}$ domain of the cerebellar rhombic lip is dependent on TGF-β signalling from the roof plate whereas the more ventrally located $Ptf1a^{+ve}$ progenitor domain does not require roof plate signalling (Chizhikov et al., 2006). Recent work has shown that physical removal of roof plate tissue from the hindbrain of E4-6 chicken embryos results in a progressive downregulation in the expression of rhombic lip *Cath1* over the course of two days when the tissue was cultured in vitro (Broom, 2011). This study also shows that the broad domain of *Cath1* expression in rostral rhombomere 1 was not lost following roof plate removal in cultured explants (**Figure 4-1 A,B**) suggesting an independent mechanism of *Cath1* regulation from roof plate-dependent rhombic lip. This preliminary data, combined with the co-expression of *Fgf8* and *Cath1* in this rostral domain suggests a potential role for the isthmus in regulating gene expression in rhombomere 1.

The isthmus is the boundary between midbrain tissue and hindbrain tissue which is induced, positioned and maintained through a network of genetic interactions between *Otx2*, *Gbx2*,

Fgf8, *Wnt1*, *Pax2/5/8* and *En1/2* (for reviews see Joyner et al. (2000) and Joyner (1996)). It has been shown that an interaction between midbrain tissue and rhombomere 1 is sufficient to induce an isthmic organiser (Irving and Mason, 1999)

Otx2 and *Gbx2* mark the territories of the mesencephalon and metencephalon respectively and are absolutely required for these respective domains as shown by loss of function studies (Acampora et al., 1995; Acampora et al., 1997; Millet et al., 1999). Furthermore these genes are sufficient to induce midbrain (*Otx2*) or hindbrain (*Gbx2*) tissue in ectopic positions both in transgenic mice (Broccoli et al., 1999; Millet et al., 1999) and by electroporation in chick (Katahira et al., 2000). Collectively these studies demonstrate a mutual repression between *Otx2* and *Gbx2*, as loss of gain of either *Otx2* or *Gbx2* results in a reciprocal shift in the boundary of expression of the other gene and an expanded domain of the territory which it specifies. For example loss of *Gbx2* results in an expansion of *Otx2* into the hindbrain territory transforming the tissue to a midbrain fate at the expense of hindbrain tissue (Millet et al., 1999).

Fgf8 is expressed at the isthmus within the *Gbx2*$^{+ve}$ domain (Crossley and Martin (1995) and see chapter 3). Whilst in mouse deletion of *Fgf8* result in a complete deletion of the midbrain and anterior hindbrain territory due to extensive cell death (Chi et al., 2003), loss of *Fgf8* in zebrafish and chick result in an expansion of *Otx2*$^{+ve}$ into the hindbrain and transforms the anterior hindbrain into midbrain tissue (Reifers et al., 1998; Jaszai et al., 2003; Sato and Nakamura, 2004). It has also been shown in zebrafish that the phenotype following loss of Fgf8 can be rescued by downregulation of *Otx2* (Foucher et al., 2006) demonstrating that *Fgf8* is not instructively required to induce cerebellar fate but instead is required to represses *Otx2*.

Two isoforms of *Fgf8* function at the isthmus, *Fgf8a* and *Fgf8b*. Of these, *Fgf8b* is more functionally active (Sato et al., 2001) and required for formation of the isthmus (Guo et al., 2010). Ectopic *Fgf8b* expression in the midbrain represses *Otx2* expression and induces *Gbx2* expression, transforming tissue to a cerebellar fate (Liu et al., 1999; Sato et al., 2001; Sato and Nakamura, 2004).

In contrast to *Fgf8b*, overexpression of *Fgf8a* does not downregulate *Otx2* and instead causes an expansion and repatterning of midbrain tissue (Lee et al., 1997; Sato et al., 2001). Lee et al. (1997) demonstrated that driving the expression of *Fgf8a* with the *Wnt1* enhancer and therefore, ectopically expressing FGF8 in the caudal midbrain resulted in a huge overgrowth of the midbrain by causing neural precursors to continue proliferating at the expense of neurogenesis. Midbrain repatterning is also seen following transplantation of the isthmus

(Marin and Puelles, 1994; Crossley et al., 1996) insertion of FGF8-soaked beads (Crossley et al., 1996; Martinez et al., 1999)and inversion of the entire midbrain (excluding the isthmus) (Martinez and Alvarado-Mallart, 1990)

Studies of *Fgf8* in mouse have used hypomorphic alleles of *Fgf8* (Meyers et al., 1998; Chi et al., 2003) and manipulation of Sprouty genes, which negatively regulate FGF signalling (Basson et al., 2008; Yu et al., 2011), to circumvent the complete loss of midbrain and hindbrain tissue observed when *Fgf8* is removed in the midbrain/hindbrain territory (Chi et al., 2003). Both hypomorphic alleles of *Ffg8* and *Sprouty2*-gain of function alleles have been demonstrated to cause a specific loss of posterior midbrain and the medial region of the cerebellum (Meyers et al., 1998; Chi et al., 2003; Basson et al., 2008). The medial region of the cerebellum, the cerebellar vermis, is derived from the most anterior part of rhombomere 1 and subsequent morphological rotation of the cerebellar hemispheres results in anterior tissue forming the medial cerebellum (Sgaier et al., 2005). Loss of *Sprouty* genes, and hence an increase in FGF signalling, can cause a lateral expansion of the cerebellar vermis but also shows reduced thickness and abnormal foliation of the granule cell layer due to later effects on granule cell proliferation (Yu et al., 2011). Sato and Joyner (2009) reported loss of *Fgf8* at progressively later time points (E8.5-10.5) to cause a progressively milder phenotype in which smaller regions of tissue are lost. The first cerebellar rhombic lip derivatives are born at around E10 (Machold and Fishell, 2005; Wang et al., 2005), and therefore the major role of *Fgf8* in specifying the domains of cerebellar tissue must occur prior to cerebellar development.

Sprouty2-gain of function mutation also result in an expansion of the roofplate and therefore it has been proposed that a possible mechanism for the loss of the cerebellar vermis is that increased BMP signalling results in roofplate expansion at the expense of progenitors for the cerebellar vermis (Basson et al., 2008). In contrast to this Alexandre and Wassef (2003) report that the isthmus promotes roofplate formation in the midbrain.

Fgf17 and *Fgf18* are also present at the isthmus (Maruoka et al., 1998) and can act partially redundantly with *Fgf8*, functioning particularly in controlling growth and proliferation (Xu et al., 2000; Liu et al., 2003)

Three FGF receptors are expressed in rhombomere 1, *fgfr1*, *fgfr2* and *fgfr3* (Walshe and Mason, 2000; Blak et al., 2005). *fgfr1* is expressed throughout the domain of the isthmus and rhombomere 1 and is required for the isthmic organiser and subsequently for mid-hindbrain development (Trokovic et al., 2003). In contrast, *fgfr2* and *fgfr3* are not expressed in or

required for the isthmus (Blak et al., 2007) but can act in a partially redundant manner with *fgfr1* (Saarimaki-Vire et al., 2007).

To investigate the relationship between the isthmus and the expression of *Cath1* and *Lhx9* in rhombomere 1, I use 3 different approaches: 1) *in vitro* culture of E3/4/5 hindbrain tissue following dissection to remove sources of isthmic and/or roof plate signalling (as per Broom (2011)), 2) overexpression of *Otx2* by *in ovo* electroporation in rhombomere 1 at E3 to induce ectopic isthmic signalling (as is reported in E2 electroporations by Katahira et al. (2000)) , and 3) E2/3 *in ovo* electroporation of *Fgf8* or a dominant-negative FGF-receptor to directly test the function of FGF signalling in rhombomere 1.

4.2 Results

4.2.1 The isthmus is required for maintenance of the broad, rostral domain of *Cath1* expression.

When the roof plate epithelium is removed from the hindbrain neuroepithelium, expression of *Cath1* in the rhombic lip is lost over the course of 2 days in culture, but *Cath1* expression in the broad rostral domain is not lost (**Figure 4-1 A,B** taken from Broom (2011)), demonstrating it is maintained independently from the rest of the roof plate-dependent rhombic lip (Broom, 2011).

To assess whether the midbrain-hindbrain interaction is required for the broad, rostral domain of *Cath1* expression I used a similar *in vitro* culture system using the hindbrain of E4 and E5 embryos, in the presence or absence of midbrain/isthmic tissue. These stages were chosen to establish whether the broad, rostral domain of *Cath1* expression could be formed (E4) and maintained (E5) in the absence of isthmic signalling. Midbrain/hindbrain tissue was removed from embryos and midbrain tissue was unilaterally removed at the level of the isthmus. The side with midbrain/isthmus intact would then provide an internal control. To ensure *Cath1* expression could not be induced/maintained through roof plate signalling, the roof plate was removed by dissection. Tissue was flat-mounted onto culture membranes atop culture medium and incubated for 2 days.

Firstly, I performed a pilot study to establish the position of dissection required to remove the isthmus. Following different dissections of unilaterally removing midbrain tissue from hindbrain tissue, explants were cultured for 2 days, fixed and processed for *in situ* hybridisation of *Otx2* and *Fgf8* to mark the midbrain and isthmus respectively. Using this

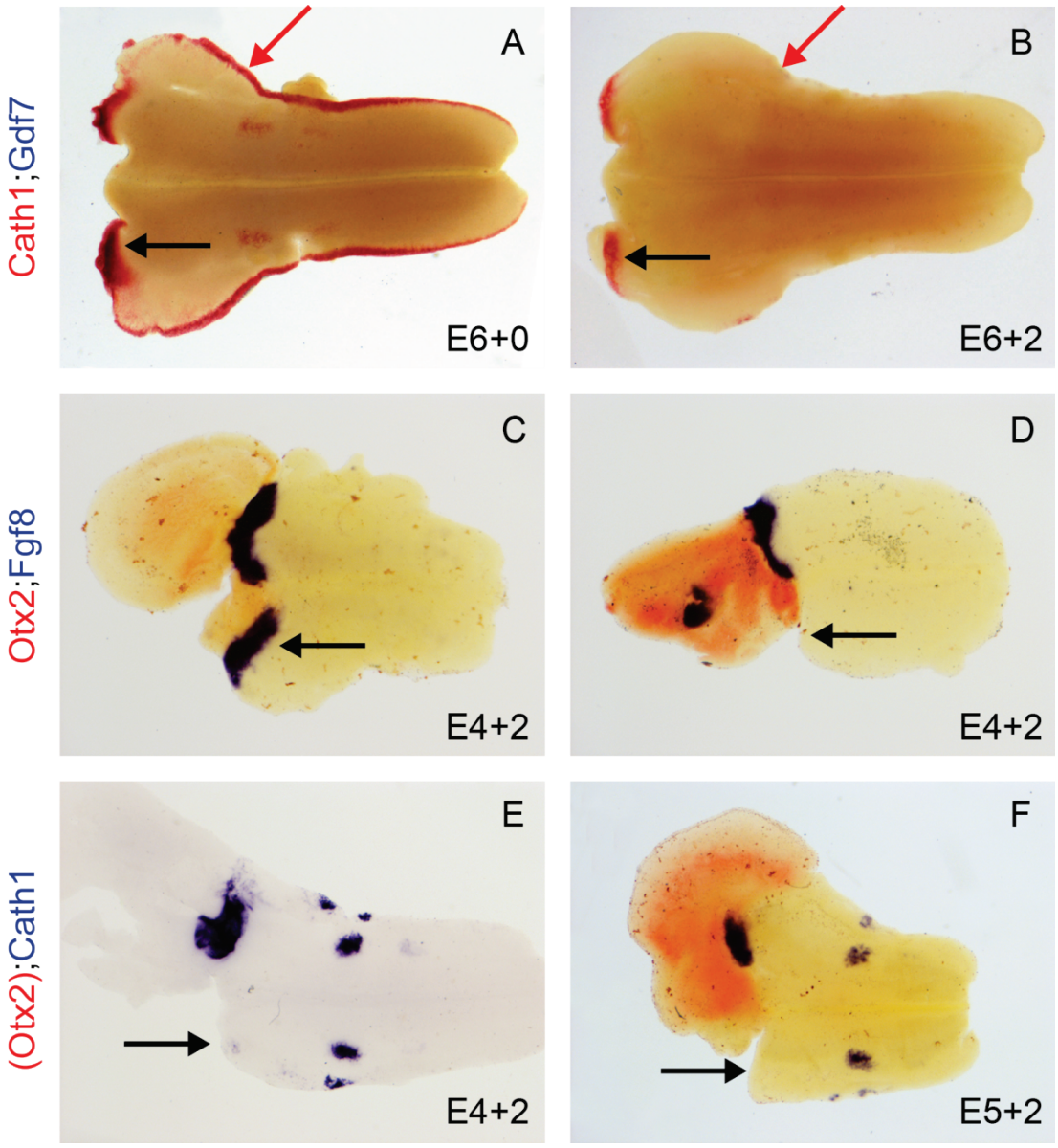

Figure 4-1 *In vitro* cultures of E4/E5/6 hindbrain tissue following roof plate and/or midbrain removal.

Previous page:

Figure 4-1 *In vitro* cultures of E4/5/6 hindbrain tissue following roof plate and/or midbrain removal

A,B) Pictures taken from (Broom, 2011). E6 flat-mount hindbrain cultured for 0 (A) or 2 days (B), following removal of roof plate tissue from hindbrain. Double *in situ* hybridisation for *Cath1* (red) and *Gdf7* (blue, showing absence of roofplate). *Cath* 1 expression is lost in the rhombic lip (red arrow) but retained in the broad rostral domain (black arrow). C,D) E4 flat-mount hindbrains cultured for 2 days following roof plate removal and insufficient (C) or sufficient (D) unilateral midbrain (*Otx2*) removal (arrows) to downregulate *Fgf8* expression shown by *in situ* hybridisation. E,F) E4 (E) or E5 (F) flat-mount hindbrain cultured for 2 days following roofplate and unilateral midbrain removal (black arrow) resulting in a loss of *Cath1* expression in rostral rhombomere 1 where midbrain is removed. All pictures orientated rostral to left.

method it could be seen which type of dissections removed all of the *Otx2*$^{+ve}$ midbrain tissue and showed no expression of *Fgf8* (**Figure 4-1C,D**).

I then repeated E4/5 dissections in which the isthmus was completely removed, cultured tissue for two days and looked at the expression of *Cath1* (and *Otx2*) by *in situ* hybridisation. Explants from E4 and E5 embryos showed a complete loss of rhombic lip expression of *Cath1 (***Figure 4-1 E,F**), as previously described following roofplate removal (Broom, 2011). A complete loss of *Cath1* expression in the broad rostral domain was observed unilaterally, only where midbrain tissue was removed. Where midbrain tissue was intact, *Cath1* expression was seen at the boundary of the two tissues, indicated by the caudal extent of *Otx2* expression (**Figure 4-1 E,F**). This isthmic domain of *Cath1* was not seen in the usual dorsal position; instead expression was often shifted more ventrally. The dorsal positioning of the broad rostral *Cath1* domain therefore may require signals which are removed in this isolated culture system, for example, signals from the roof plate or surrounding tissues, which were removed by dissection. This result shows that, whilst *Cath1* expression in the rhombic lip is dependent on the roof plate, the isthmus is sufficient to induce/maintain the expression of *Cath1* in the broad rostral domain.

To test whether the broad expression domain of *Cath1* at E3/4, which extends throughout the whole of rhombomere 1, was also dependent on signals from the isthmus I repeated these experiments using midbrain/hindbrain tissue from E3 embryos. In these dissections, roof plate tissue was not removed. After 2-3 days in culture, *Fgf8* expression was completely absent from the tissue unilaterally demonstrating successful removal of the isthmus by dissection (**Figure 4-2 A**). *Cath1* expression was retained at the rhombic lip on both sides of the hindbrain; however, the expression of *Cath1* was markedly broader adjacent to intact midbrain tissue (**Figure 4-2 B,C**). Therefore the ventral expansion of *Cath1* and resulting broader expression domain in dorsal rhombomere 1 is dependent on the isthmus. The broad expression of *Cath1* on the side of the hindbrain with midbrain intact, even after 3 days in culture, resembled the expression of *Cath1* at E4, rather than E5/6 where broad *Cath1* expression is only seen in rostral rhombomere 1. This suggests that under these culture conditions temporal progression of development is delayed.

Lhx9 is expressed in rhombic lip derivatives from E3. To assess whether reduced *Cath1* expression in E3 hindbrain cultures following midbrain removal resulted in a change in rhombic lip derivatives I next looked at the expression of *Lhx9*. After 2 or 3 days in culture, *Lhx9* expression in cultured hindbrain tissue was disrupted throughout the tissue showing abnormal, uneven loss or accumulation of *Lhx9*$^{+ve}$ cells at the edges of the tissue. No

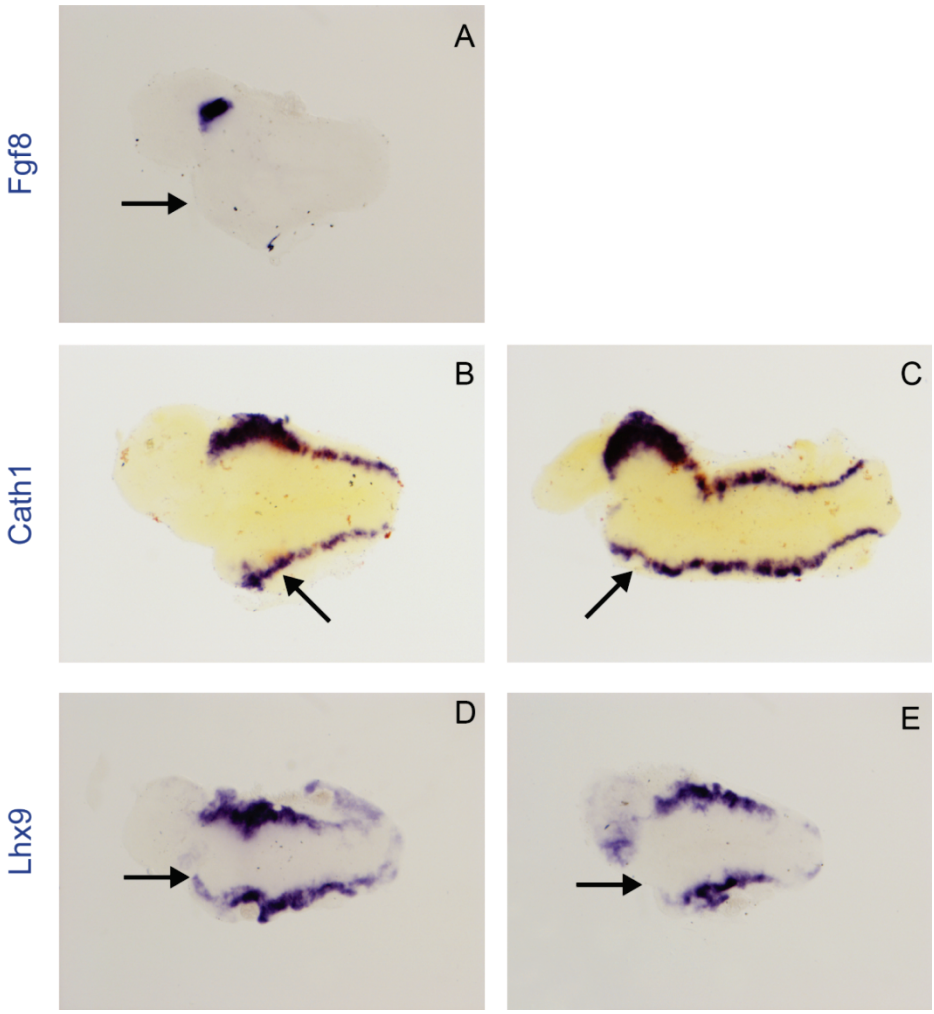

Figure 4-2 *In vitro* cultures of E3 hindbrain tissue with unilateral midbrain tissue.

E3 flat-mount hindbrains with roof plate intact cultured for 2 days following unilateral midbrain removal (bottom side/black arrow) stained by *in situ* hybridisation for *Fgf8* (A), *Cath1* (B,C) or *Lhx9* (D,E). *Fgf8* expression is lost and *Cath1*-rhombic lip expression is downregulated by midbrain removal compared to the control side. *Lhx9* expression is disturbed throughout the hindbrain.

consistent asymmetry was seen between the two sides of the hindbrain with and without midbrain tissue (**Figure 4-2 D,E**). This result suggests that the production of *Lhx9*$^{+ve}$ cells is disturbed through this *in vitro* culture technique and therefore it is not possible to assess the effects of isthmic removal on *Lhx9*$^{+ve}$ rhombic lip derivatives by this method.

4.2.2 The isthmic organiser cannot be recapitulated by the juxtaposition of E3 or E5 midbrain and hindbrain tissues *in vitro*.

Removal of the midbrain at E4/5 results in a loss of the broad domain of *Cath1* in rostral rhombomere 1. One possible explanation of these results is that the broad *Cath1*$^{+ve}$ domain may have simply been removed by dissection. In tissue dissected at E4, this is an unlikely explanation as the broad Cath1 domain extends through the whole of rhombomere 1 at the time of dissection. To confirm that the rostral domain was not simply removed by dissection in E5 hindbrains, I performed a rescue experiment in which midbrain tissue was removed from both sides of the hindbrain tissue and then the hindbrain tissue was co-cultured with a piece of midbrain tissue from a stage-matched *gfp*-transgenic chicken embryo. Based on previous observations that juxtaposition of midbrain and hindbrain tissue can induce a secondary isthmic organiser *in vivo* (Irving and Mason, 1999) and that *in vitro* co-culture of roof plate and hindbrain tissue can recapitulate the roofplate-hindbrain boundary (Broom, 2011), I hypothesised that co-culture of midbrain and hindbrain tissue would induce a secondary isthmic organiser following dissection which would be able to induce a broad domain of *Cath1* in rostral rhombomere 1.

In these experiments I dissected out the brain of E5 embryos and removed the whole midbrain at the level of the isthmus. Dissections both with, and without roof plate tissue were performed. I also dissected pieces of tissue from the dorsal half of the midbrain from stage matched *gfp*-transgenic chicken embryos, being careful to completely remove the isthmus and dorsal midline (which expresses signalling molecules such as *Wnt1*). I then co-cultured pieces of *gfp*$^{+ve}$ midbrain tissue with wildtype hindbrain tissue for 2 days. The *gfp*$^{+ve}$ midbrain tissue was placed in the position of the removed wildtype midbrain on one side of the hindbrain as shown in the schematic of this experimental technique **Figure 4-3 A.**

After 2 days *in vitro*, co-cultures of midbrain and hindbrain tissue were processed for *in situ* hybridisation for either *Fgf8* or *Cath1*. *Fgf8* expression was never seen at the boundary between the midbrain and hindbrain tissues showing that an organiser was not induced by co-culture (**Figure 4-3 B**). The broad rostral domain of *Cath1* was also absent in co-cultured explants irrespective of the presence of roof plate tissue (**Figure 4-3 C,D**). Hindbrains with roof plate tissue attached retained expression of *Cath1* in the rhombic lip.

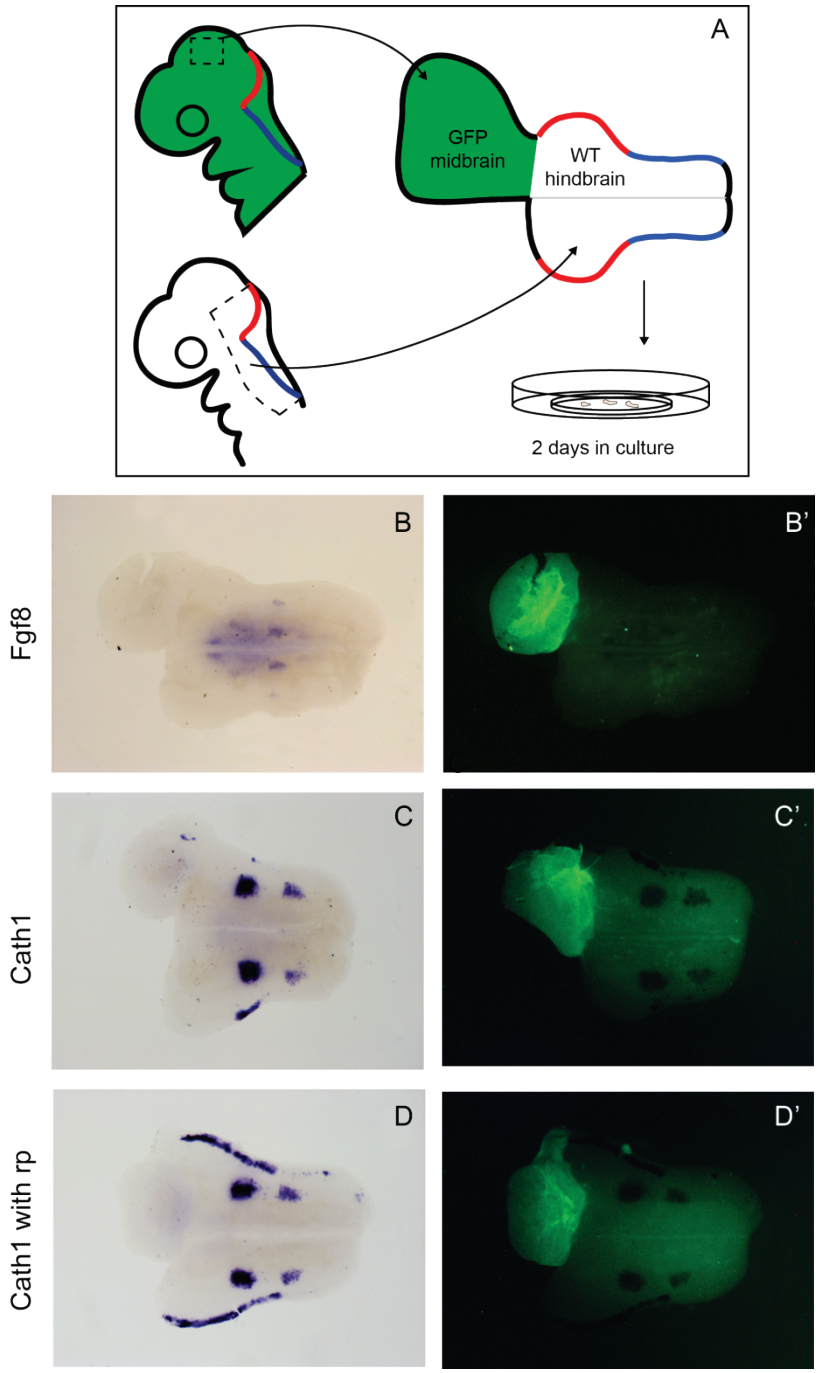

Figure 4-3 In vitro co-cultures of E5 wildtype hindbrain tissue with GFP^{+ve} midbrain tissue.

A) Shows schematic of co-culture technique. Flat-mounted wildtype midbrain tissue is co-cultured with *gfp*-transgenic midbrain tissue. B-D) E5 hindbrain and midbrain tissue co-cultured for 2 days showing no induction of Fgf8 (B) or *Cath1* (C,D) in rostral rhombomere 1. B and C have roof plate removed; D has hindbrain roof plate intact. B'-D' show GFP fluorescence.

One explanation for the lack of isthmus induction could be that at E5, the age when co-cultures were performed, *Gbx2* expression in the hindbrain is partially down regulated (see chapter 3). *Gbx2* expression is required *in vivo* for the initial formation and maintenance of the midbrain-hindbrain boundary organiser (Millet et al., 1999). I therefore repeated co-cultures at E3 when high levels of *Gbx2* expression are seen throughout the hindbrain tissue (see chapter 3). After 2 days *in vitro*, co-cultures of E3 midbrain and hindbrain explants showed no induction of *Fgf8* at the boundary between the tissues and there was no rescue of the loss of broad *Cath1* expression in rhombomere 1 (**Figure 4-4**). These cultures did show that some GFP^{+ve} axons from midbrain were present in hindbrain tissue (**Figure 4-4 A'**), suggesting lack of isthmus induction was not due to unsuccessful integration of tissue by co-culture.

4.2.3 *Otx2* overexpression in rhombomere 1 at E3 is sufficient to expanded the $Fgf8^{+ve}$ domain.

It has previously been shown that overexpression of *Otx2* in rhombomere 1 at St10/E2 in chicken embryos results in a transformation of cells in rhombomere 1 to a midbrain fate and can induce ectopic expression of *Fgf8* and other isthmic markers at the ectopic boundaries of *Otx2* expression (Katahira et al., 2000). However, this study also showed that overexpression of *Otx2* results in the majority of rhombomere 1 becoming tectum. I therefore wanted to test whether later overexpression of *Otx2* in rhombomere 1 at E3 could produce a more focal region of ectopic expression and ectopic isthmic induction without transforming the entire region to a midbrain fate. For this experiment I co-electroporated a full-length *Otx2* overexpression construct (CAβ-*Otx2*-IRES*egfp*; hereafter referred to as *Otx2*) with CAβ-*gfp* (hereafter referred to as *gfp*) or as a control, *gfp* alone, into rhombomere 1. Co-electroporation with *gfp* was used despite the *IRESegfp* within the *Otx2* overexpression construct to ensure a strong GFP signal could be detected using an anti-GFP antibody after *in situ* hybridisation.

It has previously been shown (Broom, 2011), that co-electroporation of two constructs (CAβ-*gfp* and RCAS-*rfp*) mixed in equal concentration results in 97% of electroporated cells co-expressing the two genes even with constructs containing different promoters. When co-electroporated, GFP can therefore be assumed to label cells which express *Otx2*. Using GFP signal, the position and size of each electroporation can be assessed, but when combined with in situ hybridisation, the GFP signal can sometimes be masked by the dark staining from *in situ* hybridisation.

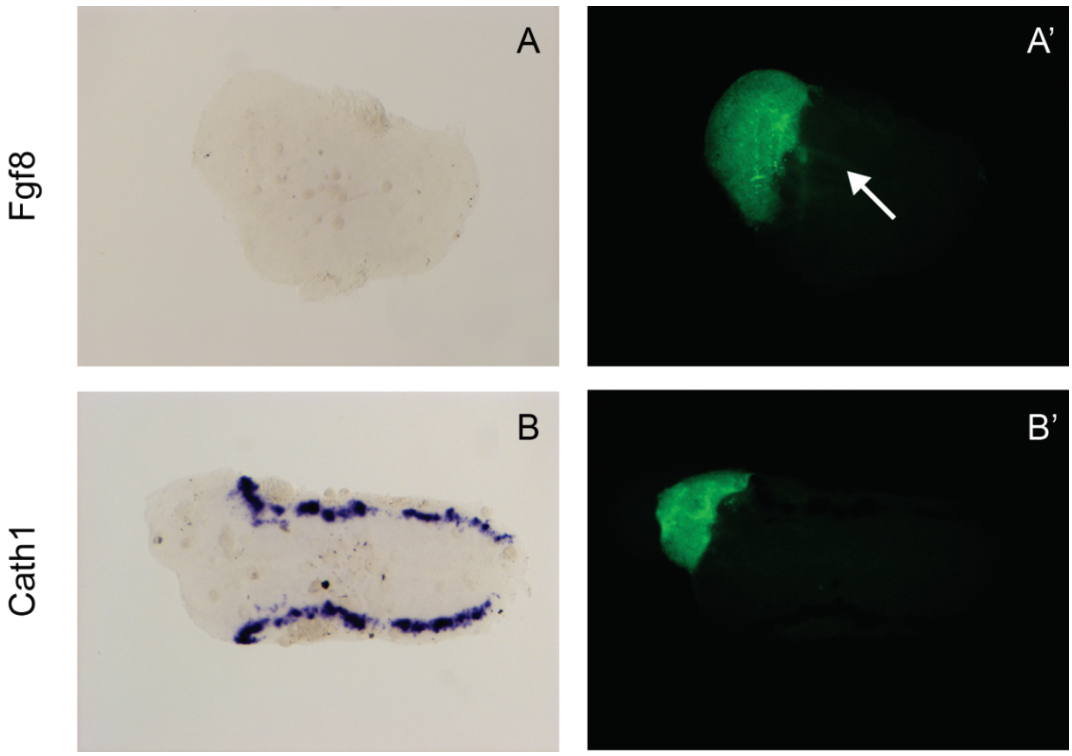

Figure 4-4 *In vitro* co-cultures of E3 wildtype hindbrain tissue with GFP^{+ve} midbrain tissue.

E3 wildtype hindbrain (roof plate intact) and *gfp*-transgenic midbrain tissue co-cultured for 2 days showing no induction of *Fgf8* (B) or rescue of broad *Cath1* expression (B) in rhombomere1. A' and B' show GFP fluorescence. White arrow indicates GFP^{+ve} axons in wildtype hindbrain.

Control *gfp* electroporations had no effect on *Fgf8* expression (**Figure 4-5 A**). However, when *Otx2* was overexpressed in a broad region throughout rhombomere 1, an expansion of the endogenous isthmic domain of *Fgf8* was seen in rostral rhombomere 1 compared to the control side (**Figure 4-5 B-E**). The majority of the GFP^{+ve} region in rhombomere 1 did not show any *Fgf8* expression and the expanded rostral domain appeared to coincide with the rostral limit of GFP expression. In higher magnification it can be seen that within the expanded domain of *Fgf8* individual cells expressing high levels of GFP (and therefore *Otx2*) did not express *Fgf8* (**Figure 4-5 C,E**). This implies that *Fgf8* is induced non-autonomously in rhombomere 1 tissue by ectopic *Otx2* overexpression.

To try and induce *Fgf8* expression in a more caudal region, I performed smaller, more focal electroporations in caudal rhombomere 1 at E3. However, no change was seen in *Fgf8* expression and no ectopic *Fgf8* was induced (**Figure 4-5 F**). Likewise, when *Otx2* was overexpressed focally in rhombomere 1 at E4, no change was seen in *Fgf8* expression compared to the control side (**Figure 4-5 G**).

The results of these experiments fit a model where overexpression of *Otx2* into rhombomere 1 can non-cell-autonomously upregulate *Fgf8* in a similar manner to the published phenotype of E2 overexpression of *Otx2* (Katahira et al., 2000). However these experiments demonstrate that in E3 embryos only the most rostral region, abutting the endogenous isthmic organiser is competent to express *Fgf8* in response to *Otx2* overexpression.

4.2.4 *Otx2* can induce an expanded domain of *Cath1* in rhombomere 1.

To test the effect of *Otx2* overexpression in rhombomere 1 on the expression of *Cath1* I co-electroporated *Otx2* with *gfp* at E3 and looked at the expression of *Cath1* two days later, at E5. Control *gfp* electroporations showed no change in *Cath1* expression (**Figure 4-6 A**) but *Otx2* overexpression in a broad region throughout rhombomere 1 (in a manner which was shown to induce an expanded domain of *Fgf8*) caused an expansion of the rostral domain of *Cath1*. However, in GFP^{+ve} cells *Cath1* expression was also cell-autonomously down-regulated both within the rhombic lip and the rostral domain (**Figure 4-6 B,C**). The caudal expansion of the rostral domain of *Cath1* mirrors the expansion of *Fgf8* expression following *Otx2* over expression. Cell autonomous downregulation of *Cath1* suggests that *Otx2* expressing cells cannot express *Cath1*.

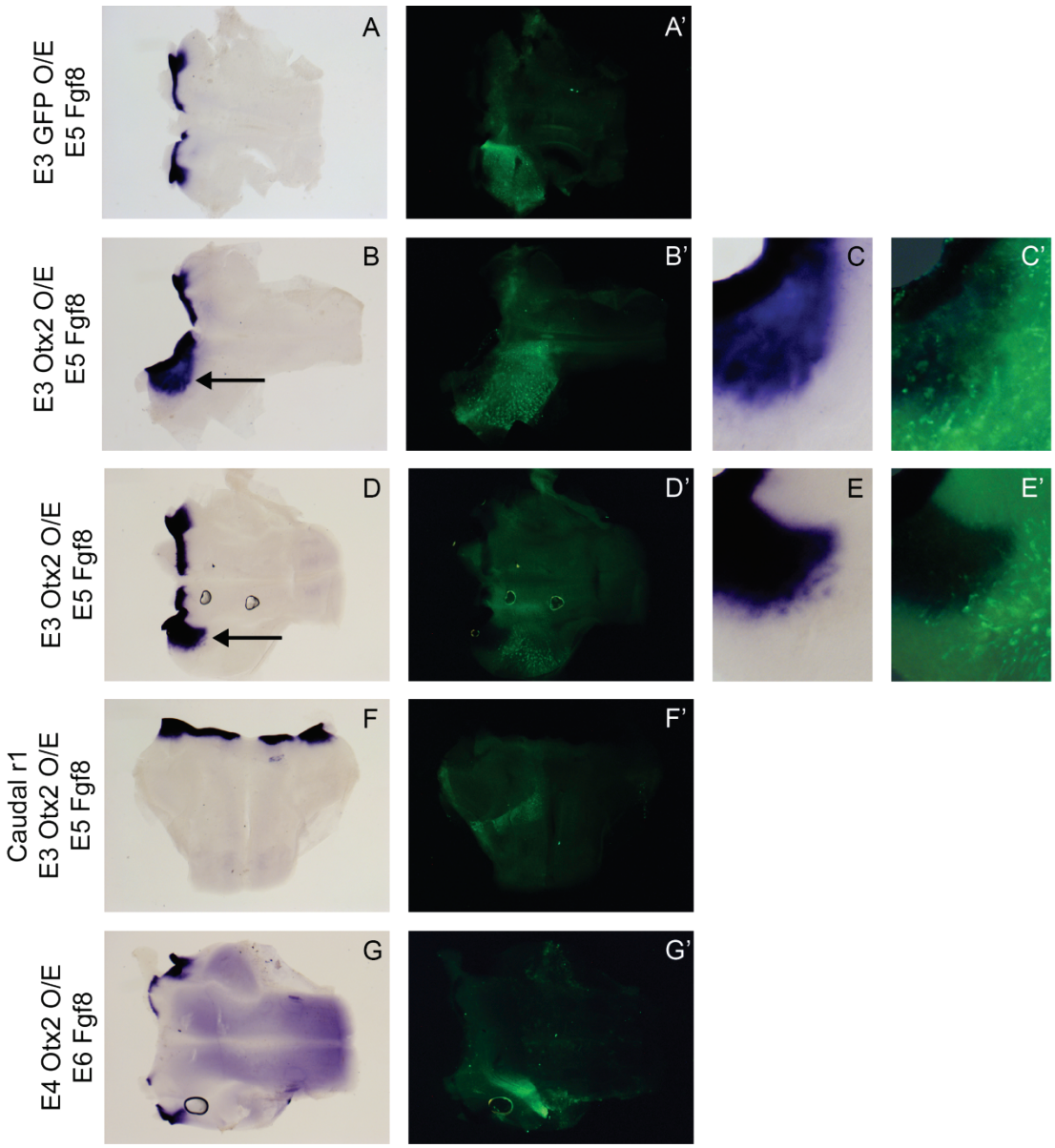

Figure 4-5 *Fgf8* expression following overexpression of *Otx2*.

E5 *In situ* hybridisation for *Fgf8* following broad rhombomere 1 E3 *gfp* electroporation (A) or *Otx2+gfp* electroporation broadly in rhombomere 1 at E3 (B-E), focally in caudal rhombomere 1 at E3 (F) or focally into caudal rhombomere 1 at E4 (G). Tissue shown in flat-mount, rostral to left (F: rostral top). C and E show magnified region of B and D where *Fgf8* expression is non-autonomously upregulated (arrow) by *Otx2* overexpression. A'-G' show GFP fluorescence, overlaid in C' and E'.

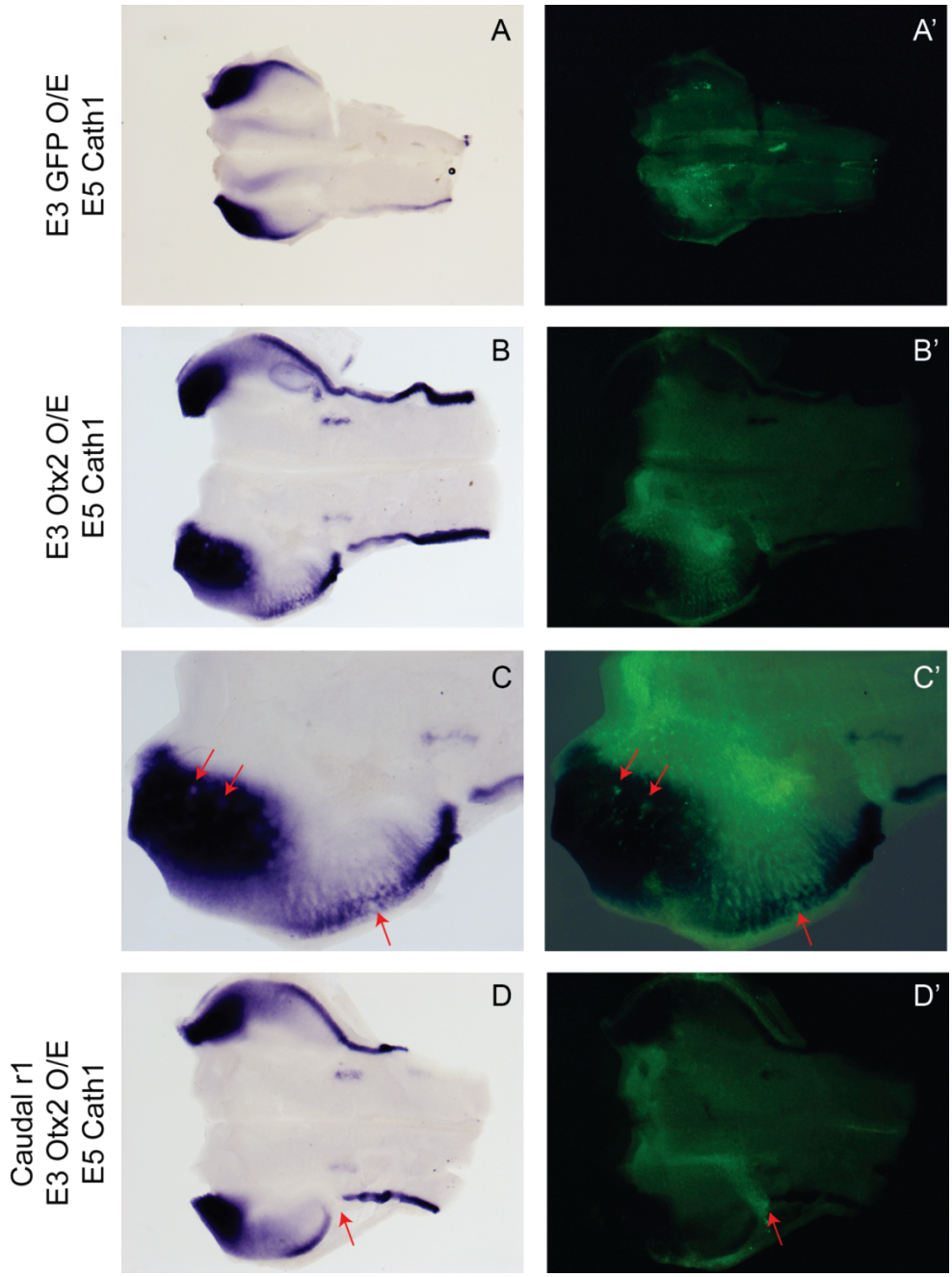

Figure 4-6 E5 *Cath1* expression following overexpression of *Otx2* at E3.

E5 *In situ* hybridisation for *Cath1* following broad rhombomere 1 E3 *gfp* electroporation (A) or *Otx2+gfp* electroporation broadly in rhombomere 1 at E3 (B,C) or focally in caudal rhombomere 1 at E3 (D). Tissue shown in flat-mount, rostral to the left. C shows magnified region of B where *Cath1* expression is autonomously downregulated (red arrows) but non-autonomously upregulated. A'-D' show GFP fluorescence, overlaid in C'. Caudal electroporation of *Otx2* only causes cell-autonomous downregulation of *Cath1* expression (D).

When *Otx2* was electroporated focally in caudal rhombomere 1 no change was seen to the rostral domain but there was a cell autonomous loss of *Cath1* in the rhombic lip (**Figure 4-6 D**). *Cath1* is therefore not induced non-autonomously by *Otx2* independently of an upregulation of *Fgf8*.

The region of the broad domain of *Cath1* expression in the rhombic lip at E3/4 and rostral domain from E5, coincides with the production of *Lhx9*-expressing cells from the rhombic lip. I therefore looked at whether overexpression of *Otx2* in rhombomere 1 at E3, which is sufficient to expand the broad rostral domain of *Cath1*, results in a changed expression of *Lhx9*. Embryos were examined 3 days after electroporation by which stage $Lhx9^{+ve}$ cells are no longer produced from the rhombic lip and *Lhx9* expression is seen in a single domain ventral/rostral to the cerebellum.

Control electroporations of *gfp* caused no change in the expression of *Lhx9* (**Figure 4-7 A**) but co-electroporation of *Otx2* and *gfp* caused a cell autonomous upregulation of *Lhx9* expression (**Figure 4-7 B,C**). Focal electroporation of *Otx2* into caudal rhombomere 1 also resulted in upregulation of *Lhx9* expression (**Figure 4-7 D,E**). Therefore, unlike *Cath1*, *Lhx9* can be upregulated by *Otx2* independently of *Fgf8*.

4.2.5 *Fgf8* is sufficient to induce a broad domain of *Cath1* in rhombomere 1.

Because *Otx2* induces changes non-autonomously (via FGF8, I hypothesise) and autonomously, I wanted to examine how much of this effect is mediated by directly by FGF8. I used a pEFX-*Fgf8b* construct (Toyoda et al., 2010) to overexpress mouse *Fgf8b* in the chick. To confirm that mouse FGF8 is capable of inducing a response in chick cells, I co-electroporated pEFX-*Fgf8b* (hereafter called *Fgf8b*) with *gfp* into the midbrain and hindbrain of E2 embryos and looked a day later at the expression of *Sprouty2*, a direct downstream target and negative feedback regulator of FGF signalling, as a read out of *FGF8* function. I also looked at the expression of *Otx2* and *Gbx2* at E5 in electroporated embryos to assess whether this construct could phenocopy published data showing a rostral shift in the *Otx2-Gbx2* boundary and loss of the tectum following *Fgf8b* overexpression at E2 (Sato et al., 2001).

Control *gfp* electroporations has no effect on the expression of *Sprouty2* surrounding the midbrain-hindbrain boundary (**Figure 4-8 A,B**). Embryos electroporated with *Fgf8b* at E2 showed an upregulation of *Sprouty2* throughout the whole of the midbrain and hindbrain compared to the control side (**Figure 4-8 C,D**). Although the tissue was electroporated evenly throughout this region, different rhombomeres showed different levels of response to

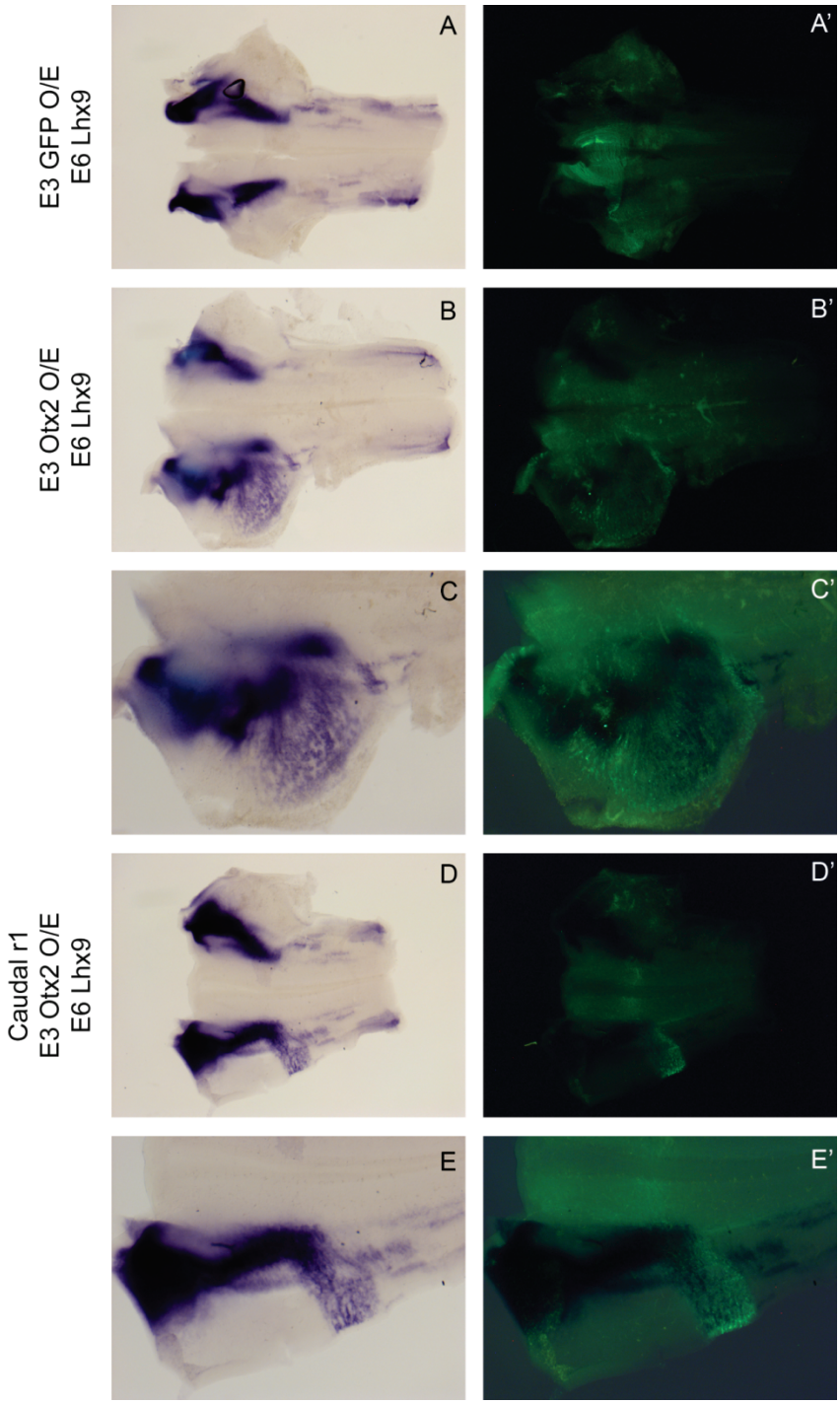

Figure 4-7 E6 *Lhx9* expression following overexpression of *Otx2* at E3.

E6 *In situ* hybridisation for *Lhx9* following broad rhombomere 1 E3 *gfp* electroporation (A) or *Otx2+gfp* electroporation broadly in rhombomere 1 at E3 (B,C) or focally in caudal rhombomere 1 at E3 (D,E). Tissue shown in flat-mount, rostral to left. C and E show magnified region of B and D where *Lhx9* expression is autonomously upregulated by *Otx2*. A'-E' show GFP fluorescence, overlaid in C' and E'.

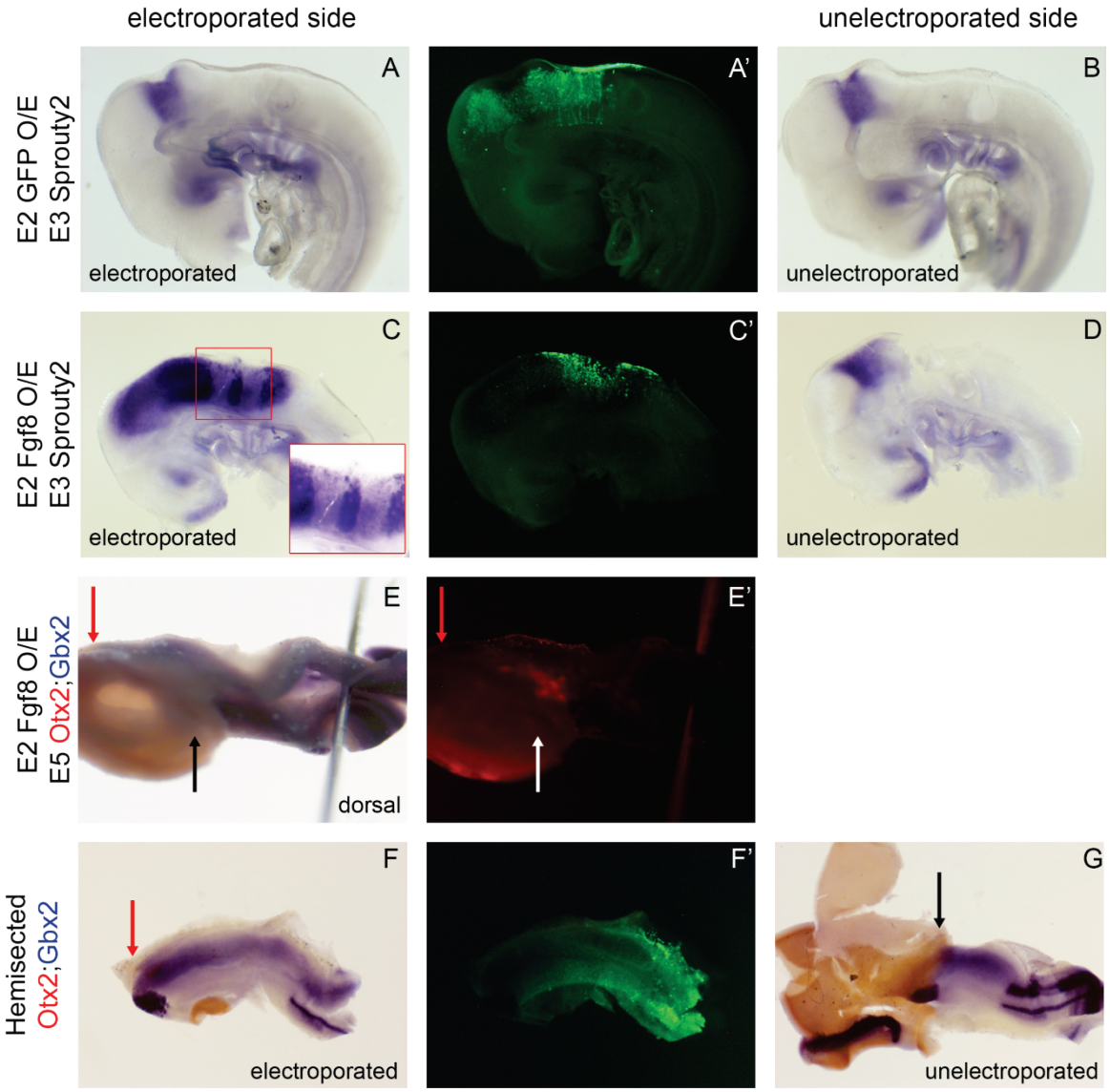

Figure 4-8 *Fgf8b* construct validation by E2 electroporation

E2 midbrain-hindbrain electroporations of *gfp* (A,B) or *Fgf8b* (C-G) stained by *in situ* hybridisation at E3 for *Sprouty2* (A-D) or E5 for *Otx2* (red) and *Gbx2* (blue) (E-G). Shown in hemisected (A-D,F,G) or dorsal view (E), orientated rostral to left. *Fgf8b* causes an upregulation of *Sprouty2* (C), magnified inset and a rostral shift in the *Otx2-Gbx2* boundary (E-G red arrow) compared to the unelectroporated side (black arrow). A'C'F') GFP fluorescence, E') red fluorescence.

the *Fgf8b* overexpression; in particular *Sprouty2* expression was higher in rhombomeres 1 and 4 (**Figure 4-8 C** inset). Furthermore, *Fgf8b* overexpression was sufficient to induce a rostral shift in the *Otx2-Gbx2* boundary on the electroporated side, causing a unilateral loss of tectum (**Figure 3-8 E-G**). These results demonstrate that *Fgf8b* causes an effective overexpression of FGF signalling in chick.

To assess the effectiveness of *Fgf8b* overexpression at E3, specifically in broad or focal electroporations, I looked at the induction of *Sprouty2* expression at E4, following E3 electroporation. Compared to the unelectroporated side (or control electroporations) *Fgf8b* overexpression resulted in a strong cell autonomous and non-autonomous upregulation of *Sprouty* 2 when electroporated in a broad region (**Figure 4-9 A,B**). *Sprouty2* upregulation in non-electroporated (GFP^{-ve}) cells shows that secreted *Fgf8b* protein is acting upon cells surrounding the electroporated region. Focal electroporation in a small region of caudal rhombomere1 caused a much smaller induction of *Sprouty2* (**Figure 4-9 C**). This highlights the importance of assessing the size and position of each individual electroporation.

I next used E3 electroporation of *Fgf8b* to test the effects of ectopic FGF signalling on *Cath1* expression in caudal rhombomere 1. In contrast to controls (**Figure 4-10 A**), co-electroporation of *Fgf8b* and *gfp* into caudal rhombomere 1 at E3 results in a broad upregulation of *Cath1* in caudal rhombomere 1 at E5 (**Figure 4-10 B-E**). At E5, *Cath1* is normally expressed in a gradient throughout rhombomere 1 (see chapter 3) which is abolished by ectopic *Fgf8* expression.

As previously demonstrated (**Figure 4-8 E-G**), E2 overexpression of *Fgf8b* through the midbrain hindbrain boundary causes a downregulation of *Otx2* and an expansion of the $Gbx2^{+ve}$ territory into the midbrain. I therefore wanted to look at how rostral *Cath1* expression was affected following this rostral expansion of $Gbx2^{+ve}$ hindbrain territory. Following E2 co-electroporation of *Fgf8b* and *gfp*, *Cath1* expression was induced throughout the dorsal half of the neural tube in the expanded $Gbx2^{+ve}$ domain (**Figure 4-11 A-D**). At the rostral boundary, *Cath1* is expressed at a much higher level. The rhombic lip also appears to extend throughout this region with the most dorsal cells expressing a slightly higher level of *Cath1*. Within rhombomere 1, there was also a slight upregulation of *Cath1* expression compared to the unelectroporated side, but, despite GFP fluorescence indicating several rhombomeres of the hindbrain were also electroporated, no change in *Cath1* expression was observed caudal to the rhombomere 1-2 boundary.

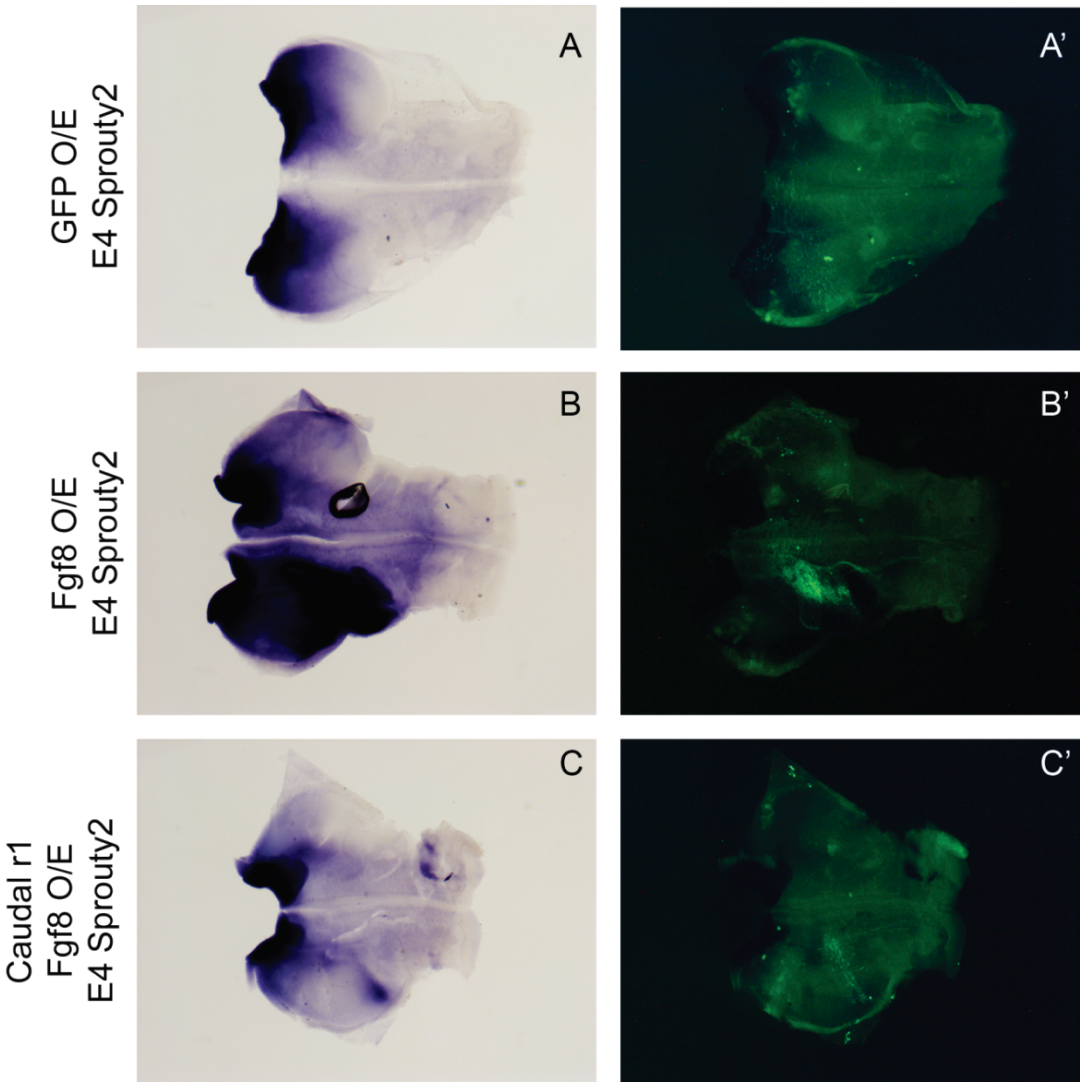

Figure 4-9 *Fgf8* construct validation by E3 electroporation.

E3 electroporations of *gfp* (A) or *Fgf8b* (B,C) in a broad (A,B) or focal (C) domain in rhombomere 1. Stained by *in situ* hybridisation at E4 for *Sprouty2*. *Fgf8b* induces *Sprouty2* cell-autonomously and non-autonomously. A'-C' show GFP fluorescence. Hindbrains shown in flat-mount, rostral to the left.

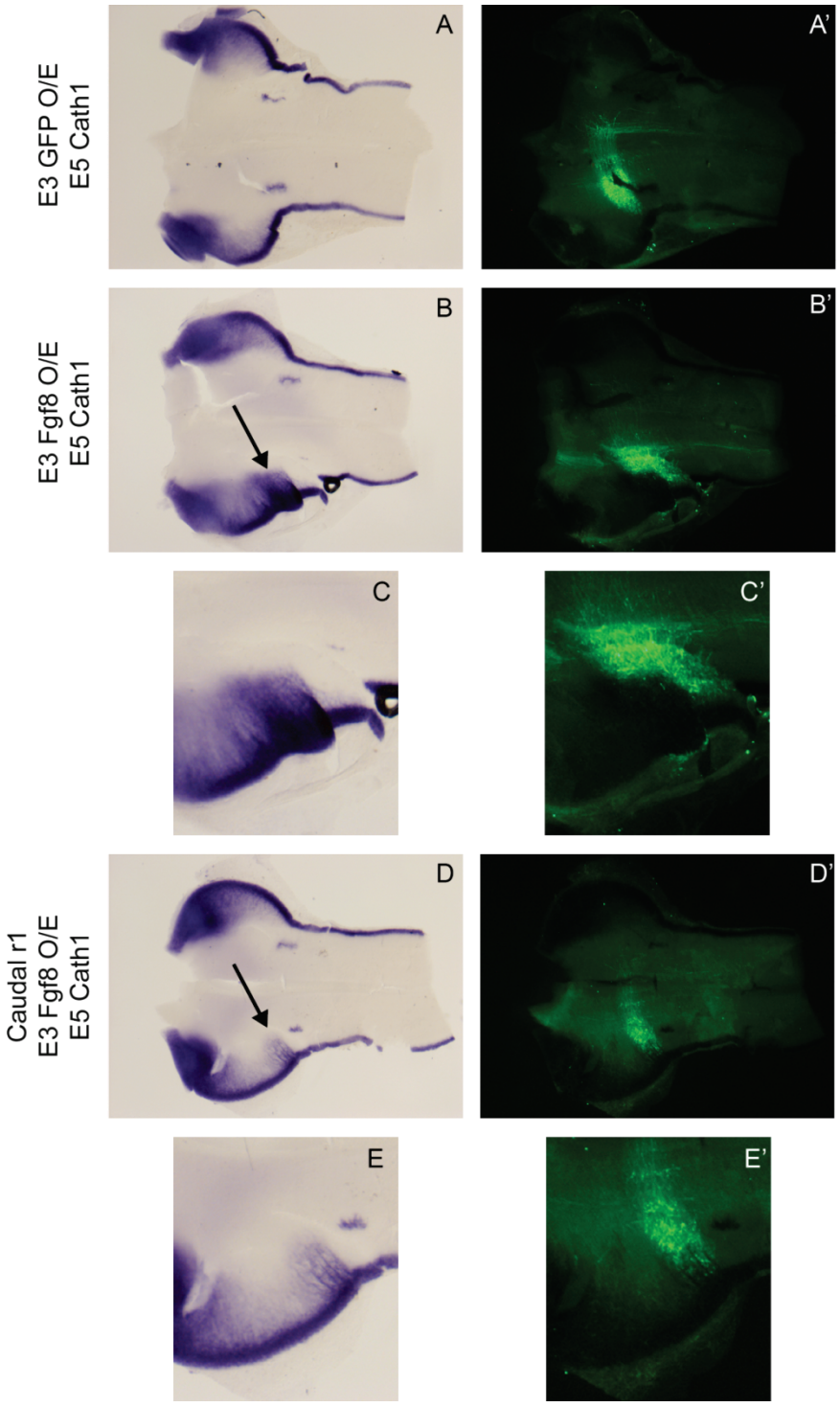

Figure 4-10 E5 *Cath1* expression following E3 overexpression of *Fgf8*.

E3 electroporations of *gfp* (A) or *Fgf8b* (B-E) in a broad (A-C) or focal (D,E) domain in rhombomere 1. Stained by *in situ* hybridisation at E5 for *Cath1*. C and E show magnified region of B and D where *Fgf8b* overexpression upregulates *Cath1* expression (arrows). A'-E' show GFP fluorescence. Hindbrains shown in flat-mount, rostral to the left.

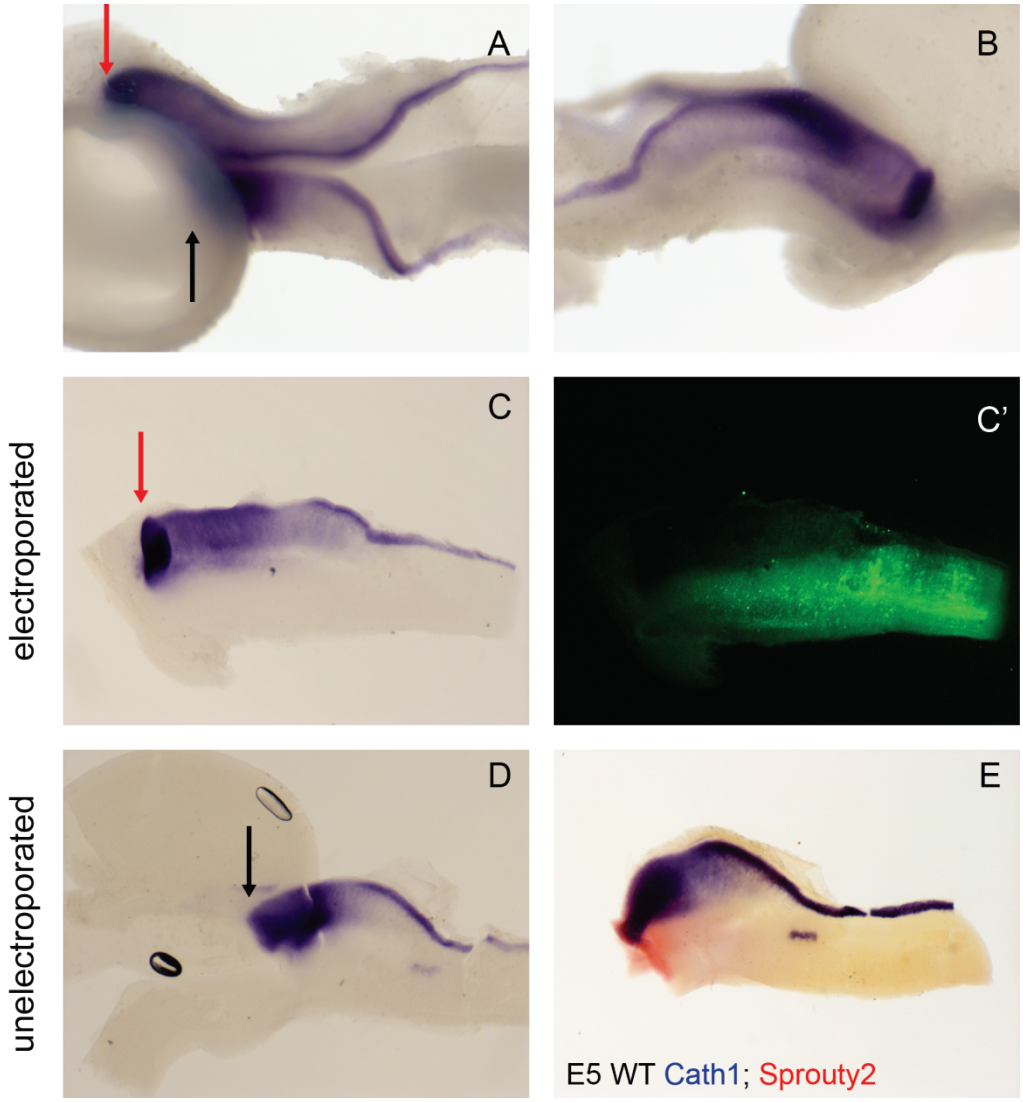

Figure 4-11 E5 *Cath1* expression following E2 overexpression of *Fgf8*.

E2 midbrain-hindbrain electroporations of *Fgf8b* (A-D stained by *in situ* hybridisation at E5 for *Cath1*. Hindbrains shown in dorsal (A), lateral (B) or hemisected (C-E) view, rostral to the left. Red arrow indicated the rostral shift of the midbrain-hindbrain boundary compared to the unelectrporated side (black arrow). *Cath1* is upregulated by Fgf8b in a broad domain in the dorsal region of expanded rhombomere 1. C' shows GFP fluorescence. E) wildtype E5 hindbrain stained for *Cath1* (blue) and *Sprouty2* (red) for comparison normal size of broad rostral Cath1 domain.

On the unelectroporated, side of the embryo there is a slight expansion of the rostral *Cath1* domain in rhombomere 1 and rhombomere 1 seems to be slightly elongated compared to wild type embryos (**Figure 4-11 D,E**). This may be due to secreted *Fgf8* signals from the electroporated half of the brain.

4.2.6 A broad rostral domain of *Cath1* is not able to form in the absence of FGF signalling.

Fgf8 is sufficient to induce expression of a broad domain of *Cath1* in dorsal rhombomere 1, so I next looked at whether this FGF signalling was required for *Cath1* expression. For these experiments I used a *pEFX-dnfgfr3c* construct. This construct contains a truncated human *fgfr3c* isoform, which lacks the intracellular tyrosine-kinase signalling domain. This construct has been shown to bind and sequester FGF8 ligand and results in a reduction in FGF signalling when electroporated into mouse cortex (Toyoda et al., 2010).

To test this *dnfgfr3c* construct in chick, I co-electroporated it with *gfp* into the midbrain and hindbrain at E2 and analysed the expression of *Sprouty2* , a downstream target of FGF signalling, a day later. I also looked at the expression of *Otx2* and *Gbx2* at E5 to see if E2 electroporation could cause a caudal shift in the *Otx-Gbx2* boundary to phenocopy the published effects of FGF knockdown by *Fgf8* siRNA and *Sprouty2* (a negative regulator of FGF signalling) overexpression (Sato and Nakamura, 2004; Suzuki-Hirano et al., 2005).

Co-electroporation of the *dnfgfr3c* and *gfp* at E2 resulted in a strong downregulation of *Sprouty2* expression at the isthmus in the electroporated region (**Figure 4-12 A-E**) demonstrating a sufficiency to abrogate FGF signalling upstream of *Sprouty2*. Furthermore, a caudal shift in the *Otx2-Gbx2* boundary was seen at E5, consistent with an effective knockdown of FGF signalling.

Electroporations of *dnfgfr3c* were also performed to demonstrate the efficiency with which FGF signalling can be reduced in rhombomere 1 at E3. E4 expression of *Sprouty2* was downregulated in caudal, rhombomere 1 following *dnfgfr3c* electroporation at E3 compared to controls (**Figure 4-13 A-C**). *Sprouty2* expression was not completely abrogated in the most rostral part of rhombomere 1, most probably due to the slightly more caudal position of electroporation.

I therefore used co-electroporation of dn*fgfr3c* and *gfp* to test the requirement of FGF signalling for the expression of C*ath1* in rhombomere1. E3 electroporation of *dnfgfr3c* resulted in a marked reduction in the size of rhombomere 1 by E5 compared to the control side. At E5, *Cath1* is expressed in a gradient throughout dorsal rhombomere and in the

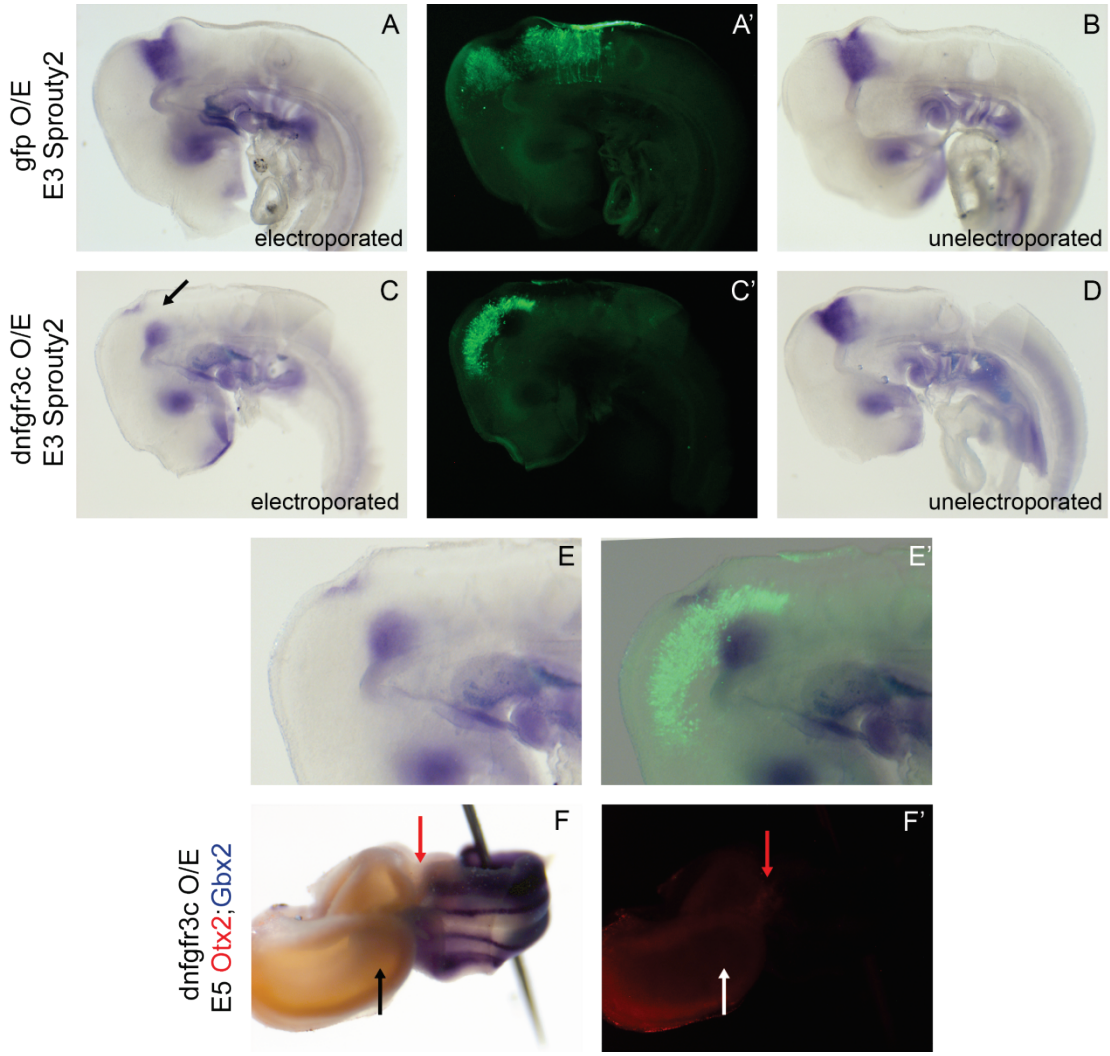

Figure 4-12 *dnfgfr3c* construct validation by E2 electroporation

E2 midbrain-hindbrain electroporations of *gfp* (A,B) or *dnfgfr3c* (C-F) stained by *in situ* hybridisation at E3 for *Sprouty2* (A-D) or E5 for *Otx2* (red) and *Gbx2* (blue) (F). Shown in hemisected (A-E) or dorsal view (F), orientated rostral to left. *dnfgfr3c* causes a downregulation of *Sprouty2* (C arrow, magnified in E) and a caudal shift in the *Otx2-Gbx2* boundary (F red arrow) compared to the unelectroporated side (black arrow). A',C',E') GFP fluorescence (overlaid in E); F') red fluorescence.

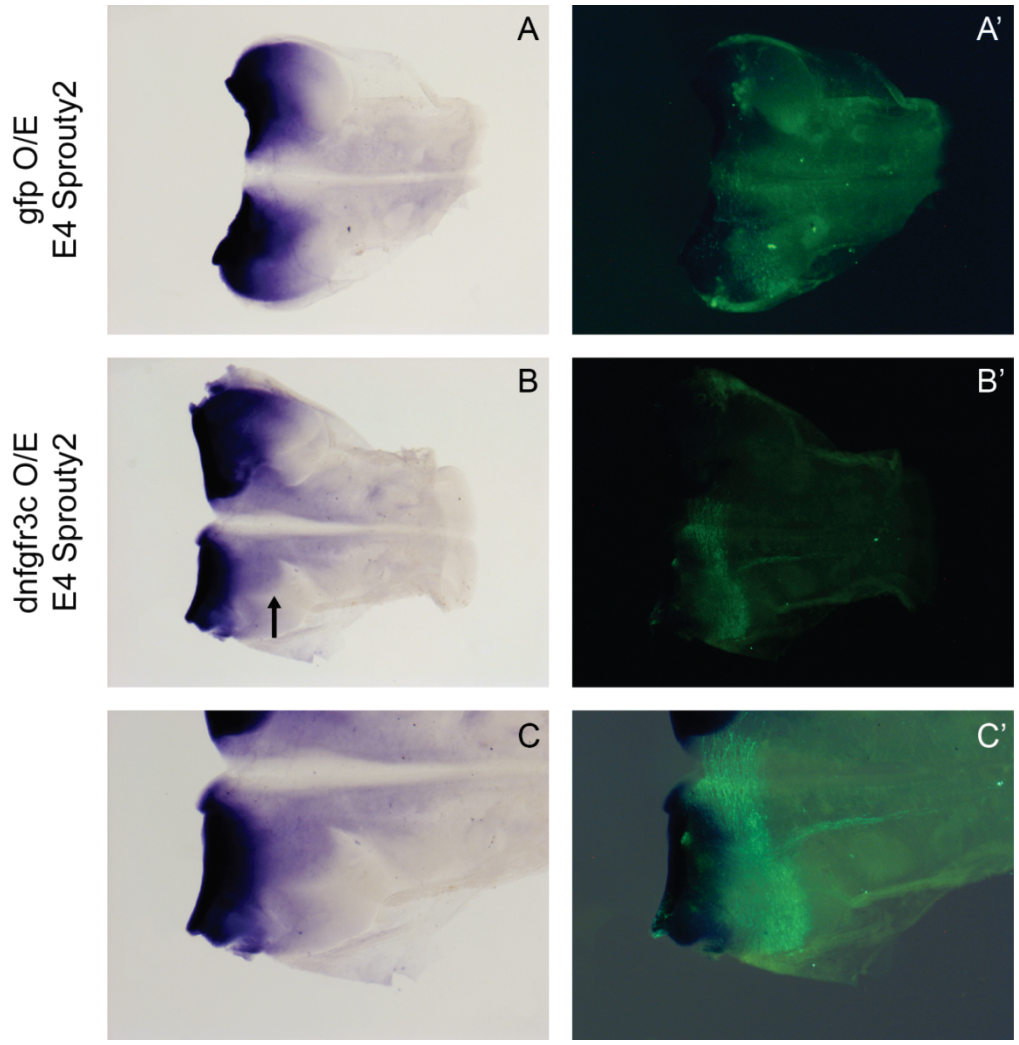

Figure 4-13 *dnfgfr3* construct validation by E3 electroporation

E3 electroporations of *gfp* (A) or *dnfgfr3c* in rhombomere 1. Stained by *in situ* hybridisation at E4 for *Sprouty2*. C shows magnified region of B where *Sprouty2* is downregulated by *dnfgfr3c* (arrow) A'-C' show GFP fluorescence. Hindbrains shown in flat-mount, rostral to the left.

rhombic lip. No loss of *Cath1* expression was ever observed within in the cerebellar rhombic lip, but a slight downregulation of *Cath1* was seen in the broad expression domain disrupting the gradient of expression compared to the unelectroporated side (**Figure 4-14 A-C**). No complete loss of the broad rostral domain of *Cath1* was observed in E3 *dnfgfr3c* electroporations consistent with the domain of *Sprouty2* expression which was retained rostrally after similar electroporations.

I next looked at the expression of *Cath1* following E2 electroporation of *dnfgfr3c* in midbrain and hindbrain which results in a caudal shift of the *Otx2*-*Gbx2* boundary (see **Figure 4-12 F**). These embryos showed a complete absence of *Cath1* in the expanded *Otx2* positive domain. Rhombic lip *Cath1* expression was seen caudal to the shifted boundary but no broad rostral domain of *Cath1* was seen (**Figure 4-15**). E3 electroporations of *Fgf8b* show this region is competent to upregulate *Cath1* expression leading to the conclusion that FGF signalling is required at the midbrain-hindbrain boundary to induce a broad domain of *Cath1* expression, which is distinct from the rest of the rhombic lip.

Together these result show that the loss of FGF signalling from the isthmus causes a complete loss of the broad *Cath1* domain in E5 embryos without affecting *Cath1* expression in the rhombic lip.

4.2.7 *Lhx9* expression is affected by, but not dependent on FGF signalling.

Broad *Cath1* expression is associated with the expression of *Lhx9* both throughout the E3/E4 broad cerebellar rhombic lip and the E5-E7 rostral domain. I therefore tested whether *Lhx9* expression is also affected by FGF signalling from the isthmus.

E3 co-electroporation of *Fgf8b* and *gfp* into rhombomere 1 showed a disruption in *Lhx9* expression at E6 compared to controls (**Figure 1-16 A-C**). Instead of *Lhx9*-positive cells forming a continuous domain in ventral rhombomere 1, small gaps in expression and ectopic streams of cells were seen the electroporated region. No *Lhx9* expression was observed at the cerebellar rhombic lip at E6 showing that *Fgf8b* was not sufficient to induce the production of *Lhx9*-positive cerebellar rhombic lip derivatives outside of the normal temporal window of specification.

Electroporations of *Fgf8b* at the rhombomere 1-2 boundary had a very different effect on *Lhx9* expression than electroporations into rhombomere 1. *Fgf8b* overexpression in rhombomere 2 caused a clear upregulation of *Lhx9* expression compared to the control side (**Figure 4-16 D,E**). Cells formed an extension of the rhombomere 1 *Lhx9*-positive domain into rhombomere 2 and expression was also seen in a stream from the rhombic lip at E6.

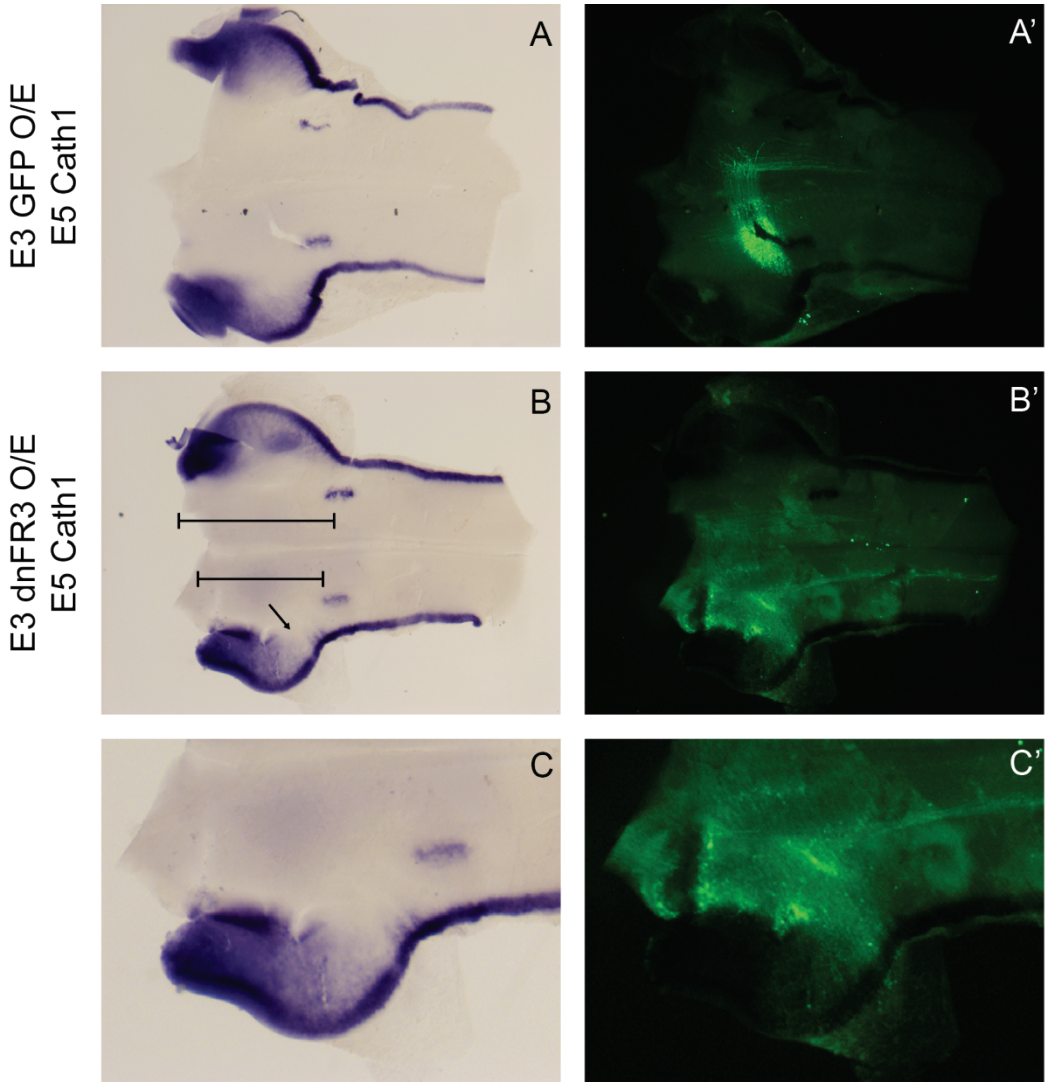

Figure 4-14 E5 *Cath1* expression following E3 overexpression of *dnfgfr3c*.

E3 electroporations of *gfp* (A) or *dnfgfr3c* (B,C) in rhombomere 1, stained by *in situ* hybridisation at E5 for *Cath1*. C shows magnified region of B where *dnfgfr3c* overexpression downregulates regulates the broad domain of *Cath1* expression (arrow) but not the rhombic lip *Cath1*. *Dnfgfr3c* also causes a reduction in the size of rhombomere 1 as indicated by line in B. A'-C' show GFP fluorescence. Hindbrains shown in flat-mount, rostral to the left.

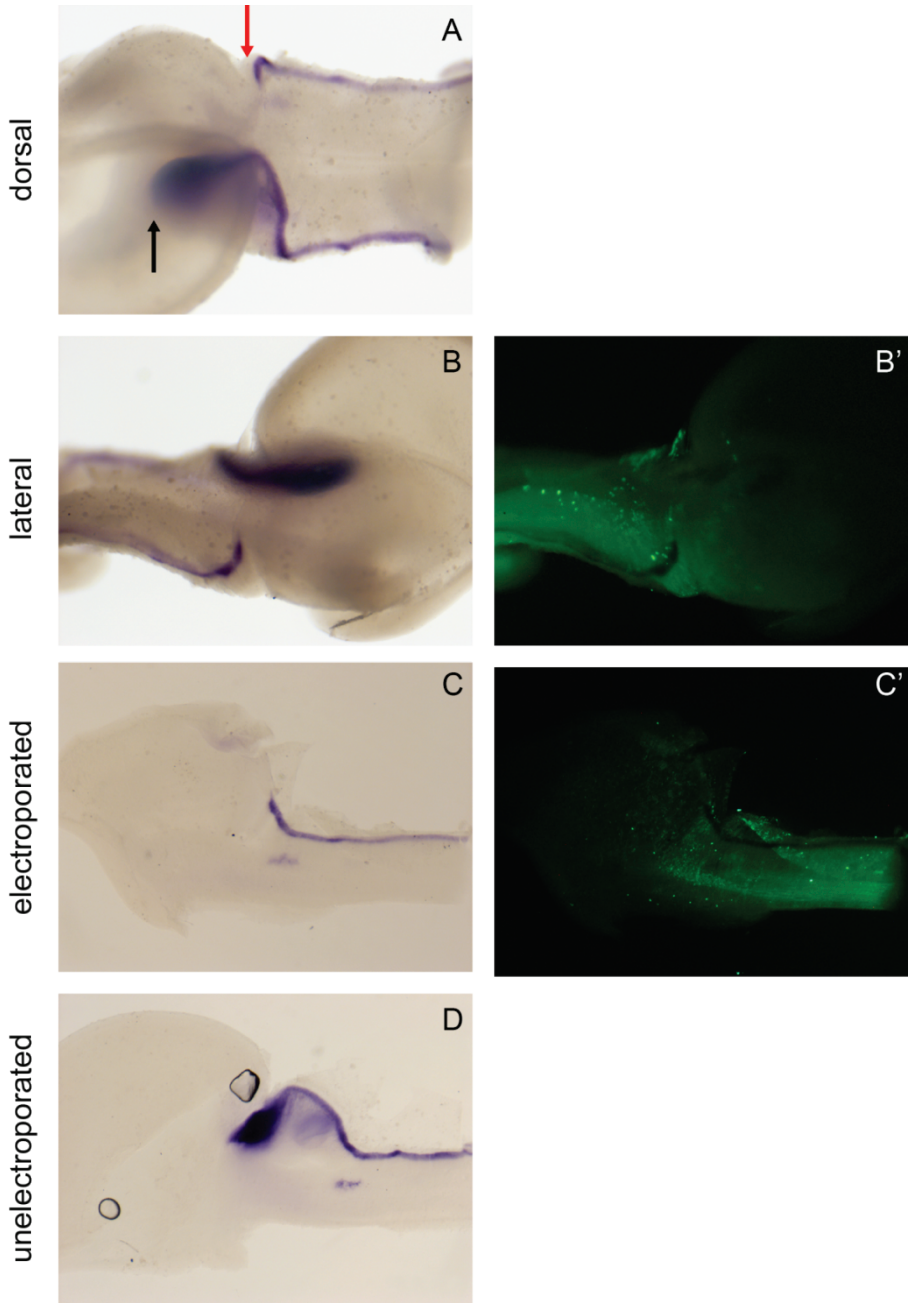

Figure 4-15 *Cath1* expression following E2 overexpression of *dnfgfr3c*.

E2 midbrain-hindbrain electroporations of *dnfgfr3c* (A-D stained by *in situ* hybridisation at E5 for *Cath1*. Hindbrains shown in dorsal (A), lateral (B) or hemisected (C,D) view, rostral to the left. Red arrow indicates the caudal shift of the midbrain-hindbrain boundary compared to the unelectroporated side (black arrow). *Cath1* is not expressed in a broad domain at the mid-hindbrain boundary following dnfgfr3c overexpression. B' and C' show GFP fluorescence.

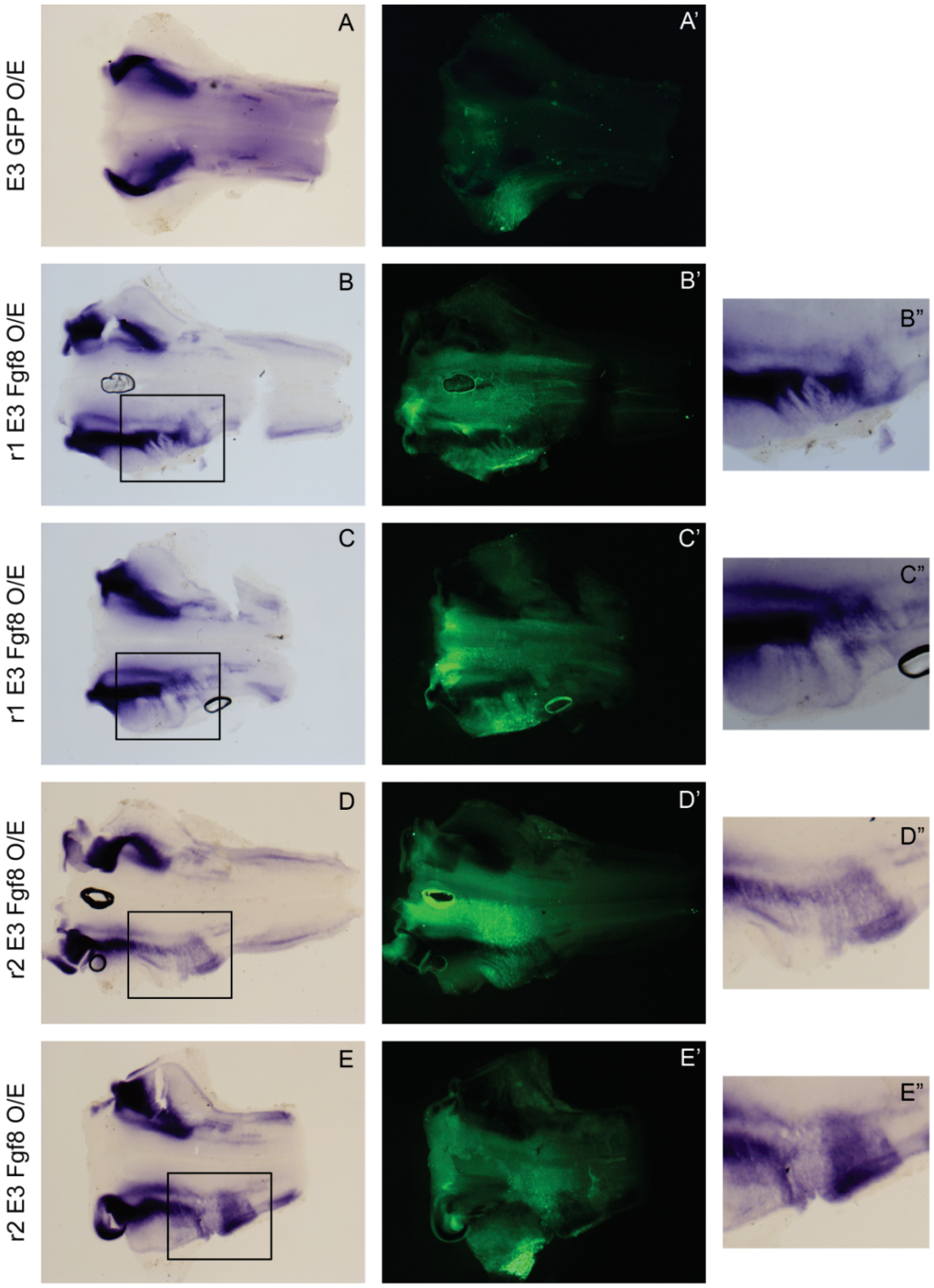

Figure 4-16 E6 *Lhx9* expression following E3 overexpression of *Fgf8b*.

E3 electroporations of *gfp* (A) or *Fgf8b* (B-E) in rhombomere 1 (A-C) or at the rhombomere 1-2 boundary (D,E), stained by *in situ* hybridisation at E6 for *Lhx9*. A'-E' show GFP fluorescence. B"-E" show magnified region in B-E where *Lhx9* expression is disturbed (B,C) or upregulated (D,E) by *Fgf8b* overexpression. Hindbrains shown in flat-mount, rostral to the left.

Cath1 is not upreguated in rhombomere 2 following *Fgf8b* overexpression (see **Figure 4-11 C**) showing that rhombomere 2 elicits a different response to *Fgf8* than rhombomere 1.

I next performed co-electroporations of *dnfgfr3c* with *gfp* into rhombomere 1 at E3 and looked at the expression of *Lhx9* at E6 to assess whether production of *Lhx9*-positive cells was disrupted. No change in *Lhx9* expression was seen in control or *dnfgfr3c* electroporated embryos (**Figure 4-17 A,B**).

Lhx9 cells are born from the cerebellar rhombic lip over the course of 2 days (E3-E5) to form the large domain seen at E6, therefore any subtle effect of *dnfgfr3c* overexpression may not be obvious at E6. I therefore repeated E3 electroporations of *dnfgfr3c* and looked at the expression of *Lhx9* a day after electroporation at E4 when only a few *Lhx9*-expressing cells have been born and are in the process of migrating ventrally. However, this also was not sufficient to cause a change in *Lhx9* expression (**Figure 4-17 C,D**).

Together these results show that FGF signalling is not required for the production of *Lhx9*-positive cells from the cerebellar rhombic lip. Ectopic *Fgf8b* expression is not sufficient to produce *Lhx9*$^{+ve}$ cells from the cerebellar rhombic lip but can affect the normal formation of *Lhx9*-positive nuclei in ventral rhombomere 1.

4.3 Discussion

In this chapter I have demonstrated that the isthmus is necessary and sufficient to induce a distinct broad domain of *Atoh1* expression in rhombomere 1 and that this is mediated via FGF8 signalling. In contrast, rhombic lip expression of *Atoh1* is independent of isthmic signalling. I have also shown that although *Lhx9* expression is closely associated with the FGF-dependent broad domain of *Atoh1* expression, *Lhx9* is not induced by or dependent on FGF signalling.

4.3.1 Technical limitations of electroporating *dnfgfr3c*

To test the effects of loss of FGF signalling I chose to electroporate a truncated human *fgfr3c*. It has been shown (Toyoda et al., 2010) that when electroporated into mouse cortex, this dominant-negative receptor is capable of binding and sequestering FGF8 protein resulting in a downregulation of phosphorylated-ERK (activated downstream signalling component) in electroporated cells and in the immediate surrounding region. By sequestering FGF8 protein, the dnFGFR3c also acts as a sink for the ligand disrupting the gradient of ligand within the rest of the tissue.

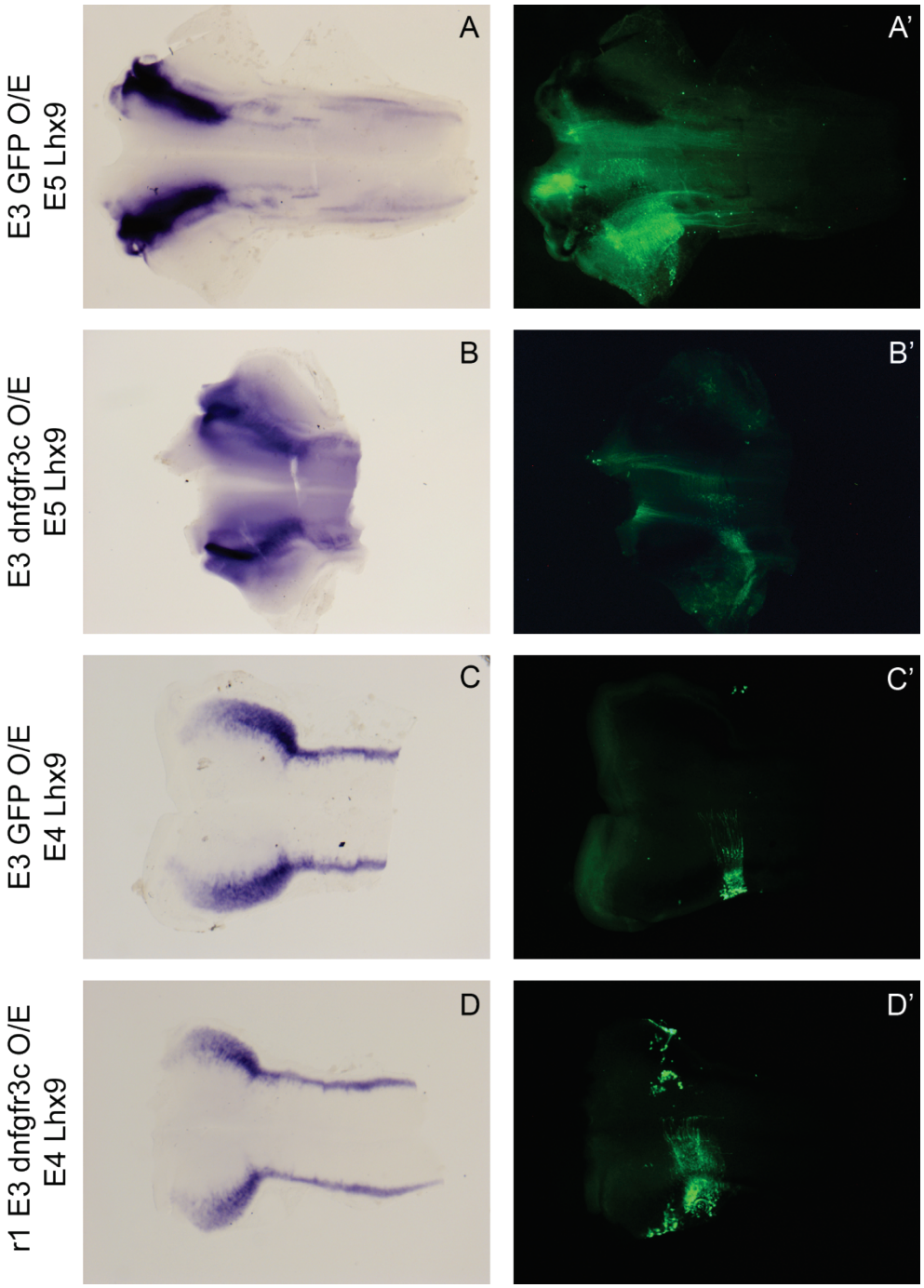

Figure 4-17 *Lhx9* expression following E3 overexpression of *dnfgfr3c*.

E3 electroporations of *gfp* (A,C) or *dnfgfr3c* (B,D) in rhombomere 1, stained by *in situ* hybridisation at E6 (A,B) or E4 (C,D) for *Lhx9*. A'-D' show GFP fluorescence. *dnfgfr3c* overexpression does not affect *Lhx9* expression. Hindbrains shown in flat-mount, rostral to the left.

It has not been shown whether this dominant-negative receptor can disrupt endogenous functional FGF receptors or just acts by competitive binding of ligand and it is not known whether this receptor can bind other FGF ligands such as FGF17 and FGF18 which are also expressed at the isthmus and play a role in cerebellar development, partially redundantly with FGF8.

FGFR3 is not the predominantly active receptor in rhombomere 1 and is only expressed in the most caudal region of the rhombomere (Walshe and Mason, 2000; Blak et al., 2007). However this truncated human receptor does seem to effectively reduce *Sprouty2* expression when electroporated into chick in both an autonomous and non-autonomous manner. *Sprouty2* expression is induced by FGF signalling and therefore provides a readout of sites of FGF signalling transduction (Chambers et al., 2000). Furthermore, *dnfgfr3c* overexpression at E2 can phenocopy FGF signalling knockdown, shifting the midbrain-hindbrain boundary caudally. Finally overexpression of this receptor appears to reduce the size rhombomere 1 on the electroporated side. This could be through cell death which is a reported effect of loss of *Fgf8* in mouse (Chi et al., 2003). However this study also shows that with partial loss of *Fgf8*, no cell death occurs (Chi et al., 2003). In my electroporations, FGF signalling is not completely abrogated and therefore it may be more likely that reduction in size of rhombomere 1 results from changes in growth and proliferation. This is supported by other observations that ectopic *Fgf8a* in the midbrain can increase proliferation (Lee et al., 1997) and that reduction in other FGF signalling molecules causes reduced proliferation in the midbrain and cerebellum, a phenotype which can be enhanced by loss of one copy of *Fgf8* (Xu et al., 2000).

Despite E3 electroporations of *dnfgfr3c* resulting in only a small reduction of broad *Cath1* expression, and no changes in rhombic lip *Cath1* or *Lhx9* expression, I am confident that these results are not due to an ineffectual reduction of FGF signalling using this dominant-negative receptor. The fact that complete loss of the broad rostral domain of *Cath1* expression was not seen following *dnfgfr3c* electroporation is consistent with the retention of *Sprouty2* expression in rostral rhombomere 1 following *dnfgfr3c* electroporation. This is likely due to technical limitations in electroporating the rostral region of rhombomere 1.

Results from E2 *dnfgfr3c* electroporation clearly show that an *Otx2*-*Gbx2* boundary lacking FGF signalling cannot induce a broad domain of *Cath1* expression in rhombomere 1. This is unlikely due to a lack of competence of more caudal tissue to form a broad domain of *Cath1*, because upregulation of *Cath1* in caudal rhombomere 1 is seen following *Fgf8b* overexpression.

4.3.2 *Otx2, Fgf8* and regional patterning

Through electroporation of *Otx2* I have been able to recapitulate the results of other studies showing non-autonomous induction of *Fgf8* (Katahira et al., 2000). However my results differ from this study showing that by electroporating a day later, at E3, it is only possibly to expand the isthmic organiser and it is not possible to non-autonomously induce *Fgf8* expression in caudal rhombomere 1. This observation may also explain why it was also not possible to induce an isthmic organiser by co-culture of E3 or E5 midbrain and rhombomere 1 in comparison to tissue from E2 embryos (Irving and Mason, 1999). Together these results demonstrate a loss of competence to induce an isthmic organiser by E3, but a maintained capacity to expand an existing isthmic organiser.

Lhx9 is expressed throughout the midbrain as well as in early born rhombic lip derivatives. Following *Otx2* overexpression, cell-autonomous upregulation of *Lhx9* occurs in a domain where *Cath1* expression is downregulated. This is consistent with a cell-autonomous transformation to a midbrain fate which is seen in previous studies of *Otx2* overexpression in rhombomere 1 (Broccoli et al., 1999; Katahira et al., 2000).

Electroporations of *Fgf8b* at E2 were also capable of recapitulating results of previous studies, causing a rostral shift in the *Otx2-Gbx2* boundary (Liu et al., 1999; Sato et al., 2001). Together *Fgf8b* electroporations at E2 and E3 demonstrated several ways in which different regions of midbrain/hindbrain respond to FGF signalling. Different levels of *Sprouty2* induction were seen in different rhombomeres, suggesting different levels of FGF signal transduction in different compartments of the hindbrain. Only dorsal tissue was capable of inducing *Cath1* in response to *Fgf8* and rhombomere 2 could upregulate *Lhx9* but not *Cath1* expression. These observations highlight that a specific combination of factors and spatial cues are important to induce the correct downstream effects of isthmic signalling.

The inability to induce *Cath1* expression in ventral rhombomere 1 following E2 *Fgf8b* electroporation can be contrasted with the observation that in *in vitro* cultures, *Cath1* expression can be induced in ventral tissue adjacent to the isthmus. In these cultures, roof plate tissue was removed which may suggest a dorsalising signal from the roof plate determines the regional competence of tissue to induce *Cath1* in response to FGF signalling.

A study in which *Hoxa2* is overexpressed in rhombomere 1 demonstrated that late but not early cerebellar rhombic lip derivatives were lost (Eddison et al., 2004). Contrasted with the result that *Lhx9* but not *Cath1* can be induced in rhombomere 2 following *Fgf8b*

overexpression suggesting there may be a unique interaction between FGF signalling and *Hox* gene expression that has yet to be explored.

4.3.3 An FGF-dependent *Atoh1* domain in rostral rhombomere 1

Using three different experimental approaches I have shown that a broad domain of *Atoh1* is expressed following isthmic/FGF signalling. In cultures, *Fgf8* and *Atoh1* were only observed where a midbrain-hindbrain boundary was intact and this was independent of roof plate signalling. *Cath1* was only induced non-autonomously by *Otx2* overexpression in a domain where *Fgf8* expression was expanded and electroporation of *Fgf8b* can directly upregulate *Cath1* expression in a broad domain.

Furthermore, culture experiments removing the isthmus showed, not only loss of the broad rostral *Cath1*$^{+ve}$ domain at E5, but showed a marked reduction in rhombic lip *Cath1* expression in E3 cultures. The inability to rescue this loss of expression by the juxtaposition of midbrain and hindbrain tissue was consistent with the inability to induce *Fgf8* expression by co-culture. Dissections at E3 and E4 would not remove broad *Cath1* expression which is expressed throughout the whole of rhombomere 1 and therefore rescue experiments are not required to confirm these results.

The fact that *Cath1* expression is reduced but not lost in E3 culture experiments demonstrates that the broad rhombic lip seen in E3/E4 brains is a result of both roofplate and isthmic influences. However it was not possible to effectively remove the roofplate from E3 hindbrain tissue and therefore it was not possible to determine whether broad *Cath1* expression in the rhombic lip represents an increase in the roof plate induced *Cath1*$^{+ve}$ domain or whether FGF signalling can induce *Cath1* independently of roof plate signalling at these stages. Further experiments could be performed to show whether FGF signalling can compensate for a loss of roof plate-dependent *Cath1*. Electroporation of *Fgf8b* in vitro following roof plate removal from hindbrain tissue at E4 or culturing with exogenous FGF protein could demonstrate whether FGF is sufficient to induce rhombic lip *Cath1* expression.

E2 *dnfgfr3c* electroporation also confirmed that broad C*ath1* expression was abolished at an *Otx2-Gbx2* boundary which is unable to respond to FGF signalling. E3 *dnfgfr3c* electroporations show a small reduction in broad *Cath1* expression however it was not possible to electroporate in the most rostral region of rhombomere 1 at E3 to test whether the entire broad rostral domain could be abolished by *dnfgfr3c* electroporation. Electroporating *dnfgfr3c* at E3 and analysing *Cath1* expression at E4 when broad expression is found

throughout rhombomere 1, may be more effective in demonstrating the function of *dnfgfr3c* electroporation at E3.

Together these results lead to a model whereby TGF-β signalling from the roof plate and FGF signalling from the isthmus can both induce *Cath1* expression in rhombomere 1 and that FGF-dependent *Cath1* expression is superimposed onto TGF-β-dependent *Cath1* expression between E3 and E4 to expand the rhombic lip. The fact that *Fgf8b* can upregulate *Cath1* expression in caudal rhombomere 1 shows the normal regression of the broad C*a*th1 domain into rostral rhombomere 1 at E5 does not reflect a loss of competence to respond to FGF signalling in caudal rhombomere 1 and therefore the progressive temporal reduction in *Fgf8* expression is likely to determine the caudal extent of broad *Cath1* expression.

4.3.4 Specification of *Lhx9*$^{+ve}$ cerebellar rhombic lip derivatives is independent of FGF signalling

Lhx9 expression is closely correlated with the broad FGF-dependent expression of *Atoh1*. However, manipulations of *Fgf8* function in the specification of *Lhx9*$^{+ve}$ cells from the cerebellar rhombic lip resulted in a breakdown in this correlated expression.

Loss or reduction of FGF signalling both in vitro, and by *dnfgfr3c* electroporation did not alter the expression of *Lhx9*, demonstrating that FGF signalling is not required for *Lhx9*$^{+ve}$ cell fate. However, as shown by *Sprouty2* expression, *dnfgfr3c* electroporation does not completely abrogate FGF signalling. Furthermore, in cultured explants the expression of *Lhx9* was globally disturbed making it difficult to assess whether cell specification was disrupted. The disrupted expression of *Lhx9* in vitro suggests that rhombic lip derivatives may not be able to migrate normally. It has previously been shown than rhombic lip derivatives require signalling from the overlying meninges for tangential migration (Zhu et al., 2002) and therefore cell migration may be disrupted by dissection and in *in vitro* culture.

Overexpression of *Fgf8b* in rhombomere 1 was unable to induce the expression of *Lhx9* in rhombic lip derivatives outside of the normal temporal window of development showing that the temporal transition between cell types is not controlled by FGF signalling. These electroporations did however, result in a disruption of *Lhx9* expression which neither appeared to be an obvious up-regulation or down-regulation of expression. This disrupted expression phenotype showed cells in clustered streams which could be a result of perturbed migration. Along the rostrocaudal axis of rhombomere 1, *Lhx9* cells exhibit different migration patterns in normal development with more caudal cells migrating further ventrally than cells that originate more rostrally. It is possible that this gradient of different migration

could be established by FGF signalling from the isthmus and therefore overexpression of *Fgf8b* in caudal rhombomere 1 could result in cells terminating their migration in an ectopic dorsal position. This hypothesis could be tested by mapping the migration of rhombic lip derivatives when *Fgf8* is overexpressed or by examining the position of *Lhx9*$^{+ve}$ rhombic lip derivatives in mice with reduced FGF signalling. These experiments are shown in chapter 5.

An alternative explanation for the disrupted expression of *Lhx9* following *Fgf8b* overexpression is that upregulation of *Cath1* in these electroporations causes a disruption in the balance of progenitor cell proliferation and differentiation to produce rhombic lip derivatives. It has been shown that ectopic *Fgf8* expression in the midbrain can promote progenitor cell proliferation at the expense of neurogenesis (Lee et al., 1997) and therefore this data may support a model whereby FGF signalling promotes progenitor cell proliferation over differentiation.

Together these results lead to the conclusion that FGF signalling does not control the specification of *Lhx9*$^{+ve}$ cell types and the temporal transition between the production of *Lhx9*$^{+ve}$ and *Lhx9*$^{-ve}$ cell types from the cerebellar rhombic lip occurs independently of FGF signalling. To confirm these conclusions, in the next chapter I will analyse the expression of early born rhombic lip derivatives in mice with reduced FGF signalling.

4.3.5 What is the significance of two different *Cath1*$^{+ve}$ domains?

In the chapter 3 I identified two distinct progenitor domains expressing *Cath1* and in this chapter I have demonstrated that these two domains are distinctly regulated. Having shown that temporal transitions in the cerebellar rhombic lip appear to be independent of FGF signalling, this raises the question: What is the significance of these two domains?

In mouse, loss of FGF signalling causes a loss of the cerebellar vermis, the medial region of the cerebellum which is derived from the most rostral region of rhombomere 1 (Meyers et al., 1998; Chi et al., 2003; Sgaier et al., 2005). Therefore, if *Atoh1* expression in rostral rhombomere 1 in mouse is also dependent on *Fgf8* then this may explain this phenotype. However it is not clear how the structure of the mammalian cerebellum, consisting of a vermis and two hemispheres, developmentally relates to the structure of the avian cerebellum which is a single structure, fused across the midline.

Alternatively, a model might begin to emerge in which FGF-dependent broad domain of *Cath1* regulates proliferation whilst TGF-β dependent rhombic lip *Cath1* regulates cell specification. This model is supported by the respective phenotypes of knocking out *Atoh1*, which results in a loss of specification of all rhombic lip derivatives (Ben-Arie et al., 1997;

Machold and Fishell, 2005; Wang et al., 2005; Rose et al., 2009a) compared to knocking out *Fgf8*, which causes loss of regions of tissue within the cerebellum (Meyers et al., 1998; Chi et al., 2003).

Chapter 5 Heterogeneity within single temporal cohorts of cerebellar rhombic lip derivatives.

5.1 Background

In chapter 2 I demonstrated that a temporal progression of cell production from the cerebellar rhombic lip results in the generation of molecularly distinct cells in chick. These populations include: extra-cerebellar cells in ventral rhombomere 1, two cerebellar nuclei and cerebellar granule cell precursors. These observations indicated that within populations born prior to granule cells there may be further patterning within each individual temporal cohort. At a particular time point multiple cell types are born, within a given nucleus, that have different projections. For example, cells of the *Tbr1*$^{+ve}$ medial cerebellar nucleus are born at E5 but give rise to cells with ascending or descending axon projections. In this chapter I will further investigate the origins of this diversity, assessing whether rostrocaudal spatial patterning cues are used to generate increased diversity.

I have used two experimental approaches to determine the nature of spatially determined diversity in the cerebellar rhombic lip. Firstly, I have labelled the derivatives of the rostral and caudal cerebellar rhombic lip by electroporating *gfp* and *rfp* into different regions of the cerebellar rhombic lip of a single embryo. And secondly, I have employed a heterotopic-heterochronic grafting assay to determine whether intrinsic or extrinsic factors determine any spatial differences within the rhombic lip. By grafting tissue from distinct locations or time points into an ectopic spatial or temporal environment it is possible to assess whether cells are intrinsically committed to a specific cell fate or whether extrinsic cues from the ectopic environment can direct cells to change their intrinsic properties. This strategy has been used in heterochronic grafting in the cortex (McConnell, 1988) and retina (Belliveau and Cepko, 1999) and in heterochronic-heterotopic grafting of cerebellar rhombic lip cells (Wilson and Wingate, 2006).

FGF signalling from the isthmic organiser is a strong candidate for influencing rostrocaudal pattern. In chapter 4 I demonstrated a requirement for isthmic *Fgf8* in inducing a broad domain of *Cath1* expression in rostral rhombomere 1. This domain is not involved in the production of rhombic lip derivatives and ultimately resolves to a domain that lies outside of the cerebellum. However a gradient of FGF signalling is present throughout the whole of rhombomere 1, before E5, which could affect early patterning and development. Although I have shown that a loss of FGF signalling cannot disrupt the expression of *Lhx9*, *Fgf8* overexpression causes a disruption in the positioning of *Lhx9*$^{+ve}$ cells which could be due to

either extrinsic influences on migration or reflect intrinsic alterations in neurogenesis. To assess the role of FGF signalling in the specification and migration of specific temporal and spatial cohorts of cerebellar rhombic lip derivatives I combined electroporation of *gfp* and *rfp* to label cells with electroporation of *Fgf8b* or a dominant-negative FGF receptor to analyse the patterns of axon projections and migration of cells following changes in FGF signalling.

In mice, a reduction in isthmic FGF signalling results in the deletion of the cerebellar vermis, the medial region of the cerebellum, which is derived from the most rostral region of the cerebellar rhombic lip (Meyers et al., 1998; Chi et al., 2003; Sgaier et al., 2005). However, the development of the earlier born cells in ventral rhombomere 1 and the cerebellar nuclei have not been examined following this loss of isthmic signalling and concomitant deletion of a large region of cerebellar tissue. In particular, the *Tbr1*$^{+ve}$ fastigial cerebellar nucleus lies within the cerebellar vermis; how then is the development of these cells affected?

Mice with conditional knockout of FGF receptors in the *Math1*$^{+ve}$ lineage have an apparently normal cerebellum (unpublished data, Rob Wechsler-Reya) showing defects following a loss of *Fgf8* result from defects in progenitor cells prior to the onset of *Math1*, either through proliferation or allocation to the rhombic lip lineage. The early born cerebellar rhombic lip derivatives of ventral rhombomere 1 and the cerebellar nuclei have not been looked at in these mice when FGF signalling from the isthmus is strong throughout rhombomere 1.

5.2 Results

5.2.1 Rostrocaudal patterning of the cerebellar rhombic lip generates cell diversity within specific temporal cohorts.

Electroporating the cerebellar rhombic lip at any given time point with *gfp* labels a heterogeneous population of cells within a given nucleus. Individual temporal cohorts derived from the cerebellar rhombic lip give rise to more than one distinct axon tract. Furthermore, scattered labelling by electroporation of Cre with Stop-*gfp* shows that no axon branching occurs and therefore different axon tracts are a result of heterogeneous populations of cells being born from the cerebellar rhombic lip at a single time point. To further investigate this apparent heterogeneity within the rhombic lip I first attempted to characterise the different patterns of cell labelling that were seen from individual electroporations at a single developmental stage.

At E7 the patterns of labelled projections following *gfp* cerebellar rhombic lip electroporations at St23 (see chapter 2), fall into three groups: 1) Axon projections in all ascending and descending tracts including the fasciculus uncinatus (**Figure 5-1 A**), 2) mostly ascending projections, including the fasciculus uncinatus (**Figure 5-1 B**), and 3) Mostly descending projections with no fasciculus uncinatus labelled (**Figure 5-1 C**).

All of these embryos were electroporated and harvested at the same developmental stages and the cells labelled were produced over the course of 3 days, therefore the different patterns of axon projections cannot be generated by different temporal changes. Most electroporations seem to have a bias towards either ascending or descending axon projections. Embryos with predominantly descending projections labelled appeared to be electroporated closer to the rhombomere 1-2 boundary than embryos with predominantly ascending axons. Therefore it seems that the variation in the exact position and size of each electroporation could account for the difference observed.

Distortions following flat-mounting make it difficult to draw direct comparisons between the position of electroporations in different embryos. The cerebellar rhombic lip was therefore electroporated at E4 using two different constructs at different rostrocaudal positions to allow for a direct comparison between electroporations in a single embryo. I performed electroporations of *rfp* into the caudal part of the cerebellar rhombic lip followed immediately by an electroporation of *gfp* into the rostral part of the cerebellar rhombic lip in the same embryo. Embryos were fixedat E7.

Using this technique the second electroporation often resulted in a co-labelling of cells with both GFP and RFP due to spread of residual DNA from the first injection site towards the second in the ventricle. *gfp* was always electroporated after *rfp*. In all pictures colours were manipulated on Photoshop to show a colour-inverted picture with RFP^{+ve} cells labelled in red and GFP^{+ve} cells labelled in black. Cells containing both GFP and RFP are shown in blue. Only cells in the second, more rostral, electroporation can be seen in blue or black, creating a clear distinction between the two adjacent electroporations. Different embryos show different degrees of separation between the two rhombic lip labels with some embryos showing complete overlap of GFP and RFP, allowing a range of different spatial separations to be analysed.

In all electroporations GFP^{+ve} and RFP^{+ve} cells were seen in parallel streams from the cerebellar rhombic lip. When the two electroporations were very close to each other or partially overlapping no difference was seen between the axon tracts labelled with GFP or RFP (**Figure 5-2 A-E**). Within this category of electroporation the same variation was seen

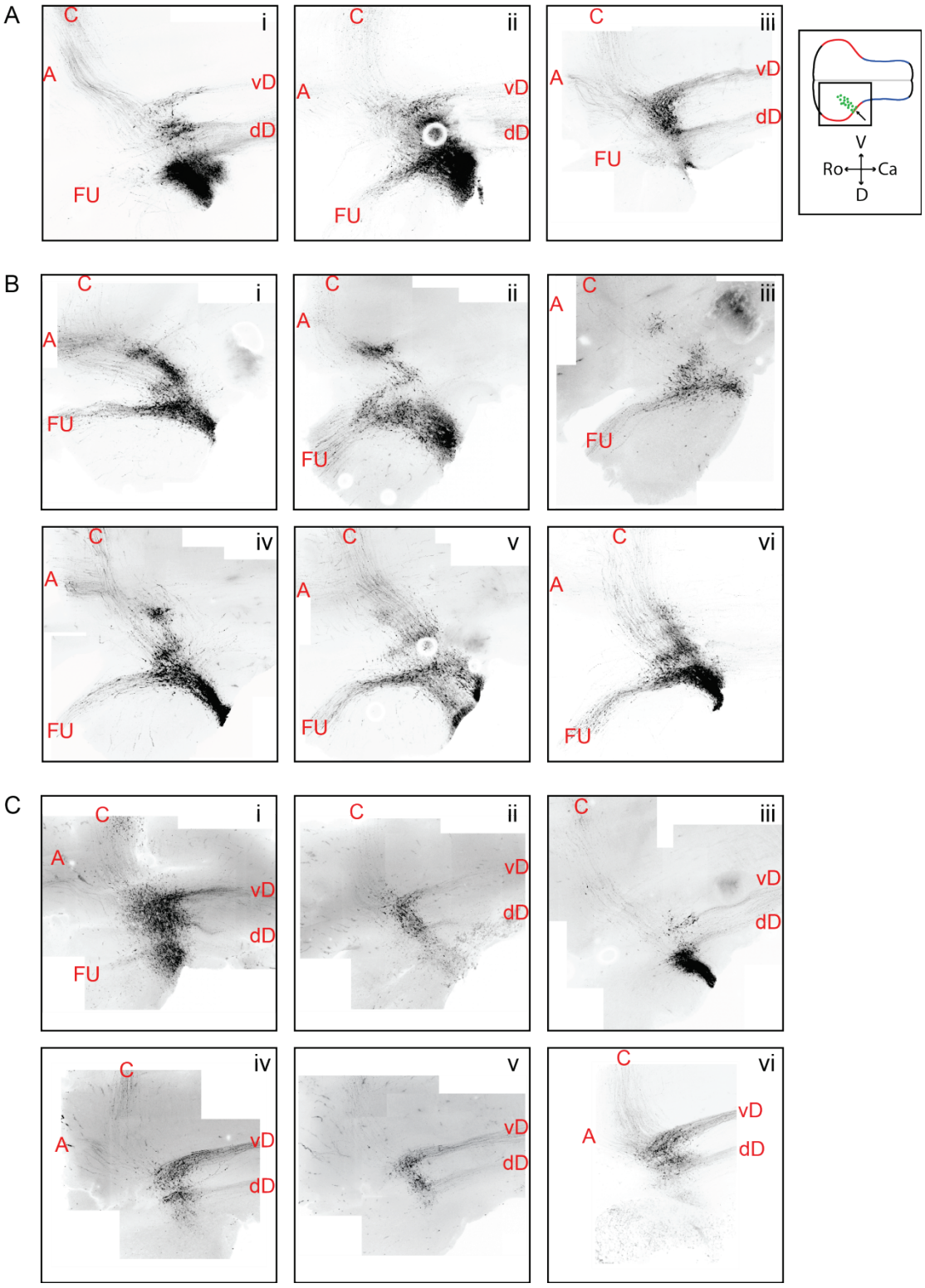

Figure 5-1 Variation in cell labelling by electroporation at St23.

Previous page:

Figure 5-1 Variation in cell labelling by electroporation at St23.

Composite projections of confocal Z-stacks taken of flat-mounted E7 hindbrain (rostral to the left) following *gfp* electroporation into the cerebellar rhombic lip at St23. Electroporations labelling: all axon tracts (A), predominantly ascending tracts (B) or predominantly descending tracts (C). Abbreviations: C: contralateral, A: ascending, vD, ventral descending, dD: dorsal descending, FU: fasciculus uncinatus.

Next page:

Figure 5-2 Double electroporations reveal spatial patterning of cerebellar rhombic lip derivatives.

Composite projections of confocal Z-stacks taken of flat-mounted E7 hindbrain (rostral to the left) following double electroporation of *gfp* into rostral cerebellar rhombic lip and *rfp* into caudal cerebellar rhombic lip at E4 (A-J) or E5 (K-M) Stage of electroporation marked on pictures. RFP^{+ve} cells shown in red, GFP^{+ve} cells shown in black and RFP^{+ve}/GFP^{+ve} cells labelled blue (colours manipulated in photoshop). A-E) close, or overlapping electroporations labelling the same cohorts of cells. F-J) spatially separated electroporations labelling different cohorts of cells. Green arrows mark different E4-born cells and blue arrows mark different E5-born cells. K-M) E5 electroporations show rostral electroporations produced more ventral cells for a longer time.

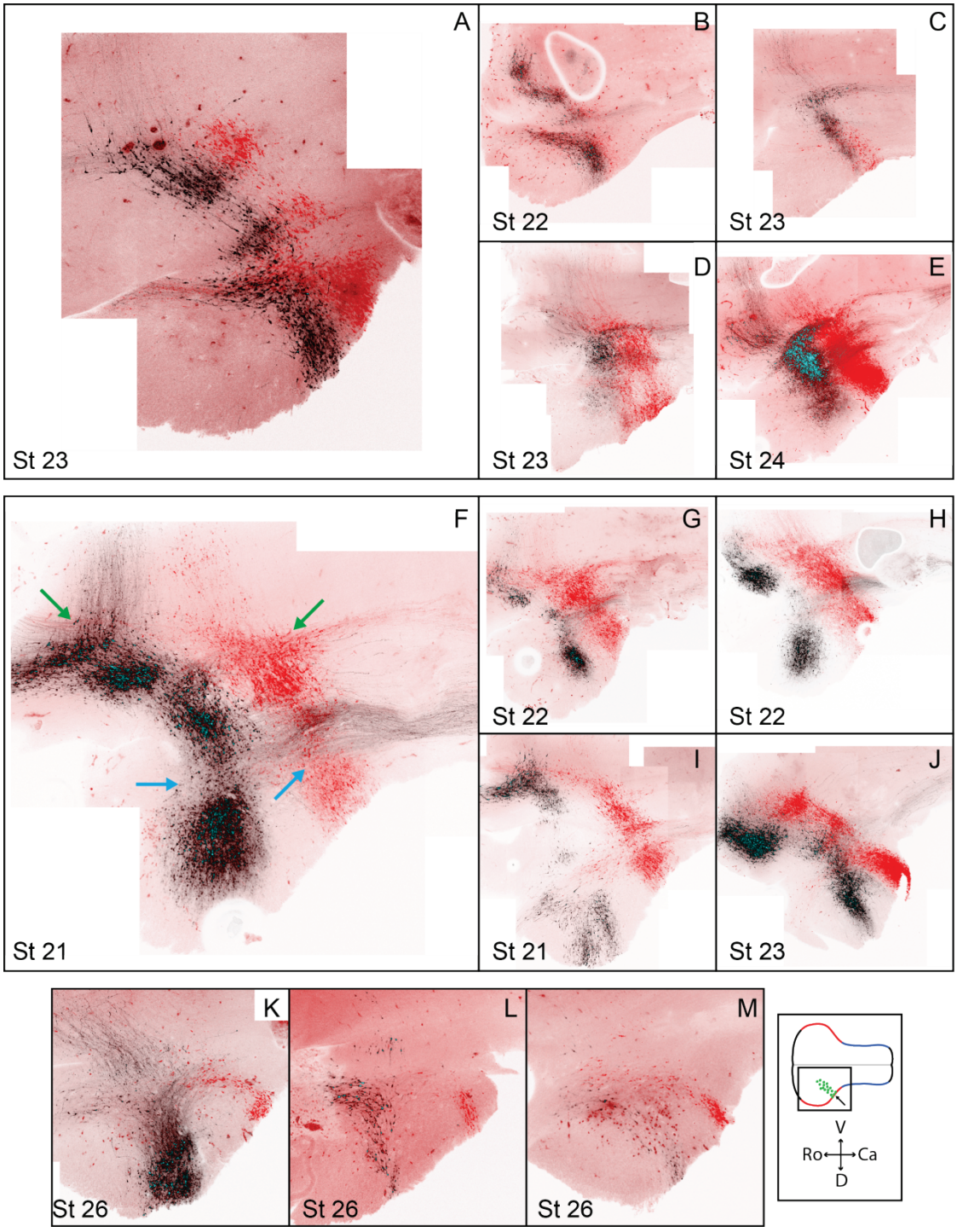

Figure 5-2 Double electroporations reveal spatial patterning of cerebellar rhombic lip derivatives.

as in single electroporations with either predominantly ascending (**Figure 5-2 A,B**), predominantly descending (**Figure 5-2 C**) or mixed ascending and descending (**Figure 5-2 D,E**) axons labelled in any single embryo.

In electroporations where GFP and RFP at the rhombic lip had a larger degree of separation, differences were observed in axon projections labelled in GFP and RFP (**Error! Reference source not found.Figure 5-2 F-J**). This demonstrates clearly that different cell types produced within a single temporal cohort can be generated from different rostrocaudal positions within the cerebellar rhombic lip.

The most common difference seen between rostrally-derived GFP^{+ve} cells and caudally-derived RFP^{+ve} cells was a separation between the predominant red or green labelling of the two descending projections (**Figure 5-2 F-H**). In these cases the more dorsal descending axon tract was predominantly labelled from rostral GFP electroporation but also by RFP, whilst the more ventral descending axon tract was only labelled by caudal RFP electroporation. These two descending axon tracts are produced at different times so it is important to consider the temporal and spatial variation together. The most ventral populations are born first, between E3 and E4. At this time point rostral cerebellar rhombic lip cells make populations with ascending axons whilst caudal cerebellar rhombic lip cells make a population of cells with descending axons (**Figure 5-2 F** green arrows). At E5 when cells of the medial cerebellar nucleus are born, GFP^{+ve} cells derived from the rostral cerebellar rhombic lip make a significant contribution to the descending axon tract, projecting to the dorsal hindbrain on the ipsilateral side, whilst caudally derived, RFP^{+ve} cells seem to make a much smaller contribution to this descending tract (**Figure 5-2 F** blue arrows). Cells with axon projections through the fasciculus uncinatus are not always labelled in electroporations suggesting they are derived from a specific region of the cerebellar rhombic lip.

Two other patterns of cell labelling were observed. In one embryo the rostrally derived GFP^{+ve} cells showed only ascending and fasciculus uncinatus projections whilst the caudally derived RFP^{+ve} cells contributed ascending, descending and fasciculus uncinatus projections (**Figure 5-2 I**). Another embryo showed both GFP^{+ve} and RFP^{+ve} ascending projections ventrally but in the medial cerebellar nucleus RFP labelled the fasciculus uncinatus projection whereas GFP labelled the descending tract (**Figure 5-2 J**).

To look more closely at the rostrocaudal allocation of cells in the medial cerebellar nucleus born at E5 I performed *gfp* and *rfp* double electroporations at E5/St26 and analysed the projections of labelled cells at E7 (**Figure 5-2 K-M**). In these electroporations caudally

derived RFP^{+ve} cells did not show any descending projections, and all RFP^{+ve} cells project only through the fasiculus uncinatus, consistent with the electroporations at E4. GFP^{+ve} cells, derived from more rostral cerebellar rhombic lip always contributed to the fasciculus uncinatus but only contribute to the descending tract from the medial cerebellar nucleus into the dorsal hindbrain in one out of the three electroporated embryos (**Figure 5-2 K**). This pattern is not consistent with the pattern seen following labelling at E4 in which very few rostral electroporations labelled the fasciculus uncinatus. This suggests that *gfp* may be diluted in E4 electroporations so later-born cells are not labelled strongly. GFP^{+ve} but not RFP^{+ve} cells were seen in ventral rhombomere 1, outside of the nuclear transitory zone. This was commonly seen in single St26 electroporations but double labelling shows that more rostral cells persist in labelling ventral cells longer than more posterior cerebellar rhombic lip.

Together, the variation between rostral and caudal labelling of the cerebellar rhombic lip at E4 demonstrates that extra-cerebellar rhombic lip derivatives in ventral rhombomere 1 show clear rostrocaudal topology in axon projections depending on their rostrocaudal origin in the rhombic lip. The projections of the medial cerebellar nucleus, produced at E5, show different rostrocaudal allocations. Both rostral and caudal cells contribute to the fasciculus uncinatus whilst descending projections are formed by cells from a more discrete region of the cerebellar rhombic lip. E5 electroporations show that the rostral cerebellar rhombic lip continues to make extra-cerebellar cells for a longer period of time than the caudal cerebellar rhombic lip.

5.2.2 Rostrocaudal differences within temporal cohorts of cerebellar rhombic lip derivatives reflect intrinsic commitment of cells.

Having shown that the rostrocaudal origin of cells within the cerebellar rhombic lip determines the specification of derivatives it is then important to distinguish between two possibilities of how this variation could occur. Either, uniform populations of cells are born from the cerebellar rhombic lip which subsequently respond to different local guidance cues throughout the rhombomere to cause different migration and axon guidance patterns, or, cells are intrinsically committed at the rhombic lip to become different cell types and migrate and grow axons accordingly. To distinguish between these two possibilities I established a cell commitment assay using microsurgical grafting based on the technique that was used to distinguish differential temporal commitment of cerebellar rhombic lip cells (Wilson and Wingate, 2006). In this previous study it was shown that E4 and E6 cerebellar rhombic lip cells grafted into dorsal rhombomere 3/4/5 of E2 chicken embryos produced migrating cells

which populated the hindbrain and extended axons. The cells migrated and showed different axonal projections in this ectopic environment based on an intrinsic temporal programme of specification. I repeated these experiments to show differences in commitment of E4, E5 and E6 cerebellar rhombic lip cells from the rostral and caudal region of rhombomere 1.

In these experiments transgenic-*gfp* chicken embryos at E4, E5 and E6 were dissected to remove the hindbrain tissue. The hindbrains were then dissected *in vitro* and small fragments of tissue were isolated from either the rostral or the caudal part of the cerebellar rhombic lip. These GFP^{+ve} tissue fragments were then transplanted heterochonically and heterotopically into dorsal rhombomere 3 of St10 (E2) wildtype chicken hindbrains. The tissue was transplanted heterotopically because grafting isotopically into rhombomere 1 can result in tissue shifting caudally resulting in an inconsistent position of grafts within the host embryo. Grafting into rhombomere 3 provides a more consistent niche for direct comparison of tissue grafted from different donor regions and ages. The chimeric embryos were incubated for 2 days and the position and axons of GFP^{+ve} cells which had migrated from the graft into the hindbrain were analysed. A schematic of this experimental procedure is shown in **Figure 5-3 A**. The benefit of using this system over an *in vitro* assay system is that the cells are transplanted into a patterned tissue which is very similar to their endogenous environment allowing cells to migrate and extend axons. Tissue from the rostral and caudal rhombic lip of a single embryo, treated in the same way and transplanted into host embryos in the same ectopic position then allows any intrinsic difference in behaviour to be established. Although the difference seen may not necessarily correlate to how the cells behave in their normal spatiotemporal environment if cells from different origins behave differently it can be concluded that the cells are intrinsically committed as different depending on their rostrocaudal origin.

When grafted cells were successfully incorporated into the hindbrain tissue of the host embryos, cells were seen to migrate away from the graft over the surface of the host hindbrain. Embryos were excluded from analysis if the graft tissue was in the incorrect position in dorsal rhombomere 3 or if cells did not integrate into the tissue properly and had no clear axons. A full list of successful and unsuccessful grafts can be found in Appendix E.

As seen by Wilson and Wingate (2006) cells of E4 and E6 donor cerebellar rhombic lip showed very different programs of migration in the same ectopic environment. Cells from E4 donors migrated ventrally and formed ascending and descending axons on the contralateral and ipsilateral side of the ventral midline (31/31) (**Figure 5-3 B,C**). Cells from E6 donors only migrated a short distance to populate dorsal hindbrain tissue and extended

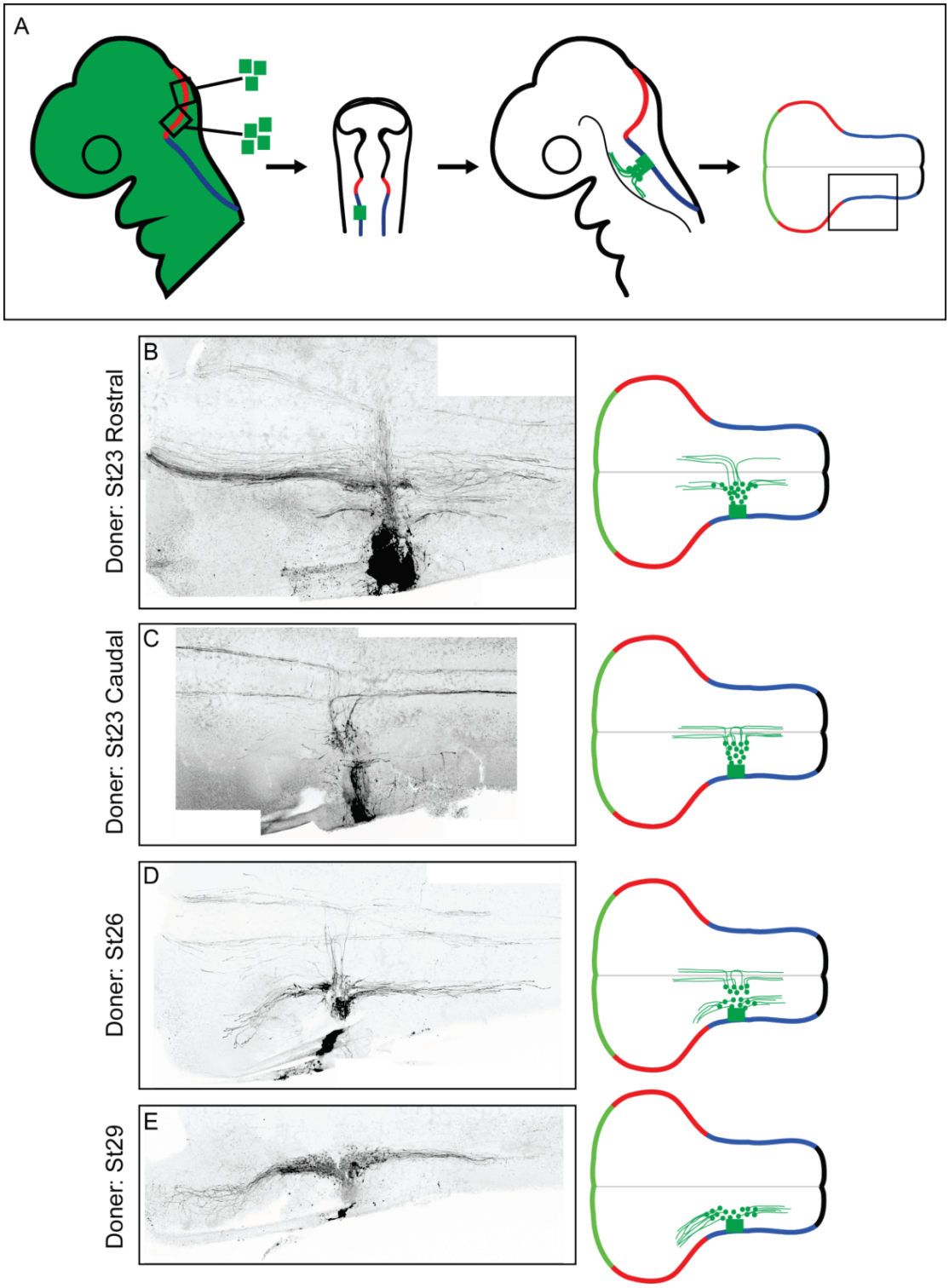

Figure 5-3 Heterochronic-heterotopic grafting of E4/5/6 rostral and caudal cerebellar rhombic lip.

Previous page:

Figure 5-3 Heterochronic-heterotopic grafting of E4/5/6 rostral and caudal cerebellar rhombic lip.

A) Schematic depicting experimental procedure for heterochronic-heterotopic grafting. Fragments of tissue from the rostral or caudal cerebellar rhombic lip of E4/5/6 *gfp*-transgenic chicken embryos are grafted into dorsal rhombomere 3 of an E2 wildtype chicken embryo and analysed after 2 days. B-D) composite projections of confocal Z-stacks taken of E4 flat-mount hindbrains (rostral to left) following grafting of cells from rostral E4 (B), caudal E4 (C), E5 (D) or E6 (E) cerebellar rhombic lip of *gfp*-transgenic embryos showing cells migrate distinctly into the host hindbrain dependent on their intrinsic commitment. Schematics to the right, summarise the patterns of migration and axon projections of grafted cells. Cells from rostral or caudal E4 cerebellar rhombic lip show distinct axon projections. Cells from E5 or E6 cerebellar rhombic lip show temporal differences in cell behaviour but no differences between rostrally and caudally derived cells.

axons rostrally or caudally in a dorsal position (24/24) (**Figure 5-3 E**). E5 transplants (which had not previously been performed) mostly showed a mixed phenotype with cells migrating to both ventral and dorsal positions and displaying a mixture of E4-like and E6-like cell behaviours (11/14) (**Figure 5-3 D**). This suggests that the E5 cerebellar rhombic lip is comprised of populations of heterogeneously committed cells. In some cases, E5 grafts only produced cells which migrated into ventral hindbrain (3/14).

In all chimeric embryos, cells which migrated from the graft tissue extended axons either caudally or rostrally but did not show a consistent bias between the production of ascending or descending axons. This shows that within an ectopic spatiotemporal environment cerebellar rhombic lip cells do not have an intrinsic commitment to form ascending or descending axon tracts and therefore cells must use local guidance cues within rhombomere 1 to control directional axon growth.

I next compared the differences between cells derived from the rostral and caudal region of the cerebellar rhombic lip of individual embryos. Cells from E5 and E6 donor embryos showed no consistent differences between grafts from rostral or caudal cerebellar rhombic lip with regards to cell migration or axon extension (**Table 5-1**). However cells derived from the rostral or caudal cerebellar rhombic lip of the same E4 donor embryo showed a consistent difference in axonal growth. Cells appeared to migrate from the graft tissue in the same manner regardless of their spatial origin but cells from caudal cerebellar rhombic lip formed ascending or descending axons directly abutting the ventral midline whereas cells derived from more rostral tissues formed ascending or descending axons in a more dorsal position, slightly away from the ventral midline (**Figure 5-3 B,C; Table 5-1**). This demonstrates that there are intrinsic differences between cells from different regions of the cerebellar rhombic lip at E4.

In grafts derived from E5 cerebellar rhombic lip some cells migrate ventrally and reflect an E4-like cell behaviour. These cells, regardless of their rostrocaudal origin, extend ascending or descending axons directly abutting the ventral midline, much like cells derived from caudal E4 cerebellar rhombic lip.

5.2.3 FGF signalling does not affect temporal or rostrocaudal allocation of cells from the cerebellar rhombic lip or their migration and axon guidance.

To test whether FGF signalling from the isthmic organiser is responsible for the rostrocaudal commitment of cells in the cerebellar rhombic lip within discrete temporal cohorts I performed double electroporations at E4 of *gfp* in rostral cerebellar rhombic lip and *rfp* in

Table 5-1 Numbers of different patterns of axon projections observed following heterochronic-heterotopic grafting of cerebellar rhombic lip cells.

Donor tissue	Ventral axons	Axons on ventral midline	Mixed (ventral midline & dorsal)	Dorsal axons	Total number of grafts (hosts)	Number of donors
E4 Rostral	15	1			16	4
E4 Caudal		15			15	5
E5 Rostral		2	7		9	4
E5 Caudal		1	4		5	3
E6 Rostral				9	9	4
E6 Caudal				15	15	3

caudal cerebellar rhombic lip mixing equal concentrations of either *dnFGFR3c* with rostral *gfp* or *Fgf8b* with caudal *rfp*. In these experiments I always co-electroporated the *gfp/Fgf8b* or the *rfp/dnfgfr3c* after the reciprocal single electroporation to ensure no mixing of *Fgf8b* or *dnfgfr3c* DNA in the ventricle could affect the single electroporation. I harvested the embryos at E7 and looked at the combinations of patterns of cell migration and axon guidance.

In these electroporations there was no change to cell migration or axon guidance when cells were electroporated with *dnfgfr3c* or *Fgf8b* (**Figure 5-4**) when compared to electroporation of *gfp* or *rfp* alone (**Figure 5-2**). Both the temporal and spatial allocation of cell types were undisturbed following FGF manipulation suggesting that from E4 onwards FGF signalling has no role in specifying individual cell types or of patterning the derivatives of the cerebellar rhombic lip.

All of the derivatives of the cerebellar rhombic lip appear to be specified normally in the presence of ectopic *Fgf8*. These results show that *Fgf8* overexpression and the subsequent effects on genes expressed at the rhombic lip do not disturb the normal spatiotemporal production of specific cell types from the cerebellar rhombic lip.

5.2.4 *Fgf8* hypomorphic mice

The reduction of *Fgf8* in rhombomere 1 in mouse results in a loss of the cerebellar vermis. However the early born rhombic lip derivatives which make *Lhx9*$^{+ve}$ cells of ventral rhombomere 1 and the cerebellar nuclei have not been analysed in these mutants. I therefore analysed an allelic series of *Fgf8* mutant mouse embryos to establish how individual temporal cohorts of rhombic lip derivatives might be affected with increasing loss of functional FGF8.

The hypomorphic allele of *Fgf8*, *Fgf8*^{neo}, contains a neomycin-resistance (neo) expression cassette within the first intron of the *Fgf8* gene. Cryptic splice sites within the neo cassette result in the production of hybrid RNAs which produce non-functional FGF8 protein. The level of *Fgf8* RNA which produces functional protein in *Fgf8*$^{neo/neo}$ embryos is about 40% of the level in wildtype embryos. Combining the *Fgf8*^{neo} allele with an *Fgf8*^{null} allele results in a further reduction in the amount of functional FGF8 and a more severe phenotype. For a full description of the generation of this allelic series see Meyers et al. (1998).

Mice carrying heterozygous null (*Fgf*$^{null/+}$) or hypomorphic (*Fgf8*$^{neo/+}$) alleles for *Fgf8* (Meyers et al., 1998) were used in two separate crosses to generate hypomorphic (*Fgf8*$^{neo/neo}$) and severe hypomorphic (*Fgf8*$^{neo/null}$) embryos which were harvested at E15.5 (mice embryos

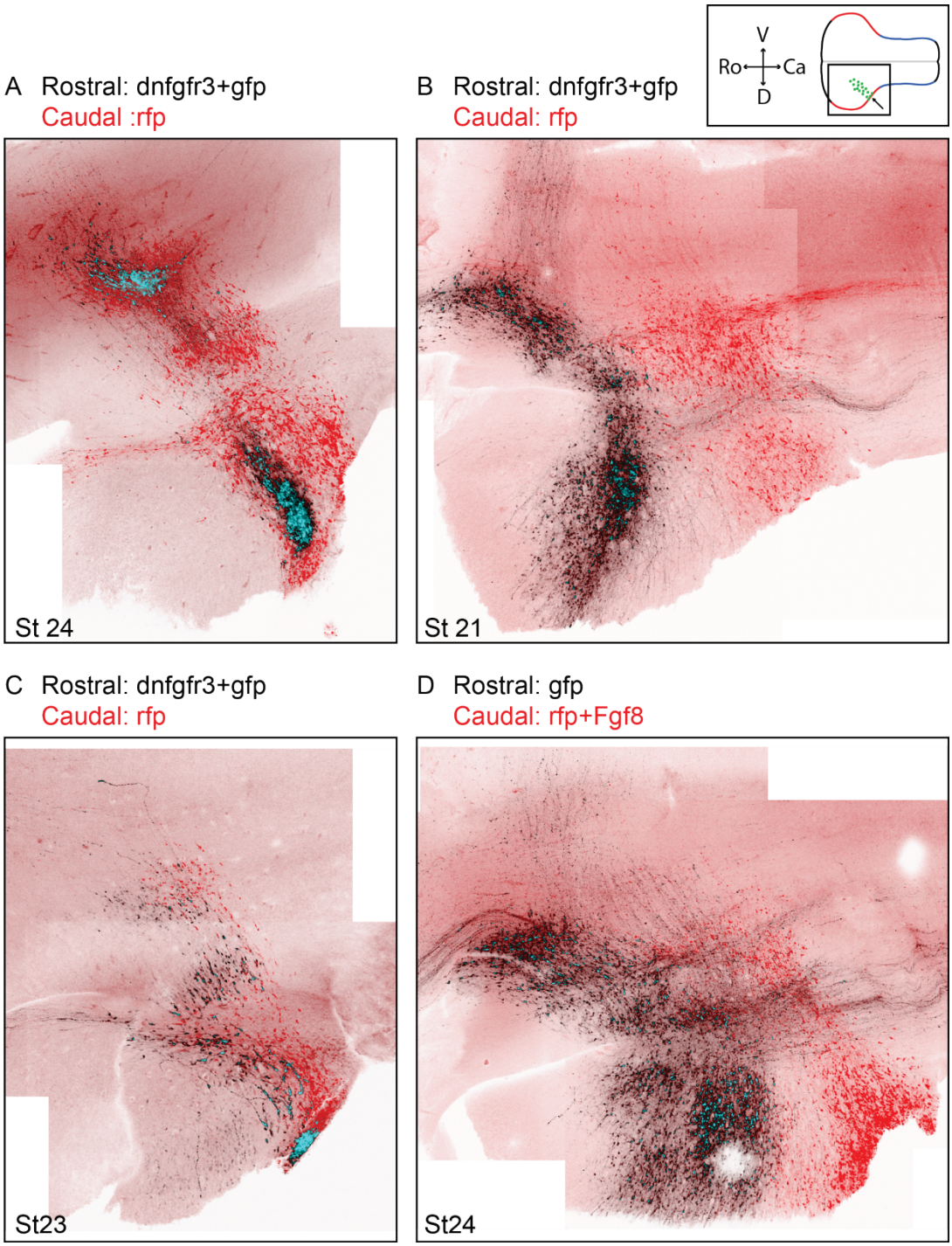

Figure 5-4 Double electroporations with Fgf8b or dnfgfr3c.

Composite projections of confocal Z-stacks taken of flat-mounted E7 hindbrain (rostral to the left) following E4 double electroporation of *gfp+dnfgfr3c* into rostral cerebellar rhombic lip and *rfp* alone into caudal cerebellar rhombic lip (A-C) or *gfp* alone into rostral cerebellar rhombic lip and *gfp+Fgf8b* into caudal cerebellar rhombic lip (D). All cells show normal patterns of migration and axon projection.

donated and genotyped by Albert Basson/Tian Yu, King's College London). Heterozygous and wildtype littermates were used as controls. The brains of embryos were cryosectioned in a sagittal plane and serial sections were processed for in situ hybrisidation for *Lhx9*, *Math1* and *Tbr1* (**Figure 5-5**). Between these 3 markers all of derivatives of the mouse cerebellar rhombic lip are labelled.

Gene expression in wild type embryos show that *Lhx9* is expressed in lateral sections within rhombomere 1 in two distinct domains, ventral rhombomere 1 and the nuclear transitory zone (NTZ) (**Figure 5-5 A,D**). *Lhx9* is also expressed throughout the whole of the tectum except at the ventricular surface. *Math1* is expression can be seen in the rhombic lip and external granule layer (**Figure 5-5 B,E**). *Tbr1* is expressed in lateral-midsagittal sections in the NTZ but not in the most medial sections (**Figure 5-5 C,F**).

As previously reported (Meyers et al., 1998; Chi et al., 2003) in $Fgf8^{neo/null}$ embryos the majority of the tectum and the entire cerebellum is absent in these embryos in both medial and sagittal sections (**Figure 5-5 G-L**). There is no expression of *Math1* or *Tbr1* in any tissue abutting the roofplate of the forth ventricle, showing that the cerebellar rhombic lip is not even formed in these embryos. *Lhx9* is expressed abutting the roofplate but not in ventral rhombomere 1. It has previously been shown that the most anterior tectal tissue is intact in these embryos and therefore *Lhx9* would be expressed. Thus no $Lhx9^{+ve}$ cerebellar rhombic lip derivatives are present. Wildtype, $Fgf8^{null/+}$ and $Fgf8^{neo/+}$ embryos all showed the same normal expression patterns of these 3 genes (not shown).

The less severe phenotype of $Fgf8^{neo/neo}$ embryos (**Figure 5-6**) shows only very mild defects in lateral sections with a small reduction in tectal tissue and a shift in the position of the NTZ. The expression of *Lhx9, Tbr1* and *Math1* in the remaining lateral tissue appears unchanged compared to the wildtype showing that all of the early born cells types are present and the cerebellar nuclei are, at least initially, formed normally (**Figure 5-6 G-I**). However in more medial sections there is a complete loss of cerebellar tissue and a reduction in midbrain tissue. No expression of *Math1* is seen in these sections showing there is no cerebellar rhombic lip between the roofplate of the forth ventricle and the tectal tissue which expresses *Lhx9* in pial layers (**Figure 5-6 J-L**).

This loss of medial cerebellar tissue (the cerebellar vermis) is a well characterised defect of reduction of FGF signalling at the isthmus. The lack of expression of *Math1* in the medial domain is consistent with data in the chick showing a medial/rostral region of *Cath1*

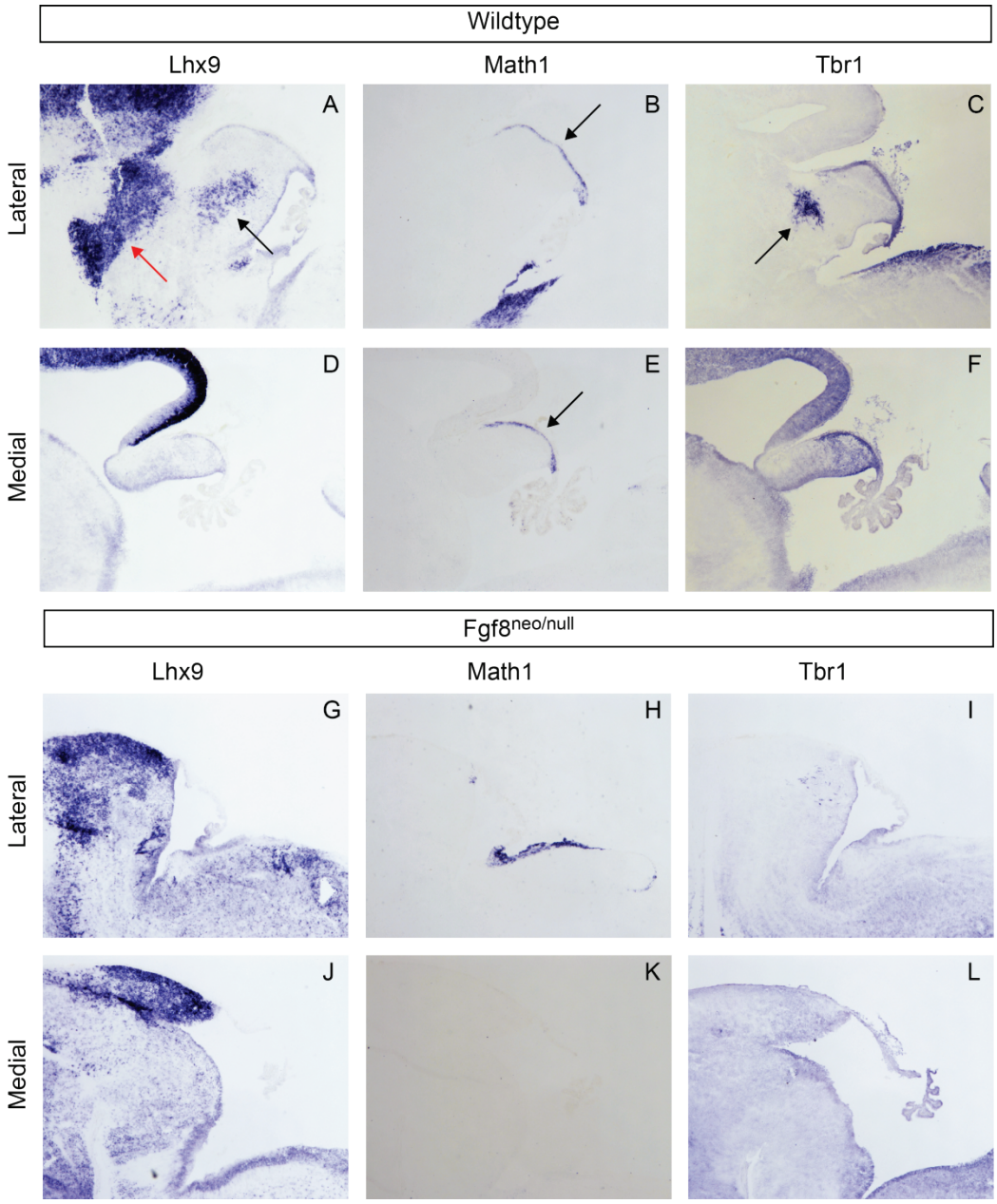

Figure 5-5 *Lhx9*, *Math1* and *Tbr1* expression in E16.5 *Fgf8* severe hypomorphic mice.

Sagittal serial cryosections of E16.5 wildtype (A-F) and *Fgf8*$^{neo/.null}$ mice (G-L). Sections stained by *in situ* hybridisation for *Lhx9*, *Math1* or *Tbr1*, showing anterior hindbrain and posterior midbrain, orientated rostral to left. A-F) Wildtype sections show *Lhx9* in extra-cerebellar ventral rhombomere 1 (red arrow) and nuclear transitory zone (black arrow) populations laterally but only inferior colliculus expression medially (A,D), *Math1* in the external granule layer (A,E arrows) and *Tbr1* in the nuclear transitory zone laterally (C,F arrow). G-L) *Fgf8*$^{neo/null}$ mice lack the entire cerebellum and posterior midbrain and show no *Math1* or *Tbr1* expression and only superior colliculus *Lhx9* expression (G-L)

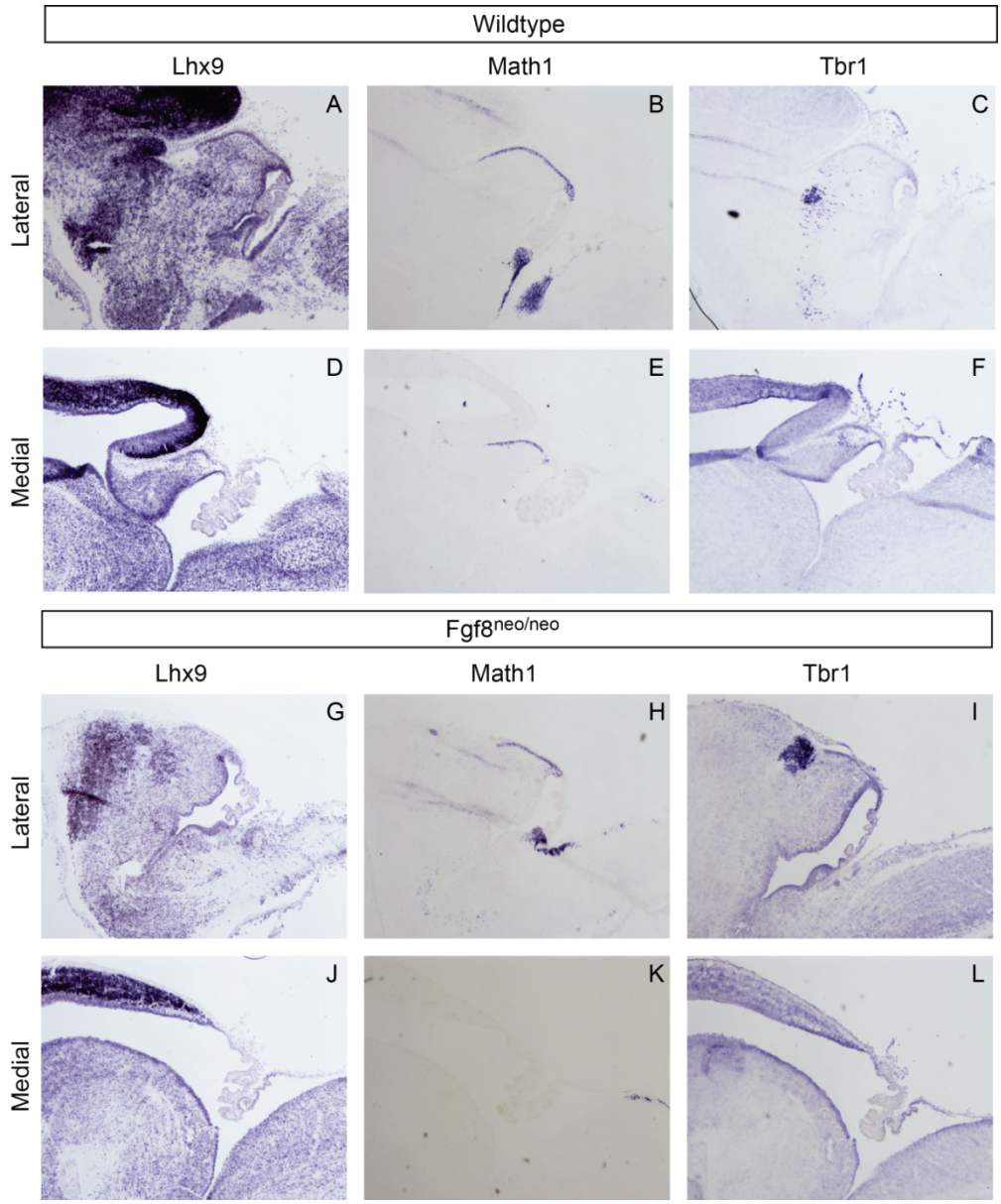

Figure 5-6 *Lhx9*, *Math1* and *Tbr1* expression in E16.5 *Fgf8* hypomorphic mice

Sagittal serial cryosections of E16.5 wildtype (A-F) and *Fgf8*$^{neo./neo}$ mice (G-L). Sections stained by *in situ* hybridisation for *Lhx9*, *Math1* or *Tbr1*. Lateral and medial sections show anterior hindbrain and posterior midbrain, orientated rostral to left. A-F) Wildtype sections show *Lhx9* in extracerebellar ventral rhombomere 1(red arrow) and nuclear transitory zone (black arrow) populations laterally but only inferior colliculus expression medially (A,D), *Math1* in the external granule layer (A,E arrows) and *Tbr1* in the nuclear transitory zone laterally (C,Farrows). G-L) *Fgf8*$^{neo/neo}$ mice show normal expression of *Lhx9*, *Math1* and *Tbr1* in lateral sections and a loss of medial tissue showing only midbrain *Lhx9* expression.

expression is dependent on FGF signalling from the isthmus. Despite the fact that the *Tbr1*$^{+ve}$ fastigial cerebellar nucleus normally lies within the cerebellar vermis and receives efferent input from vermal Purkinje cells it must be produced from more lateral cerebellar rhombic lip and is still formed in embryos which lack vermal tissue. These results show that with reduced FGF signalling the lateral cerebellar rhombic lip can produce its normal sequence of cells.

5.2.5 Conditional triple FGFR knockout in the *Math1* lineage has no effect on the development of the cerebellum.

Fgf8 hypomorphic embryos show a normal allocation of rhombic lip derivatives in lateral cerebellar tissue. However, these embryos still have low levels of functional FGF8 and may have other partially functionally redundant FGFs. I therefore looked at mice which completely lack FGF receptors in all the cells of the *Math1* lineage (Mice donated by Rob Wechsler-Reya, Sanford-Burnham Medical Research Institute).

Mice homozygous for two floxed FGF receptor alleles: *fgfr1*$^{flox/flox}$ and *fgfr2*$^{flox/flox}$ with an FGFR4 germline knockout (*fgfr4*$^{-/-}$) crossed with mice expressing Cre-recombinase under the control of the *Math1* enhancer (*Math1-Cre*) lack expression of all three FGF receptors in the *Math1* lineage. Previously, these mice mice were found to have no defects in cerebellar development (unpublished data, Rob Wechsler-Reya) but the early rhombic lip derivatives had not been analysed.

The brains of P2 *Math1*-TKO (triple FGF receptor knock out) mice were cryosectioned sagittally and serial sections were stained by *in situ* hybridisation for *Lhx9*, *Tbr1* and *Math1* to look at all of the cells of the *Math1* lineage. The *Math1*-TKO mice showed expression of *Lhx9*, *Tb1* and *Math1* in all of the expected population and showed no defects in any of the cerebellar rhombic lip derivatives (**Figure 5-7**).

Together these results show that all defects in cerebellar formation due to loss of *Fgf8* must be either due to a loss of proliferation or the allocation of cells to the *Math1* lineage. This is entirely consistent with the results of experiments in chick embryos.

5.2.6 The gradient of *Wnt1* in the cerebellar rhombic lip does not determine rostrocaudal identity of cerebellar rhombic lip derivatives.

FGF signalling from the isthmus does not direct rostrocaudal patterning or cell specification in the rhombic lip. I therefore decided to look at whether *Wnt1*, which is expressed in a gradient within the cerebellar rhombic lip from E3 to E5, could possibly have a role in

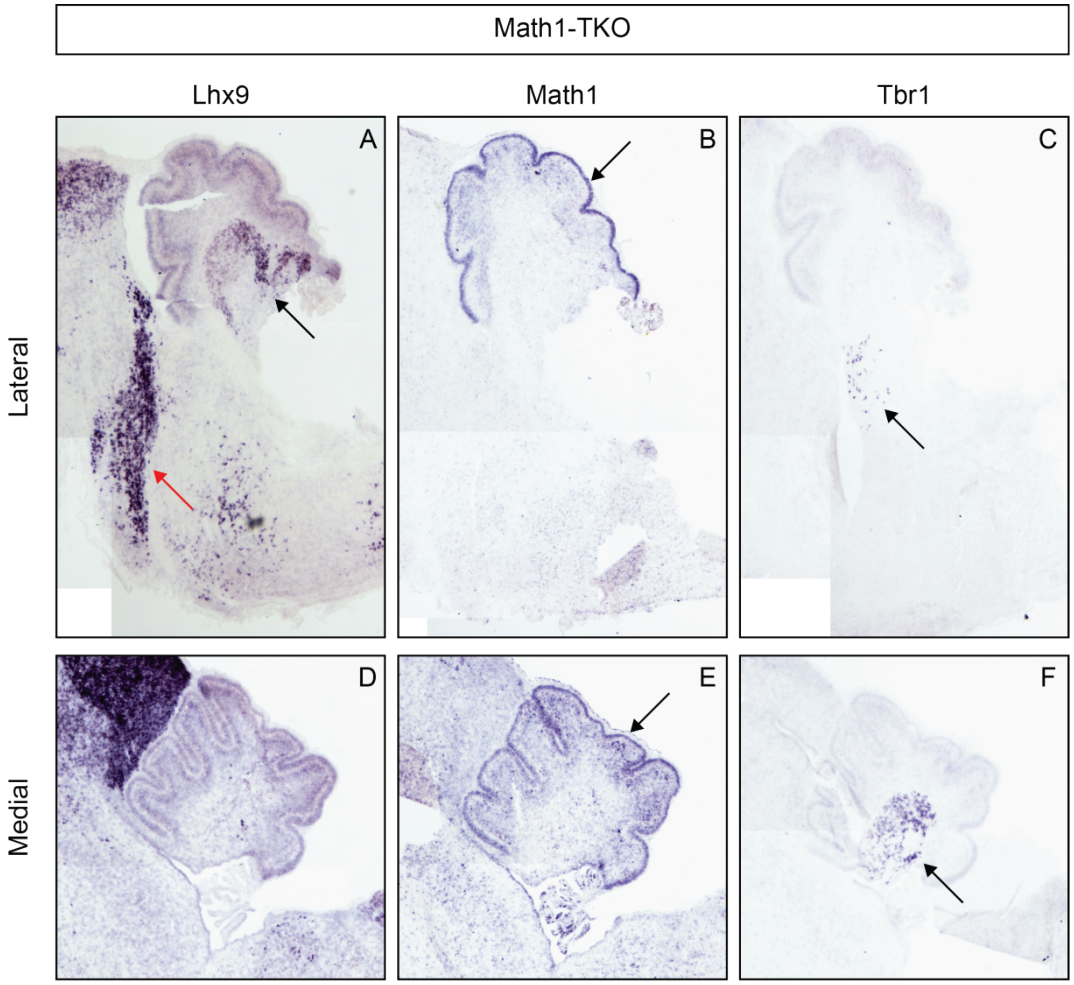

Figure 5-7 *Lhx9*, *Math1* and *Tbr1* expression in P2 Math1-TKO mice.

Sagittal serial cryosections of P2 Math1-TKO mice showing lateral sections of rhombomere 1 and medial sections of the cerebellum, orientated rostral to left. Sections stained by *in situ* hybridisation for *Lhx9*, *Math1* or *Tbr1*. *Lhx9* is expressed laterally in ventral rhombomere 1(red arrow) and the cerebellar nuclei (black arrow)(A) but only in the midbrain medially (D). *Math1* is expressed in the EGL (B,E arrows). *Tbr1* is expressed in the cerebellar nuclei sparsely in lateral and strongly in medial sections (C,E arrows)

regional cell specification. Exogenous FGF8 protein has previously been shown to downregulate *Wnt1* expression in the rhombic lip (Irving and Mason, 2000) suggesting the *Wnt1* gradient may be established downstream of FGF signalling, which does not affect allocation of cell fate in the cerebellar rhombic lip.

To test whether isthmic expression of *Fgf8* establishes the *Wnt1* gradient in rhombomere 1 I focally co- electroporated *Fgf8b* or *dnfgfr3c* with *gfp* into rhombomere 1 at St10 (E2) and looked at the gradient of *Wnt1* expression in rhombomere 1 at E4.

Control electroporations of *gfp* alone had no effect on the expression of *Wnt1* (**Figure 5-8 A,B**). *Fgf8b* overexpression resulted in a cell autonomous downregulation of *Wnt1* expression but no cell non-autonomous effects to the gradient of *Wnt1* expression were seen (**Figure 5-8 C-F**). Overexpression of the dominant-negative FGF receptor had no effect on the expression of *Wnt1* (**Figure 5-8 G,H**). Leading to the conclusion that *Fgf8* can cell-autonomously disrupt *Wnt1* but is not instructive in establishing the gradient of *Wnt1* in rhombomere 1 through a gradient of signalling.

Because *Fgf8b* overexpression causes a loss of *Wnt1* and also does not affect the specification of cerebellar rhombic lip derivatives, it can be inferred that *Wnt1* is not required for the correct allocation of cell fate at the cerebellar rhombic lip.

5.3 Discussion

The results of this chapter highlight the complexity of cell specification at the cerebellar rhombic lip showing that combined temporal and spatial patterning is required to generate the full complement of cell types within the cerebellar rhombic lip lineage. These data demonstrate for the first time that the cerebellar rhombic lip is not a homogeneous population of cells. Furthermore, I have shown that FGF-signalling is not acutely required for the specification, migration or axon guidance of any populations of cells from the cerebellar rhombic lip.

5.3.1 Spatial diversity in the cerebellar rhombic lip

Two models could possibly be used to explain rostrocaudal differences in cell allocation at the cerebellar rhombic lip: 1) a localised source of extrinsic signalling could differentially pattern the rhombic lip territory in a morphogen-like manner, or 2) a temporal wave of maturation from caudal to rostral cerebellar rhombic lip may determine different populations of cells at a single time point.

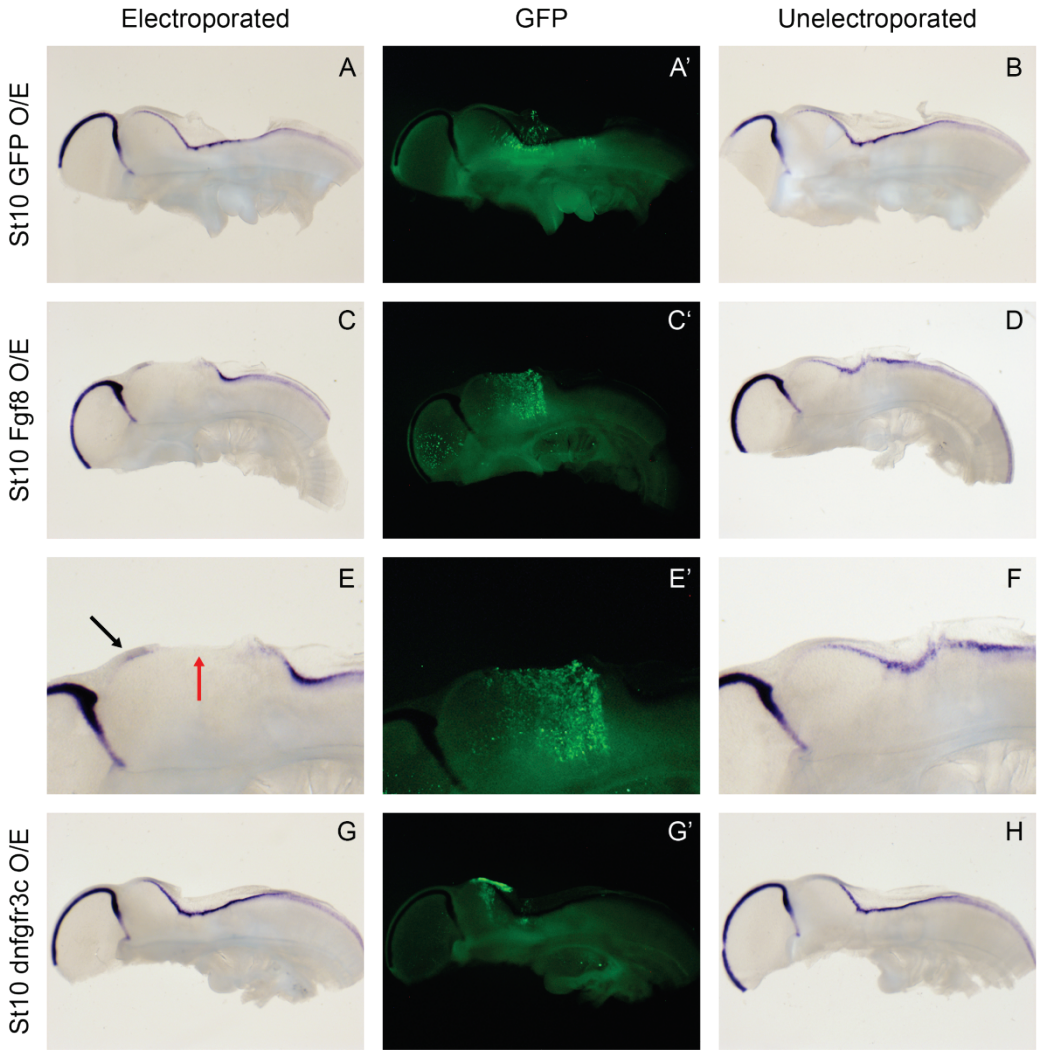

Figure 5-8 E4 *Wnt1* expression following overexpression of *Fgf8b* or *dnfgfr3c*.

E4 hemisected hindbrains (orientated rostral to left) stained for *Wnt1* by *in situ* hybridisation following E2 rhombomere 1 electroporation of *gfp* (A,B), *Fgf8b+gfp* (C-F) or *dnfgfr3c+gfp* (G,H). E shows magnified region in C showing cell-autonomous (red arrow), but not non-autonomous (black arrow), downregulation of *Wnt1* by *Fgf8b* overexpression. A',C',E',G') GFP fluorescence.

Cells produced from rostral or caudal cerebellar rhombic lip at E3/E4 show a distinct commitment to produce cells with ascending or descending axon tracts respectively. Heterochronic-heterotopic grafting also suggests that these two populations have intrinsically determined differences. However this grafting assay highlighted differences in dorsoventral axon guidance rather than rostrocaudal commitment suggesting the normal rostrocaudal differences in axon guidance in these cells is based on local extrinsic cues within rhombomere 1. However, this experiment does demonstrate that cells of rostral and caudal cerebellar rhombic lip have some intrinsic differences at E4. It is not clear how this intrinsic commitment is achieved but it is not determined by acute FGF signalling from the isthmus or a gradient of *Wnt1* expression within the cerebellar rhombic lip.

Within the populations of cells born from the cerebellar rhombic lip at E5, which form the medial cerebellar nucleus, both temporal and spatial patterning are apparent. E4 electroporations show cells in the medial cerebellar nucleus with descending axons are born from predominantly rostral, but also caudal cerebellar rhombic lip. E4 and E5 electroporations together show that cells projecting through the fasciculus uncinatus are variably born from both rostral and caudal regions of the cerebellar rhombic lip. E5 electroporations showed that the rostral cerebellar rhombic lip produces cells which migrate ventrally to the nuclear transitory zone for a longer time window.

Heterochronic-heterotopic grafting of rostral and caudal cerebellar rhombic lip from E5 embryos showed no obvious differences between the two populations, supporting electroporation mapping showing mixed origins of ascending and descending axons tracts from E5-born cells. These E5 grafts did produce a mixture of cells which migrate to ventral ("E4-like") and dorsal ("E6-like") positions in the host embryo. This suggests that at E5 a mixture of different cell types are born throughout the cerebellar rhombic lip and may possibly point to a temporal overlap between the production of different cell types.

Finally, the characteristics of cells which migrated into ventral neural tube from E5 cerebellar rhombic lip displayed axons which behaved like caudal E4 cerebellar rhombic lip cells. This observation may point to temporal wave of maturation across the rhombic lip where the "E4 caudal" identity is later seen in the whole E5 rhombic lip.

Cells derived from different regions of the E6 cerebellar rhombic lip behave in the same manner both in the grafting assay and in *gfp*-electroporated cells. Granule cell precursors, born from the cerebellar rhombic lip from E6, are also seemingly homogenous in their appearance across the external granule layer and uniformly project to overlying Purkinje cells in their mature state in the internal granule layer.

Together these observations show spatial patterning is most important at E4, in cells which migrate into ventral rhombomere 1. At E5 mixed populations are produced from the cerebellar rhombic lip partially determined by both spatial and temporal cues and by E6, no spatial patterning is observed.

5.3.2 Does a rostrocaudal pre-pattern determine the fate of rhombic lip cells?

Electroporations of *Fgf8b* and *dnfgfr3c* at E4 did not show any changes in cell specification, migration or axon guidance. It is possible that rhombomere 1 is patterned by isthmic signals prior to E4 and that acute changes in FGF signalling are unable to change this "pre-pattern".

Possible candidates for pre-pattern genes include *Enrailed1* and *Engrailed2*. it has been shown that different regions of the cerebellum show different sensitivity to the expression of the two engrailed genes, *En1* and En2 , both of which are induced by isthmic signals before the first rhombic lip derivatives are produced and through different spatial and temporal expression patterns are important for different regions of the cerebellum (Sgaier et al., 2005; Sgaier et al., 2007). Furthermore En1/2 have been shown to determine rostrocaudal patterning within the midbrain (Itasaki and Nakamura, 1996). It is possible that graded isthmic signals differentially activate genes, such as *En1/2*, to determine rostrocaudal identity and that the alteration of FGF signalling after this early patterning is not sufficient to alter cell commitment.

Wnt1 is expressed in a gradient in the cerebellar rhombic lip prior to E5. Temporal genetic fate mapping of murine *Wnt1*$^{+ve}$ cells in the cerebellar rhombic lip reveals that *Wnt1*$^{+ve}$ cells may be progenitors for *Math1*$^{+ve}$ cells (Hagan and Zervas, 2012). Together these observations suggest that cerebellar rhombic lip expression of *Wnt1* could direct cell specification. The function of *Wnt1* within the rhombic lip is unknown. This is largely due to that fact that *Wnt1* is also expressed at and required for the isthmus and therefore deletions of *Wnt1* result in a complete loss of the posterior midbrain and anterior hindbrain (McMahon and Bradley, 1990; McMahon et al., 1992).

Results in this chapter show that a gradient of FGF signalling does not define the gradient of rhombic lip expression of *Wnt1*, suggesting this is not a pre-pattern established by isthmic signalling. Instead *Fgf8b* overexpression causes a cell-autonomous downregulation of *Wnt1*. This may account for the absence of *Wnt1* expression within the broad rostral domain of *Cath1* expression in rhombomere 1. *Fgf8b* overexpression does not affect the specification of cells from the rhombic lip and therefore that the concomitant loss of *Wnt1* in these experiments does also not affect rhombic lip specification.

Therefore, whilst rostrocaudal patterning of the cerebellar rhombic lip may be determined by a pre-pattern at early stages by isthmic *Fgf8*, these experiments show that cerebellar rhombic lip cells do not acutely require FGF signalling or *Wnt1* for their correct fate allocation, migration or axon guidance. Alternatively, rostrocaudal patterning within rhombomere 1 could be conferred by signals from the isthmus that are not FGFs, or potentially even signals from the caudal boundary between rhombomere 1 and rhombomere 2 but currently there are no obvious candidate signals from either of these sources.

5.3.3 FGF signalling is not required for any cell type in the rhombic lip lineage.

Analysis of hypomorphic *Fgf8* mice show that as long as the entire cerebellar primordium is not lost ($Fgf8^{neo/null}$) then all of the individual cell types born from the rhombic lip are produced normally, and only medial cerebellar tissues are lost ($Fgf8^{neo/neo}$). Importantly, when the cerebellar vermis is lost in $Fgf8^{neo/neo}$ mice the fastigial cerebellar nucleus, to which vermal cells project, is at least initially, formed normally. It would be interesting therefore to follow these $Tbr1^{+ve}$ cells later in development to establish how cerebellar circuits are altered by the loss of vermal tissue. This could lead to an interesting insight into the mechanisms of circuit formation between Purkinje cells and the various cerebellar nuclei. Do Purkinje cells of the cerebellar hemispheres alter their connections to the cerebellar nuclei or is the fastigial nucleus eventually lost due to a lack of innervation?

Removal of FGF receptors in the $Math1^{+ve}$ lineage causes no obvious alterations in cerebellar development. This demonstrates that FGF signalling is not required for the allocation of any specific cell types from the *Math1* lineage and that the defects in cerebellar development due to loss of FGF signalling must occur through effects on cells prior to the onset of *Math1* expression, possibly in progenitor proliferation. Alternatively, FGFs may act on other cell types of the cerebellum to indirectly affect cerebellar development.

Observations from the hypomorphic *Fgf8* and Math1-TKO mice support data from chick experiments which show FGF signalling does not affect cell specification in the cerebellum. Furthermore, results in this chapter confirm that cell migration is normal following *Fgf8b* overexpression and therefore the results in chapter 4 showing disturbed expression of *Lhx9* following *Fgf8b* are not due to migratory defects and are likely due to changes in progenitor proliferation and differentiation.

Chapter 6 The role of thyroid hormone signalling in the cerebellar rhombic lip

6.1 Background

The rhombic lip gives rise to different temporal cohorts of neurons with different projections and molecular identities at different time points. Whilst the factor(s) regulating temporal progression are unknown there is some evidence that an extrinsic factor is responsible for the switch between different cell fates rather than an intrinsic program of development (Wilson and Wingate, 2006).

How would you determine whether an extrinsic signal is conferring temporal signals? It is important to distinguish between a requirement for a factor in the differentiation of a specific cell type and a factor than can induce a temporal shift in cell production. In searching for a signal which could initiate the temporal transition between the production of different cell types from the rhombic lip at a specific time point, when any given cell type is lost it would be expected that there would be an extended window of production of other cell types in the lineage. However, if a signal was just required for the differentiation of one specific cell type in the lineage, no compensation would be expected in the other cells types. For example, if a specific factor was required for the temporal transition to the onset of granule cell production, removal of this factor may be expected to result in an extended period of cerebellar nuclei production. Likewise, if this factor was applied at an earlier time point, it would be expected that there would be loss of earlier born cell types accompanied with the production of precocious granule cells. This model is outlined in **Figure 6-1**.

Thus far I have excluded signals from the diminishing isthmic organiser in the specification of specific temporal cohorts from the rhombic lip. Another possible source of temporal signal to the cerebellum is the developing roof plate of the fourth ventricle. Whilst the boundary between the expanded roof plate epithelium of the fourth ventricle and dorsal neuroepithelium has been established as an organising centre which is required to establish and maintain the rhombic lip progenitor pool (Chizhikov et al., 2006), the expression of genes involved in orchestrating these interactions (e.g. *Gdf7* and Notch-delta signalling components) are static during the early periods of rhombic lip cell production when different cohorts of cells are born (E3-7) (Broom, 2011).

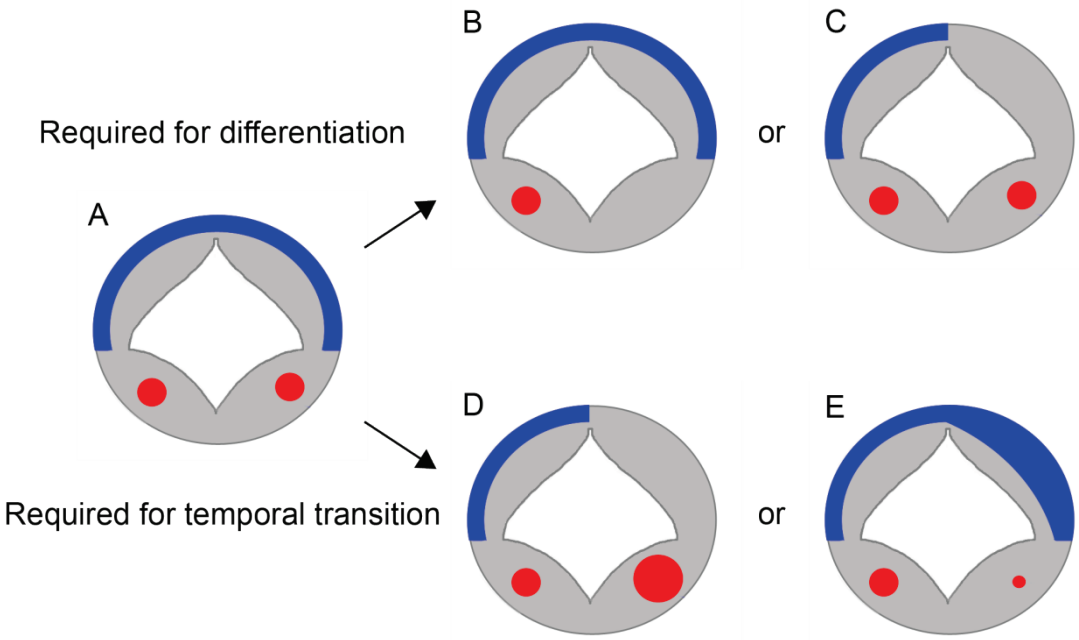

Figure 6-1 Theoretical model for the action of factor regulating temporal transitions.

A) Diagram representing transverse section through the cerebellum indicating dorsal granule cells (blue) and early-born ventral populations of cerebellar rhombic lip derivatives (red). B-C) indicate expected outcome for manipulation of a signal that is required to specify an individual population of cells where only one specific population of cells is lost. D-E) Bottom row indicates expected outcome for manipulation of a signal which regulates the transition between early and late-born cell types. If the switch is lost, an increase in early-born cells and a loss of late-born cells would be seen (D) or if a premature switch occurs an excess of late-born cells would be seen at the expense of early born population (E).

A third possible local source of temporal patterning is the choroid plexus. From as early as E3 in the chicken embryo the roof plate of the ventricle begins to develop into choroid plexus epithelium. Choroid plexuses develop from all of the ventricle roof plates (lateral, third and fourth) and are highly vascularised tissues which form the blood-cereberospinal fluid (CSF) barrier and regulate the internal environment of the brain. The choroid plexus is responsible for the presence of many signalling molecules within the CSF such as sonic hedgehog (Shh), retinoic acid and thyroid hormone. In mouse, transventricular Shh signalling has been shown to be involved in cerebellar ventricular zone development but not in the rhombic lip or its derivatives at this stage of development (Huang et al., 2010). Other candidate molecules are retinoic acid and thyroid hormones, synthesising enzymes for which are both expressed within the developing choroid plexus epithelium (Verhoelst et al., 2004; Wilson et al., 2007). Thyroid hormone is transported through the choroid plexus using the protein Transthyretin (Ttr). *Ttr* is expressed in the fourth ventricle roofplate from St20 (E3.5) suggesting that thyroid hormone can be transported into the CSF at a stage when different temporal cohorts of rhombic lip cells are specified (Thomas et al., 1988; Broom, 2011).

There has been no study of the early phase of thyroid hormone synthesis but thyroid hormone is known to have a profound effect on late cerebellar development. Postnatal hypothyroidism results in a failure of most cells types within the cerebellum to fully mature. Most prominently, many cerebellar granule cells fail to differentiate and undergo radial migration to the inner granule cell layer. Instead cells remain in the proliferative external granule layer for a prolonged period of time where they eventually die by apoptosis. In contrast, early postnatal hyperthyroidism results in a premature differentiation of granule cells, resulting in a reduced cell number (Nicholson and Altman, 1972a; Lauder, 1977). Maturation of Bergman glia cells, Purkinje cells and GABAergic interneurons in the cerebellum are also perturbed by reduced thyroid hormone resulting in reduced synaptogenesis in the molecular layer (Nicholson and Altman, 1972b; Morte et al., 2004; Manzano et al., 2007; Boukhtouche et al., 2010) . The development and connections of the cerebellar nuclei have not been studied in these experimental models.

Thyroid hormone has been shown to regulate the cerebellar expression of the genes *Barhl1* and *Neurod1*, both of which are expressed in post-mitotic granule cells (Chantoux and Francon, 2002; Dong et al., 2011). However, both of these genes are also expressed in a subset of early-born cerebellar nuclei. This, combined with the early appearance of Transthyretin and other thyroid hormone transporters/regulators (Mct8, Oatp1c1 and iodothyronine deiodoinase type 3) in the fourth ventricle choroid plexus (Geysens et al.,

2012) suggest that thyroid hormone could also play a role in the early cerebellar development.

A schematic depicting the mechanism of thyroid hormone signalling is shown in **Figure 6-2** and is reviewed by Forrest et al. (2002). Thyroid hormone receptors (TRs) form either homodimers or heterodimers with retinoid X receptors (RXRs) and bind to DNA at a specific motif (Thyroid hormone response element, T3RE). In the absence of thyroid hormone the thyroid hormone receptors recruit co-repressors and inhibit the transcription of specific genes. Upon ligand binding co-repressors are dissociated and a co-activator complex is formed resulting in the transcription of target genes. Signalling is tightly regulated by the availability of an active form of the ligand. The inactive form of thyroid hormone, T4 (3,5,3',5'-tetraiodothyronine also known as thyroxine) circulates in the blood. At the site where it is required it is converted into the active form, T3 (3,3',5-triiodothyronine) by the removal of an iodine molecule by the enzyme iodothyronine deiodoinase type 2 (D2). T3 can enter into cells and bind directly to thyroid hormone receptors. T3 is inactivated by the further deiodination to form T2 (3,3'-diiodothyronine) by the enzyme D3 (iodothyronine deiodinase type 3). The enzymes D2 and D3 are expressed within specific tissues of the cerebellum in late embryonic development (E18) but in early development (E3-10) their expression is not apparent in cerebellar tissues, and is only found in the roof plate (Verhoelst et al., 2005; Geysens et al., 2012) however detailed analysis of cerebellar expression has not been performed.

There are two classes of thyroid hormone receptor that bind T3, TRα and TRβ. TRα is expressed in the brain from at least E4 and is highly expressed in the cerebellum at E9 (earlier expression not analysed) but TRβ is not expressed in the chicken cerebellum until at least E19 (Forrest et al., 1990; Forrest et al., 1991). In early postnatal mice *TRα* expression is found ubiquitously in the cerebellum with higher expression in postmitotic cells whereas and *TRβ* is limited to specific cell types (Bradley et al., 1989; Mellstrom et al., 1991; Wallis et al., 2010). Thyroid hormone receptor knockouts have a surprisingly mild phenotype compared to hypothyroidism and removal of thyroid hormone receptors can partially rescue the phenotype of hypothyroid mice. This suggests that a large part of the hypothyroid phenotype is due to the repressor effects of the unliganded receptor, a model which is supported by the hypothyroid-like phenotype of mice expressing a dominant-negative mutation in the TRα resulting in loss of its activator but not the repressor effects (Fauquier et al., 2011).

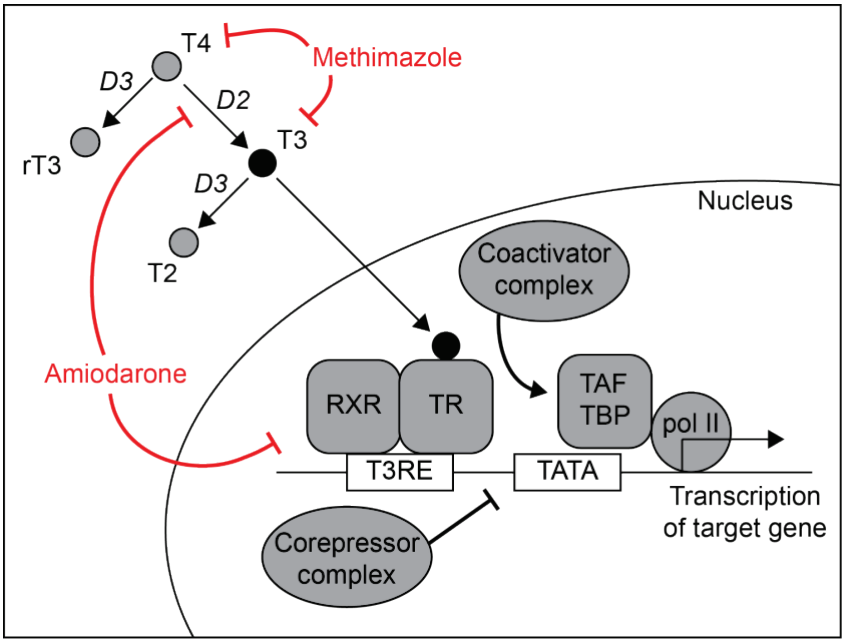

Figure 6-2 Thyroid hormone signalling pathway.

Adapted from review by Forrest et al. (2002). Schematic showing the pathway of thyroid hormone signalling and the interactions of pharmacological agents amiodarone and methimazole. T4 is converted to an active form, T3, and transported into the nucleus of cells where it can bind to thyroid hormone receptor (TR). TRs form heterodimers with retinoid X receptors (RXR) and bind to Thyroid hormone response elements (T3RE). Ligand binding causes a displacement of the co-repressor complex associated with TR and a co-activator complex is formed resulting in transcription of target genes. Amiodarone competitively inhibits T3 binding to TR and inhibits the conversion of T4 to T3. Methimazole inhibits the production of both T4 and T3.

Genetic approaches of manipulating thyroid hormone signalling by electroporation directly into the cerebellar rhombic lip are complicated by the requirement for both activator and repressor function of the receptors. To be sure to compensate for both functions, receptor knockout (for example by shRNA) and overexpression of dominant-negative and dominant-active forms of the receptor would need to be compared. Alternatively, knockdown of transporters or synthesising enzymes in the roofplate epithelium could be used. However, it would not be possible to target the entire fourth ventricle roofplate by electroporation so a viral overexpression technique would be required. For these reasons I chose a pharmacological approach to investigate the actions of thyroid hormone on early cerebellar development through direct application of 3,3',5-triiodo-L-thyronine (T3), the active form of thyroid hormone, or two inhibitors of thyroid hormone signalling, methimazole and amiodarone (Burger et al., 1976; Ha et al., 2000; Hasebe et al., 2008)

Amiodarone is an antiarrhythmic agent which is used to treat cardiac dysrhythmias through its inhibitory effect on potassium channels. However amiodarone structurally resembles T4 and therefore acts as a competitive inhibitor of thyroid hormone signalling by both the inhibition of the enzyme D2 which converts T4 into T3 and by competitively binding directly to thyroid hormone receptors (reviewed by Unger et al. (1993)). Methimazole is a drug used to treat hyperthyroidism and it acts to inhibit the synthesis of both T3 and T4 by the inhibition of the enzyme thyroperoxisade, which oxidises iodide ions to iodine to allow for incorporation into T3 and T4 molecules (reviewed by Cooper (2005)). The site of action of each inhibitor is indicated in Figure 6-2.

6.2 Results

6.2.1 *Pax6* and *Tbr1* expression in the nuclear transitory zone are specifically lost following thyroid hormone inhibition.

To test whether thyroid hormone is able to instruct the production of cerebellar granule cell precursors or cerebellar nuclei cells from the rhombic lip outside of the endogenous temporal window of production, T3 (the active form of thyroid hormone) was injected into chicken embryos at E3 or E4. Injections of 3 different concentrations of T3 were either performed directly into the fourth ventricle (filling the ventricle) or into the bloodstream of embryos by targeting an artery overlying the yolk (5µl). Embryos were collected a day after injection and processed for *Pax6 in situ* hybridisation. In wildtype embryos *Pax6* is not expressed in the cerebellum until E6 when expression is found in the nuclear transitory zone, granule cell precursors and the rhombic lip (See chapter 3).

No precocious expression of *Pax6* was observed at E4 or E5 following injection of T3 (not shown) showing T3 alone was not sufficient to induce cerebellar nuclei or granule cell production. Numbers of embryos injected for each treatment are shown in **Table 6-1A**.

A cocktail of two thyroid hormone inhibitors, methimazole and amiodarone, was also injected into embryos to see if the production of cerebellar nuclei cells or cerebellar granule neurons could be disrupted. Three different doses of the mix of two inhibitors were injected into the fourth ventricle or into the bloodstream at E4 or E5. Injected embryos were collected at E6 and processed for *Pax6 in situ* hybridisation.

Injections of the thyroid hormone inhibitors at E4 or E5 into the bloodstream or the forth ventricle resulted in a complete downregulation of *Pax6* expression in the medial cerebellar nucleus at E6 whilst *Pax6* expression in cerebellar granule cells was unperturbed (E4 injection: 25/41; E5 injection: 14/31) (**Figure 6-3 A-D**). The loss of *Pax6* expression in the nuclear transitory zone was confirmed in vibratome sections of the injected embryos (**Figure 6-3 E-J**). Numbers of affected embryos following the different injection conditions are summarised in **Table 6-1B**.

Since there was no different between injection techniques, in subsequent experiments I only performed injections directly into the fourth ventricle. Embryos showed no morphological defects in the hindbrain following ventricle injection compared to uninjected embryos and no general developmental delays were observed based on standard staging in this, and all subsequent experiments.

To confirm that the medial cerebellar nucleus is disrupted by the presence of thyroid hormone inhibitors, I performed E4 ventricular injections of methimazole and amiodarone and analysed the expression of *Tbr1* at E6 to specifically mark the nuclear transitory zone. Whilst stage matched, uninjected embryos always showed strong expression of *Tbr1* in the nuclear transitory zone at E6 (n=6), embryos injected with thyroid hormone inhibitors showed a complete lack of *Tbr1* expression in the nuclear transitory zone in 10 out of 13 embryos (**Figure 6-4 A-D**). Vibratome sections of injected embryos revealed that a very small amount of *Tbr1* expression was present in some embryos in the most lateral part of the NTZ (**Figure 6-4 E-J**).

Table 6-1 Numbers of embryos with altered *Pax6* expression following injection of T3 or methimazone and amiodarone

A			
Injection	Fix	Dose T3	Number no Effect
E3 Blood	E4 *Pax6*	50nM	7/7
		5nM	4/4
		0.5nM	7/7
E3 Ventricle	E4 *Pax6*	50nM	9/9
		5nM	8/8
		0.5nM	8/8
E4 Blood	E5 *Pax6*	50nM	7/7
		5nM	5/5
		0.5nM	8/8
E4 Ventricle	E5 *Pax6*	50nM	6/6
		5nM	6/6
		0.5nM	8/8
B			
Age Inject	Age Fix	Dose M/A	Number Lose mCbN
E4 Blood	E6 *Pax6*	A	5/5
		B	2/6
		C	3/6
E4 Ventricle	E6 *Pax6*	A	6/9
		B	2/7
		C	7/8
E5 Blood	E6 *Pax6*	A	3/6
		B	3/6
		C	1/5
E5 Ventricle	E6 *Pax6*	A	1/5
		B	3/4
		C	3/5
A= 1µM Amiodarone + 2mM Methimazole B = 0.1µM Amiodarone + 0.2mM Methimazole C = 0.01µM Amiodarone + 0.02mM Methimazole			

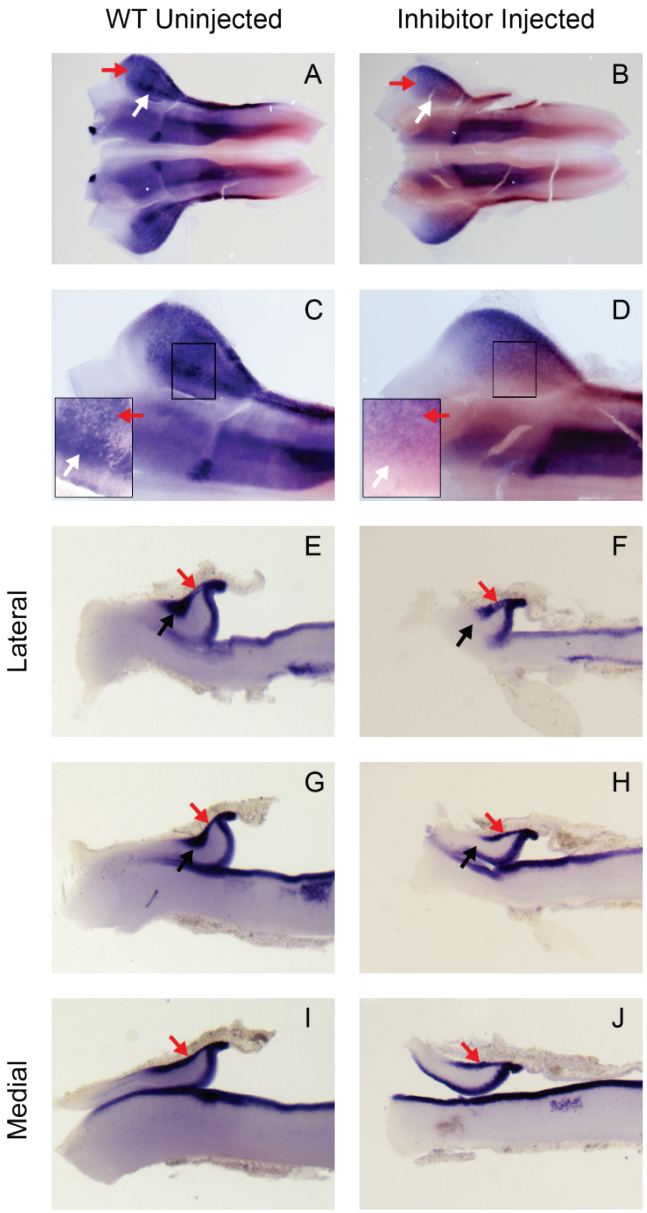

Figure 6-3 *Pax6* expression is lost specifically in the nuclear transitory zone following thyroid hormone inhibition.

E6 *Pax6* expression detected by *in situ* hybridisation in uninjected controls (A,C,E,G,I) and embryos injected with methimazole and amiodarone at E4 (B,D,F,H,J). Expression in the nuclear transitory zone (white and black arrows) is lost in injected embryos but granule cell expression (red arrows) is unaltered. A and B show flat-mount hindbrain view magnified in C and D with inset region of red box further magnified with increased contrast. E-J show sagittal sections of hindbrains taken from lateral (E,F) and mid-parasagittal (G,H) regions which include the nuclear transitory zone and medial sections (I,J) which do not. Tissue orientated with rostral to the left.

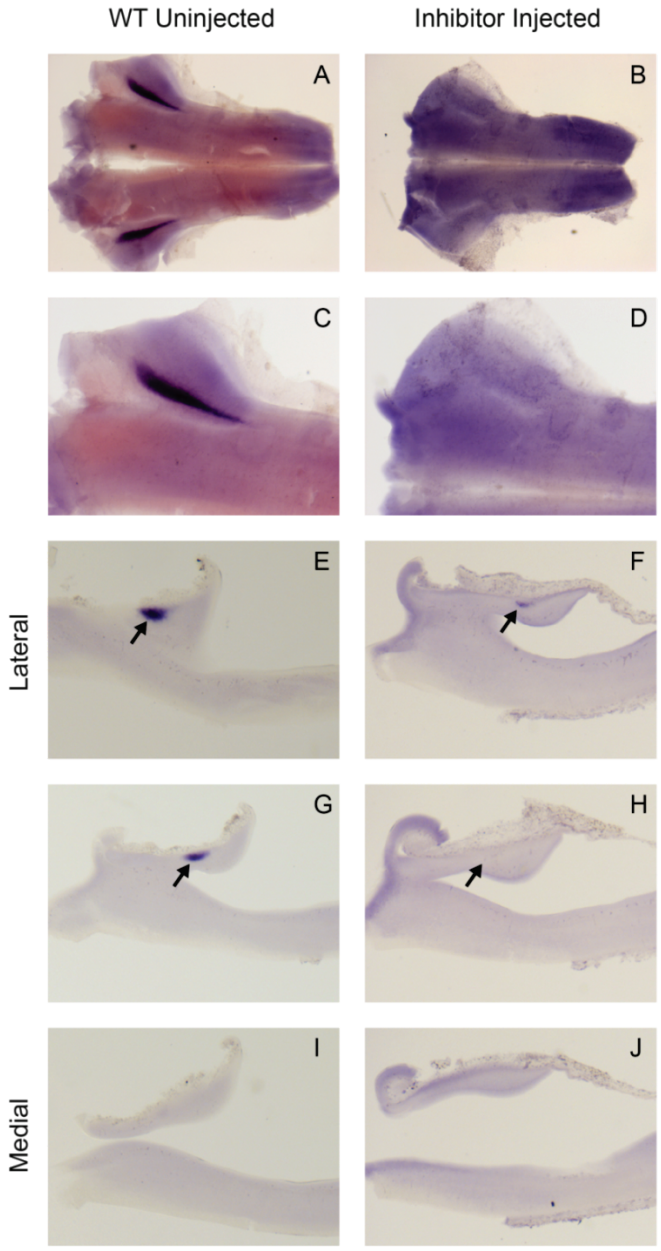

Figure 6-4 *Tbr1* expression is lost in the nuclear transitory zone following thyroid hormone inhibition.

E6 *Tbr1* expression detected by *in situ* hybridisation in uninjected controls (A,C,E,G,I) and embryos injected with methimazole and amiodarone at E4 (B,D,F,H,J). Expression in the nuclear transitory zone (black arrows) is lost in injected embryos. A and B show flat-mount hindbrain view magnified in C and D. E-J show sagittal sections of hindbrains taken from lateral (E,F) and mid-parasagittal (G,H) regions which include the nuclear transitory zone and medial sections (I,J) which do not. Tissue is orientated with rostral to the left.

6.2.2 The degree of *Tbr1*/*Pax6* loss depends on the concentration and timing of pharmacological agent delivery.

One hundred fold serial dilutions of the cocktail of inhibitors were injected into the fourth ventricle of E4 embryos and the expression of *Tbr1* was analysed at E6. Consistent with a specific pharmacological effect, fewer embryos showing loss of *Tbr1* expression were observed with increasingly lower doses of the inhibitors (**Table 6-2; Figure 6-**5). Most affected embryos showed a complete abrogation of *Tbr1* expression, however in some cases (4/43) a very low level of *Tbr1* expression could be seen. This low level expression phenotype was counted as an affected embryo. The incidence of the partial phenotype was not correlated with the dose of inhibitors injected.

Embryos injected with a high concentration of the thyroid hormone inhibitors at E3 showed reduced, weak expression of *Tbr1* at E6 (n= 4/5). Unlike 24 hour survival *Tbr1* was not fully lost in any embryos demonstrating a limited efficacy of treatments, possibly due to the effect of dilution after two days in the ventricle.

6.2.3 *Lhx9* and *Cath1* expression following inhibition of thyroid hormone signalling.

Following injection of thyroid hormone inhibitors at E4, nuclear transitory zone expression of *Pax6* and *Tbr1* are lost but *Pax6*$^{+ve}$ granule cell precursors are still present at E6. This could indicate that thyroid hormone is required specifically for the specification of cells of the medial cerebellar nucleus (and therefore other cells in the cerebellar rhombic lip lineage would not be affected) or that a thyroid hormone is required for the temporal shift between production of different cell types from the cerebellar rhombic lip. According to the working model outlined in Figure 6-1, if thyroid hormone was acting as a temporal signal then an extended period of production of early-born cell types (*Lhx9*$^{+ve}$) or a precocious production of later-born cell types (*Cath1*$^{+ve}$ granule cell precursors) would be seen. To test this I looked at the expression of *Lhx9* and *Cath1* following injection of thyroid hormone inhibitors.

Ventricular injections of methimazole and amiodarone at E4 showed no change in the expression of *Lhx9* at E6 (n=6) compared to stage-matched uninjected embryos. This shows the period of *Lhx9*$^{+ve}$ cell production from the cerebellar rhombic lip was not extended following thyroid hormone inhibition.

To look for precocious production of cerebellar granule cells with inhibition of thyroid hormone I performed ventricular injections of methimazole and amiodarone at E4 and looked at the expression of *Cath1* at E5. *Cath1*$^{+ve}$ granule cells are never observed prior to

Table 6-2 Numbers of embryos showing a loss of *Tbr1* expression following ventricular injections of methimazone and amiodarone.

Stage Injected	Methimazole	Amiodarone	E6 *Tbr1* loss
St17-18 (E3)	2mM	1µM	4/5 partial loss
St22-24 (E4)	2mM	1µM	10/13 (2 partial)
St22-24 (E4)	20µM	10nM	7/7 (1 partial)
St22-24 (E4)	200nM	0.1nM	0/4
St22-24 (E4)	2nM	0.001nM	1/5 (partial)
St22-24 (E4)	0.2nM	0.01pM	1/8
St22-24 (E4)	0.0002nM	0.0001pM	0/6

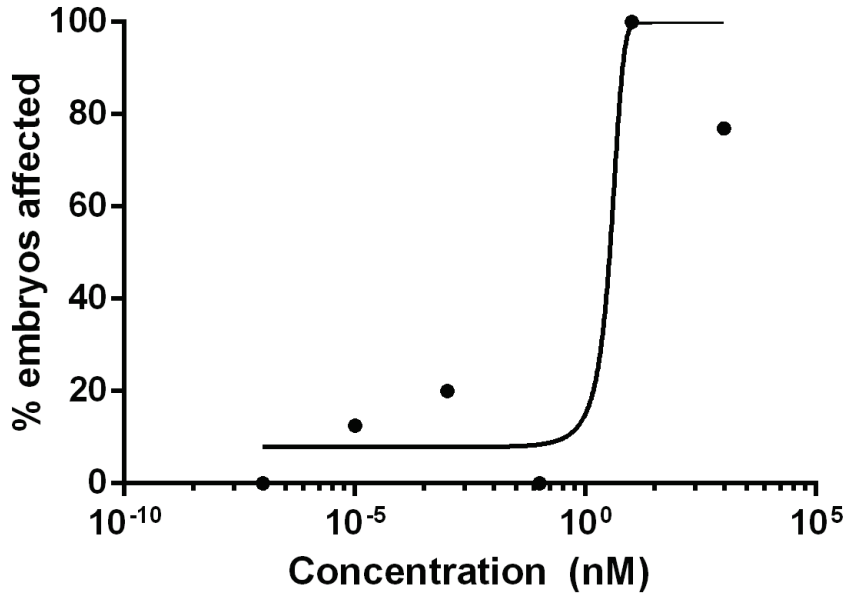

Figure 6-5 Dose response curve for E4 amiodarone and methimazole treatments.

Graph indicating percentage of embryos which lose *Tbr1* expression in the nuclear transitory zone following different doses of injected methimazole and amiodarone at E4. Concentration in a logarithmic scale. Data from **Table 6-2**. Decreasing dose causes a decrease in efficacy, consistent with a specific pharmacologic effect.

St28/E6 in normal development. Inhibitor injection at E4 resulted in an apparent increase in *Cath1* expression on the surface of the cerebellum away from the cerebellar rhombic lip at St27/E5 (n=13/19; **Figure 6-6 A-D**) compared to uninjected staged matched controls (n=5). Vibratome sections of injected and uninjected embryos showed *Cath1* expression on the pial surface of the cerebellum in injected embryos whereas in uninjected embryos *Cath1* expression was confined to the rhombic lip and broad, FGF-dependent rostral domain (**Figure 6-6 E-H).** This result suggests inhibition of thyroid hormone results in the early onset of cerebellar granule cell production from the rhombic lip. However, at early stages during E5, the FGF-dependent broad *Cath1*$^{+ve}$ domain in rostral rhombomere 1 forms which can result in broad *Cath1* expression in more caudal regions of dorsal rhombomere1 (see discussion) so other granule cell markers would need to be assessed to confirm that ectopic *Cath1* expression compared to stage-matched uninjected controls was indicative of precocious granule cell production.

Another set of embryos was injected with methimazole and amiodarone at St15-16/E3 and the embryos were collected at St 24/E4 (n = 11) and early E6/St28 (n=5). No *Cath1* expression consistent with precocious granule cell production was observed at either stage. This is consistent with the reduced efficacy of E3 inhibitor injections in disrupting *Tbr1* expression.

6.2.4 T3 injections offer inconclusive evidence of *Cath1* downregulation.

I next looked at whether injections of T3, the active form of thyroid hormone, could alter the production of cells from the cerebellar rhombic lip. In a series of pilot experiments I injected 50nM T3 into the fourth ventricle of E5 and E6 embryos and analysed the expression of *Cath1*, *Tbr1*, *Pax6* and *Lhx9* at E7. No changes were seen in expression of *Tbr1*, *Lhx9* or *Pax6*, but in 1/3 embryos injected at E5 and 1/3 embryos injected at E6 there was a marked decrease in *Cath1*$^{+ve}$ granule cells (**Figure 6-7 A-F; Table 6-3**).

Following this preliminary data, I performed extensive repeats of this experiment but could never see the same loss of granule cells. In some embryos expression of *Cath1* in the cerebellum was significantly disrupted (**Figure 6-7 G-I**) but this effect was also seen following control injections of high pH saline and therefore was presumed to be a toxic effect of the high pH saline in which T3 was dissolved. Three different batches of T3 were used for injections and no consistent change was seen in *Cath1*$^{+ve}$ expression. The dose of T3 injected was increased until it became toxic (resulting in significant deaths) and no effect was seen. Injections into the blood stream and the fourth ventricle were both used. Results are summarised in **Table 6-4**.

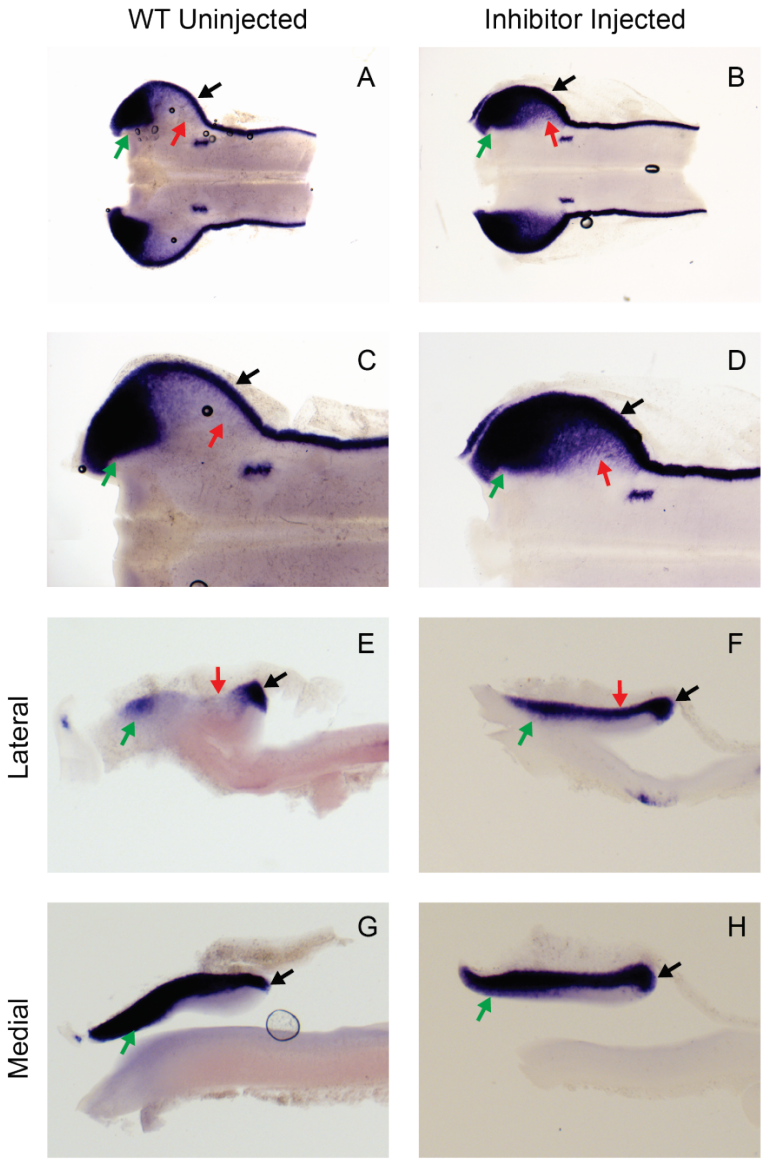

Figure 6-6 *Cath1* expression is induced prematurely in the external granule layer following thyroid hormone inhibition.

E5 *Cath1* expression detected by *in situ* hybridisation in uninjected controls (A,C,E,G) and embryos injected with methimazole and amiodarone at E4 (B,D,F,H). Normal expression is seen in the broad rostral domain of rhombomere 1 (green arrows) and in the rhombic lip (black arrows) but expression is induced prematurely on the pial surface of the cerebellum (red arrows) in injected embryos. A and B show flat-mount hindbrain view magnified in C and D. E-H show sagittal sections of hindbrains taken from lateral (E,F) regions showing ectopic Cath1 expression and medial regions (G-H) showing normal expression in rhombic lip and broad rostral domain of rhombomere1. Tissue is orientated with rostral to the left.

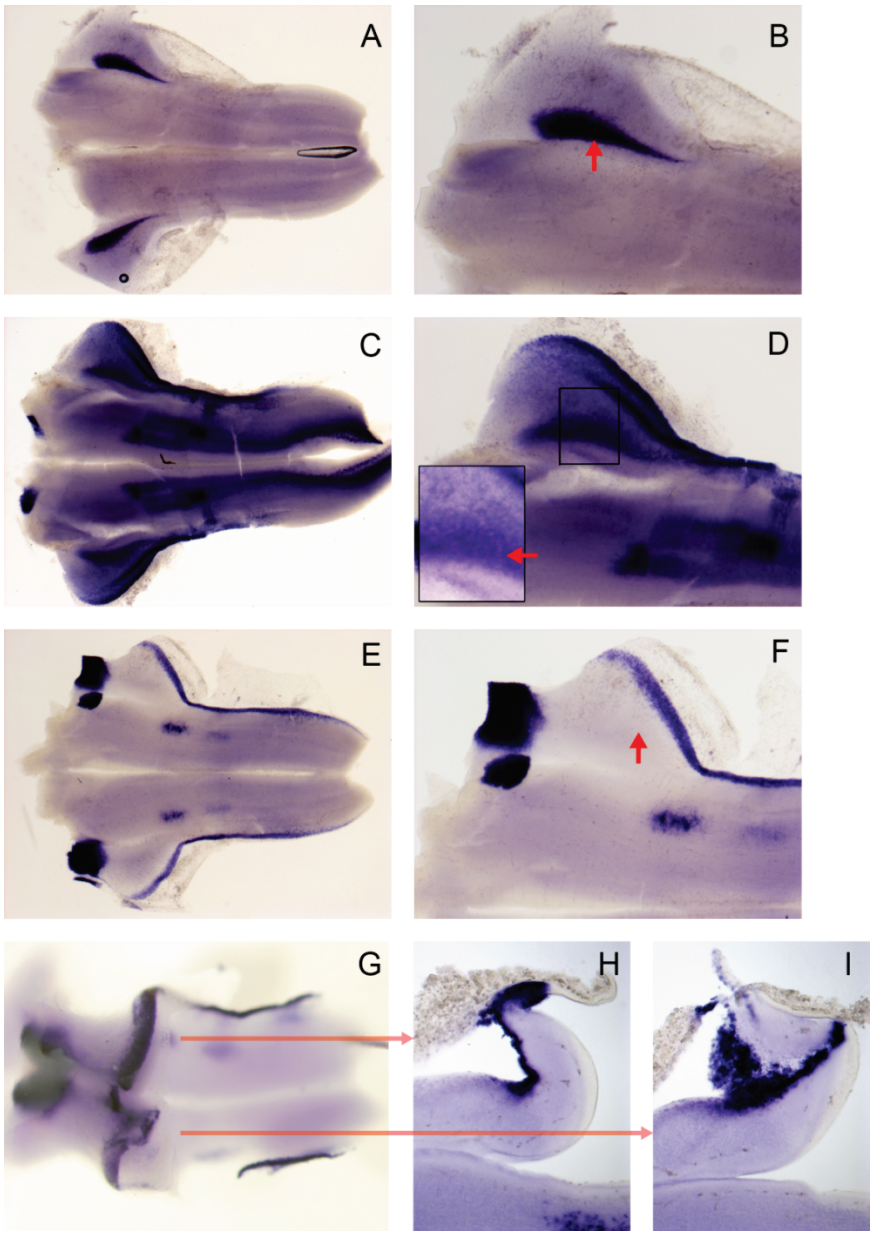

Figure 6-7 Expression of *Tbr1*, *Pax6* and *Cath1* following injection of T3.

A-F show embryos from pilot experiments and G-I show experiment from subsequent experiments. E7 embryos injected with T3 at E5 processed for *in situ* hybridisation for *Tbr1* (A,B), *Pax6* (C,D) or *Cath1* (E-G). Nuclear transitory zone (red arrow) expression of *Tbr1* and *Pax6* are normal. Cath1 expression in the rhombic lip and broad rostral domain of rhombomere 1 are normal but expression in the external granule layer is absent (E,F red arrow) or disturbed (G-I). A,C and E show flat-mount hindbrain view magnified in B,D and F with further magnification and adjusted contrast of boxed region inset in D. G shows whole-mount hindbrain and H and I show sagittal section of G at the level indicated with red line. Tissue orientated rostral to the left.

Table 6-3 Numbers of embryos showing a change in *Cath1*, *Tbr1*, *Pax6* or *Lhx9* expression following ventricular injections of T3.

Stages Injected	Dose	Gene expression	Embryos affected
E5 (ventricle)	50nM	Cath1	1/3
E6 (ventricle)	50nM	Cath1	1/3
E5 (ventricle)	50nM	*Tbr1*	0/3
E6 (ventricle)	50nM	*Tbr1*	0/2
E5 (ventricle)	50nM	*Pax6*	0/4
E6 (ventricle)	50nM	*Pax6*	0/3
E5 (ventricle)	50nM	*Lhx9*	0/3
E6 (ventricle)	50nM	*Lhx9*	0/3

Table 6-4 Numbers of embryos showing a change in *Cath1* expression following injections of T3.

	Injection	Dose	Disturbed *Cath1* expression at E7
Round 1	E5 (Ventricle)	1.5mM	0/4
	E5 (Ventricle)	150nM	0/3
	E5 (Ventricle)	15nM	0/6
	E5 (Ventricle)	1.5nM	0/2
	E5 (Ventricle)	150pM	1/5
Round 2	E5 (Ventricle)	50nM	0/8
	E5 (Ventricle)	30nM*	2/14
	E5 (Ventricle)	3nM*	2/14
	Uninjected	/	0/15
Round 3	Uninjected	/	0/10
	E5 (Blood)	Control	0/3
	E6 (Blood)	Control	0/1
	E5 (Blood)	30nM*	1/6
	E5 (Ventricle)	30nM*	1/6
	E6 (Blood)	30nM*	1/1
	E6 (Ventricle)	30nM*	0/1
	E5 (Blood)	50nM	1/12
Round 4	E5 (Blood)	1.5mM**	0/2 (7/9 dead)
	E5 (Blood)	150nM**	1/5
	E5 (Blood)	15nM**	2/7
	E5 (Blood)	Control	3/8
	E6 (Blood)	1.5mM**	0/2 (7/9 dead)
	E6 (Blood)	150nM**	2/5
	E6 (Blood)	15nM**	2/7
	E6 (Blood)	Control	1/11
* and ** indicate different batches of T3. Control: high pH saline injections.			

6.3 Discussion

In this chapter I have shown that inhibition of thyroid hormone signalling in early development has very specific effects on a single temporal cohort of the rhombic lip lineage which forms the *Tbr1*$^{+ve}$ medial cerebellar nucleus. Furthermore, some evidence suggests that the loss *Tbr1*$^{+ve}$ cells following inhibition of thyroid hormone may also result in a temporal shift in the production of later-born cerebellar granule neurons, though further evidence is required to confirm the identity of the ectopic *Cath1*$^{+ve}$ cells. Despite the clear effect on cerebellar nuclei production following pharmacological treatments to block thyroid hormone signalling, no converse effects of exogenous thyroid hormone treatments were observed.

6.3.1 Thyroid hormone manipulations have inconclusive effects on granule cell precursor production.

Experiments in which thyroid hormone signalling was inhibited by injection of methimazole and amiodarone superficially suggest that precocious granule cells are produced at E5. However, this precocious "granule cell" expression of *Cath1*strongly resembles the expression of *Cath1* in wildtype embryos at a slightly younger stage (**Figure 6-8 compare B and E**). It is therefore possible that the difference between injected and control embryos may reflect a developmental delay. At E5, embryos are staged by the shape of their limbs. It is possible that focal inhibition of thyroid hormone in the hindbrain could cause a localised delay in development or possibly slow the regression of FGF-dependent *Cath1* expression into rostral rhombomere 1. To ascertain the nature of altered *Cath1* expression with thyroid hormone inhibition other markers of granule cells, such as *Pax6* and *NeuroD* could be used.

If thyroid hormone inhibition could shift the production of granule cells to an earlier time point it would logically follow that the addition of exogenous thyroid hormone would abolish granule cell production. However, following injections of T3, no consistent loss of granule cells was seen. This observation supports a model whereby thyroid hormone is only required specifically for the specification of the *Tbr1*$^{+ve}$ population of cells. However several factors must be considered when drawing this conclusion.

The lack of any effects on cerebellar development may suggest that the method of T3 administration was ineffective. T3 is soluble at a high pH or in inorganic solvents (eg DMSO) but can easily precipitate from solution when diluted for injection. This is the reason that a high pH saline carrier was used; however control injections occasionally caused a toxic effect on granule cell production. To circumvent these problems, other methods could

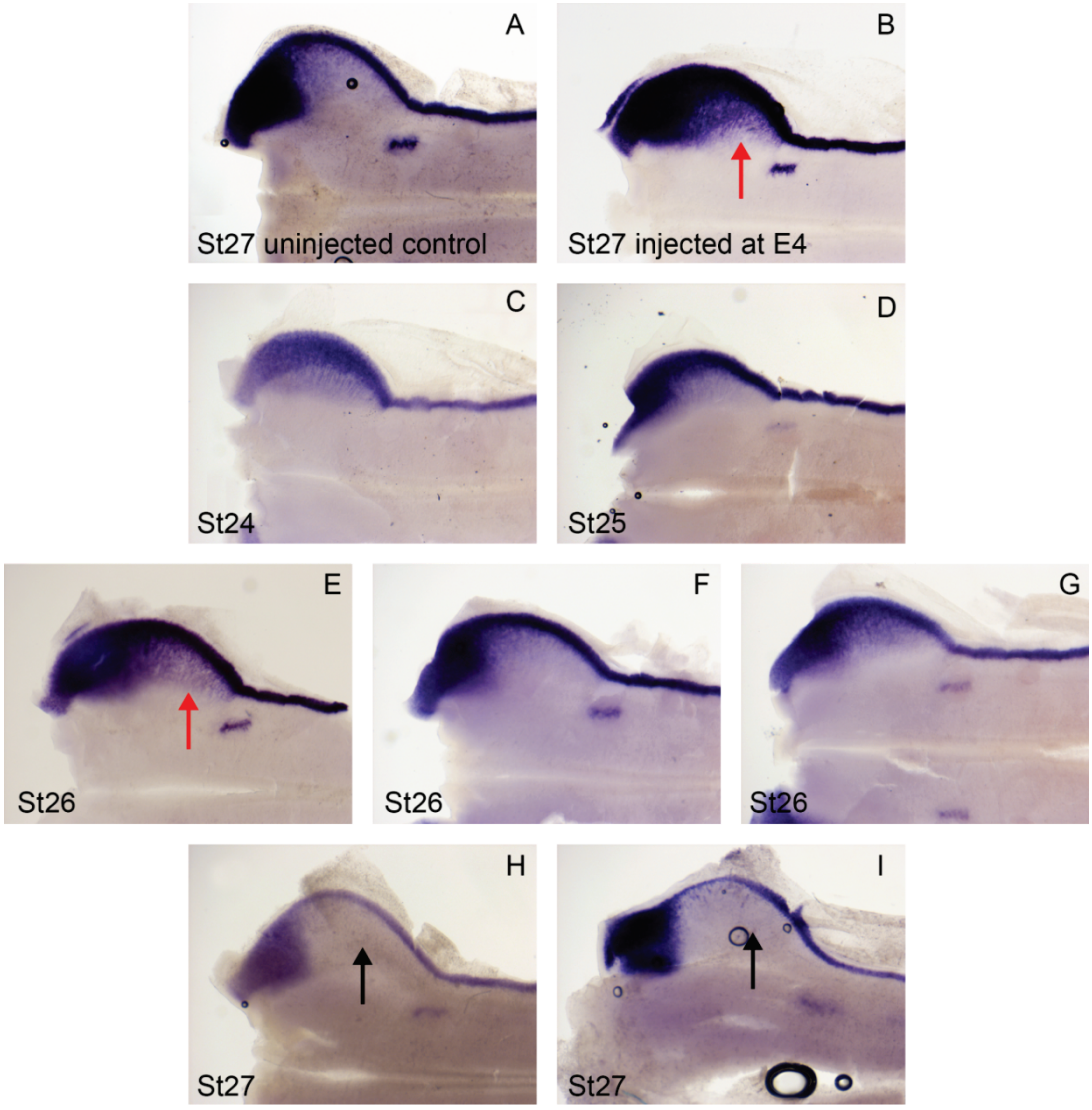

Figure 6-8 Variation in *Cath1* expression at E5.

Hindbrain flat-mount orientated rostral to left showing *Cath1* expression by *in situ* hybridisation. A and B) taken from Figure 6-5 showing no *Cath1* expression on pial surface of St27 uninjected control (A) but increased *Cath1* (red arrow) in St27 hindbrain injected with methimazole and amiodarone at E4. C-I) Cath1 expression in a series of wild type hindbrains showing the variation in *Cath1* expression. At St27 no *Cath1* expression is seen on the pial surface of the cerebellum (H,I black arrows) but at St26 *Cath1* expression is more variable and in some embryos (E) *Cath1* is seen on the pial surface of the cerebellum (red arrow) in a gradient from rostral to caudal. This is comparable to the expression seen in injected embryos (B).

be used to dissolve T3, eg DMSO. Alternatively, injections of T4 could be used instead of T3. However, the rate limiting step of T4 to T3 conversion could prevent a phenotype. A simple experiment could be used to test whether the method of T3 treatments is effective. Co-injection of T3 and the competitive inhibitor of thyroid hormone, amiodarone, should rescue the loss of *Tbr1* expression observed with amiodarone and methimazole injections.

Another explanation of the lack of a reciprocal effect with T3 injections is that the working model of how an extrinsic factor would alter the succession of cell types produced from the cerebellar rhombic lip (**Figure 6-1**) may be too simple. Other factors may act in conjunction with thyroid hormone to elicit an effect on the cerebellar rhombic lip meaning that thyroid hormone could be necessary but not sufficient to cause a temporal shift in cell production.

The requirement for thyroid hormone receptor action in both repressive and active forms must also be considered when interpreting the results of pharmacological manipulations. Inhibition of ligand binding to thyroid hormone receptors may cause an effect due to overactive repressor functions of the receptor complex similarly to dominant-negative thyroid receptor experiments in mice (Fauquier et al., 2011). However addition of T3 may result in no obvious change if the thyroid hormone receptors are already saturated.

Finally, it is also important to consider results of thyroid hormone manipulations in the context of the normal levels of thyroid hormone at different times in development. The initial reason for studying the function of thyroid hormone in cerebellar rhombic lip was the coincident temporal development of the choroid plexus expressing thyroid hormone transporters and regulators. If inhibition of thyroid hormone is responsible for or required for the onset of granule cell production, then in normal development cerebellar rhombic lip cells must become insensitive the thyroid hormone, the levels of which would presumably be increasing in the fourth ventricle (based on gene expression in the choroid plexus). In order to study this further a better understanding of the levels of thyroid hormone availability in the cerebrospinal fluid and activity of the receptor signalling at different times in development would be required (see future work, below).

6.3.2 Thyroid hormone inhibition disrupts gene expression in the nuclear transitory zone.

Inhibition of thyroid hormone at E4 causes a robust loss of *Pax6/Tbr1* expression in the nuclear transitory zone after 2 days. This result was validated by a dilution series showing a loss of the effect with reduced doses, indicating a specific pharmacologic effect. Furthermore, two different methods of injection into the ventricle or the bloodstream were

used, producing the same specific result. Injections of methimazole and amiodarone at E3 showed a reduced effect after 3 days which may either indicate a dilution of the drug over time or that the effect can only occur within a specific time window.

It is unlikely that the loss of *Tbr1/Pax6* expression in the nuclear transitory zone reflects a delay in development as was the possible explanation of altered *Cath1* expression. Robust expression of *Tbr1* in a very specific domain is always seen in wildtype embryos at St28 (early E6) and all experimental embryos were fixed at St29. Furthermore, in wildtype embryos when *Pax6* expression is first seen in the cerebellum it appears simultaneously in the nuclear transitory zone and granule cells at E6 suggesting *Pax6*, like *Tbr1* is not switched on in medial cerebellar nuclei cells until they terminate their tangential migration (see chapter 3). The *Pax6* expression pattern observed in injected embryos where expression is seen on the pial surface but not in nuclear transitory zone is therefore not representative of a younger expression pattern. To definitively confirm this, E4 inhibitor injected embryos could be analysed for *Tbr1* expression at E7, instead of E6.

The loss of *Tbr1/Pax6* expression in the nuclear transitory zone could represent three different outcomes of the experiment. 1) the cells are absent, 2) there is a loss of specification due to migration failure and 3) the cells are present but no longer express *Pax6* or *Tbr1*. The function of *Pax6* in the nuclear transitory zone is not known but *Tbr1* expression is not required for cerebellar nuclei formation (Fink et al., 2006).

To distinguish between these three potential situations injection of thyroid hormone inhibitors could be paired with electroporation of GFP into the cerebellar rhombic lip to label cells. If the cells are absent (1), there would be a complete lack of GFP^{+ve} cells in the region of the nuclear transitory zone. If the cells migrate erroneously (2) GFP^{+ve} cells would absent in the region of the nuclear transitory zone but an ectopic population would be found elsewhere. If cells are present and only expression of *Tbr1*/*Pax6* is absent (3) then cells would be labelled in the nuclear transitory zone as normal.

6.3.3 Thyroid hormone as a temporal regulator of cell fate?

Results in this chapter support a role for thyroid hormone as an extrinsic signal which can control cell specification at the cerebellar rhombic lip. This is strongly supported by the loss of *Tbr1/Pax6* expression in a very specific temporal cohort of rhombic lip cells. However, there is only partial evidence that granule cells from the rhombic lip are altered to compensate for the loss of a temporal specific cohort according to the model for temporal

transitions outlined in **Figure 6-1**. The evidence for temporal compensation by the granule cell population is very weak, as discussed above.

There is no evidence that the temporal production of earlier-born, *Lhx9*$^{+ve}$ cells from the cerebellar rhombic lip is altered. However, inhibitor injections were performed at E4, after the majority of *Lhx9*$^{+ve}$ cells are produced. Further experiments to analyse the expression of *Lhx9* following E3 injections of inhibitors are needed to conclusively answer this.

One other possibility is that inhibition of thyroid hormone alters the temporal allocation of different cell types of the cerebellar nuclei. The population of cells born immediately before the *Tbr1*$^{+ve}$ cells of the medial cerebellar nucleus are cells of lateral cerebellar nucleus which do not express *Tbr1* or *Lhx9*. Without a specific molecular marker for this population of cells it would be difficult to assess whether the transition between these two cell types was affected, but labelling cells of the cerebellar rhombic lip by focal electroporation with GFP could help to discriminate between these two cerebellar nuclei populations based on the cell positioning and axon projections.

A temporal transition between the production of *Lhx9*$^{+ve}$ and *Pax6*$^{+ve}$ (*Barhl1*$^{+ve}$) cells from the rhombic lip is observed throughout the entire hindbrain (see chapter 3 and (Bermingham et al., 2001; Rose et al., 2009a)). The specific loss of *Pax6*$^{+ve}$ cells in the nuclear transitory zone suggests that thyroid hormone may contribute to this more general transition, but *Pax6*$^{+ve}$ granule cells are still produced when thyroid hormone signalling is blocked. Analysis of populations of cells from the lower rhombic lip could show whether the effects observed within the cerebellum are specific or reflect a more general program of development in the hindbrain which is reliant on thyroid hormone.

6.3.4 Thyroid hormone as a regulator of migration?

To complete this study it is very important to understand how the migration of rhombic lip derivatives is altered when thyroid hormone signalling is inhibited. Changes in gene expression may not be an accurate representation of the actual behaviour cells within the brain.

Pharmacological treatments utilised two antithyroid drugs, methimazole and amiodarone. Whilst these drugs are known to antagonise the thyroid hormone signalling pathway it possible that they may have other, off target effects on development. In particular, amiodarone is primarily used as an anti-arrhythmic drug due to its ability to block potassium channels. The specification or migration of neurons from the cerebellar rhombic lip could be altered by changes in electrical activity of cells through the inhibition of potassium channels.

In the *weaver* mouse which carries a mutation in the GIRK2 potassium channel, the differentiation and radial migration of cerebellar granule cells is disrupted (Kofuji et al., 1996). Therefore in order to confirm that the loss of cerebellar nuclei gene expression is specific to thyroid hormone and not activity dependent another method of thyroid inhibition should be used. One possibility would be to perform single injections of methimazole, without amiodarone.

One well characterised effect of hypothyroidism is the loss of radial migration of cerebellar granule cells (Nicholson and Altman, 1972a; Lauder, 1977). Bergman Glia cells (which granule cells attach to for radial migration) are also show disrupted in hypothyroid mice (Morte et al., 2004; Manzano et al., 2007). It is therefore important to understand if the migration of cerebellar rhombic lip derivatives is disrupted by thyroid hormone inhibition during the production of cerebellar nuclei cells. However, changes in migration of cells may only be as a consequence of disrupted differentiation.

6.3.5 Thyroid hormone as a differentiation factor?

An alternative explanation of the results obtained following pharmacological treatments is that thyroid hormone may just be required for the correct differentiation of cells of the medial cerebellar nucleus. Although the expression of *Pax6* and *Tbr1* in the nuclear transitory zone is completely abolished following thyroid hormone inhibition, this could reflect a failure of cells to differentiate properly rather than a complete loss of cells. Both *Pax6* and *Tbr1* do not mark cerebellar nuclei cells as they tangentially migrate and are only expressed when cells reach the nuclear transitory zone and begin to differentiate (see chapter 3). Again, labelling of cells by electroporations alongside treatments could confirm this hypothesis.

Most of the documented phenotypes of loss of thyroid hormone signalling in the cerebellum result in an inability of cells to terminally differentiate. Late embryonic/early postnatal hypothyroidism results in a failure of cerebellar granule cells to terminally differentiate and radially migrate form mature granule cells in the inner granule layer (Nicholson and Altman, 1972a; Lauder, 1977). Purkinje cells display markedly reduced arborisation and do not form mature connections with afferent climbing fibres following thyroid hormone deficiency (Crepel et al., 1981; Boukhtouche et al., 2010). GABAergic interneurons in the cerebellar cortex show delayed differentiation and maturation and show reduced connectivity (Manzano et al., 2007). Despite most of these effects being demonstrated in late cerebellar development the differentiation of cerebellar nuclei cells in the nuclear transitory zone may be disturbed in a similar manner.

Without clear evidence for a shifted temporal progression of rhombic lip cell specification and without a phenotype following T3 administration the data reported from these treatments is more consistent with a model whereby thyroid hormone is required for the correct differentiation of cerebellar nuclei cells.

6.3.6 Future work.

The work in this chapter has provided evidence that thyroid hormone can alter cell derived from the cerebellar rhombic lip. However, further work will be required to understand the nature of these observed changes.

Further characterisations of the effects observed with pharmacological treatments is required including: labelling cells by GFP electroporation, determining whether precocious granule cells are born with thyroid hormone inhibition by the use of other markers and testing that T3 injections can rescue inhibitor injections to determine whether the technique is working, and confirm the absence of an effect with over-activation of thyroid hormone.

To understand the role of the choroid plexus in the regulation of thyroid hormone during development, further characterisation of the temporal expression of thyroid hormone transporters and regulating enzymes would be informative. Analysis of the levels of thyroid hormone in the blood and cerebrospinal fluid at different stages would also be informative. Levels of T3 and T4 can be analysed using a radioimmunoassay as described by Van der Geyten et al. (2001).

To understand the activity of thyroid hormone receptors in wildtype and manipulated situations I would construct a reporter of the thyroid hormone response similar to that used to detect activation of retinoic acid signalling by placing a series of thyroid hormone receptor binding sites, which are coded by a specific motif, with a minimal promoter upstream of *gfp*. Electroporation of this construct into the rhombic lip would give a read-out of where thyroid hormone signalling was endogenously activated and when combined with pharmacological treatments would give a better understanding of how thyroid hormone is acting at the level of the receptors.

Chapter 7 General Discussion

In this thesis I have sought to further understand the development of the cerebellum using the chick as a model organism. By analysis of the temporal progression of cell production from the cerebellar rhombic lip and through detailed analysis of cell migration, axon projections, gene expression and temporally changing signalling systems, I have given new insights into the mechanisms which are required to orchestrate this developmental regime. Through comparison with published data, this detailed study allows for comparisons across different species to be made with important consequences for evolutionary changes in the structure and function of the cerebellum.

This thesis also addresses the function of the isthmus in rhombomere 1 during the period of cerebellar development. I have demonstrated a novel mechanism of *Atoh1* induction in dorsal rhombomere 1 which is dependent on FGF signalling. This domain is independent of the *Atoh1*$^{+ve}$ rhombic lip and its derivatives are produced in sequential order regardless of the level of FGF signalling. This work suggests a role of FGF signalling in tissue growth rather than in cell specification in rhombomere1.

7.1 Temporal controls of cell fate specification

By studying the temporal allocation of cell fate at the cerebellar rhombic lip I have shown that different cerebellar nuclei, with differing functions, are born sequentially from the cerebellar rhombic lip in chick. Furthermore, I have demonstrated that the different cerebellar nuclei occupy distinct dorsoventral domains of the neural tube prior to migration of cerebellar nuclei into the white matter of the cerebellum. Cells of the lateral cerebellar nucleus migrate more ventrally than later-born cells of the medial cerebellar nucleus, which occupy the nuclear transitory zone.

Dorsal restriction in the migration of late born cerebellar rhombic lip derivatives has previously been shown to be mediated by a temporal change in sensitivity to Netrin signalling (Gilthorpe et al., 2002). This mechanism can likely be extended to the intermediate populations of the cerebellar nuclei, such that successive populations have a stepwise reduction in Netrin response. Migratory capacity could be a cell fate determinate. However, homologous populations in mouse and chick have distinct genetic properties allocated at the rhombic lip, suggesting fate is determined prior to, and may govern, migration.

A temporal axis determines the diversity of cells produced from a continuous stream of cells migrating from the cerebellar rhombic lip. This suggests a simple model for generating

increased diversity by temporal subdivisions of this lineage which could provide a possible evolutionary model for altering the populations of cells within the cerebellum.

7.2 Evolutionary changes of temporal fate specification

The ventral to dorsal restriction of cell types born from the cerebellar rhombic lip seems invariant between species as diverse as zebrafish, chick and mouse, all of which show early ventral and later dorsal cell migration from the cerebellar rhombic lip (Gilthorpe et al., 2002; Machold and Fishell, 2005; Wang et al., 2005; Volkmann et al., 2010). However, the number of distinct cerebellar nuclei made from this migratory lineage does vary between species from none (zebrafish/goldfish) to five distinct nuclei in humans. This suggests that the temporal allocation of cells to different fates occurs by variable subdivision of the continuous migratory stream from the cerebellar rhombic lip. The evolutionary relationship between different species and their respective number of cerebellar nuclei (Nieuwenhuys, 1998) is outlined in the phylogenetic tree in **Figure 7-1**.

The presence of single cerebellar nucleus in both paddlefish (basal ray-finned fish) and shark suggest that their common ancestor would have possessed a single cerebellar nucleus. In zebrafish/goldfish (teleosts) the function of the cerebellar nuclei is replaced by a unique cell class called eurydendroid cells. Eurydendroid cells are situated in the cerebellar cortex and receive inputs from Purkinje cells and parallel fibres to form the output of the cerebellum (Ikenaga et al., 2006). Like cerebellar nuclei cells, eurydendroid cells can be both GABAergic and glutamatergic and are derived from ventricular zone and rhombic lip respectively (Kani et al., 2010). It is not clear whether these cells are homologues of the cerebellar nuclei or have evolved functional equivalents.

In order to understand the evolutionary mechanisms by which the number of cerebellar nuclei has increased in the amniote lineages (reptile/avian and mammalian), analysis of lizard cerebellar nuclei and the cerebellar nuclei of other, more basal mammals could be particularly informative. Do the three cerebellar nuclei of mice originate from a common ancestor with reptile and birds which possess two nuclei or have distinct mechanisms generated multiple nuclei in both lineages from a common ancestor with a single cerebellar nucleus?

The efferent connections of shark, zebrafish, frog, chick and mouse cerebellum are broadly outlined in **Figure 7-2** (Nieuwenhuys, 1998). Despite different pathways through the cerebellar nuclei, the connections of shark, zebrafish, frog and chick cerebella are remarkably conserved, with variation only in connections to vestibular nuclei and a minor connection to the thalamus in chick. Mammals also preserve this pattern of efferent

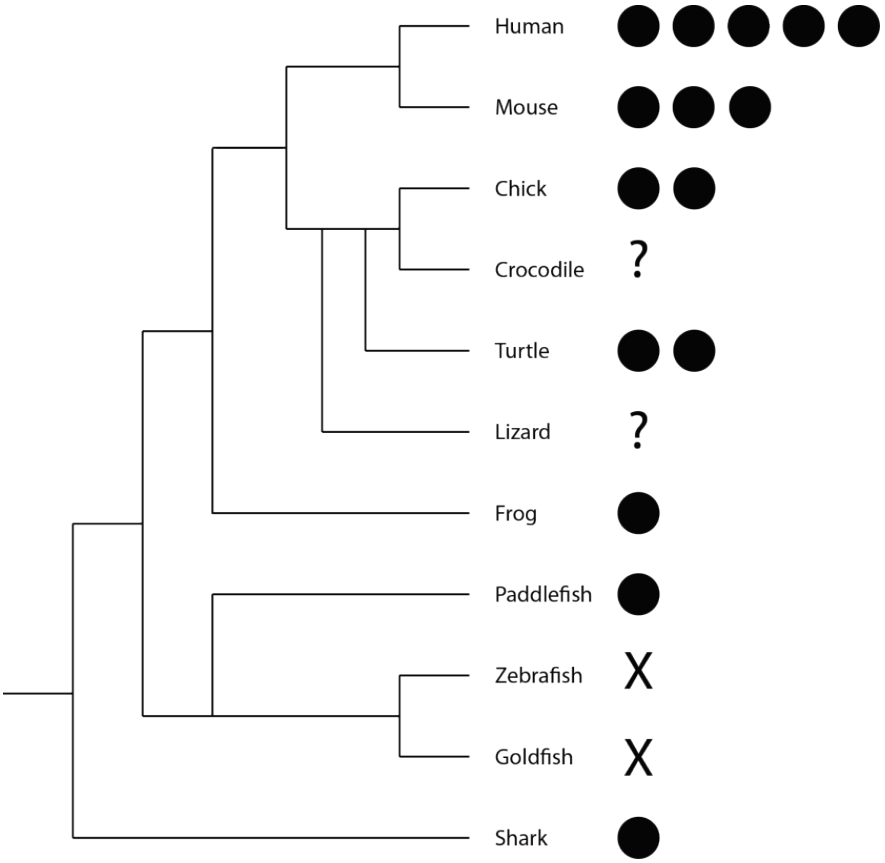

Figure 7-1 Phylogenetic tree showing the number of cerebellar nuclei in different vertebrate species.

Phylogenetic tree showing the evolutionary relationship between different vertebrate species. To the right, the number of black circles shows the number of cerebellar nuceli in each species varying from none (X) in fish to 5 in humans based on the descriptions in Nieuwenhuys (1998). The number of cerebellar nuclei in crocodiles and lizards is unknown.

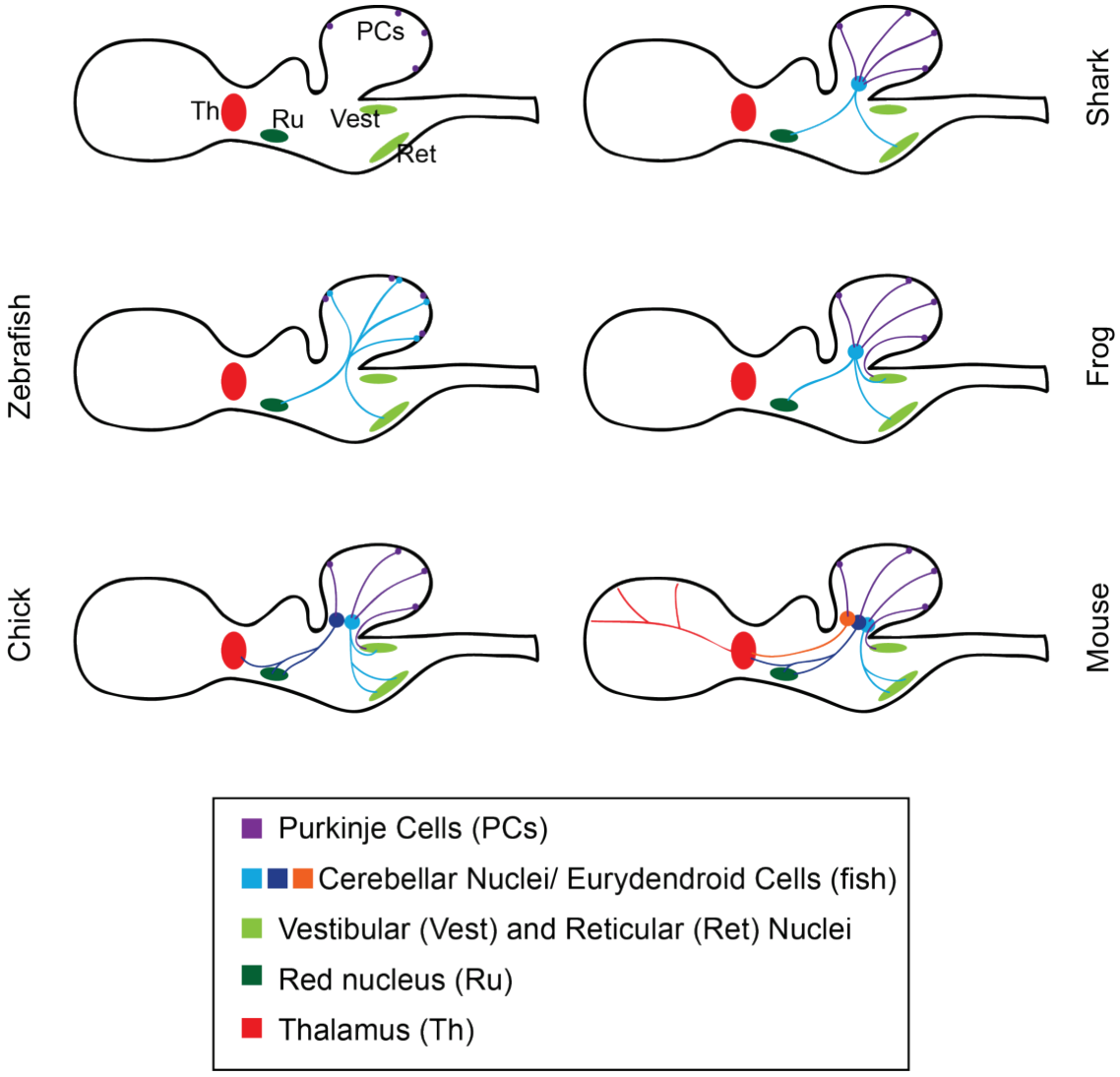

Figure 7-2 Comparative efferent connections of the cerebellum.

Schematic depicting the variation in cerebellar output between shark, zebrafish, frog, chick and mouse based on description by Nieuwenhuys (1998). Projections from the cerebellar cortex, via variable cerebellar nuceli, project to vestibular and reticular nuclei, the red nucleus and variably to the thalamus.

connections within the fastigial and interposed nuclei (suggesting a common origin) but the addition of a dentate nucleus forges a major connection between the cerebellum and the cortex, via the thalamus.

The results of this thesis suggest that the functional change to connect extensively to the thalamus and hence the cortex, arises with the addition of *Lhx9* expression within a subset of the cerebellar nuclei. In chick, *Lhx9* expression is confined to non-cerebellar cells in ventral rhombomere 1, which are born before cerebellar nuclei. The single cerebellar nucleus of the frog is also *Lhx9*-negative (Moreno et al., 2005). This is highly significant because, in chick, the majority of *Lhx9*$^{+ve}$ cells in ventral rhombomere 1 project directly to the thalamus/hypothalamus. Therefore the extension of the temporal window of *Lhx9*$^{+ve}$ cell production may be responsible for the innovation of new connections between the cerebellum and the cortex, a pathway which is important for the non-motor, as well as motor functions, of the cerebellum. Differential expression of LIM-homeodomain genes specify the axon targeting to different classes of motor neurons in the drosophila ventral nerve cord (Thor et al., 1999) and in *Lhx9*$^{+ve}$ spinal cord interneurons in the mouse and chick (Wilson et al., 2008; Avraham et al., 2009; Kohl et al., 2012) which are derived from dorsal *Atoh1*$^{+ve}$ progenitors (Helms and Johnson, 1998; Bermingham et al., 2001). This strongly supports a role for *Lhx9* in targeting axonal projections of early born rhombic lip derivatives.

Together these observations suggests an evolutionary model where an invariant dorsal restriction of cell migration from the cerebellar rhombic lip occurs beginning with the production of *Lhx9*$^{+ve}$ ventral populations and terminating with dorsal cerebellar granule cells. Altering the temporal controls of genetic programs of specification which are superimposed onto this lineage can then subdivide the lineage to generate novel cerebellar nuclei and functional connections within the brain (**Figure 7-3**).

Compared to the highly conserved circuitry in the rest of the cerebellum (granule cells and Purkinje cells) the variation in cerebellar nuclei is quite distinct. This suggests that evolutionarily, functional changes to the cerebellum have mostly occurred via adaptation of the cerebellar nuclei and their respective connections, which is controlled by temporal fate specification at the cerebellar rhombic lip.

The cortical connections of the mammalian cerebellum form part of closed-loop system which projects back to the cerebellum via the pontine nucleus (Kelly and Strick, 2003). The pons is also a (lower) rhombic lip derived structure (Rodriguez and Dymecki, 2000) almost uniquely present in mammals (Nieuwenhuys, 1998), although there is some evidence of a reduced pons in chick (Brodal et al., 1950; Marin and Puelles, 1995). This suggests a

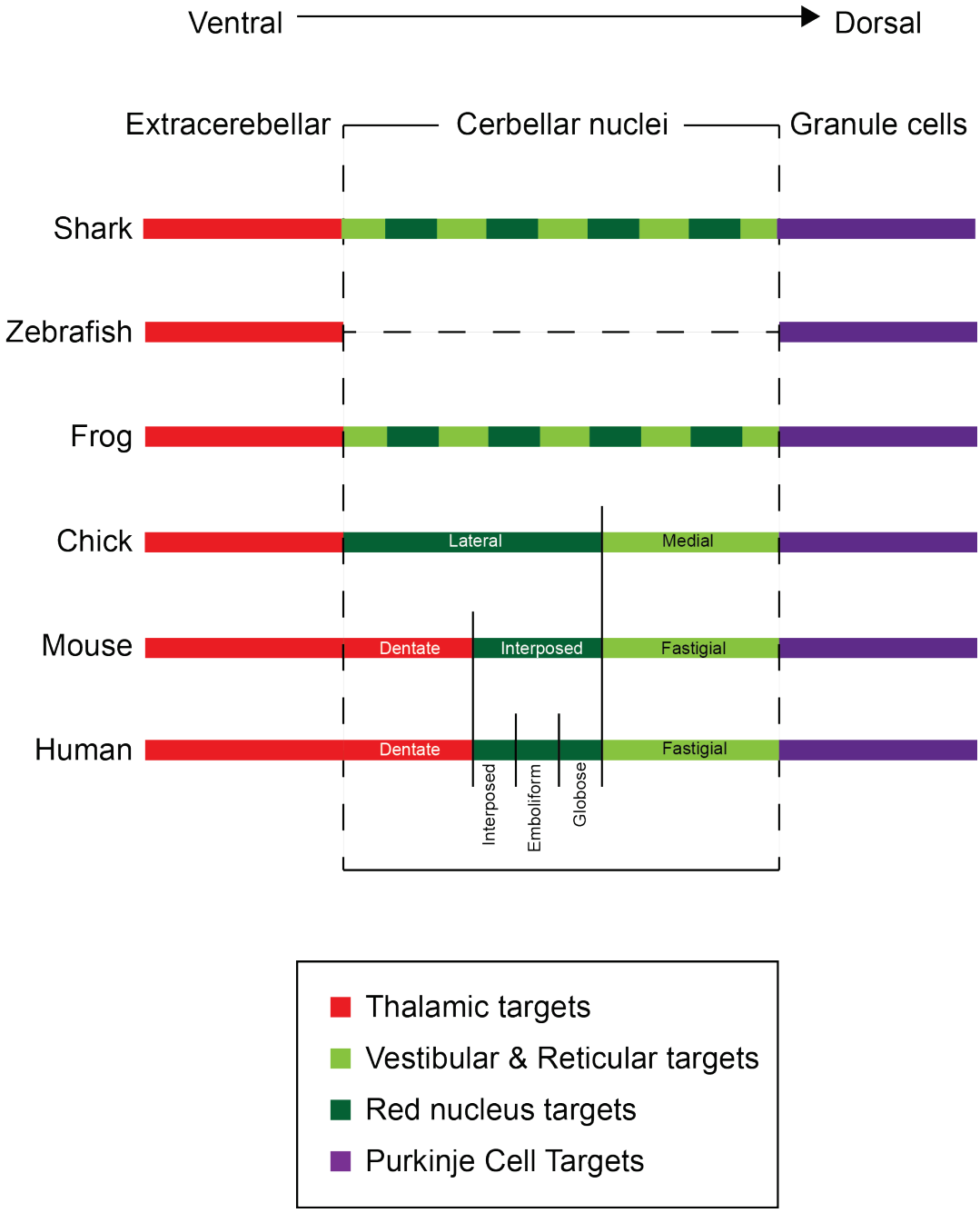

Figure 7-3 Comparative temporal subdivisions of the cerebellar rhombic lip lineage.

Model for temporal origins of diversity through evolution. Each horizontal line represents the invariable lineage of cells from the cerebellar rhombic lip. This lineage is then subdivided into 3 broad populations: extracerebellar cells, cerebellar nuceli and granule cells. Further temporal subdivisions or heterochronic shifts in cells produced within this lineage result in diverse specification.

common evolutionary adaptation in the rhombic lip may alter both the cerebellar nuclei and pons to create this functional circuit in mammals.

7.3 Gene regulatory networks across brain regions

Within the *Atoh1* lineage, throughout the hindbrain there are two, temporally distinct programs of development characterised by the expression of *Lhx2*/9 and *Barhl1*/*Pax6* which together result in the development of several different components of proprioceptive pathways in the brain including the cerebellum (Bermingham et al., 2001; Rose et al., 2009a). The temporal switch between these two programs occurs across the entire rhombic lip and I have shown that an alteration to the relative temporal window of expression of *Lhx9* coincides with the addition of an extra cerebellar nucleus and altered cerebellar circuitry. I have also demonstrated that, in chicken there is gap between the expression of *Lhx9* and *Pax6*, in which cells of the lateral cerebellar nucleus are born, which does not appear to be present in mice. Further work is required to define whether these cells may express other genes which characterise the two temporal phases, such as *Lhx2* or *Barhl1*, of whether a third temporal program of development may exist.

Although it is not clear whether *Lhx9* itself is required for the specification of the early-born cells, or whether this gene acts to control cell migration and axon guidance, this phase of development is notably negative for *Pax6* and *NeuroD1* expression. The onset of expression of *Pax6*, *NeuroD1* and *Tbr1* (and presumably *Tbr2* (Fink et al., 2006)) with the production of the medial cerebellar nucleus suggests a switch to a distinctly different program of development, which is similar to that found in multiple different sites of glutamatergic cell specification such the cortex and hippocampus (Reviewed by Hevner et al. (2006)). Expression of these genes in the medial cerebellar nucleus, granule cells and cortical pyramidal cells are outlined in **Figure 7-4**. Although these two systems show several differences such as by different bHLH proneural genes (*Atoh1* in hindbrain and *Ngn2* in cortex (see review by Guillemot et al. (2006)) and differential expression of *Atoh1* (cerebellar granule neurons) or *Tbr2* (cortex) during transit amplification (Noctor et al., 2004; Englund et al., 2005) the transcriptional networks indicate several commonalities which could provide insight into general principals of cell specification in the brain.

The expression of *Lhx9* and *Barhl1* are both dependent on *Atoh1* expression (Bermingham et al., 2001; Wang et al., 2005; Rose et al., 2009a) but only *Barhl1* has been shown to be directly regulated by *Math1* binding to its enhancer (Kawauchi and Saito, 2008; Lai et al., 2011). Throughout the hindbrain *Lhx9* and *Barhl1* are expressed in complementary population however in the spinal cord, these genes are expressed in the same population of

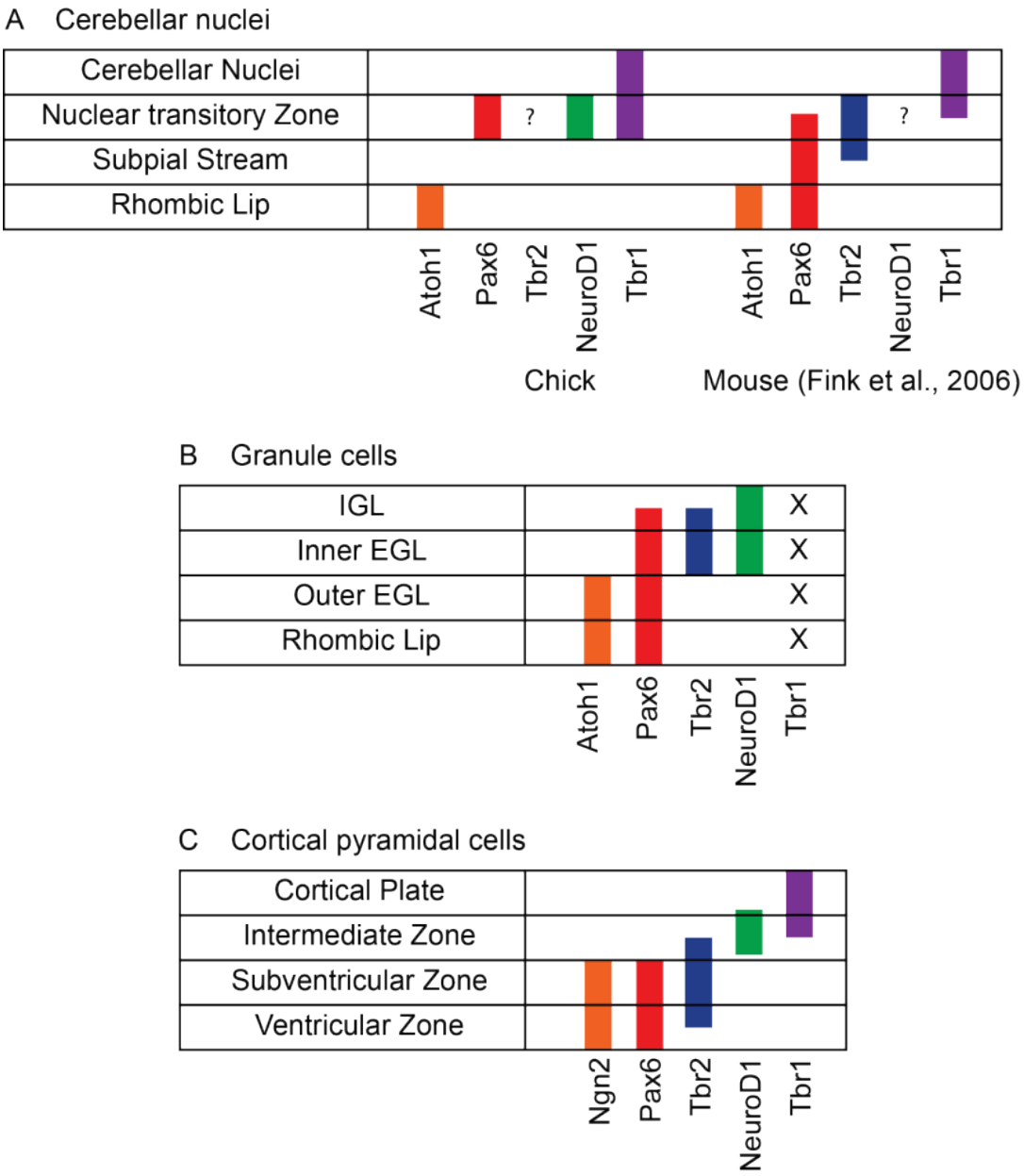

Figure 7-4 Comparative gene expression in cerebellar nuceli, cerebellar granule cells and cortical pyramidal neurons.

Diagram showing the common, but variable, network of transcription factors: *Pax6*, *Tbr2*, *NeuroD1*, *Tbr1*. In the development of multiple different cells types: cerebellar nuceli, granule cells and cortical pyramidal neurons. Reviewed by (Hevner et al., 2006). Both my data, and published data in mouse (Fink et al., 2006) are included.

Atoh11-dependent cells, the DI1 population of interneurons and differential expression of *Barhl1*/*Lhx9* and closely related genes *Barhl2* and *Lhx2* control the specification of subtypes of neurons within this population (Bermingham et al., 2001; Saba et al., 2003; Wilson et al., 2008; Ding et al., 2012). *Barhl1* and *Barhl2* are both present in cerebellar granule cells with partially redundant functions (Kawauchi and Saito, 2008) and *Barhl2* is expressed in a subset of other cerebellar rhombic lip derivatives, all of which are *Lhx9*-negative. *Barhl1*-null mice have a mild cerebellar phenotype affecting granule cells (attenuated cerebellar foliation, defective radial migration and increased apoptotic death) and precerebellar nuclei (aberrant migration and increased apoptosis) (Li et al., 2004) suggesting *Barhl1* is not a major factor in granule cell specification. Although there are clear differences between the generation of *Atoh1*-derived spinal cord commissural neurons and cerebellar cells, the commonalties between expression in the two distinct regions of the brain suggest *Atoh1* can induce different combinations of common downstream effectors in a context dependent manner.

Studying common transcriptional programs in different regions of the brain including the *Pax6, Tbr2, NeuroD1, Tbr1* network and the *Math1, Lhx9, Barhl1* network offers a potential window into factors that orchestrate temporal cell fate allocation at the cerebellar rhombic lip. Furthermore to understand how extrinsic factors such as thyroid hormone, retinoic acid and organiser signalling molecules can regulate and possibly even link common modes of cell specification across the brain to organise functional systems such as the proprioceptive network.

7.4 Spatial controls of cell fate specification

Through focal mapping of cerebellar rhombic lip derivatives I have demonstrated that the different axon projections from a single cerebellar nucleus are determined by the rostro-caudal origin of cells within the rhombic lip. Although the precise patterning mechanism which generates the subcompartments of the cerebellar nuclei from different regions of the cerebellar rhombic lip remains elusive, I have shown that patterning at the level of the rhombic lip precursors, at least in part, determines the heterogeneity of cell types in the cerebellar nuclei. Despite the later morphological changes of the cerebellum which result in the cerebellar nuclei transitioning from the edge of the cerebellar primordium to within the while matter of the cerebellum, the spatial organisation of different projections from individual cerebellar nuclei is retained in the adult cerebellum, where labelling of different regions of the medial or lateral cerebellar nuclei labels different subsets of projections (Arends and Zeigler, 1991a).

Purkinje cells throughout the majority of the cerebellar cortex, project directly to the cerebellar nuclei below them (Arends and Zeigler, 1991b) regardless of their species specific number of cerebellar nuclei. This suggests that the early spatial organisation of the cerebellar nuclei, which is determined by rostrocaudal origin within the cerebellar rhombic lip, may, in part, determine and the topographic organisation of circuits in the cerebellum and therefore the functional subdivisions of the cerebellum.

7.5 The role of the isthmus in rhombomere 1.

The work of this thesis has extensively examined the role of signalling from the isthmus in rhombomere 1. Despite the initial observation of a correlation between FGF signalling and the expression of *Lhx9* in early-born cerebellar rhombic lip derivatives, I have shown that FGFs are not directly responsible for the specification of any individual cells types within the cerebellum. This is consistent with observations in zebrafish that Fgf8 is not required instructively for cerebellar development but acts to prevent *Otx2* expansion and therefore is required to maintain cerebellar territory (Foucher et al., 2006). However, it is clear from mouse conditional *Fgf8* mutants (Chi et al., 2003) and the data presented in this thesis that the repression of *Otx2* expression is not the only function of isthmic FGF signalling in the developing cerebellum.

I have demonstrated a novel mechanism by which *Fgf8* can induce *Cath1* expression in rhombomere 1 in a manner which is entirely independent from the roof plate-dependent *Cath1* expression in the rhombic lip. This domain of *Cath1* expression does not appear to directly contribute to the cerebellum based on gene expression (no *Pax6*$^{+ve}$ granule cells are seen to migrate from this domain) and tissue morphogenesis (the domain becomes segregated outside of the cerebellar tissue). Furthermore, the rostral domain of *Cath1* expression is *Wnt1*-negative and genetic fate-mapping of the *Wnt1*$^{+ve}$ lineage in rhombomere 1 shows that the *Wnt1*$^{+ve}$ precursor pool accounts for all cerebellar rhombic lip derivatives (Hagan and Zervas, 2012). I show that *Fgf8* overexpression does not induce the production of *Lhx9* outside of its endogenous temporal window and the *Lhx9*$^{+ve}$ domain in rhombomere 1 does not appear to increase in size significantly following the termination of *Lhx9*$^{+ve}$ cell production from the rhombic lip. Together, these observations suggest it is unlikely that the rostral FGF-dependent domain of *Atoh1* produces tangentially migrating cells. Fate mapping this region from E5 could verify these conclusions.

I propose that the more likely function of the FGF signalling in rostral rhombomere 1 is to direct orientated growth of the cerebellum. This idea is supported by experiments showing that loss of FGF signalling results in a marked decrease in the size of the cerebellar

primordium (chapter 4,(Chi et al., 2003; Basson et al., 2008)) and conversely, that an increase in FGF signalling can laterally expand the cerebellum (Yu et al., 2011). Furthermore loss of FGF receptors after commitment of cells to the *Atoh1*$^{+ve}$ lineage causes no cerebellar defects in *Math1*-TKO (triple FGF-receptor knockout) mice (chapter 5). This suggests that FGF signalling directs precursor proliferation prior to the allocation of cells to the *Atoh1* lineage.

In attempting to fate map the most rostral region of rhombomere 1, electroporations consistently labelled more caudal cells after 2-3 days of development. This caudal shift of tissue is also seen in rhombomere 1/mesencephalic grafts which exclude the isthmus (Millet et al., 1996). A surprisingly large expansion of tissue forming the posterior midbrain and anterior cerebellum hindbrain has been observed by labelling cells very close to the isthmus by grafting (Hallonet et al., 1990; Hallonet and Le Douarin, 1993; Le Douarin, 1993; Millet et al., 1996), DiI labelling (Alexandre and Wassef, 2003; Louvi et al., 2003; Chaplin et al., 2010) and genetic fate mapping (Zervas et al., 2004). All of these experiments were performed by labelling the isthmus from E2 and growth from the isthmus into rhombomere 1 been interpreted as midbrain tissue contributing to the cerebellum by growth or migration. However, I have performed labelling at E3, when midbrain tissue is definitely not labelled and see a similar caudal shift in tissue. Genetically inducible fate mapping of *Otx2*$^{+ve}$ midbrain cells could be used to confirm that no part of the cerebellum is derived from the mesencephalon.

This model would propose that cerebellar growth is identical to the midbrain. Here growth from a narrow strip of *Wnt1*$^{+ve}$ cells at the posterior, isthmic region of the mesencephalon forms the entire inferior colliculus (Zervas et al., 2004). This study also demonstrated that there is no increased cell division at the isthmus. One possibility of how this growth can be achieved is by regulating the ratio of asymmetric and symmetric division. By increasing symmetric divisions of progenitor cells a territory can be expanded whereas increasing asymmetric divisions promotes the production of differentiated cells.

7.6 Models of cerebellar growth

Based on the evidence in this thesis I propose two possible models of growth directed by anterior rhombomere 1 which are summarised in **Figure 7-5 A,B**. Model 1 suggests the rostral FGF-dependent domain of Cath1 to be a proliferating “node” which feeds cells directly into the rhombic lip. This model indicates a functional role for *Atoh1* expression in the anterior region of rhombomere 1. However, the lack of *Wnt1* expression in this domain is not consistent with the observation that all cerebellar rhombic lip derivatives express *Wnt1*,

most likely prior to the onset of *Atoh1*$^{+ve}$ expression (Hagan and Zervas, 2012). Nor is this model consistent with the observation from chimeric isthmic grafting experiments which show that, although midbrain/isthmic tissue contributes to tissue of the medial cerebellum, it does not give rise to granule cells (Louvi et al., 2003).

By comparison, this model is supported by work showing the isthmic organiser to be a node for producing roof plate cells in the midbrain and rhombomere 1 (Alexandre and Wassef, 2003), but rhombic lip cells were not specifically assessed in this study. Furthermore, a similar mechanism is proposed for the production of midbrain tissue from a thin strip of *Wnt1*$^{+ve}$ cells in caudal rhombomere1 (Zervas et al., 2004).

The second model of cerebellar growth is that rostral rhombomere 1 is an entirely distinct domain from the rest of the cerebellum, which is initially very small in comparison to the broad FGF-dependent domain of *Atoh1*. In this model FGF signalling from this domain causes proliferation of surrounding tissues and therefore contributes to the growth of the cerebellum. This model is more consistent with the apparent physical separation of the rostral *Atoh1*$^{+ve}$ domain and the cerebellar rhombic lip as the cerebellum grows.

Either model of FGF-directed growth could explain the specific loss of cerebellar vermis tissue in hypomorphic *Fgf8* or Sprouty-gain of function mutations in mice (Meyers et al., 1998; Chi et al., 2003; Basson et al., 2008). In these mice, vermal dysplasia would arise through the failure to generate (model 1) or sufficiently expand (model 2) the rostral region of vermal rhombic lip progenitors. A possible mechanism for this loss of cerebellar vermis was proposed to be the expansion of roofplate tissue at the expense of vermal progenitors by the loss of antagonism to BMP signalling (Basson et al., 2008). The mediolateral expansion of the cerebellar vermis in mice with conditional loss of Sprouty genes (which negatively regulate FGF signalling) is most consistent with a proliferative model of FGF in rostral rhombomere 1 (Yu et al., 2011).

A simple experiment might distinguish between these two growth models. By applying DiI at E4 to a discrete domain at the most anterior region of rhombomere 1, abutting the isthmus at the dorsal midline this anterior domain can be fate mapped, circumventing the problems of targeting the anterior *Atoh1*$^{+ve}$ domain by electroporation. For comparison, more caudal cerebellar rhombic lip can also be labelled to assess changes in the relative growth of different regions of the cerebellar primordium. **Figure 7-5 C** outlines the expected outcomes of this experiment with the two different models of cerebellar growth. In model 1, labelling at the isthmus would be expected to contribute to cells to the rhombic lip and migratory derivatives should be been throughout the newly generated region. In model 2, isthmic

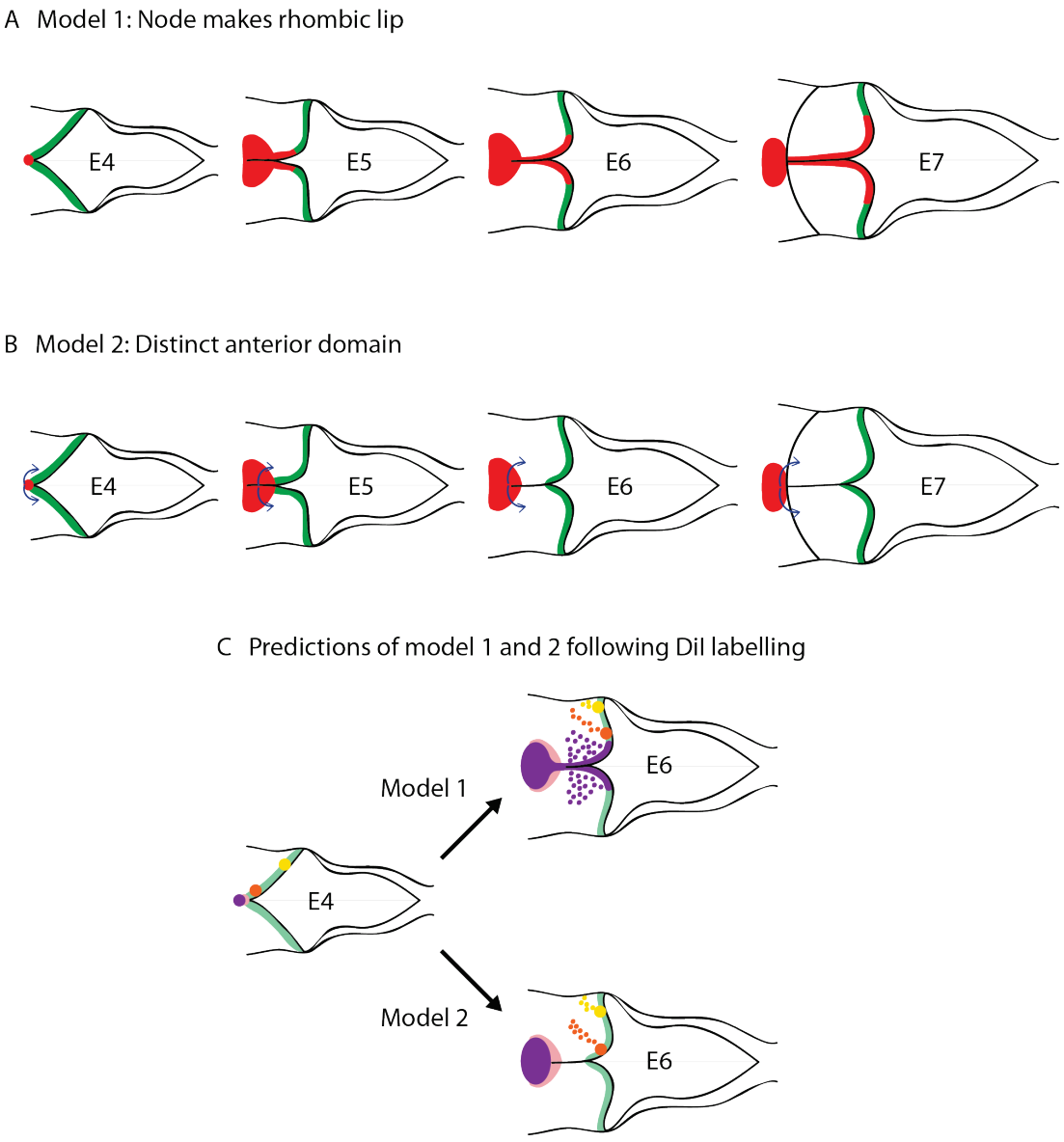

Figure 7-5 Models of cerebellar growth.

A,B) Two models of how growth from the rostral domain of *Atoh1* could be orchestrated. Model 1: suggests that FGF-dependent Atoh1 domain feeds cells into the rhombic lip as a node. Model 2: suggests that the FGF-dependent rostral domain signals to the surrounding tissues to direct growth. C) An experiment to test these model by discrete labelling of the rostral domain of rhombomere 1 and the expected outcomes with the two models.

labelling would be expected to remain in a discrete region in rostral rhombomere 1. Both models would see a caudal shift in rhombic lip DiI labelling but model 1 would predict a lateral shift of rhombic lip progenitors to accommodate the newly generated rhombic lip tissue.

7.7 Evolutionary significance of the FGF-dependent Atoh1^{+ve} domain.

Although not widely discussed, a rostral domain of *Atoh1* expresssion abutting the isthmus appears to be a feature that is conserved in a number of vertebrate embryos.

Teleost fish have a structure called the valvulus at the most anterior end of their cerebellum which produces cerebellar cells in the adult fish. Zebrafish have three *Atoh1* genes, *Atoh1a*, *Atoh1b* and *Atoh1c*. *Atoh1a*/b are expressed in the rhombic lip and presumptive valvulus at 2 days but by 4 days are expressed only in the presumptive valvulus. In contrast *Atoh1c* is not expressed in the presumptive valvulus and is expressed in the rhombic lip from 3 days (Chaplin et al., 2010) however *Atoh1c* expression is reported in the valvulus of adult fish (Kani et al., 2010). The valvulus is a cerebellar structure that is unique to fish and it is not known whether it has a dependence on FGF signalling for its development. However, the progression of *Atoh1* expression is strikingly similar to the two distinct domain of *Atoh1* identified in chick.

Xenopus laevis tadpoles, like chick embryos, have a domain of *Atoh1* expression at the most anterior region of rhombomere 1 which is separate from expression at the rhombic lip. Similarly to chick, *Lhx9* is expressed in a domain either side of this rostral *Atoh1* domain. (Thomas Butts, unpublished observations). It is not known whether this domain is dependent on FGF signalling.

In mice, a distinct domain of *Atoh1* expression in dorsal rhombomere 1 abutting the isthmus has been reported at E14.5 (Louvi et al., 2003). However, no further details were investigated and no other studies have recognised such a domain. Alternatively, it is possible that the most anterior region of the cerebellar rhombic lip (which generates the cerebellar vermis (Sgaier et al., 2005)) may be of equivalence to the rostral *Atoh1* domain of chick. The rostral region of rhombic lip, abuts the isthmus at E13.5 (prior to midline fusion) (Louvi et al., 2003) and is sensitive to the loss of FGF signalling prior to E10.5 (Sato and Joyner, 2009), demonstrated by the loss of tissue derived from this region (the vermis) of rhombic lip following loss of FGF signalling.

In order to establish whether, evolutionarily, the rostral domain of rhombomere 1 is co-opted into the cerebellum, it will be important to study the fate of this region of tissue across different species. In mouse, the region of tissue between the caudal extent of the cerebellum and the inferior colliculus at the dorsal midline has no neurons and becomes the acellular medullary velum (Louvi et al., 2003). In chick, which lacks an overt inferior colliculus, the presence of *Lhx9* and *Atoh1* expression suggest, at least between E5 and E10, the presence of neurons in this region.

The models and questions arising from the identification of a distinct rostral domain of *Atoh1*, highlight the need for accurate fate mapping to interpret functional data. The need to understand when and where neurons are born remains an essential prerequisite to mechanistic questions of how development is organised.

Chapter 8 Materials and Methods

8.1 Common solutions

ddH_2O	double-distilled H_2O. Autoclave.
PBS	phosphate buffered saline (Oxoid). Autoclave.
PFA	4% paraformaldehyde (Sigma) in PBS.
PBSTr	PBS with 1% Triton-X 100 (VWR)
PBTw	PBS with 0.1% Tween-20 (Sigma).
Tris-HCL	Trizma base, minimum (Sigma) in ddH_2O. pH to desired pH with 2M HCl. Autoclave.
20x SSC (pH 4.5)	3M NaCl (BDH), 0.3M sodium citrate (Fisher Scientific). pH using 5M citric acid. Autoclave.
5x MAB pH7.5	500mM maleic acid (Sigma), 750mM NaCl (BDH). pH using 2M NaOH. Autoclave.
MABT	1xMAB with 0.1% Tween-20 (Sigma).
10% BBR	Boehringer Blocking Reagent (Boehringer) dissolved in 1x MAB.
Detergent mix	1% IGEPAL CA-630 (Sigma), 1% SDS (Sigma), 0.5% deoxycholate (Fluka), 50mM Tris-HCL (pH8), 1mM EDTA (Ambion), 150mM NaCl (BDH).

Whole-mount hybridisation buffer	50% formamide (Sigma), 5x SSC (pH4.5), 2% SDS (Sigma), 2% BBR.
Solution X	50% formamide (Sigma), 2x SSC (pH4.5), 1% SDS (Sigma).
Heat-inactivated sheep serum	Sheep Serum (Sigma) heated to 56°C for 30 min.
Blocking solution	2% Boehringer Blocking Reagent, 20% heat-inactivated sheep serum in MABT. (filtered with Whatman filter paper for use on cryostat section)
Whole-mount pH 8 NTMT	100mM NaCl (BDH), 100mM Tris-HCL (pH8), 50mM $MgCl_2$ (BDH), 1% Tween-20 (Sigma). Made up on the day it was to be used.
Whole-mount pH 9.5 NTMT	100mM NaCl (BDH), 100mM Tris-HCL (pH9.5), 50mM $MgCl_2$ (BDH), 1% Tween-20 (Sigma). Made up on the day it was to be used.
10x Salts	114g NaCl (BDH), 14.04g Trizma ® HCL (Sigma), 1.34g Trizma ® base minimum (Sigma), 7.1g $NaH_2PO_4.2H_2O$ (BDH), 0.5M EDTA (Sigma) in 1L ddH_2O.
Cryostat hybridisation buffer	1x Salts, 50% formamide (Sigma), 10% dextran sulphate (Fluka), 250µg/ml Yeast tRNA (Ambion), 1x Denhardt's (Fluka).
Cryostat washing solution	1x SSC pH7 (Sigma), 50% formamide (Sigma) 0.1% Tween-20 (Sigma).

Cryostat pH 9.5 NTMT	100mM NaCl (BDH), 100mM Tris-HCL (pH9.5), 50mM $MgCl_2$ (BDH), 0.1% Tween-20 (Sigma). Made up on the day it was to be used.
X-gal base solution	10mM Tris-HCL (pH7.3), 0.005% Na-deoxycholate (Sigma), 0.01% IPEGAL (Sigma), 5mM $K_4Fe(CN)_6$ (Sigma), 5mM $K_3Fe(CN)_6$ (Sigma), 2mM $MgCl_2$ (Sigma) in PBS
Tyrodes	137.0mM NaCl (BDH), 2.7mM KCl (Sigma), 2.4mM $CaCl_2$ (Sigma), 2.1mM $MgCl_2.6H_2O$ (BDH), 0.4mM $NaH_2PO_4.2H_2O$ (BDH), 5.6mM glucose (Sigma). Autoclave. Before use add 100U/ml penicillin, 100µg/ml streptomycin, 0.3 µg/ml Fungizone (Gibco).
Culture medium	Basal Medium Eagle (Gibco) supplemented with 0.5% D-(+)-glucose (Sigma), 1x B27 NeuroMix (PAA Laboratories Ltd.), 2mM L-Glutamine (Sigma), 100U/ml penicillin, 100µg/ml streptomycin, 0.25 µg/ml Fungizone® (Gibco).
10x MEMFA salts	1M MOPS (Sigma), 20mM EGTA (Sigma), 10mM $MgSO_4$ (Sigma) solution. pH to 7.4 using NaOH pellets (BDH). Autoclave and store in dark.
MEMFA	1x MEMFA salts, 3.7% formaldehyde (Sigma).

8.2 Molecular techniques

8.2.1 Amplification of DNA constructs

DNA solutions were transformed into Subcloning Efficiency 5-alpha competent *E. coli* (NEB) according the manufacturer's instructions. Transformed cells were plated out on appropriately selective LB agar (Sigma) plates and grown overnight at 37°C. Individual colonies were picked to inoculate 50-150ml of appropriately selective LB (sigma) and grown overnight at 37°C, shaking at 213rpm. DNA was purified from cultures using QIAfilter

Plasmid Maxi Kit (Qiagen) for electroporation constructs or QIAfilter Plasmid Midi Ki (Qiagen) for *in situ* hybridisation plasmids according the manufacturer's instructions.

8.2.2 Generation of antisense riboprobes for *in situ* hybridisation

DNA *in situ* plasmids (Appendix C) were linearised with the appropriate restriction enzyme (Roche) by incubating 10ug DNA with 10U of enzyme in a 30µl volume with the appropriate concentration of buffer for 2 hours at 37°C for 2 hours. Linearised DNA was purified using an illustra GFX PCR DNA and Gel Band purification kit (GE Healthcare) according the manufacturer's instructions. 1µg of linearised DNA was then mixed with 30U of the appropriate RNA polymerase (Roche) in a 20µl volume with 1x transcription buffer (Roche), 20U Protector RNase inhibitor (Roche) and either 1x DIG RNA labelling mix (Roche) or 1x fluorescein RNA labelling mix (Roche). Reaction was incubated for 4 hours at 37°C before adding 2µl DNase 1 (Roche) and incubating for a further 30 minutes. The reaction was diluted to a volume of 50µl and the riboprobe was purified using illusta Microspin G50 Columns (GE Healthcare). Fluorescein-labelled ribroprobes were purified twice to improve the signal during *in situ* hybridisation. Reactions were checked by running 2µl of the reaction diluted with 6 µl ddH_2O and 2µl 5x DNA loading buffer (Bioline) on a 1% agarose (Sigma) in TBE (Severn Biotech) gel stained with SYBR Safe DNA gel stain (Invitrogen) alongside 5µl Hyperladder 1 (Bioline). RNA concentration was quantified using a NanoVue Plus Spectrophotometer (GE Healthcare).

8.2.3 Generation of Math1-*mCherry* reporter construct.

Full length *mCherry* was amplified using primers designed to include restriction sites EcoR1 (forward) and HindIII (reverse). The forward primer used was: 5'GCGGCGGAATTCGCTGCCATGGTGAGCAAGGGCGAG 3' and the reverse primer used was: 5'GCGGCGAAGCTTGTCGACTTACTTGTACAGCTCGTC 3' (Primers ordered from Sigma). 0.5µl each of 10µM forward and reverse primers was mixed with 1µl DNA, 0.5µl dNTPs (NEB), 0.125µl Phusion® Taq polymerase (NEB) and 1x buffer (NEB) in a 25µl reaction. The following conditions were used for the PCR amplification: Template DNA was denatured by heating to 95°C for 2mins then 35 cycles of amplification (30sec at 95°C for denaturing, 30sec at 50°C for annealing, 1min at 72°C DNA extension) followed by 5mins at 72°C to ensure all DNA was fully extended. The PCR product mixed with 5µl 5x DNA loading buffer (Bioline) and run on a gel made from 1% agarose (Sigma) in TBE (Severn Biotech) stained with SYBR Safe DNA gel stain (Intirogen) alongside 5µl Hyperladder 1 (Bioline) (Hereafter described as "run on a 1% agarose gel"). A band of the

expected size (approximately 700bp) was seen and was cut out with a razor blade and the DNA was purified using illustra GFX PCR DNA and Gel Band purification kit (GE Healthcare) as per the manufacturer's instructions (hereafter described as "DNA was gel purified").

Both the purified PCR product and the Math1-LacZ reporter construct were digested with EcoR1 by incubating DNA (2µl vector or all PCR product) with 1µl EcoR1 (Roche) and 2.5µl BufferH (Roche) in a 25µl volume for 2 hours at 37°C. The DNA was gel purified, then digested in the same manner using the enzyme HindIII (Roche) and BufferB (Roche). The linearised products were run on a 1% agarose gel (*mCherry*) or a 0.7% agarose gel (vector). Bands of approximately 700bp for mCherry and 4.5kb for the vector (minus the 3kb *LacZ*) were cut with a razor blade and the DNA was gel purified.

mCherry and the vector were mixed in a ratio of 7:1 with 1µl T4 DNAligase (Roche) and 1µl ligation buffer (Roche) in a 10µl volume. The reaction was left at RT for 1 hour and then put at 4°C overnight. One shot Top10 chemically competent *E. Coli* (Invitrogen) were transformed with 5µl of the ligation reaction according to the manufacturer's instructions, and the resulting transformed cells were plated out on LB agar (Sigma) plates containing 100µg/ml ampicillin (Sigma) and grown overnight at 37°C. 24 colonies were picked and grown in 3ml LB (Sigma) containing 100µg/ml ampicillin (Sigma) overnight at 37°C shaking at 213rpm. DNA was purified from the cultures using a QIAprep Spin MiniPrep Kit (Qiagen) according to the manufacturer's instructions. A diagnostic sequential double digest with EcoR1 then HindIII was carried out using 5µl of each miniprep in the same manner as outlined for the digest above and linearised DNA was run on a 1% agarose gel. Six clones showed bands the correct size for the vector and insert and one was selected for sequencing (Eurofins). Sequencing confirmed thecorrect sequence of *mCherry* was successfully inserted into the correct position in the Math-reporter vector to replace *LacZ.*

8.3 Animals

8.3.1 Chicken embryos

Fertilised wild type eggs (Henry Stewart, UK) and GFP-transgenic eggs (Helen Sang, Roslin Institute) were incubated at 38°C for 2 to 10 days. For *in ovo* manipulations, eggs were windowed with sharp surgical scissors and closed with selotape after adding 0.5ml Tyrodes solution. Embryos were staged according to Hamburger and Hamilton (1951)(See Appendix A). Embryos were removed from windowed eggs using hooked forceps and ophthalmic scissors to cut membranes. From E7 heads of embryos were severed immediately upon

removal from egg and the bodies were discarded. Younger embryos were left intact to allow accurate staging. Intact heads or whole embryos were fixed overnight at 4°C in PFA or MEMFA. Embryos were stored in fix or transferred to PBS with 0.02% NaN_3 (Sodim Azide, Sigma). Sodium azide prevents bacterial growth during long-term storage.

8.3.2 Mouse embryos

Mouse embryos and postnatal dissected brains were obtained from Albert Basson and Rob Weschler-Reya, stored in PBS after fixation in PFA. Genotyping was completed before donation of the embryos by the respective labs.

8.4 *In ovo* electroporation

Eggs incubated at 38°C for 2-6 days were windowed and the vitelline membrane was removed using the point of a hypodermic needle. For E2 embryos is was occasionally necessary to inject the yolk underlying the embryo with Fount India ink (Pelikan) diluted 1 in 5 in Tyrodes to give visual contrast. DNA constructs (Listed in AppendixB) at 1-2µg/µl were mixed with trace amounts of fast green (Sigma) and injected into the lumen of the neural tube at hindbrain/midbrain level (E2 electroporations) or into the fourth ventricle, directly below the targeted region (E3-6 electroporations). Where two or more constructs were co-electroporated DNA was mixed in equal concentrations, to give a final concentration of 1-2 µg/µl for each construct. A negative electrode was placed to the left of the neural tube (at E3-E6 the electrode is hooked underneath the embryo) and a positive electrode was placed to the right of the neural tube to target a specific region, ie the cerebellar rhombic lip. Three 50 ms/10 V square waveform electrical pulses were passed between electrodes so that DNA entered the right side of the neural tube. Eggs were then sealed and incubated at 38°C until the embryos were harvested and fixed overnight at 4°C in PFA or MEMFA (used only following RFP electroporation).

When two electroporations in different positions were performed in the same embryo, the first construct was injected and a current passed then the second construct was injected at a different position and another current was passed with the positive electrode aimed at the different region.

8.5 Explant cultures

Embryos were incubated at 38°C for 3-5 days and immediately, upon removal from the egg to a dish of Tyrodes solution, the hindbrain and midbrain tissue was dissected from the head using ridged forceps (Fine Science Tools) and Lumsden bioscissors (Fine Science Tools). In

E3 embryos the roofplate tissue was kept intact with the hindbrain tissue but in E4 and E6 embryos the roofplate tissue was removed upon dissection. Brains were dissected along the dorsal midline and midbrain tissue was removed unilaterally (or bilaterally in GFP co-cultures) at the level of the isthmus. 0.4µm culture plate inserts (Millicel – CM, Millipore) were placed in 60mm tissue culture dishes (Nunc) containing 3ml of culture medium pre-warmed to 37°C and dissected tissue was positioned on the membrane of the inserts with ventricular surface of the tissue facing down in contact with the membrane. Explants were cultured for 2 days at 37°C with 6% CO_2 in a Sanyo CO_2 incubator, then fixed by replacing the 3ml slice media with 3ml 4% PFA and leaving the plates for 30 minutes at room temperature. 4% PFA was then applied directly to the explant tissue and left for a further 30 minutes at room temperature. The Millipore inserts were transferred to 6 well plates (Nunc) with fresh PFA and fixed overnight at 4°C, ready for *in situ* hybridisation.

For co-cultures, dorsal midbrain tissue from stage-matched *gfp*-transgenic chicken embryos was dissected in Tyrodes solution, removing the dorsal midline, isthmic and most posterior tissue. GFP^{+ve} midbrain tissue was then co-cultured abutting the dissected hindbrain tissue. The midbrain tissue was very slightly overlaid on the midbrain tissue to ensure the tissues did not retract away from each other during the culture process.

8.6 Microsurgical grafting

The hindbrain was dissected from heads of E4,5 or 6 *gfp*-transgenic embryos in Tyrodes, immediately after removal from the egg. Roofplate tissue was removed from the hindbrain and small strips of tissue from the rostral and caudal part of the cerebellar rhombic lip (excluding region where the cerebellum is joined at the midline in E5 and E6 embryos) on both sides of the hindbrain were removed using a flame-sharpened 0.1mm tungsten wire and transferred to separate dishes with fresh Tyrodes using a goat serum coated pipette tip. Using tungsten wire the strips of rhombic lip tissue were cut into small fragments. Wild type host embryos incubated for 2 days at 38°C to St10 were windowed and the yolk underlying the embryos was injected with Fount India ink (Pelikan) diluted 1 in 5 in Tyrodes. 0.5ml Tyrodes solution was added before microsurgery so that the grafted tissue was not disturbed later. A small window was made in the vitelline membrane over the hindbrain using the point of a hypodermic needle and then a small piece of tissue, corresponding to the size of the GFP^{+ve} fragments dissected, was removed from dorsal rhombomere 3 on the right side of the embryo. GFP^{+ve} rhombic lip fragments were then transferred to the host egg using a goat serum-coated pipette tip and positioned, into the space created by removal of wild type tissue, using the tungsten wire. Eggs were sealed and incubated for 2 days before harvesting and fixing in PFA.

8.7 *In ovo* pharmacological injections.

3,3′,5-Triiodo-L-thyronine (T3, Sigma) was dissolved in high pH saline and diluted to the appropriate concentration for injection. Amiodarone (Sigma) was dissolved in DMSO (Sigma) to make a 1mM stock solution. Methimazole (Sigma) was dissolved in Tyrodes solution. Stock solutions of amiodarone and methimazole were mixed and diluted in Tyrodes solution to the appropriate concentration for injection. Drugs were mixed with trace amounts of fast green (Sigma) and 5µl was injected into the bloodstream by targeting an artery overlying the yolk. Alternatively drugs were injected directly into the fourth ventricle, filling the ventricle. 0.5ml of Tyrodes was added, eggs were sealed and incubated for a further 1-3 days before harvesting and fixing in PFA.

8.8 Histological techniques

8.8.1 Sectioning

8.8.1.1 Vibratome sectioning

Following *in situ* hybridisation embryos were washed in PBS 3 times for 10 minutes and placed into pre-warmed 20% gelatine (Fluka) in PBS at 65°C for 1 hour. Embryos were transferred to fresh pre-warmed 20% gelatine in PBS in moulds and orientated appropriately before allowing gelatine to set by cooling the mould in an ice bath. Once set, gelatine blocks were cooled for a further 30mins at 4°C and then removed from moulds and cut using a razor blade into blocks appropriate for sectioning. Blocks were fixed in PFA overnight at 4°C.

To section, blocks were washed in PBS three times for 10mins, dried slightly with tissue and glued with superglue to the chuck of a vibratome (Leica VT1000S). The block was submerged in PBS and 50µm sections were cut and mounted under a coverslip on twin-frost glass slides using 90% glycerol (MP) in PBS. Slides were sealed using nail varnish.

8.8.1.2 Cyrostat sectioning

Mouse embryos/brains, stored in PBS post fixation, were dissected (if required) and washed in PBS three times for 10 minutes. Tissue was perfused with 10% sucrose (sigma) in PBS for 1 hour, then 20% sucrose in PBS for 1 hour and finally 30% sucrose in PBS overnight at 4°C. Tissue was perfused with OCT compound (VWR) for 1 hour at RT before being transferred to fresh OCT compound in moulds. Tissue was orientated appropriately and blocks were frozen by placing the mould into a foil boat floating on liquid nitrogen. Blocks were stored at -80°C until required.

To section blocks were placed in the cryostat chamber for 30mins to raise their temperature prior to mounting on cryostat chuck using OCT compound. 20µm sections were cut using with the cryostat (Zeiss Microm HM 560) and collected on SuperFrost® Plus slides (VWR). Sections were left to dry at RT for 2 hours and stored at -80°C until needed.

8.8.2 RNA *in situ* hybridisation

8.8.2.1 Whole-mount *in situ* hybridisation

Post-fixation embryos were dissected for *in situ* hybridisation by either removal of the midbrain/hindbrain tissue from the embryo or, where younger, whole embryos or heads were used, a hole was made in the dorsal midline of the forebrain, midbrain and hindbrain to prevent riboprobe or antibody trapping. Tissue was washed twice in PBSTw for 10mins and was then gradually dehydrated by washing for 5mins in 25%, 50% then 75% methanol in PBSTw and then twice for 5 mins in 100% methanol. Tissue was bleached for 1hr at RT in 1.8% H_2O_2 (Sigma) in methanol, washed twice for 5mins in 100%methanol and gradually rehydrated by washing for 5mins in 75%, 50% then 25% methanol in PBSTw. Tissue was washed a further three times for 5mins with PBSTw before two 20min washes with detergent mix and 20mins fixation in PFA. PFA was washed off with two 5min washes and then tissue was incubated at 70°C in pre-warmed hybridisation buffer for 1-4hours. 1µg/ml of DIG-labelled riboprobe (with 1ug/ml Fluorescein-labelled riboprobe for double *in situ* hybridisation) was added to fresh pre-warmed hybridisation buffer and incubated for 10mins at 70°C before tissue was hybridised with this solution overnight at 70°C. After hybridisation, tissue was washed in pre-warmed solution X at 70ºC twice for 5mins, then twice for 30mins before five 5min and two 30min washes in MABT at room temperature. Tissue was placed in blocking solution for 1-2hrs and incubated overnight at 4°C with alkaline phosphatase-conjugated anti-DIG antibody (Roche) diluted 1:2000 in blocking solution. Tissue was washed in MABT three times for 5mins, twice for 1hr and then overnight at 4°C. Tissue was washed for 10mins in pH9.5 NTMT and blue signal was developed to detect DIG-labelled probes using 5µl/ml NBT/BCIP (Roche) in pH9.5 NTMT at RT in the dark. Staining solution was replaced every 4-5hrs. If colour reaction progressed for longer than a day, tissue was stored in MABT overnight at 4°C and continued the following day. When the appropriate level of staining was achieved tissue was washed for 5mins in MABT then twice for 10mins in PBSTw. For single *in situ* hybridisation, tissue was then fixed in PFA overnight at 4°C and stored in PBS with 0.02%NaN_3.

For double *in situ* hybridisation, after the blue signal was developed and tissue was washed in MABT and PBSTw, the tissue was treated with 5mM EDTA in PBS for 1hr at 70°C to

denature the alkaline phosphatase-conjugated anti-DIG antibody. Tissue was washed twice in PBS for 5mins and then fixed overnight in PFA at 4°C. Tissue was washed three times in MABT for 5mins before 1-2 hours in blocking solution and overnight incubation at 4°C with alkaline phosphatase-conjugated anti-fluorescein antibody (Roche) diluted 1:2000 in blocking solution. Tissue was washed in MABT three times for 5mins, twice for 1hr, then overnight at 4°C and 10mins in pH8 NTMT. Red signal was developed at 4°C using a filtered (0.2µm syringe filter) solution of 1 tablet of Fast-red (Roche) dissolved in 10ml pH8 NTMT which was replaced every 4-5 hours (storing in MABT overnight if required). When the red signal had fully developed tissue was washed for 5mins in MABT, twice for 10mins in PBSTw, fixed overnight at 4°C and stored in PBS with 0.02%NaN_3.

8.8.2.2 Whole-mount *in situ* hybridisation on cultured explants

Tissue from cultured explants was processed for *in situ* hybridisation in the same manner as whole embryos or dissected brains except tissue was left attached to culture plate inserts until after solution X washes at 70°C. After this, tissue was removed from the culture insets to allow for more stringent washing. Hybridising tissue attached to the culture membranes prevented damage to the very fragile tissue.

8.8.2.3 *In situ* hybridisation on cryostat sections

Slides were defrosted for 2hrs at RT and washed for 10mins in PBS to remove OCT compound. 1ug/ml DIG-labelled riboprobe in cryostat hybridisation buffer was denatured at 70°C for 5mins and 200µl was added to each slide (after slides were dried around the sections with tissue). A coverslip was put on each side and slides were incubated overnight at 65°C in a sealed box containing paper wetted with cryostat washing solution. Slides were washed once for 15mins (to remove coverslips) and twice for 30mins at 65°C with pre-warmed washing solution followed by three 10min washes at RT with MATB. Slides, dried with tissue, were then covered with 400µl/slide filtered blocking solution for 1hr at RT. Block was removed and replaced with 250-400µl filtered blocking solution with 1:2000 dilution of alkaline phosphatase-conjugated anti-DIG antibody (Roche) and incubated overnight at 4°C in a humidified box. Slides were washed three times for 10mins in MABT and blue colour was developed by adding 400µl of cryostat pH9.5NTMT with 20µl/ml NBT/BCIP (Roche) to each slide. The colour reaction was developed in a dark, humidified box and, when complete, slides were washed twice for 10mins with 0.25%Triton-X +2mM EDTA in PBS to terminate the reaction. Slides were mounted with coverslips using 90% glycerol (MP) in PBS and sealed with nail varnish.

8.8.3 Whole-mount immunohistochemical staining

Post-fixation, tissue is washed three times for 10mins with PBSTr then three times for 1hr with 5% neonatal calf serum (NCS, Sigma) in PBSTr. Tissue was then incubated for 2-3 nights at 4°C with 1:100 dilution of rabbit anti-GFP,IgG (Invitrogen) in 5%NCS 0.02%NaN_3 PBSTr. Primary antibody was retained and used a total of three times. Tissue was washed three times for 5mins and four times for 30mins with 1% goat serum (Sigma) in PBSTr before overnight incubation at 4°C with secondary antibody, Alexa Fluor 488-conjucated goat anti-rabit IgG (1:1000; Invitrogen) with 1% goat serum in PBSTr. Secondary antibody was washed off with three 5min washes followed by four 30min washed in 1% goat serum in PBSTr. Tissue was then fixed overnight at 4°C in PFA.

8.8.4 LacZ staining

The hindbrain was dissected from embryos for LacZ staining prior to fixation. Hindbrain tissue was then short fixed for 20mins in PFA at RT and washed three times for 5mins with PBS. Tissue was incubated in the dark at 37°C in a solution of 1.25mg/ml X-gal (1:80 dilution from 100mg/ml stock solution in DMF) in X-gal base solution until the stain has appropriately developed. Tissue was then washed three times for 5mins in PBS and fixed in PFA overnight at 4°C.

8.9 Imaging

Low magnification pictures of whole mount or hemisected embryos or dissected brains were captured using a Zeiss dissecting scope fitted with an OlympusDP70 digital camera or a Leica stereoscope fitted with a Q-imaging Retiga EXi camera. Embryos were photographed in PBS in sylgard-coated dishes and insect pins were used to orientate some embryos correctly.

Hindbrains dissected in PBS were flat-mounted by cutting along the dorsal midline of the tissue and mounting brains pial-side up on twinfrost glass slides. Hemisected brains were cut along the dorsal and ventral midline and both halves were mounted pial-side. Silicon grease (RS) was used to support a coverslip and tissues were mounted in 90% glycerol (MP) in PBS.

Low magnification images of mounted brains or vibratome sections were photographed using Leica stereoscope fitted with a Q-imaging Retiga EXi camera. High magnification images of mounted brains or cyrosections were photographed with a Nikon DS-Ri1 camera fitted to a Nikon Elipse80i compound microscrope.

Confocal stacks were collected using an Olympus Fluoview AX70 and images shown are projections of z-stacks compiled in ImageJ. Optical sections in z-stacks were taken at 10µm intervals.

All images were processed using Photoshop CS5.1 (Adobe).

Appendix A

Relationship between embryonic day (E) and Hamburger and Hamilton (1951) stages (st).

Embryonic day	Hamburger and Hamilton stages	Defining features
E2	St10 – St13	Number of somites/shape of neural tube
E2.5	St14 – St15	Angle between head and trunk
E3	St16 – St19	Angle between head and trunk
E4	St20 – St24	Shape of forelimb/ eye pigmentation
E4.5	St25	Shape of forelimb
E5	St26 – St27	Shape of forelimb
E6	St28 – St29	Shape of forelimb
E7	St30 - St31	Appearance of egg tooth / number scleral papillae
E7.5	St32-33	Number scleral papillae
E8	St34	Shape of eye/eyelid
E9	St35	Shape of eye/eyelid
E10	St36	Shape of eye/eyelid

Appendix B

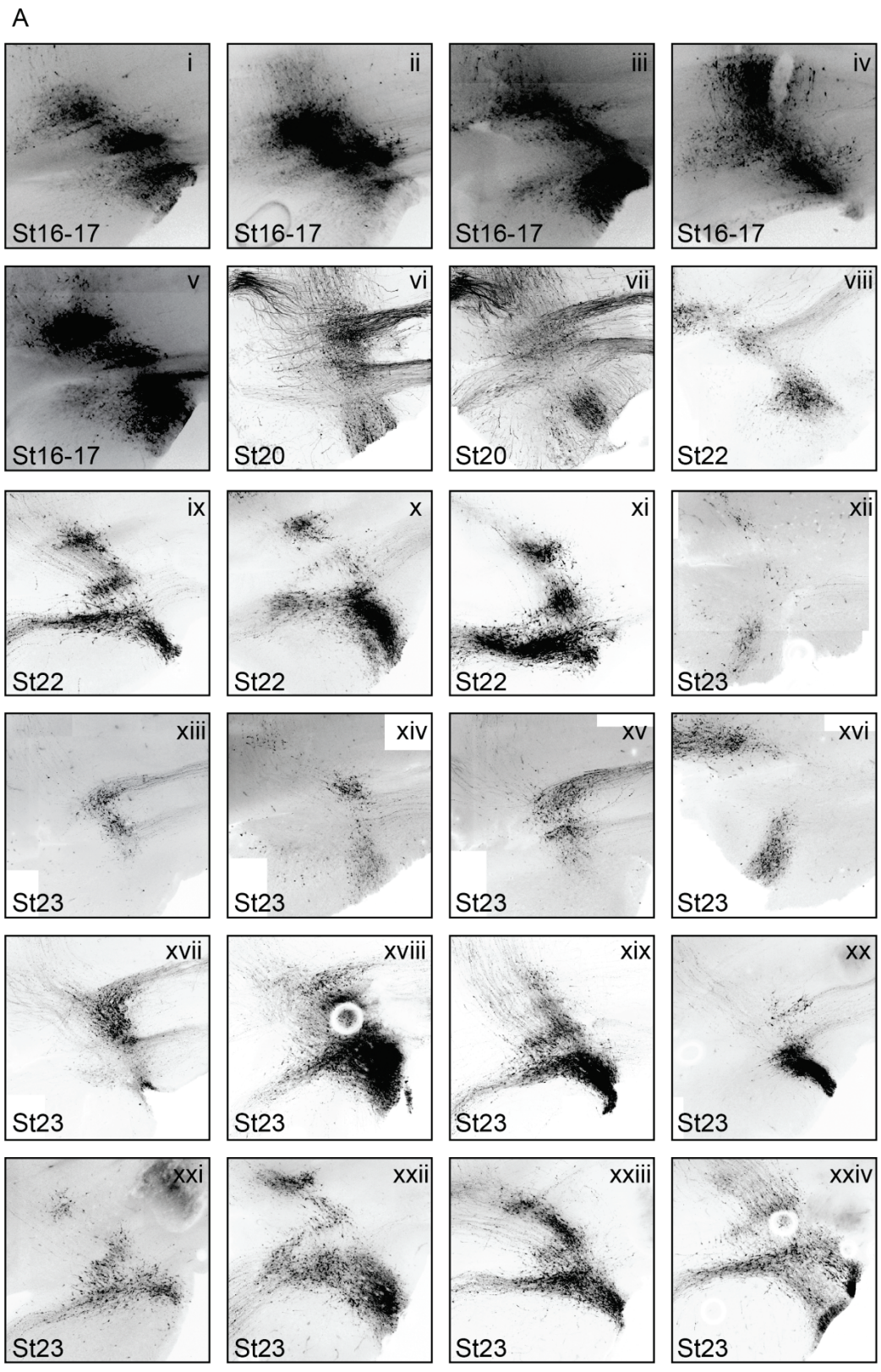
A
i
St16-17
ii
St16-17
iii
St16-17
iv
St16-17
v
St16-17
vi
St20
vii
St20
viii
St22
ix
St22
x
St22
xi
St22
xii
St23
xiii
St23
xiv
St23
xv
St23
xvi
St23
xvii
St23
xviii
St23
xix
St23
xx
St23
xxi
St23
xxii
St23
xxiii
St23
xxiv
St23

B

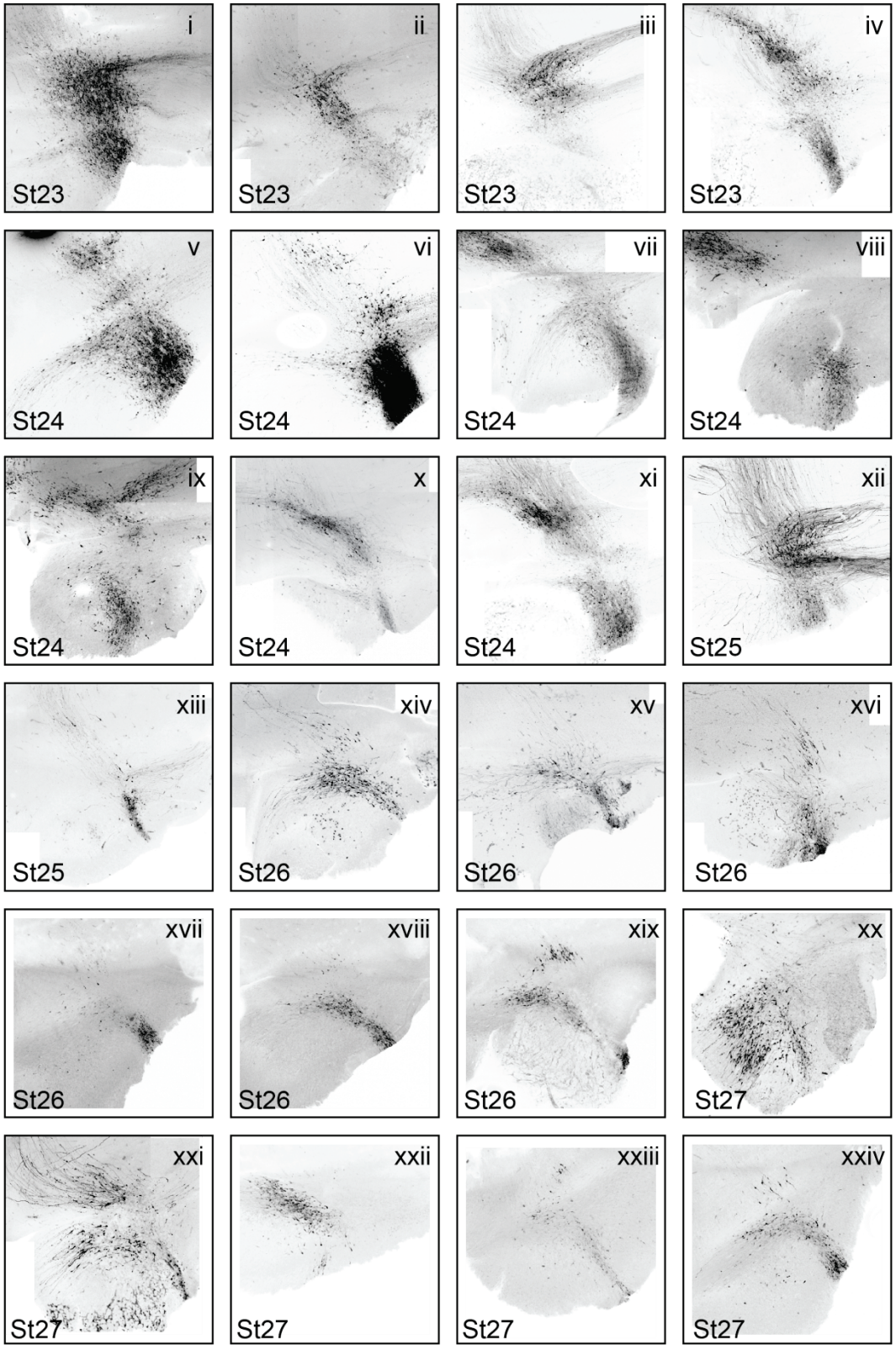
i
St23
ii
St23
iii
St23
iv
St23
v
St24
vi
St24
vii
St24
viii
St24
ix
St24
x
St24
xi
St24
xii
St25
xiii
St25
xiv
St26
xv
St26
xvi
St26
xvii
St26
xviii
St26
xix
St26
xx
St27
xxi
St27
xxii
St27
xxiii
St27
xxiv
St27

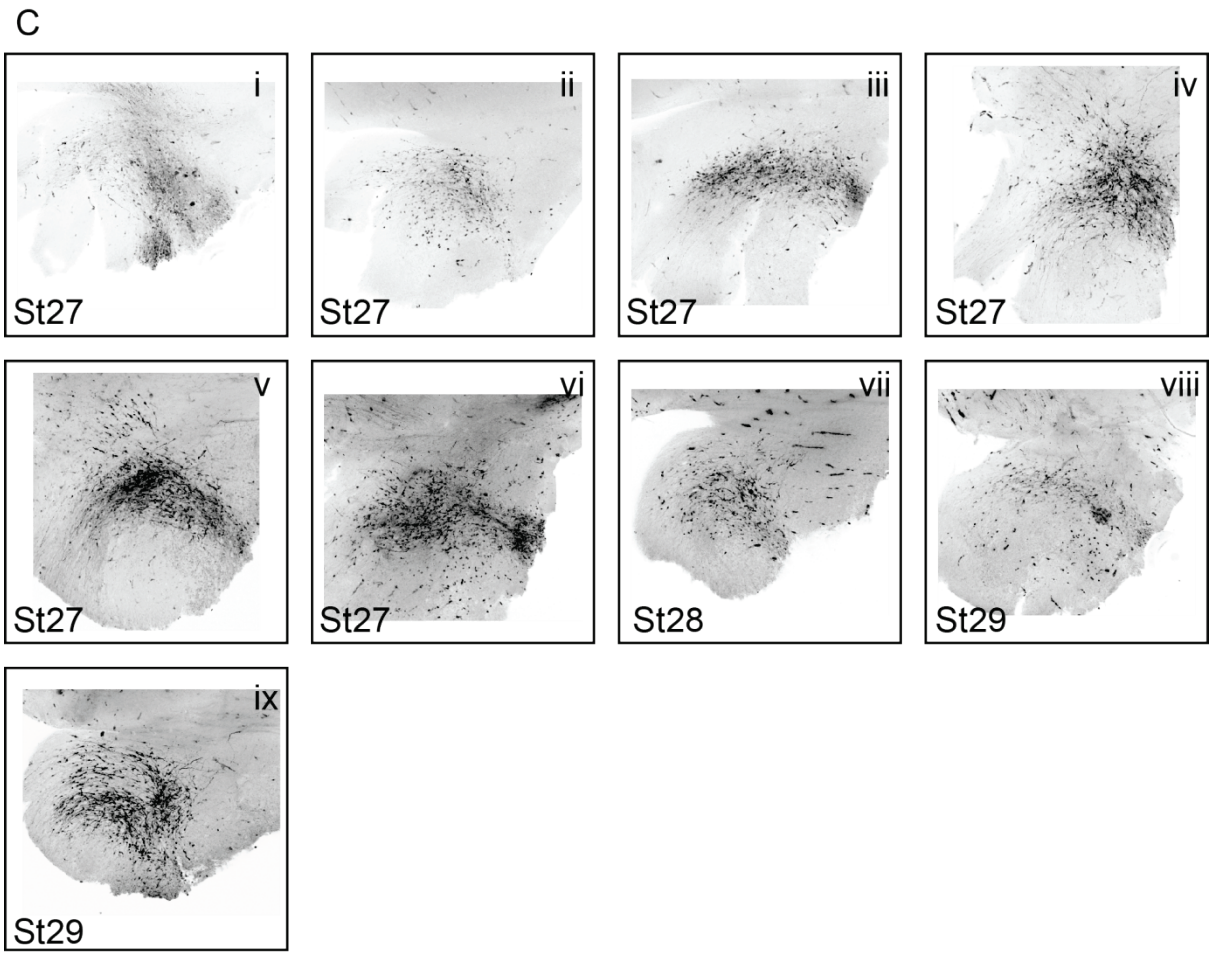

Collection of all St16-St29 cerebellar rhombic lip electroporations, fixed at E7 from composite projections of confocal Z-stacks. (see **Figure 2-1**)

Appendix C

List of DNA constructs used in electroporation studies.

Electroporation construct	Reference
pCAβ-*GFP*	pCAβ-*eGFPm5* (Yaneza et al., 2002)
pCX-Cre	Morin et al. (2007)
pFlox-pA-EGFP	Morin et al. (2007) (“Stop-GFP”)
MATH1-LacZ	(Helms et al., 2000)
MATH1-mCherry	This study
pCAβ-*Otx2*IRES*egfp*	Robin Golgoi, Antonio Simeone (unpublished)
pEFX-*Fgf8b*	Toyoda et al. (2010)
pEFX-dnfgfr3c	Toyoda et al. (2010)
pCAβ-*RFP*	Wingate lab (unpublished).

Appendix D

Plasmids for the generation of RNA *in situ* hybridisation riboprobes:

Chick probes	For antisense riboprobe:		
Gene	Cut:	Transcribe with:	Obtained from/ Reference
Cath1	NotI	T3	Wilson and Wingate (2006)
Fgf8	BamHI	T7	Chambers and Mason (2000)
Gbx2	BglII	T3	Kiecker and Lumsden (2004)
Lhx9	SpeI	T7	Alessio Delogu
NeuroD1	SacI	T3	Thomas Butts
Otx2	NotI	T7	Millet et al. (1996)
Pax6	EcoRI	T7	Martyn Goulding (unpublished)
Sprouty2	KpnI	T3	Chambers and Mason (2000)
Tbr1	BamHI	T7	Puelles et al. (2000)
Wnt1	EcoRI	T7	Hollyday et al. (1995)
Mouse Probes	For antisense riboprobe:		
Gene	Cut:	Transcribe with:	Obtained from/ Reference
Lhx9	EcoR1	T3	Alessio Delogu
Math1	Kpn1	T3	Albert Basson
Tbr1	Sal1	T7	Alessio Delogu

Appendix E

Full list of numbers of heterochronic-heterotopic grafts (See **figure 5-3 / table 5-1**)

Date	Donor	A	B	B+C	C	D	E	n
24.4.10	29 Rostral				1	2	3	5
	29 Caudal				5			5
23.4.10	26 Rostral			1		1	2	4
	26 Caudal					1	2	3
15.4.10	26 Rostral			1		2	2	5
	26 Caudal			1		2	1	4
21.4.10	24 Rostral	1	1			2		4
	24 Caudal		2			1	1	4
14.4.10	22 Rostral	2						2
	22 Caudal		7					7
11.9.10	22 Rostral	7					3	10
	22 Caudal		1				2	3
12.9.10	26 Rostral		2	1		1	2	6
	26 Caudal		1	2		2	1	6
10.9.10	29 Rostral				3		2	5
	29 Caudal				6*	1		7

15.9.10	23 Rostral	5*				1		6
	23 Caudal		4*					4
16.9.10	26 Rostral			4*			1	5
	26 Caudal			1			1	2
18.9.10	29 Rostral				4		2	6
	29 Caudal				4	2	2	8
22.9.10	24 Rostral						2	2
	24 Caudal		1				4	5
23.9.10	26 Caudal						1	1
24.9.10	29 Rostral				1		2	3
	29 Caudal						2	2

A = ventral axons

B = midline axons

C = dorsal axons

D = no axons (discounted)

E = incorrect position of grafted tissue (discounted)

* = example shown in figure 5-3

Bibliography

Acampora D, Avantaggiato V, Tuorto F, Simeone A (1997) Genetic control of brain morphogenesis through Otx gene dosage requirement. Development 124:3639-3650.

Acampora D, Mazan S, Lallemand Y, Avantaggiato V, Maury M, Simeone A, Brulet P (1995) Forebrain and midbrain regions are deleted in Otx2-/- mutants due to a defective anterior neuroectoderm specification during gastrulation. Development 121:3279-3290.

Akazawa C, Ishibashi M, Shimizu C, Nakanishi S, Kageyama R (1995) A mammalian helix-loop-helix factor structurally related to the product of Drosophila proneural gene atonal is a positive transcriptional regulator expressed in the developing nervous system. The Journal of biological chemistry 270:8730-8738.

Albus JS (1971) A theory of cerebellar function. Mathematical biosciences 10:25-61.

Alder J, Cho NK, Hatten ME (1996) Embryonic precursor cells from the rhombic lip are specified to a cerebellar granule neuron identity. Neuron 17:389-399.

Alder J, Lee KJ, Jessell TM, Hatten ME (1999) Generation of cerebellar granule neurons in vivo by transplantation of BMP-treated neural progenitor cells. Nature neuroscience 2:535-540.

Alexandre P, Wassef M (2003) The isthmic organizer links anteroposterior and dorsoventral patterning in the mid/hindbrain by generating roof plate structures. Development 130:5331-5338.

Altman J, Bayer SA (1978) Prenatal development of the cerebellar system in the rat. I. Cytogenesis and histogenesis of the deep nuclei and the cortex of the cerebellum. The Journal of comparative neurology 179:23-48.

Altman J, Bayer SA (1985a) Embryonic development of the rat cerebellum. I. Delineation of the cerebellar primordium and early cell movements. The Journal of comparative neurology 231:1-26.

Altman J, Bayer SA (1985b) Embryonic development of the rat cerebellum. II. Translocation and regional distribution of the deep neurons. The Journal of comparative neurology 231:27-41.

Apps R, Garwicz M (2005) Anatomical and physiological foundations of cerebellar information processing. Nature reviews Neuroscience 6:297-311.

Arends JJ, Zeigler HP (1991a) Organization of the cerebellum in the pigeon (Columba livia): II. Projections of the cerebellar nuclei. The Journal of comparative neurology 306:245-272.

Arends JJ, Zeigler HP (1991b) Organization of the cerebellum in the pigeon (Columba livia): I. Corticonuclear and corticovestibular connections. The Journal of comparative neurology 306:221-244.

Aroca P, Lorente-Canovas B, Mateos FR, Puelles L (2006) Locus coeruleus neurons originate in alar rhombomere 1 and migrate into the basal plate: Studies in chick and mouse embryos. The Journal of comparative neurology 496:802-818.

Avraham O, Hadas Y, Vald L, Zisman S, Schejter A, Visel A, Klar A (2009) Transcriptional control of axonal guidance and sorting in dorsal interneurons by the Lim-HD proteins Lhx9 and Lhx1. Neural development 4:21.

Basson MA, Echevarria D, Ahn CP, Sudarov A, Joyner AL, Mason IJ, Martinez S, Martin GR (2008) Specific regions within the embryonic midbrain and

cerebellum require different levels of FGF signaling during development. Development 135:889-898.
Baumgardt M, Karlsson D, Terriente J, Diaz-Benjumea FJ, Thor S (2009) Neuronal subtype specification within a lineage by opposing temporal feed-forward loops. Cell 139:969-982.
Belliveau MJ, Cepko CL (1999) Extrinsic and intrinsic factors control the genesis of amacrine and cone cells in the rat retina. Development 126:555-566.
Belliveau MJ, Young TL, Cepko CL (2000) Late retinal progenitor cells show intrinsic limitations in the production of cell types and the kinetics of opsin synthesis. The Journal of neuroscience : the official journal of the Society for Neuroscience 20:2247-2254.
Ben-Arie N, Bellen HJ, Armstrong DL, McCall AE, Gordadze PR, Guo Q, Matzuk MM, Zoghbi HY (1997) Math1 is essential for genesis of cerebellar granule neurons. Nature 390:169-172.
Bermingham NA, Hassan BA, Wang VY, Fernandez M, Banfi S, Bellen HJ, Fritzsch B, Zoghbi HY (2001) Proprioceptor pathway development is dependent on Math1. Neuron 30:411-422.
Berry M, Rogers AW (1965) The migration of neuroblasts in the developing cerebral cortex. Journal of anatomy 99:691-709.
Berry M, Rogers AW, Eayrs JT (1964) Pattern of Cell Migration During Cortical Histogenesis. Nature 203:591-593.
Bertrand N, Castro DS, Guillemot F (2002) Proneural genes and the specification of neural cell types. Nature reviews Neuroscience 3:517-530.
Blak AA, Naserke T, Weisenhorn DM, Prakash N, Partanen J, Wurst W (2005) Expression of Fgf receptors 1, 2, and 3 in the developing mid- and hindbrain of the mouse. Developmental dynamics : an official publication of the American Association of Anatomists 233:1023-1030.
Blak AA, Naserke T, Saarimaki-Vire J, Peltopuro P, Giraldo-Velasquez M, Vogt Weisenhorn DM, Prakash N, Sendtner M, Partanen J, Wurst W (2007) Fgfr2 and Fgfr3 are not required for patterning and maintenance of the midbrain and anterior hindbrain. Developmental biology 303:231-243.
Boukhtouche F, Brugg B, Wehrle R, Bois-Joyeux B, Danan JL, Dusart I, Mariani J (2010) Induction of early Purkinje cell dendritic differentiation by thyroid hormone requires RORalpha. Neural development 5:18.
Bradley DJ, Young WS, 3rd, Weinberger C (1989) Differential expression of alpha and beta thyroid hormone receptor genes in rat brain and pituitary. Proceedings of the National Academy of Sciences of the United States of America 86:7250-7254.
Broadus J, Doe CQ (1997) Extrinsic cues, intrinsic cues and microfilaments regulate asymmetric protein localization in Drosophila neuroblasts. Current biology : CB 7:827-835.
Broccoli V, Boncinelli E, Wurst W (1999) The caudal limit of Otx2 expression positions the isthmic organizer. Nature 401:164-168.
Brodal A, Kristiansen K, Jansen J (1950) Experimental demonstration of a pontine homologue in birds. The Journal of comparative neurology 92:23-69.
Broom ER (2011) Studies of the hindbrain roof plate organiser in the chick embyro. In: MRC Centre for Developmental Neurobiology: King's College London.

Bulfone A, Smiga SM, Shimamura K, Peterson A, Puelles L, Rubenstein JLR (1995) T-Brain-1: A homolog of Brachyury whose expression defines molecularly distinct domains within the cerebral cortex. Neuron 15:63-78.
Bulfone A, Martinez S, Marigo V, Campanella M, Basile A, Quaderi N, Gattuso C, Rubenstein JLR, Ballabio A (1999) Expression pattern of the Tbr2 (Eomesodermin) gene during mouse and chick brain development. Mechanisms of development 84:133-138.
Burger A, Dinichert D, Nicod P, Jenny M, Lemarchand-Beraud T, Vallotton MB (1976) Effect of amiodarone on serum triiodothyronine, reverse triiodothyronine, thyroxin, and thyrotropin. A drug influencing peripheral metabolism of thyroid hormones. The Journal of clinical investigation 58:255-259.
Butts T, Chaplin N, Wingate R (2011) Can Clues from Evolution Unlock the Molecular Development of the Cerebellum? Molecular Neurobiology 43:67-76.
Cajal Ry (1990 (1894)) New ideas on the structure of the nervous sytem in man and vertebrates: Massachusetts institute of technology (translation from French).
Cepko CL, Austin CP, Yang X, Alexiades M, Ezzeddine D (1996) Cell fate determination in the vertebrate retina. Proceedings of the National Academy of Sciences of the United States of America 93:589-595.
Chambers D, Mason I (2000) Expression of sprouty2 during early development of the chick embryo is coincident with known sites of FGF signalling. Mechanisms of development 91:361-364.
Chambers D, Medhurst AD, Walsh FS, Price J, Mason I (2000) Differential display of genes expressed at the midbrain - hindbrain junction identifies sprouty2: an FGF8-inducible member of a family of intracellular FGF antagonists. Molecular and cellular neurosciences 15:22-35.
Chang WS, Harris WA (1998) Sequential genesis and determination of cone and rod photoreceptors in Xenopus. Journal of neurobiology 35:227-244.
Chantoux F, Francon J (2002) Thyroid hormone regulates the expression of NeuroD/BHF1 during the development of rat cerebellum. Molecular and cellular endocrinology 194:157-163.
Chaplin N, Tendeng C, Wingate RJ (2010) Absence of an external germinal layer in zebrafish and shark reveals a distinct, anamniote ground plan of cerebellum development. The Journal of neuroscience : the official journal of the Society for Neuroscience 30:3048-3057.
Cheng Y, Sudarov A, Szulc KU, Sgaier SK, Stephen D, Turnbull DH, Joyner AL (2010) The Engrailed homeobox genes determine the different foliation patterns in the vermis and hemispheres of the mammalian cerebellum. Development 137:519-529.
Chi CL, Martinez S, Wurst W, Martin GR (2003) The isthmic organizer signal FGF8 is required for cell survival in the prospective midbrain and cerebellum. Development 130:2633-2644.
Chizhikov VV, Lindgren AG, Currle DS, Rose MF, Monuki ES, Millen KJ (2006) The roof plate regulates cerebellar cell-type specification and proliferation. Development 133:2793-2804.
Chizhikov VV, Lindgren AG, Mishima Y, Roberts RW, Aldinger KA, Miesegaes GR, Currle DS, Monuki ES, Millen KJ (2010) Lmx1a regulates fates and location of cells originating from the cerebellar rhombic lip and telencephalic

cortical hem. Proceedings of the National Academy of Sciences of the United States of America 107:10725-10730.
Cooper DS (2005) Antithyroid drugs. The New England journal of medicine 352:905-917.
Corrales JD, Blaess S, Mahoney EM, Joyner AL (2006) The level of sonic hedgehog signaling regulates the complexity of cerebellar foliation. Development 133:1811-1821.
Corrales JD, Rocco GL, Blaess S, Guo Q, Joyner AL (2004) Spatial pattern of sonic hedgehog signaling through Gli genes during cerebellum development. Development 131:5581-5590.
Crepel F, Delhaye-Bouchaud N, Dupont JL (1981) Fate of the multiple innervation of cerebellar Purkinje cells by climbing fibers in immature control, x-irradiated and hypothyroid rats. Brain research 227:59-71.
Crossley PH, Martin GR (1995) The mouse Fgf8 gene encodes a family of polypeptides and is expressed in regions that direct outgrowth and patterning in the developing embryo. Development 121:439-451.
Crossley PH, Martinez S, Martin GR (1996) Midbrain development induced by FGF8 in the chick embryo. Nature 380:66-68.
Dahmane N, Ruiz i Altaba A (1999) Sonic hedgehog regulates the growth and patterning of the cerebellum. Development 126:3089-3100.
Dailey L, Ambrosetti D, Mansukhani A, Basilico C (2005) Mechanisms underlying differential responses to FGF signaling. Cytokine & Growth Factor Reviews 16:233-247.
Daniel H, Levenes C, Crépel F (1998) Cellular mechanisms of cerebellar LTD. Trends in neurosciences 21:401-407.
Danielian PS, Muccino D, Rowitch DH, Michael SK, McMahon AP (1998) Modification of gene activity in mouse embryos in utero by a tamoxifen-inducible form of Cre recombinase. Current biology : CB 8:1323-S1322.
Dean P, Porrill J, Ekerot C-F, Jorntell H (2010) The cerebellar microcircuit as an adaptive filter: experimental and computational evidence. Nature reviews Neuroscience 11:30-43.
Ding Q, Joshi PS, Xie ZH, Xiang M, Gan L (2012) BARHL2 transcription factor regulates the ipsilateral/contralateral subtype divergence in postmitotic dI1 neurons of the developing spinal cord. Proceedings of the National Academy of Sciences of the United States of America 109:1566-1571.
Dong H, Yauk CL, Wade MG (2011) Barhl1 is directly regulated by thyroid hormone in the developing cerebellum of mice. Biochemical and biophysical research communications 415:157-162.
Eccles JC, Ito,M. & Szentagothai, J. (1967) The cerbellum as a neuronal machine: Springer, Berlin.
Eddison M, Toole L, Bell E, Wingate RJ (2004) Segmental identity and cerebellar granule cell induction in rhombomere 1. BMC biology 2:14.
Elliott J, Jolicoeur C, Ramamurthy V, Cayouette M (2008) Ikaros Confers Early Temporal Competence to Mouse Retinal Progenitor Cells. Neuron 60:26-39.
Engelkamp D, Rashbass P, Seawright A, van Heyningen V (1999) Role of Pax6 in development of the cerebellar system. Development 126:3585-3596.
Englund C, Kowalczyk T, Daza RA, Dagan A, Lau C, Rose MF, Hevner RF (2006) Unipolar brush cells of the cerebellum are produced in the rhombic lip and

migrate through developing white matter. The Journal of neuroscience : the official journal of the Society for Neuroscience 26:9184-9195.
Englund C, Fink A, Lau C, Pham D, Daza RA, Bulfone A, Kowalczyk T, Hevner RF (2005) Pax6, Tbr2, and Tbr1 are expressed sequentially by radial glia, intermediate progenitor cells, and postmitotic neurons in developing neocortex. The Journal of neuroscience : the official journal of the Society for Neuroscience 25:247-251.
Espinosa JS, Luo L (2008) Timing neurogenesis and differentiation: insights from quantitative clonal analyses of cerebellar granule cells. The Journal of neuroscience : the official journal of the Society for Neuroscience 28:2301-2312.
Fauquier T, Romero E, Picou F, Chatonnet F, Nguyen XN, Quignodon L, Flamant F (2011) Severe impairment of cerebellum development in mice expressing a dominant-negative mutation inactivating thyroid hormone receptor alpha1 isoform. Developmental biology 356:350-358.
Fink AJ, Englund C, Daza RA, Pham D, Lau C, Nivison M, Kowalczyk T, Hevner RF (2006) Development of the deep cerebellar nuclei: transcription factors and cell migration from the rhombic lip. The Journal of neuroscience : the official journal of the Society for Neuroscience 26:3066-3076.
Flace P, Benagiano V, Lorusso L, Girolamo F, Rizzi A, Virgintino D, Roncali L, Ambrosi G (2004) Glutamic acid decarboxylase immunoreactive large neuron types in the granular layer of the human cerebellar cortex. Anatomy and embryology 208:55-64.
Flora A, Klisch TJ, Schuster G, Zoghbi HY (2009) Deletion of Atoh1 disrupts Sonic Hedgehog signaling in the developing cerebellum and prevents medulloblastoma. Science 326:1424-1427.
Forrest D, Sjoberg M, Vennstrom B (1990) Contrasting developmental and tissue-specific expression of alpha and beta thyroid hormone receptor genes. The EMBO journal 9:1519-1528.
Forrest D, Reh TA, Rusch A (2002) Neurodevelopmental control by thyroid hormone receptors. Current opinion in neurobiology 12:49-56.
Forrest D, Hallbook F, Persson H, Vennstrom B (1991) Distinct functions for thyroid hormone receptors alpha and beta in brain development indicated by differential expression of receptor genes. The EMBO journal 10:269-275.
Foucher I, Mione M, Simeone A, Acampora D, Bally-Cuif L, Houart C (2006) Differentiation of cerebellar cell identities in absence of Fgf signalling in zebrafish Otx morphants. Development 133:1891-1900.
Frantz GD, McConnell SK (1996) Restriction of late cerebral cortical progenitors to an upper-layer fate. Neuron 17:55-61.
Fujiyama T, Yamada M, Terao M, Terashima T, Hioki H, Inoue YU, Inoue T, Masuyama N, Obata K, Yanagawa Y, Kawaguchi Y, Nabeshima Y, Hoshino M (2009) Inhibitory and excitatory subtypes of cochlear nucleus neurons are defined by distinct bHLH transcription factors, Ptf1a and Atoh1. Development 136:2049-2058.
Gardner CA, Darnell DK, Poole SJ, Ordahl CP, Barald KF (1988) Expression of an engrailed-like gene during development of the early embryonic chick nervous system. Journal of neuroscience research 21:426-437.

Gavalas A, Davenne M, Lumsden A, Chambon P, Rijli FM (1997) Role of Hoxa-2 in axon pathfinding and rostral hindbrain patterning. Development 124:3693-3702.
Geysens S, Ferran JL, Van Herck SL, Tylzanowski P, Puelles L, Darras VM (2012) Dynamic mRNA distribution pattern of thyroid hormone transporters and deiodinases during early embryonic chicken brain development. Neuroscience.
Gilthorpe JD, Papantoniou EK, Chedotal A, Lumsden A, Wingate RJ (2002) The migration of cerebellar rhombic lip derivatives. Development 129:4719-4728.
Glasgow SM, Henke RM, Macdonald RJ, Wright CV, Johnson JE (2005) Ptf1a determines GABAergic over glutamatergic neuronal cell fate in the spinal cord dorsal horn. Development 132:5461-5469.
Grandel H, Kaslin J, Ganz J, Wenzel I, Brand M (2006) Neural stem cells and neurogenesis in the adult zebrafish brain: origin, proliferation dynamics, migration and cell fate. Developmental biology 295:263-277.
Grosskortenhaus R, Pearson BJ, Marusich A, Doe CQ (2005) Regulation of Temporal Identity Transitions in Drosophila Neuroblasts. Developmental cell 8:193-202.
Guillemot F, Molnár Z, Tarabykin V, Stoykova A (2006) Molecular mechanisms of cortical differentiation. European Journal of Neuroscience 23:857-868.
Guo C, Qiu HY, Huang Y, Chen H, Yang RQ, Chen SD, Johnson RL, Chen ZF, Ding YQ (2007) Lmx1b is essential for Fgf8 and Wnt1 expression in the isthmic organizer during tectum and cerebellum development in mice. Development 134:317-325.
Guo Q, Li K, Sunmonu NA, Li JY (2010) Fgf8b-containing spliceforms, but not Fgf8a, are essential for Fgf8 function during development of the midbrain and cerebellum. Developmental biology 338:183-192.
Ha HR, Stieger B, Grassi G, Altorfer HR, Follath F (2000) Structure-effect relationships of amiodarone analogues on the inhibition of thyroxine deiodination. European journal of clinical pharmacology 55:807-814.
Hagan N, Zervas M (2012) Wnt1 expression temporally allocates upper rhombic lip progenitors and defines their terminal cell fate in the cerebellum. Molecular and cellular neurosciences 49:217-229.
Hallonet ME, Le Douarin NM (1993) Tracing neuroepithelial cells of the mesencephalic and metencephalic alar plates during cerebellar ontogeny in quail-chick chimaeras. The European journal of neuroscience 5:1145-1155.
Hallonet ME, Teillet MA, Le Douarin NM (1990) A new approach to the development of the cerebellum provided by the quail-chick marker system. Development 108:19-31.
Hanashima C, Li SC, Shen L, Lai E, Fishell G (2004) Foxg1 suppresses early cortical cell fate. Science 303:56-59.
Hasebe M, Matsumoto I, Imagawa T, Uehara M (2008) Effects of an anti-thyroid drug, methimazole, administration to rat dams on the cerebellar cortex development in their pups. International journal of developmental neuroscience : the official journal of the International Society for Developmental Neuroscience 26:409-414.
Hawkes R (1992) Antigenic markers of cerebellar modules in the adult mouse. Biochemical Society transactions 20:391-395.

Hawkes R, Colonnier M, Leclerc N (1985) Monoclonal antibodies reveal sagittal banding in the rodent cerebellar cortex. Brain research 333:359-365.
Heffner CD, Lumsden AG, O'Leary DD (1990) Target control of collateral extension and directional axon growth in the mammalian brain. Science 247:217-220.
Helms AW, Johnson JE (1998) Progenitors of dorsal commissural interneurons are defined by MATH1 expression. Development 125:919-928.
Helms AW, Johnson JE (2003) Specification of dorsal spinal cord interneurons. Current opinion in neurobiology 13:42-49.
Helms AW, Abney AL, Ben-Arie N, Zoghbi HY, Johnson JE (2000) Autoregulation and multiple enhancers control Math1 expression in the developing nervous system. Development 127:1185-1196.
Hevner RF, Miyashita-Lin E, Rubenstein JLR (2002) Cortical and thalamic axon pathfinding defects in Tbr1, Gbx2, and Pax6 mutant mice: Evidence that cortical and thalamic axons interact and guide each other. The Journal of comparative neurology 447:8-17.
Hevner RF, Hodge RD, Daza RA, Englund C (2006) Transcription factors in glutamatergic neurogenesis: conserved programs in neocortex, cerebellum, and adult hippocampus. Neuroscience research 55:223-233.
Hevner RF, Shi L, Justice N, Hsueh Y-P, Sheng M, Smiga S, Bulfone A, Goffinet AM, Campagnoni AT, Rubenstein JLR (2001) Tbr1 Regulates Differentiation of the Preplate and Layer 6. Neuron 29:353-366.
Hidalgo-Sanchez M, Martinez-de-la-Torre M, Alvarado-Mallart RM, Puelles L (2005) A distinct preisthmic histogenetic domain is defined by overlap of Otx2 and Pax2 gene expression in the avian caudal midbrain. The Journal of comparative neurology 483:17-29.
Higashijima S, Shishido E, Matsuzaki M, Saigo K (1996) eagle, a member of the steroid receptor gene superfamily, is expressed in a subset of neuroblasts and regulates the fate of their putative progeny in the Drosophila CNS. Development 122:527-536.
Hobert O, Westphal H (2000) Functions of LIM-homeobox genes. Trends in Genetics 16:75-83.
Hollyday M, McMahon JA, McMahon AP (1995) Wnt expression patterns in chick embryo nervous system. Mechanisms of development 52:9-25.
Holmes G (1917) The symptoms of acute cerebellar injuries due to gunshot injuries. Brain 40:461-535.
Holmes G (1922a) The Croonian Lectures on the clinical symptoms of cerebellar disease and their interpretation. The Lancet 199:1177-1182.
Holmes G (1922b) The Croonian Lectures on the clinical symptoms of cerebellar disease and their interpretation. The Lancet 200:59-65.
Holt CE, Bertsch TW, Ellis HM, Harris WA (1988) Cellular determination in the xenopus retina is independent of lineage and birth date. Neuron 1:15-26.
Hoshino M, Nakamura S, Mori K, Kawauchi T, Terao M, Nishimura YV, Fukuda A, Fuse T, Matsuo N, Sone M, Watanabe M, Bito H, Terashima T, Wright CV, Kawaguchi Y, Nakao K, Nabeshima Y (2005) Ptf1a, a bHLH transcriptional gene, defines GABAergic neuronal fates in cerebellum. Neuron 47:201-213.
Huang X, Liu J, Ketova T, Fleming JT, Grover VK, Cooper MK, Litingtung Y, Chiang C (2010) Transventricular delivery of Sonic hedgehog is essential to cerebellar ventricular zone development. Proceedings of the National Academy of Sciences of the United States of America 107:8422-8427.

Ikenaga T, Yoshida M, Uematsu K (2006) Cerebellar efferent neurons in teleost fish. Cerebellum 5:268-274.
Irving C, Mason I (1999) Regeneration of isthmic tissue is the result of a specific and direct interaction between rhombomere 1 and midbrain. Development 126:3981-3989.
Irving C, Mason I (2000) Signalling by FGF8 from the isthmus patterns anterior hindbrain and establishes the anterior limit of Hox gene expression. Development 127:177-186.
Isshiki T, Pearson B, Holbrook S, Doe CQ (2001) Drosophila neuroblasts sequentially express transcription factors which specify the temporal identity of their neuronal progeny. Cell 106:511-521.
Itasaki N, Nakamura H (1996) A Role for Gradient en Expression in Positional Specification on the Optic Tectum. Neuron 16:55-62.
Ito M (2008) Control of mental activities by internal models in the cerebellum. Nature reviews Neuroscience 9:304-313.
Ito M, Sakurai M, Tongroach P (1982) Climbing fibre induced depression of both mossy fibre responsiveness and glutamate sensitivity of cerebellar Purkinje cells. The Journal of physiology 324:113-134.
Jaszai J, Reifers F, Picker A, Langenberg T, Brand M (2003) Isthmus-to-midbrain transformation in the absence of midbrain-hindbrain organizer activity. Development 130:6611-6623.
Joyner AL (1996) Engrailed, Wnt and Pax genes regulate midbrain--hindbrain development. Trends in genetics : TIG 12:15-20.
Joyner AL, Liu A, Millet S (2000) Otx2, Gbx2 and Fgf8 interact to position and maintain a mid-hindbrain organizer. Current opinion in cell biology 12:736-741.
Kalinichenko SG, Okhotin VE (2005) Unipolar Brush Cells – a New Type of Excitatory Interneuron in the Cerebellar Cortex and Cochlear Nuclei of the Brainstem. Neuroscience and Behavioral Physiology 35:21-36.
Kani S, Bae YK, Shimizu T, Tanabe K, Satou C, Parsons MJ, Scott E, Higashijima S, Hibi M (2010) Proneural gene-linked neurogenesis in zebrafish cerebellum. Developmental biology 343:1-17.
Karlsson D, Baumgardt M, Thor S (2010) Segment-specific neuronal subtype specification by the integration of anteroposterior and temporal cues. PLoS biology 8:e1000368.
Kaslin J, Ganz J, Geffarth M, Grandel H, Hans S, Brand M (2009) Stem cells in the adult zebrafish cerebellum: initiation and maintenance of a novel stem cell niche. The Journal of neuroscience : the official journal of the Society for Neuroscience 29:6142-6153.
Katahira T, Sato T, Sugiyama S, Okafuji T, Araki I, Funahashi J, Nakamura H (2000) Interaction between Otx2 and Gbx2 defines the organizing center for the optic tectum. Mechanisms of development 91:43-52.
Kawauchi D, Saito T (2008) Transcriptional cascade from Math1 to Mbh1 and Mbh2 is required for cerebellar granule cell differentiation. Developmental biology 322:345-354.
Kelly RM, Strick PL (2003) Cerebellar loops with motor cortex and prefrontal cortex of a nonhuman primate. The Journal of neuroscience : the official journal of the Society for Neuroscience 23:8432-8444.

Keynes R, Krumlauf R (1994) Hox genes and regionalization of the nervous system. Annual review of neuroscience 17:109-132.
Kiecker C, Lumsden A (2004) Hedgehog signaling from the ZLI regulates diencephalic regional identity. Nature neuroscience 7:1242-1249.
Kim EJ, Battiste J, Nakagawa Y, Johnson JE (2008) Ascl1 (Mash1) lineage cells contribute to discrete cell populations in CNS architecture. Molecular and cellular neurosciences 38:595-606.
Klein C, Butt SJ, Machold RP, Johnson JE, Fishell G (2005) Cerebellum- and forebrain-derived stem cells possess intrinsic regional character. Development 132:4497-4508.
Kofuji P, Hofer M, Millen KJ, Millonig JH, Davidson N, Lester HA, Hatten ME (1996) Functional analysis of the weaver mutant GIRK2 K+ channel and rescue of weaver granule cells. Neuron 16:941-952.
Kohl A, Hadas Y, Klar A, Sela-Donenfeld D (2012) Axonal Patterns and Targets of dA1 Interneurons in the Chick Hindbrain. Journal of Neuroscience 32:5757-5771.
Koster RW, Fraser SE (2006) FGF signaling mediates regeneration of the differentiating cerebellum through repatterning of the anterior hindbrain and reinitiation of neuronal migration. The Journal of neuroscience : the official journal of the Society for Neuroscience 26:7293-7304.
Kramer S, Okabe M, Hacohen N, Krasnow MA, Hiromi Y (1999) Sprouty: a common antagonist of FGF and EGF signaling pathways in Drosophila. Development 126:2515-2525.
Lai HC, Klisch TJ, Roberts R, Zoghbi HY, Johnson JE (2011) In vivo neuronal subtype-specific targets of Atoh1 (Math1) in dorsal spinal cord. The Journal of neuroscience : the official journal of the Society for Neuroscience 31:10859-10871.
Lainé J, Axelrad H (1994) The candelabrum cell: A new interneuron in the cerebellar cortex. The Journal of comparative neurology 339:159-173.
Landsberg RL, Awatramani RB, Hunter NL, Farago AF, DiPietrantonio HJ, Rodriguez CI, Dymecki SM (2005) Hindbrain rhombic lip is comprised of discrete progenitor cell populations allocated by Pax6. Neuron 48:933-947.
Lauder JM (1977) The effects of early hypo- and hyperthyroidism on the development of rat cerebellar cortex. III. Kinetics of cell proliferation in the external granular layer. Brain research 126:31-51.
Le Douarin NM (1993) Embryonic neural chimaeras in the study of brain development. Trends in neurosciences 16:64-72.
Lee J-K, Cho J-H, Hwang W-S, Lee Y-D, Reu D-S, Suh-Kim H (2000a) Expression of neuroD/BETA2 in mitotic and postmitotic neuronal cells during the development of nervous system. Developmental Dynamics 217:361-367.
Lee KJ, Mendelsohn M, Jessell TM (1998) Neuronal patterning by BMPs: a requirement for GDF7 in the generation of a discrete class of commissural interneurons in the mouse spinal cord. Genes & development 12:3394-3407.
Lee KJ, Dietrich P, Jessell TM (2000b) Genetic ablation reveals that the roof plate is essential for dorsal interneuron specification. Nature 403:734-740.
Lee SM, Danielian PS, Fritzsch B, McMahon AP (1997) Evidence that FGF8 signalling from the midbrain-hindbrain junction regulates growth and polarity in the developing midbrain. Development 124:959-969.

Leto K, Carletti B, Williams IM, Magrassi L, Rossi F (2006) Different types of cerebellar GABAergic interneurons originate from a common pool of multipotent progenitor cells. The Journal of neuroscience : the official journal of the Society for Neuroscience 26:11682-11694.
Leto K, Bartolini A, Di Gregorio A, Imperiale D, De Luca A, Parmigiani E, Filipkowski RK, Kaczmarek L, Rossi F (2011) Modulation of cell-cycle dynamics is required to regulate the number of cerebellar GABAergic interneurons and their rhythm of maturation. Development 138:3463-3472.
Lewis PM, Gritli-Linde A, Smeyne R, Kottmann A, McMahon AP (2004) Sonic hedgehog signaling is required for expansion of granule neuron precursors and patterning of the mouse cerebellum. Developmental biology 270:393-410.
Li S, Qiu F, Xu A, Price SM, Xiang M (2004) Barhl1 regulates migration and survival of cerebellar granule cells by controlling expression of the neurotrophin-3 gene. The Journal of neuroscience : the official journal of the Society for Neuroscience 24:3104-3114.
Lin JC, Cai L, Cepko CL (2001) The external granule layer of the developing chick cerebellum generates granule cells and cells of the isthmus and rostral hindbrain. The Journal of neuroscience : the official journal of the Society for Neuroscience 21:159-168.
Liu A, Losos K, Joyner AL (1999) FGF8 can activate Gbx2 and transform regions of the rostral mouse brain into a hindbrain fate. Development 126:4827-4838.
Liu A, Li JY, Bromleigh C, Lao Z, Niswander LA, Joyner AL (2003) FGF17b and FGF18 have different midbrain regulatory properties from FGF8b or activated FGF receptors. Development 130:6175-6185.
Livesey FJ, Cepko CL (2001) Vertebrate neural cell-fate determination: Lessons from the retina. Nature reviews Neuroscience 2:109-118.
Llinás RR (1969) Neurobiology of cerebellar evolution and development: American medical association/Education and research foundation, Chicago.
Logan C, Wizenmann A, Drescher U, Monschau B, Bonhoeffer F, Lumsden A (1996) Rostral optic tectum acquires caudal characteristics following ectopic engrailed expression. Curr Biol 6:1006-1014.
Louvi A, Alexandre P, Metin C, Wurst W, Wassef M (2003) The isthmic neuroepithelium is essential for cerebellar midline fusion. Development 130:5319-5330.
Lumsden A, Keynes R (1989) Segmental patterns of neuronal development in the chick hindbrain. Nature 337:424-428.
Luskin MB, Shatz CJ (1985) Studies of the earliest generated cells of the cat's visual cortex: cogeneration of subplate and marginal zones. The Journal of neuroscience : the official journal of the Society for Neuroscience 5:1062-1075.
Machold R, Fishell G (2005) Math1 is expressed in temporally discrete pools of cerebellar rhombic-lip neural progenitors. Neuron 48:17-24.
Machold RP, Kittell DJ, Fishell GJ (2007) Antagonism between Notch and bone morphogenetic protein receptor signaling regulates neurogenesis in the cerebellar rhombic lip. Neural development 2:5.
Manzano J, Cuadrado M, Morte B, Bernal J (2007) Influence of thyroid hormone and thyroid hormone receptors in the generation of cerebellar gamma-

aminobutyric acid-ergic interneurons from precursor cells. Endocrinology 148:5746-5751.
Marin F, Puelles L (1994) Patterning of the embryonic avian midbrain after experimental inversions: a polarizing activity from the isthmus. Developmental biology 163:19-37.
Marin F, Puelles L (1995) Morphological fate of rhombomeres in quail/chick chimeras: a segmental analysis of hindbrain nuclei. The European journal of neuroscience 7:1714-1738.
Marquardt T, Ashery-Padan R, Andrejewski N, Scardigli R, Guillemot F, Gruss P (2001) Pax6 Is Required for the Multipotent State of Retinal Progenitor Cells. Cell 105:43-55.
Marr D (1969) A theory of cerebellar cortex. The Journal of physiology 202:437-470.
Martinez S, Alvarado-Mallart RM (1990) Expression of the homeobox Chick-en gene in chick/quail chimeras with inverted mes-metencephalic grafts. Developmental biology 139:432-436.
Martinez S, Crossley PH, Cobos I, Rubenstein JL, Martin GR (1999) FGF8 induces formation of an ectopic isthmic organizer and isthmocerebellar development via a repressive effect on Otx2 expression. Development 126:1189-1200.
Maruoka Y, Ohbayashi N, Hoshikawa M, Itoh N, Hogan BL, Furuta Y (1998) Comparison of the expression of three highly related genes, Fgf8, Fgf17 and Fgf18, in the mouse embryo. Mechanisms of development 74:175-177.
Matsumoto K, Nishihara S, Kamimura M, Shiraishi T, Otoguro T, Uehara M, Maeda Y, Ogura K, Lumsden A, Ogura T (2004) The prepattern transcription factor Irx2, a target of the FGF8/MAP kinase cascade, is involved in cerebellum formation. Nature neuroscience 7:605-612.
Matsunaga E, Katahira T, Nakamura H (2002) Role of Lmx1b and Wnt1 in mesencephalon and metencephalon development. Development 129:5269-5277.
McConnell SK (1988) Fates of visual cortical neurons in the ferret after isochronic and heterochronic transplantation. The Journal of neuroscience : the official journal of the Society for Neuroscience 8:945-974.
McConnell SK, Kaznowski CE (1991) Cell cycle dependence of laminar determination in developing neocortex. Science 254:282-285.
McMahon AP, Bradley A (1990) The Wnt-1 (int-1) proto-oncogene is required for development of a large region of the mouse brain. Cell 62:1073-1085.
McMahon AP, Joyner AL, Bradley A, McMahon JA (1992) The midbrain-hindbrain phenotype of Wnt-1-/Wnt-1- mice results from stepwise deletion of engrailed-expressing cells by 9.5 days postcoitum. Cell 69:581-595.
Mellstrom B, Naranjo JR, Santos A, Gonzalez AM, Bernal J (1991) Independent expression of the alpha and beta c-erbA genes in developing rat brain. Mol Endocrinol 5:1339-1350.
Meyers EN, Lewandoski M, Martin GR (1998) An Fgf8 mutant allelic series generated by Cre- and Flp-mediated recombination. Nature genetics 18:136-141.
Miale IL, Sidman RL (1961) An autoradiographic analysis of histogenesis in the mouse cerebellum. Experimental neurology 4:277-296.

Miesegaes GR, Klisch TJ, Thaller C, Ahmad KA, Atkinson RC, Zoghbi HY (2009) Identification and subclassification of new Atoh1 derived cell populations during mouse spinal cord development. Developmental biology 327:339-351.
Millen KJ, Gleeson JG (2008) Cerebellar development and disease. Current opinion in neurobiology 18:12-19.
Millen KJ, Wurst W, Herrup K, Joyner AL (1994) Abnormal embryonic cerebellar development and patterning of postnatal foliation in two mouse Engrailed-2 mutants. Development 120:695-706.
Millet S, Bloch-Gallego E, Simeone A, Alvarado-Mallart RM (1996) The caudal limit of Otx2 gene expression as a marker of the midbrain/hindbrain boundary: a study using in situ hybridisation and chick/quail homotopic grafts. Development 122:3785-3797.
Millet S, Campbell K, Epstein DJ, Losos K, Harris E, Joyner AL (1999) A role for Gbx2 in repression of Otx2 and positioning the mid/hindbrain organizer. Nature 401:161-164.
Millonig JH, Millen KJ, Hatten ME (2000) The mouse Dreher gene Lmx1a controls formation of the roof plate in the vertebrate CNS. Nature 403:764-769.
Miyata T, Maeda T, Lee JE (1999) NeuroD is required for differentiation of the granule cells in the cerebellum and hippocampus. Genes & development 13:1647-1652.
Mizuhara E, Minaki Y, Nakatani T, Kumai M, Inoue T, Muguruma K, Sasai Y, Ono Y (2010) Purkinje cells originate from cerebellar ventricular zone progenitors positive for Neph3 and E-cadherin. Developmental biology 338:202-214.
Morales D, Hatten ME (2006) Molecular markers of neuronal progenitors in the embryonic cerebellar anlage. The Journal of neuroscience : the official journal of the Society for Neuroscience 26:12226-12236.
Moreno N, Bachy I, Retaux S, Gonzalez A (2005) LIM-homeodomain genes as territory markers in the brainstem of adult and developing Xenopus laevis. The Journal of comparative neurology 485:240-254.
Morin X, Jaouen F, Durbec P (2007) Control of planar divisions by the G-protein regulator LGN maintains progenitors in the chick neuroepithelium. Nature neuroscience 10:1440-1448.
Morte B, Manzano J, Scanlan TS, Vennstrom B, Bernal J (2004) Aberrant maturation of astrocytes in thyroid hormone receptor alpha 1 knockout mice reveals an interplay between thyroid hormone receptor isoforms. Endocrinology 145:1386-1391.
Nicholson JL, Altman J (1972a) The effects of early hypo- and hyperthyroidism on the development of rat cerebellar cortex. I. Cell proliferation and differentiation. Brain research 44:13-23.
Nicholson JL, Altman J (1972b) The effects of early hypo- and hyperthyroidism on the development of the rat cerebellar cortex. II. Synaptogenesis in the molecular layer. Brain research 44:25-36.
Nieuwenhuys R, tenDonklaar, H.J., Nicholson, C. (1998) The central nervous system of vertebrates: Springer, Berlin.
Noctor SC, Martinez-Cerdeno V, Ivic L, Kriegstein AR (2004) Cortical neurons arise in symmetric and asymmetric division zones and migrate through specific phases. Nature neuroscience 7:136-144.

Novotny T, Eiselt R, Urban J (2002) Hunchback is required for the specification of the early sublineage of neuroblast 7-3 in the Drosophila central nervous system. Development 129:1027-1036.
O'Leary DD (1987) Remodelling of early axonal projections through the selective elimination of neurons and long axon collaterals. Ciba Foundation symposium 126:113-142.
O'Leary DD, Fawcett JW, Cowan WM (1986) Topographic targeting errors in the retinocollicular projection and their elimination by selective ganglion cell death. The Journal of neuroscience : the official journal of the Society for Neuroscience 6:3692-3705.
Ozaki K, Kadomoto R, Asato K, Tanimura S, Itoh N, Kohno M (2001) ERK Pathway Positively Regulates the Expression of Sprouty Genes. Biochemical and biophysical research communications 285:1084-1088.
Pascual M, Abasolo I, Mingorance-Le Meur A, Martinez A, Del Rio JA, Wright CV, Real FX, Soriano E (2007) Cerebellar GABAergic progenitors adopt an external granule cell-like phenotype in the absence of Ptf1a transcription factor expression. Proceedings of the National Academy of Sciences of the United States of America 104:5193-5198.
Pearson BJ, Doe CQ (2003) Regulation of neuroblast competence in Drosophila. Nature 425:624-628.
Pearson BJ, Doe CQ (2004) Specification of temporal identity in the developing nervous system. Annual review of cell and developmental biology 20:619-647.
Prince V, Lumsden A (1994) Hoxa-2 expression in normal and transposed rhombomeres: independent regulation in the neural tube and neural crest. Development 120:911-923.
Puelles L, Kuwana E, Puelles E, Bulfone A, Shimamura K, Keleher J, Smiga S, Rubenstein JLR (2000) Pallial and subpallial derivatives in the embryonic chick and mouse telencephalon, traced by the expression of the genes Dlx-2, Emx-1, Nkx-2.1, Pax-6, and Tbr-1. The Journal of comparative neurology 424:409-438.
Qian X, Shen Q, Goderie SK, He W, Capela A, Davis AA, Temple S (2000) Timing of CNS Cell Generation: A Programmed Sequence of Neuron and Glial Cell Production from Isolated Murine Cortical Stem Cells. Neuron 28:69-80.
Ramoa AS, Campbell G, Shatz CJ (1989) Retinal ganglion beta cells project transiently to the superior colliculus during development. Proceedings of the National Academy of Sciences of the United States of America 86:2061-2065.
Rapaport DH, Patheal SL, Harris WA (2001) Cellular competence plays a role in photoreceptor differentiation in the developing Xenopus retina. Journal of neurobiology 49:129-141.
Reid CB, Tavazoie SF, Walsh CA (1997) Clonal dispersion and evidence for asymmetric cell division in ferret cortex. Development 124:2441-2450.
Reifers F, Bohli H, Walsh EC, Crossley PH, Stainier DY, Brand M (1998) Fgf8 is mutated in zebrafish acerebellar (ace) mutants and is required for maintenance of midbrain-hindbrain boundary development and somitogenesis. Development 125:2381-2395.
Rodriguez CI, Dymecki SM (2000) Origin of the precerebellar system. Neuron 27:475-486.

Rose MF, Ahmad KA, Thaller C, Zoghbi HY (2009a) Excitatory neurons of the proprioceptive, interoceptive, and arousal hindbrain networks share a developmental requirement for Math1. Proceedings of the National Academy of Sciences of the United States of America 106:22462-22467.
Rose MF, Ren J, Ahmad KA, Chao HT, Klisch TJ, Flora A, Greer JJ, Zoghbi HY (2009b) Math1 is essential for the development of hindbrain neurons critical for perinatal breathing. Neuron 64:341-354.
Ryder EF, Cepko CL (1994) Migration patterns of clonally related granule cells and their progenitors in the developing chick cerebellum. Neuron 12:1011-1029.
Saarimaki-Vire J, Peltopuro P, Lahti L, Naserke T, Blak AA, Vogt Weisenhorn DM, Yu K, Ornitz DM, Wurst W, Partanen J (2007) Fibroblast growth factor receptors cooperate to regulate neural progenitor properties in the developing midbrain and hindbrain. The Journal of neuroscience : the official journal of the Society for Neuroscience 27:8581-8592.
Saba R, Nakatsuji N, Saito T (2003) Mammalian BarH1 confers commissural neuron identity on dorsal cells in the spinal cord. The Journal of neuroscience : the official journal of the Society for Neuroscience 23:1987-1991.
Sato T, Nakamura H (2004) The Fgf8 signal causes cerebellar differentiation by activating the Ras-ERK signaling pathway. Development 131:4275-4285.
Sato T, Joyner AL (2009) The duration of Fgf8 isthmic organizer expression is key to patterning different tectal-isthmo-cerebellum structures. Development 136:3617-3626.
Sato T, Araki I, Nakamura H (2001) Inductive signal and tissue responsiveness defining the tectum and the cerebellum. Development 128:2461-2469.
Sgaier SK, Millet S, Villanueva MP, Berenshteyn F, Song C, Joyner AL (2005) Morphogenetic and cellular movements that shape the mouse cerebellum; insights from genetic fate mapping. Neuron 45:27-40.
Sgaier SK, Lao Z, Villanueva MP, Berenshteyn F, Stephen D, Turnbull RK, Joyner AL (2007) Genetic subdivision of the tectum and cerebellum into functionally related regions based on differential sensitivity to engrailed proteins. Development 134:2325-2335.
Simpson TI, Price DJ (2002) Pax6; A pleiotropic player in development. BioEssays 24:1041-1051.
Steinlin M (2008) Cerebellar disorders in childhood: cognitive problems. Cerebellum 7:607-610.
Strick PL, Dum RP, Fiez JA (2009) Cerebellum and nonmotor function. Annual review of neuroscience 32:413-434.
Suzuki-Hirano A, Sato T, Nakamura H (2005) Regulation of isthmic Fgf8 signal by sprouty2. Development 132:257-265.
Suzuki A, Harada H, Nakamura H (2012) Nuclear translocation of FGF8 and its implication to induce Sprouty2. Development, growth & differentiation.
Swanson DJ, Goldowitz D (2011) Experimental Sey mouse chimeras reveal the developmental deficiencies of Pax6-null granule cells in the postnatal cerebellum. Developmental biology 351:1-12.
Swanson DJ, Tong Y, Goldowitz D (2005) Disruption of cerebellar granule cell development in the Pax6 mutant, Sey mouse. Brain research Developmental brain research 160:176-193.

Thomas T, Power B, Hudson P, Schreiber G, Dziadek M (1988) The expression of transthyretin mRNA in the developing rat brain. Developmental biology 128:415-427.
Thor S, Andersson SG, Tomlinson A, Thomas JB (1999) A LIM-homeodomain combinatorial code for motor-neuron pathway selection. Nature 397:76-80.
Tossell K, Kiecker C, Wizenmann A, Lang E, Irving C (2011) Notch signalling stabilises boundary formation at the midbrain-hindbrain organiser. Development 138:3745-3757.
Toyoda R, Assimacopoulos S, Wilcoxon J, Taylor A, Feldman P, Suzuki-Hirano A, Shimogori T, Grove EA (2010) FGF8 acts as a classic diffusible morphogen to pattern the neocortex. Development 137:3439-3448.
Trokovic R, Trokovic N, Hernesniemi S, Pirvola U, Vogt Weisenhorn DM, Rossant J, McMahon AP, Wurst W, Partanen J (2003) FGFR1 is independently required in both developing mid- and hindbrain for sustained response to isthmic signals. The EMBO journal 22:1811-1823.
Turner DL, Cepko CL (1987) A common progenitor for neurons and glia persists in rat retina late in development. Nature 328:131-136.
Unger J, Lambert M, Jonckheer MH, Denayer P (1993) Amiodarone and the thyroid: pharmacological, toxic and therapeutic effects. Journal of internal medicine 233:435-443.
Van der Geyten S, Segers I, Gereben B, Bartha T, Rudas P, Larsen PR, Kuhn ER, Darras VM (2001) Transcriptional regulation of iodothyronine deiodinases during embryonic development. Molecular and cellular endocrinology 183:1-9.
Verhoelst CH, Roelens SA, Darras VM (2005) Role of spatiotemporal expression of iodothyronine deiodinase proteins in cerebellar cell organization. Brain research bulletin 67:196-202.
Verhoelst CH, Darras VM, Roelens SA, Artykbaeva GM, Van der Geyten S (2004) Type II iodothyronine deiodinase protein in chicken choroid plexus: additional perspectives on T3 supply in the avian brain. The Journal of endocrinology 183:235-241.
Volkmann K, Chen YY, Harris MP, Wullimann MF, Koster RW (2010) The zebrafish cerebellar upper rhombic lip generates tegmental hindbrain nuclei by long-distance migration in an evolutionary conserved manner. The Journal of comparative neurology 518:2794-2817.
Voogd J, Glickstein M (1998) The anatomy of the cerebellum. Trends in neurosciences 21:370-375.
Waid DK, McLoon SC (1995) Immediate differentiation of ganglion cells following mitosis in the developing retina. Neuron 14:117-124.
Waid DK, McLoon SC (1998) Ganglion cells influence the fate of dividing retinal cells in culture. Development 125:1059-1066.
Wallace VA (1999) Purkinje-cell-derived Sonic hedgehog regulates granule neuron precursor cell proliferation in the developing mouse cerebellum. Current biology : CB 9:445-448.
Wallis K, Dudazy S, van Hogerlinden M, Nordstrom K, Mittag J, Vennstrom B (2010) The thyroid hormone receptor alpha1 protein is expressed in embryonic postmitotic neurons and persists in most adult neurons. Mol Endocrinol 24:1904-1916.

Walshe J, Mason I (2000) Expression of FGFR1, FGFR2 and FGFR3 during early neural development in the chick embryo. Mechanisms of development 90:103-110.
Walther C, Gruss P (1991) Pax-6, a murine paired box gene, is expressed in the developing CNS. Development 113:1435-1449.
Wang VY, Rose MF, Zoghbi HY (2005) Math1 expression redefines the rhombic lip derivatives and reveals novel lineages within the brainstem and cerebellum. Neuron 48:31-43.
Wassarman KM, Lewandoski M, Campbell K, Joyner AL, Rubenstein JL, Martinez S, Martin GR (1997) Specification of the anterior hindbrain and establishment of a normal mid/hindbrain organizer is dependent on Gbx2 gene function. Development 124:2923-2934.
Wechsler-Reya RJ, Scott MP (1999) Control of Neuronal Precursor Proliferation in the Cerebellum by Sonic Hedgehog. Neuron 22:103-114.
Wetts R, Fraser SE (1988) Multipotent precursors can give rise to all major cell types of the frog retina. Science 239:1142-1145.
Wilkinson DG, Bailes JA, McMahon AP (1987) Expression of the proto-oncogene int-1 is restricted to specific neural cells in the developing mouse embryo. Cell 50:79-88.
Wilson LJ, Wingate RJ (2006) Temporal identity transition in the avian cerebellar rhombic lip. Developmental biology 297:508-521.
Wilson LJ, Myat A, Sharma A, Maden M, Wingate RJ (2007) Retinoic acid is a potential dorsalising signal in the late embryonic chick hindbrain. BMC developmental biology 7:138.
Wilson SI, Shafer B, Lee KJ, Dodd J (2008) A molecular program for contralateral trajectory: Rig-1 control by LIM homeodomain transcription factors. Neuron 59:413-424.
Wingate RJ (2001) The rhombic lip and early cerebellar development. Current opinion in neurobiology 11:82-88.
Wingate RJ, Hatten ME (1999) The role of the rhombic lip in avian cerebellum development. Development 126:4395-4404.
Wunderlich FT, Wildner H, Rajewsky K, Edenhofer F (2001) New variants of inducible Cre recombinase: a novel mutant of Cre-PR fusion protein exhibits enhanced sensitivity and an expanded range of inducibility. Nucleic acids research 29:E47.
Wurst W, Auerbach AB, Joyner AL (1994) Multiple developmental defects in Engrailed-1 mutant mice: an early mid-hindbrain deletion and patterning defects in forelimbs and sternum. Development 120:2065-2075.
Xu J, Liu Z, Ornitz DM (2000) Temporal and spatial gradients of Fgf8 and Fgf17 regulate proliferation and differentiation of midline cerebellar structures. Development 127:1833-1843.
Yamasaki T, Kawaji K, Ono K, Bito H, Hirano T, Osumi N, Kengaku M (2001) Pax6 regulates granule cell polarization during parallel fiber formation in the developing cerebellum. Development 128:3133-3144.
Ye W, Bouchard M, Stone D, Liu X, Vella F, Lee J, Nakamura H, Ang S-L, Busslinger M, Rosenthal A (2001) Distinct regulators control the expression of the mid-hindbrain organizer signal FGF8. Nature neuroscience 4:1175-1181.

Yu T, Yaguchi Y, Echevarria D, Martinez S, Basson MA (2011) Sprouty genes prevent excessive FGF signalling in multiple cell types throughout development of the cerebellum. Development 138:2957-2968.
Zervas M, Millet S, Ahn S, Joyner AL (2004) Cell behaviors and genetic lineages of the mesencephalon and rhombomere 1. Neuron 43:345-357.
Zhang XM, Yang XJ (2001) Regulation of retinal ganglion cell production by Sonic hedgehog. Development 128:943-957.
Zhao H, Ayrault O, Zindy F, Kim JH, Roussel MF (2008) Post-transcriptional down-regulation of Atoh1/Math1 by bone morphogenic proteins suppresses medulloblastoma development. Genes & development 22:722-727.
Zhu Y, Yu T, Zhang XC, Nagasawa T, Wu JY, Rao Y (2002) Role of the chemokine SDF-1 as the meningeal attractant for embryonic cerebellar neurons. Nature neuroscience 5:719-720.
Zordan P, Croci L, Hawkes R, Consalez GG (2008) Comparative analysis of proneural gene expression in the embryonic cerebellum. Developmental dynamics : an official publication of the American Association of Anatomists 237:1726-1735.